Tropical Phenology In A Time Of Change

Emma R Bush

December 2018

A thesis submitted for the degree of

Doctor of Philosophy

Faculty of Natural Sciences

The University of Stirling

UNIVERSITY OF STIRLING

SUMMARY ABSTRACT

Phenology is increasingly recognized as an important indicator to measure the impacts of global environmental change. Changes to the phenology of tropical ecosystems are likely to have wide-reaching impacts on species, human society and even feedback onto climate. However, tropical phenology data are often unavailable and analyses have been constrained by dependence on geographically limited, non-circular indicators and lack of power in statistical analyses. This thesis addresses these challenges by making available and analysing for the first time a 32-year long record of monthly focal-crown observations (>1000 individuals of >80 species) from western equatorial Africa (Lopé National Park, Gabon).

In Chapter 2, I developed a novel application of Fourier analysis to objectively and quantitatively describe flowering phenology at Lopé (856 trees of 70 species). I tested the power of this approach under different scenarios of data noise (regularity of the cycle and detectability of phenological events) and data length using both simulations and field data. Most individual trees monitored at Lopé flower at regular intervals (59%) and most species have dominant annual flowering modes (88%). I showed that at least six years of data are necessary to confidently detect flowering cycles using this method.

In Chapter 3, I considered how both existing, and emerging, tropical phenology monitoring programs could be made most effective for change analyses by investigating major sources of noise in data collection. Using Fourier analyses of focal crown observations from Lopé (827 trees of 61 species) I showed that regular annual cycles are more common among reproductive than vegetative phenophases. Using expert knowledge and Generalized Linear Mixed Modelling I showed that experienced field observers can provide important information on major sources of noise in data collection and that observation length, phenophase visibility and phenophase duration are all important positive predictors of cycle detectability.

In Chapter 4, I assessed how local weather has changed in western equatorial Africa using Wavelet analysis and Generalised Linear Mixed Models of the long-term weather record from Lopé (34 years of rainfall and temperature observations). Lopé is characterised by a cool, cloudy, long dry season that contrasts with two bright rainy

seasons. Lopé has warmed at a rate of 0.23°C per decade (minimum daily temperature) and dried at a rate of -52mm per decade (total annual precipitation) since 1984. Interannual variation in rainfall and temperature is significantly influenced by global weather patterns such as the El Niño Southern Oscillation and the Atlantic Cold Tongue.

Given this context of change, in Chapter 5 I selected focal-crown observations from a representative subset of canopy tree species at Lopé (108 trees of 8 species representative of 63% of total canopy volume) to assess seasonal and interannual variation in leaf phenology. I found that the tree community is evergreen with dominant species exchanging leaves incrementally and that new leaf development is suppressed during the long dry season. Using Generalised Linear Mixed Models I demonstrated that moisture, light and leaf herbivory are all important positive predictors of new leaf production at seasonal scales. The community-wide probability of leaf flush at Lopé has declined since 1986 and is most strongly predicted by the rise in atmospheric CO_2.

Finally, in Chapter 6 I applied the knowledge accumulated in the previous chapters to assess the impacts of fluctuating resource availability on commercialisation of Moabi Oil, a traditional non-timber forest product in west central Africa. I combined over 15 years' scientific monitoring of the phenology of *Baillonella toxisperma* at Lopé National Park with interviews of indigenous knowledge of Moabi oil producers in rural Gabon, to describe the factors that influence Moabi harvest success and explore its impacts on the rest of the Moabi oil value chain. Because of the temporal and regional variability of wild Moabi fruit availability I recommended a multi-species approach to NTFP commercialisation in the Gabonese NP buffer zones.

In summary, I have shown that regularly cycling phenology is common in tropical tree communities although a wide range of strategies is evident. The evidence from Lopé supports the idea that western equatorial Africa experiences a strongly seasonal environment with a uniquely light deficient long dry season and that this seasonality in environmental conditions directly impacts the phenology of the plant community. The potential stresses on the plant community associated with the long-term warming and drying trends at Lopé appear to be compensated by CO_2 fertilisation

and the characteristic light deficiency of the region which improve water use efficiency.

This thesis answers numerous calls for more quantitative assessment of tropical phenology data by making available evidence from a previously unpublished long-term dataset. This thesis also serves to link the cycles of tropical forest productivity and reproduction to global socio-ecological issues such as forest regeneration, climate mediation and resource availability for threatened animal species and human forest-users.

DECLARATION OF AUTHORSHIP

I, Emma R Bush, declare that this thesis has been composed by myself and that it embodies the results of my own research. Where appropriate, I have acknowledged the nature and extent of the work carried out in collaboration with others

Signed……..

Date……..

ACKNOWLEDGEMENTS

I would like to start by thanking the field scientists who have not only made this work possible but whose dedication and expertise have resulted in a rare and valuable ecological resource to study the effects of our changing world. There have been many that have contributed to this long-term record over the years but particular recognition must go to the core team of phenology observers - Caroline Tutin, Katharine Abernethy, Lee White, Edmond Dimoto and JT Dikangadissi - whose commitment to observe, record and learn from the forest is unrivalled.

Next to my principal supervisors: Nils Bunnefeld and Kate Abernethy. Nils you are a generous and inspirational academic who, throughout this PhD journey, has never let me forget The Big Picture. There are other things I will also never forget…. like watching you discover mirror dancing in a bar in Lopé or your home-dyed "tropical green" fieldwork shirt! Thank you for your mentorship and friendship. Kate, your knowledge and insight into the natural world is incredible and it has been an honour to work with you studying the Lopé landscape that you love so much. Thank you for opening up your home and family to me. Kath, Al and Daisy, you have been such an encouragement to me and I have really enjoyed benefitting from so much supervision.

Arriving at my new office at the University of Stirling, I first stumbled across Izzy, then Katie, then Jess, Bekah and finally Kirstie (who turned up a year later). My coffee room chatter was complete and I was surrounded by a band of ambitious, kind, adventurous women with whom to figure out this PhD thing. I've ended up completing after all of you and you've been an unwavering support throughout. There are so many others who have contributed to this journey - Chris, Robbie, Saro, Patri, Lynsey, all of my office mates, TEAC, STICS - far too many to mention you all, but thank you.

And to those outside of the University bubble who have kept me grounded. Rachie, I think you have sent me a care package for every major life event since we met aged 14 and this has been no different. Thank you for always seeing me through, believing in me and making me laugh.

To my family, my Grandma, my wonderful parents and parents-in-law who have supported us as a family in our commitment to this PhD in so many ways. To my big sister Katie, who has always been my biggest cheerleader and has taken a keen interest in my work since she started tutoring me at an early age!

And last but very much not least, to the other two thirds of myself. Andrew, people ask how I have managed to complete this PhD alongside becoming a mum for the first time, and the answer has to be because of you. You have solo-parented at many a weekend and taken on far too many household chores. But more than that, you believe I've got an important contribution to make and you're willing to put in the hard work to get us there. You are so wonderful and I am so deeply thankful for you. I loved sharing a field season at Lopé with you although I'm sorry about the bees… let's go adventuring again soon?

And my PhD baby, the one whose sleepless nights and boundless energy have added extra "challenges" to completing this PhD but to whom I dedicate this work: May we love the world we live in and learn to tread more lightly upon it, so that when you take your first steps to go out and explore, you may see as many wonderful things as we have seen.

Also one of your first words was "tree"... I think I must take responsibility.

TABLE OF CONTENTS

FIGURES

TABLES

CHAPTER 1

General Introduction

1.1 PHENOLOGY, TROPICAL FORESTS AND GLOBAL ENVIRONMENTAL CHANGE

Phenology is the study of cyclical living processes and questions related to why organisms respond the way they do (adaptation), when (timing) and how often (periodicity) lie at the heart of ecology (Newstrom *et al.* 1994). Recurrent biological events (often referred to as phenophases) occur across many temporal and spatial scales and for plants, range from daily fluctuations in photosynthetic activity (e.g. Koch *et al.* 1994) to seasonal and even multi-annual cycles of woody growth, leaf turnover and reproduction (e.g. Alfaro-Sánchez *et al.* 2017). Temperate plants are broadly synchronized around an annual cycle with growth limited during the winter season (Hanes *et al.* 2013). However there are fewer restrictions on tropical plant growth and many more ecological niches to fill meaning that tropical phenological cycles are much more diverse with less synchrony between individuals and species and cycles other than 12-months long (van Schaik *et al.* 1993).

Phenology as an Essential Biodiversity Variable

Phenology is increasingly recognised as a major global change indicator and has been proposed as an Essential Biodiversity Variable required to study,

report and manage biodiversity change (Pereira *et al.* 2013). In the 4th report of the Intergovernmental Panel on Climate Change (IPCC), Rosenzweig *et al.* (2007) described phenology as "the simplest process in which to track changes in the ecology of species in response to climate change". There is indeed abundant evidence that global warming has led to progressively advancing spring events in temperate regions which can be tracked using a suite of Spring Indicators (e.g. date of leaf out, flowering etc.; Walther *et al.* 2002; Parmesan & Yohe 2003; Rosenzweig *et al.* 2007). However tracking changes in tropical phenology is not as straightforward. The tropics lag far behind temperate regions in terms of data availability and understanding of the mechanistic links between climate and phenology (Abernethy *et al.* 2018). Even where tropical phenology data are available, the measured responses of tropical plants are so complicated that it is difficult to condense the information into coherent, replicable indicators of directional change (equivalent to the temperate Spring Indicators), such as could be included in ecosystem and biome-wide modelling approaches. Thus tropical phenology is largely missing from global meta-analyses of the impacts of climate change on natural systems (Feeley *et al.* 2017; although see section 1.3 for a review of recent publications using long-term tropical phenology).

Phenology is a key adaptive trait determining individual growth and survival (Cleland *et al.* 2007) as well as species distributions (Chuine 2010). It determines the regeneration of species and the composition of future tropical forest plant communities. Both vegetative and reproductive phenology influence the availability of resources to animal and human users of the forest (Butt *et al.* 2015; Morellato *et al.* 2016). Hughes (2000) mapped out potential pathways via which atmospheric and climate changes are likely to impact natural systems (adapted in Figure 1.1). They show that climate changes (increased temperatures, changes to precipitation and changes to frequency and severity of events) will either lead to *in situ* adaptation, extinction or changes to physiology, phenology and species distributions. In this framework, CO_2 enrichment was postulated to directly impact physiology only (e.g. changes to photosynthesis, respiration and plant growth), however there are a small number of studies showing CO_2 impacts

on plant phenology, such as delayed autumnal senescence (Tricker *et al.* 2004; Taylor *et al.* 2008) and increased duration of tropical flowering (Pau *et al.* 2017). Climate change, CO_2 enrichment and nitrogen deposition have also contributed to extensive greening (increased leaf area index, LAI) of the world's land areas (including the tropics; Zhu *et al.* 2016). We have included this link between CO_2 and phenology in Figure 1.1. Together, these changes to physiology, phenology and species distributions will impact species interactions in the community, causing further distribution shifts and in some cases extinctions, and finally species compositional change (Hughes 2000).

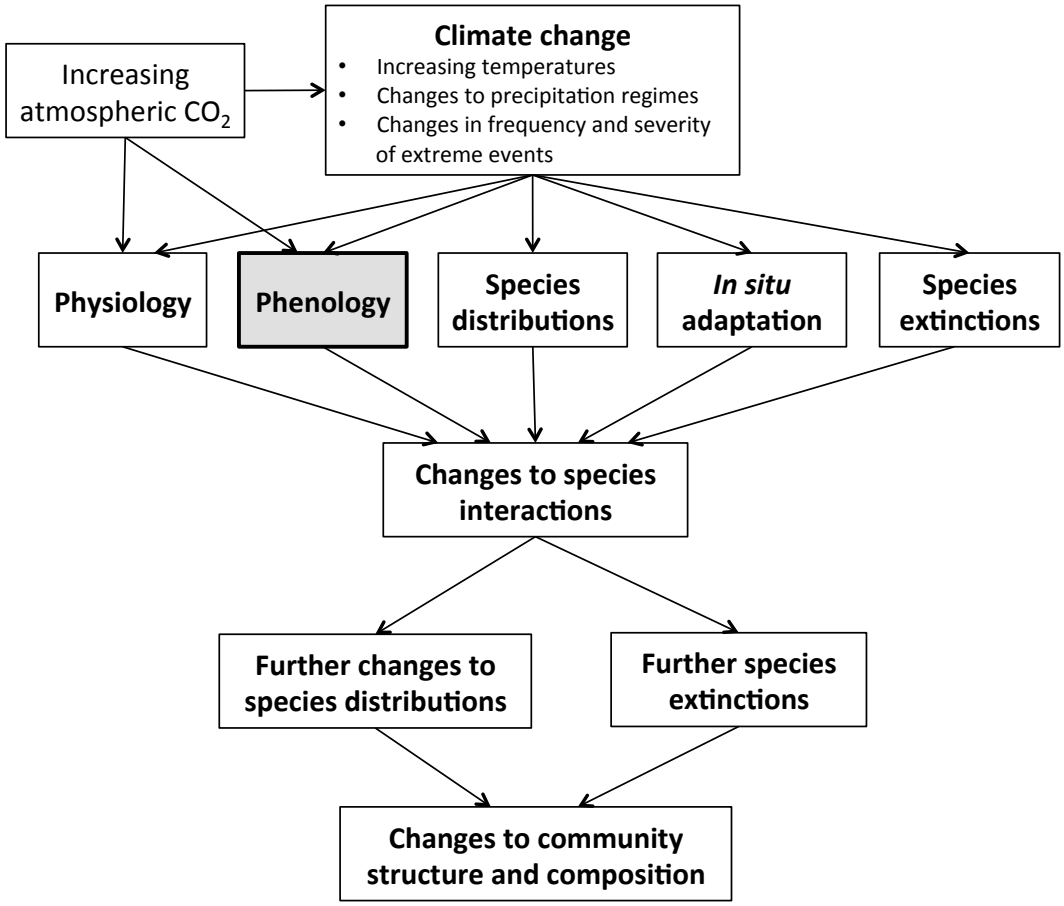

Figure 1.1. Pathways of climate change impacts on plant communities. *Adapted from Hughes 2000.*

Phenology as a climate mediator

Recent Earth System Models (ESMs) show large uncertainty over tropical land areas due to disagreement on the impacts of climate and atmospheric composition on primary productivity (Mitchard 2018). This uncertainty

alongside absence of data is problematic because the phenological responses of tropical ecosystems are a key piece of the global change jigsaw. Tropical forests contain ~25% of land carbon, account for ~33% net primary productivity (NPP; Bonan 2008) and are both source and sink of CO_2 emissions. Land use change (mostly tropical deforestation) is responsible for 20% of CO_2 emissions since 1960 while tropical forest growth is responsible for between a quarter to a third of all CO_2 emissions taken up by the Earth system (Mitchard 2018). Leafy tropical canopies also reduce air temperature because evaporative cooling offsets the heating effect of sunlight absorbed due to low canopy albedo (Bonan 2008).

The future of tropical forests will play a pivotal role in global climate mediation with current debate over whether tropical forests will continue to act as a carbon sink under changing climate and land-use scenarios (Mitchard 2018). Seasonal, interannual and long-term changes to leaf phenology determine the leaf area and demography of leaves in the canopy and thus directly influence structural and physiological processes such as NPP, carbon flux and local microclimatic conditions.

Intersection between phenology, tropical ecology and global environmental change

In summary, it is clear that better knowledge is needed of the environmental and biotic drivers of tropical phenology on seasonal and interannual scales to inform climate change projections, to predict the future species make-up of tropical forests and to understand resource availability for forest-dependent people and animals. However, while we know that phenology and tropical forest ecosystems both influence and respond to global environmental change (GEC), the former relationship (phenology-GEC; Figure 1.2) is based almost solely on temperate data and mechanisms (e.g. widespread evidence of advancing spring events) while the latter (tropical forests-GEC; Figure 1.2) is dominated by climate impacts on forest growth, mortality and long-term species turnover. There is a growing tropical phenology databank (both short and long-term) that is being used to describe and understand seasonal

responses of tropical vegetation (phenology-tropical forests). However the three-way intersection between tropical forest ecology, phenology and GEC is largely missing and has only been addressed by a very small number of scientific studies despite its global importance (Figure 1.2).

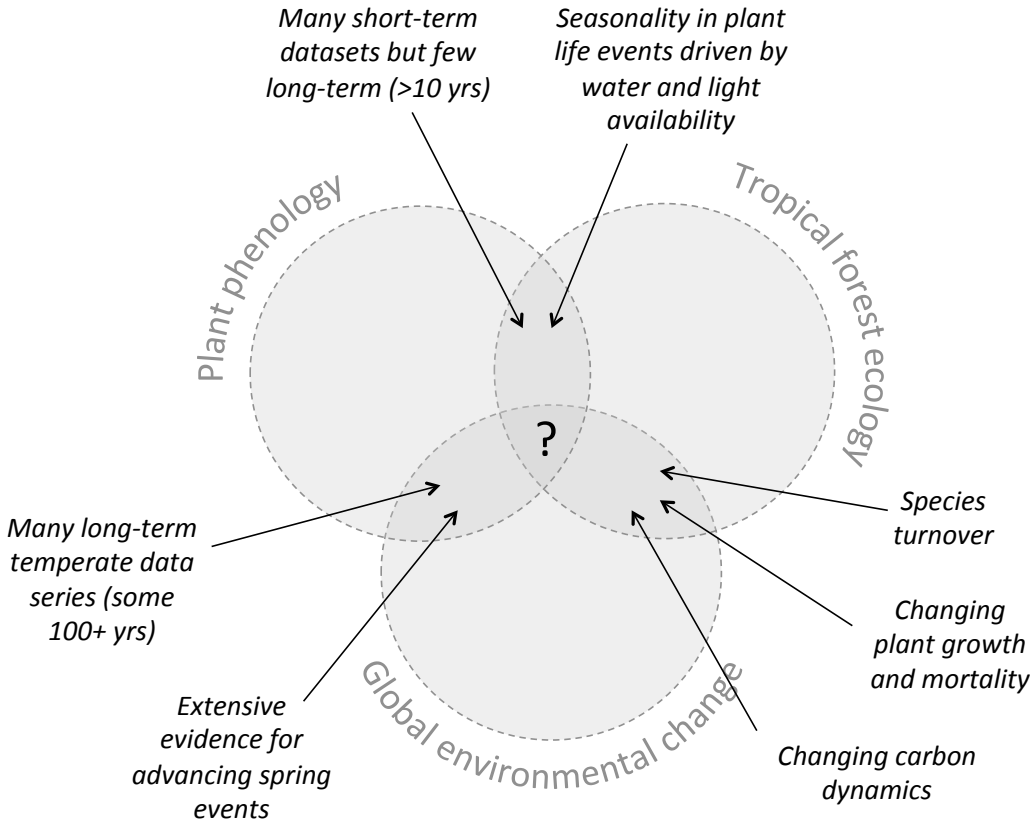

Figure 1.2. The intersection of global environmental change, tropical forests and phenology.

In the following sections we review the mechanisms that determine plant phenology and then give an overview of recent publications on long-term phenology throughout the tropics. Finally we describe the motivation for this thesis including the political and environmental context of our long-term research site in Gabon and pathways to impact for the work presented.

1.2 INTRODUCTION TO PLANT PHENOLOGY

Phenological events vary in their timing, frequency, duration, synchronicity and the scale at which they occur, from individual plant components (such as inflorescences and branches) to individuals, populations, species, guilds and communities (Figure 1.3; van Schaik *et al.* 1993).

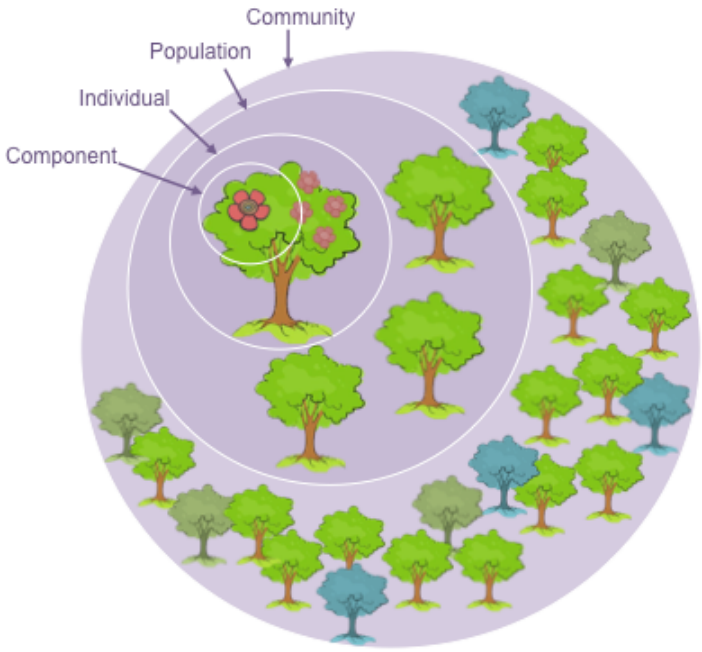

Figure 1.3: Plant phenology occurs at varying spatial scales from branches and individual plants to populations and communities.

The scale of phenological observations determines the questions that can be investigated. Plant physiology and phytochemistry require information at the component or individual-level (e.g. Zhang *et al.* 2017) while population-level data opens up opportunities for assessment of phenotypic variation and the mechanisms and adaptive significance of synchrony between individuals (e.g. Wich & Schaik 2000). At the species and guild level, questions arise regarding faunal interactions with plants, such as the availability of flowers and fruits for nectarivores and frugivores (e.g. Tutin *et al.* 1997). Guild patterns may demonstrate a continual multispecies sequence or sustain nonflowering / fruiting intervals, the nature of which will influence plant processes such as cross-pollination and competition for pollination and fruit dispersal (Newstrom *et al.* 1994). At the community level, research has thus far focussed on the phenological profile – or dominant pattern of phenology - of major forest ecosystems. For example, southeast Asia's dipterocarp-dominated tropical forests are characterised by supra-annual synchronised masting events at the community level, where as sub-annual and annual flowering patterns are more common in Amazonian and African forests (Sakai 2001; Adamescu *et al.* 2018).

Classic reviews of tropical phenology have emphasised a distinction between proximate cues and ultimate selective agents (van Schaik *et al.* 1993; Wright 1996), and between abiotic and biotic causes of phenological events (Sakai 2001). Whilst these distinctions are important, their binary nature falls short of the complex ecological situation. Figure 1.4 represents current knowledge of the chains of causality between exogenous variables of interest in the climate and environment through to those factors which the plant can sense and interact with mechanistically and thus are likely to directly determine plant phenological activity.

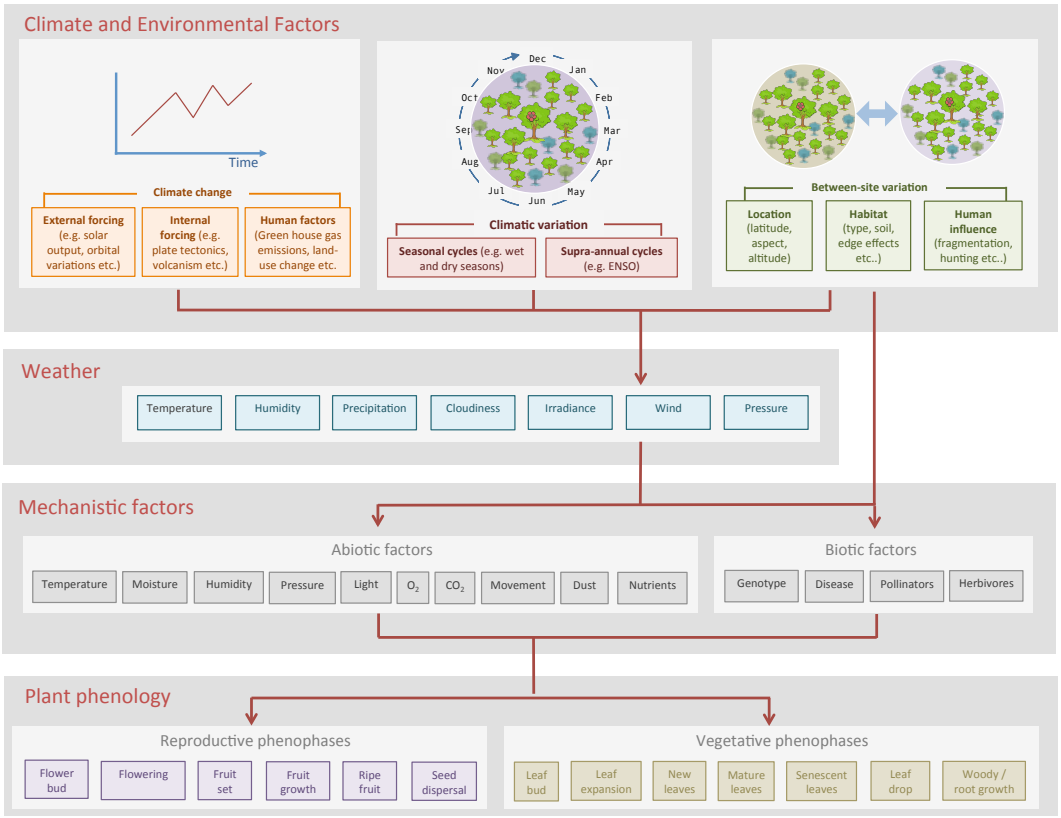

Figure 1.4. Chain of causality between climate and other external factors and the mechanistic factors that directly impact plant phenology.

Mechanistic factors that interact with plant phenology directly can either be abiotic (e.g. photo-period, irradiation, atmospheric pressure, temperature, moisture and mineral nutrients) or biotic (e.g. competition, predation and dispersal; Sakai 2001) and represent physiological demands and genetic limitations on plant growth and reproduction (Menzel 2002; Figure 1.4). The mechanistic relationship between these factors and the phenology of plants

is often unknown and must be addressed at a cellular level (e.g. carbohydrate reserves postulated as the physiological mechanism linking solar radiation and flowering; Wright & Calderón 2018).

Environmental variables and processes interact to determine the availability of the biotic and abiotic factors upon which a plant relies (Menzel 2002). In Figure 1.4, we show that these factors are dependent on site-specifics such as aspect, altitude and habitat as well as local weather conditions (precipitation, temperature, humidity etc.). Local weather is itself determined by a combination of cyclic climatic variables such as seasonality and multi-annual teleconnections (e.g. the El Niño Southern Oscillation, ENSO) but also by long-term climate variation (e.g. anthropogenic climate change) as well as site-level characteristics.

While annual climatic variability is more limited in the tropics than the temperate regions, predictable seasonal patterns do exist (van Schaik *et al.* 1993). Much of the seasonality in the tropics is due to the movements of the inter-tropical convergence zone (ITCZ), a band of clouds and high precipitation encircling the equator formed by the convergence of the trade winds. The ITCZ moves north in the northern summer and south in the northern winter and rainfall is most intense when the sun passes the equator (March and September) forming two dry seasons and two wet seasons annually at the equator (Wright 1996; National Weather Service 2018). Periodic supra-annual climate cycles such as ENSO - where sea surface temperatures (El Niño) and air pressure (Southern Oscillation) fluctuate periodically across the Pacific Ocean every two to seven years – impact weather conditions across the tropics (National Climate Data Centre 2014). In the neotropics, moisture availability is usually lowest in the dry seasons where it is exacerbated by high transpiration demand from increased irradiance. The extent of moisture shortfall in this season is instrumental in determining the tropical vegetation type (Wright 1996) with drought intensity associated with increased deciduousness, shorter trees, simplified canopy structure and decreased leaf-area index (van Schaik *et al.* 1993).

Photosynthetically active radiation is usually limited in the forest understorey and so seasonal variation in irradiance due to changes in cloud cover, day length and solar elevation, are likely candidates for selection on phenological activity (Wright 1996). Newly mature leaves are the most efficient at photosynthesis and it is most energetically efficient to grow reproductive organs when assimilate production is high, rather than to store them (van Schaik *et al.* 1993), thus many forests (especially in neotropics) show flowering and fruiting peaks towards the end of the dry season when irradiance and thus photosynthetic activity peak (Wright & van Schaik 1994; Sakai 2001).

The availability of mineral nutrients has also been considered as a possible determinant of phenological activity as it varies seasonally. At Barro Colorado Island (BCI) in Panama, magnesium and calcium availability increase throughout the wet season as leaf litter decays while elsewhere rapid changes in moisture availability are associated with shorter-term pulses of nitrogen and phosphate due to decomposition of microbes in the soil (Wright 1996). However Wright (1996) warns that many tropical plants are able to effectively store nutrients and so the impact of seasonal fluctuations might be minimal.

While, increasingly, the aim for many phenology studies is to monitor the impacts of climate change on living systems, it is important to consider the complexity of the interactions between climate and plant phenology (as shown in Figure 1.4). For example a positive correlation was found between ENSO and ripe fruit availability at Kibale NP, Uganda, however the relationship is indirect and infers changes at a number of mechanistic levels (e.g. local weather, abiotic and biotic variables), many of which are not well understood and difficult to interpret (Chapman *et al.* 2018).

1.3 REVIEW OF RECENT PUBLICATIONS ON TROPICAL PHENOLOGY

In general tropical plant phenology lags far behind temperate phenology in terms of the data available, establishment of research networks and the

number of published analyses (Mendoza *et al.* 2017; Abernethy *et al.* 2018). However in the last five years there have been a number of new analyses of long-term ground-based tropical plant phenology published in the scientific literature. In this section we briefly review this recent literature to give an indication of the current state of the tropical phenology field.

Alongside the work presented in this thesis, Barro Colarado Island (BCI) in Pamana hosts an equally long continuous reproductive and vegetative phenology monitoring study in the neotropics. For over three decades (1986 to the present), researchers at BCI have used litter traps to collect evidence of plant phenophases from the forest community. The work has been published at regular intervals throughout this period and has made a substantial contribution to our understanding of tropical forest dynamics (e.g. Wright & Calderon 1995; Pau *et al.* 2013). The most recent analyses from this neotropical moist forest show that flowering activity is better predicted by irradiance than rainfall (Wright & Calderón 2018) and has increased across tropical forest growth forms since 1986, related primarily to rising atmospheric CO_2 (Pau *et al.* 2017). At the same site, another recent analysis has shown that elevated leaf and seed fall is associated with the dry, bright conditions of El Niño years, mirroring the community response to the annual dry season (Detto *et al.* 2018).

Other recent analyses from the Neotropics originate from Luquillo in Puerto Rico and Nourages Research Station in Guiana. Luquillo (1992-2007) is a wet tropical forest and seasonal analyses showed an increase in flowering with temperature increases on seasonal and interannual scales. While phenology observations at Nourages ceased in 2011, the full 10 years of phenology data (2001-2001) had not previously been analysed and Mendoza et al. (2018) demonstrated a community-wide annual peak in fruiting at the site coinciding with the peak of the rainy season.

Other sites of significant long-term interest include Kibale, NP, Uganda, where phenology monitoring has taken place discontinuously since 1970 (Chapman *et al.* 2005). A new analysis of a 15-year record (1998-2013) from Kibale showed no long-term trends in fruiting but that inter-annual variation

in fruit production is associated with the El Niño Southern Oscillation (ENSO) and solar radiation (Chapman *et al.* 2018). In a contrasting set of recent analyses of African forest phenology, upward trends in fruiting have been reported for Bwindi Impenetrable NP, Uganda (1998-2010; Polansky & Boesch 2013) and Tai NP, Cote d'Ivoire (2005-2012; Polansky & Robbins 2013), while a decline in flowering and fruiting was detected from a discontinuous dataset from Budongo Forest Reserve, Uganda (1993-2017; Babweteera *et al.* 2018). However the trend in the latter study occurred mostly in the early 1990s with relative stasis since. An 11-year record of epiphytic orchids from Yaoundé Living Collection, Cameroon, supplemented by *in situ* observations, demonstrated a predominately annual flowering mode associated with photoperiod and precipitation as climatic triggers (Texier *et al.* 2018). A newly available large dataset originating in the 1940s from Luki Reserve, Democratic Republic of Congo described a dominant annual rhythm to leaf and reproductive tropical tree phenology strongly associated with rainfall (1947-1958; Couralet *et al.* 2013).

Asian tropical phenology is characterised by mast flowering events where many species reproduce simultaneously on irregular, multi-year cycles. 13 years of flowering records from litter traps at Pasoh Forest Reserve, Malaysia (2001-2014; Chen *et al.* 2017) showed that drought and cool temperatures interact to predict general flowering events for five species of the Dipterocarp genus *Shorea* that are indicative of community-wide general flowering. A similar association between flowering and drought (linked to the transition between ENSO phases) was found in an earlier study of Dipterocarp general flowering at Lambir Hills National Park, Borneo (1993-2003; Sakai *et al.* 2006).

The last two years have seen the first continent-wide analyses and reviews of tropical phenology published. A review of African plant phenology literature (tropical and other) uncovered 130 publications with 75% published between 2000 and 2015 and 70% relying on remote sensing rather than ground-based data. Adole *et al.* (2016) found only five ground-based phenology studies from central Africa (the focus of this thesis). A major

development since then has been the publication of a pan-African analysis of ground-based reproductive phenology at 12 tropical sites throughout west, central and east Africa (sampling length = 6-29 years; Adamescu *et al.* 2018). This study represents the first time that the phenological data from a number of the participating sites has been analysed and demonstrates both the diversity of phenological activity in tropical forest ecosystems (>50% individuals with no detectable regular cycle) and the dominance of annual flowering and fruiting patterns among regularly cyclic species, confirming previously published site-specific findings (Chapman *et al.* 2005; Polansky & Boesch 2013; Chapter 2 / Bush *et al.* 2017). A review of reproductive phenology literature for the Neotropics (sites = 218 sites; median sampling length = 18 months; Mendoza *et al.* 2017) revealed the low density of phenological research in the region (~1 dataset per 78000km^2) and the paucity of long-term data (only ten sites with >10 years data). The authors found that rainfall was the most common driver included in explanatory analyses of fruiting activity with fruiting peaks most often reported during the rainy seasons in both rainforests and cerrado woodlands.

Finally there has also been much recent development in the use of alternative data sources to study tropical phenology including living collections at botanic gardens (Texier *et al.* 2018), herbaria data (Zalamea *et al.* 2011; Davis *et al.* 2015), tree-ring analysis (Battipaglia *et al.* 2015; Alfaro-Sánchez *et al.* 2017), phenocams (Lopes 2016; Alberton *et al.* 2017) and remote sensing techniques (Gond *et al.* 2013; Wu *et al.* 2018) .

1.4 INTRODUCTION TO THE CONSERVATION AGENDA IN GABON AND THE LOPÉ LONG-TERM PHENOLOGY STUDY

1.4.1 GABON AND THE NATIONAL PARK NETWORK

Gabon is an equatorial country on the Atlantic coast of central Africa bordering Equatorial Guinea and Cameroon to the North and the Republic of Congo to the east and south. The second largest river in the Congo-Ogooué

basin - the river Ogooué - runs through the heart of the country. Gabon is heavily forested (>85% land area in 2010; Blaser et al. 2011) with more forest per capita than any other African country (Parcs Gabon 2018) and the largest area of African humid forest after the Democratic Republic of Congo (Mayaux *et al.* 2013). The annual rate of deforestation for central Africa from 2000-2010 was 0.11%, between three and ten times lower than that for west Africa and Madagascar respectively (Mayaux *et al.* 2013).

The human population in Gabon numbered just over two million in 2017 but due to rapid urbanisation only 13% of the population (~260,000 people) remain in rural areas (UNdata 2018). GDP per capita in Gabon is ~ 7900 US dollars (UNdata 2018) and the country is classified as an upper middle-income country according to the World Bank (World Bank 2018). Most of Gabon's wealth is derived from oil and is distributed unequally with a third of the population living under the national poverty line (3.4% under the international $1.90 a day poverty line; World Bank 2018). Agricultural development is minimal (just 3.8% of gross value added, GVA) and most employment is in the services industry (UNdata 2018). Unemployment, especially in rural areas, is high (countrywide unemployment in 2017 = 18%; UNdata 2018).

In 2002, the President of the Gabonese Republic designated more than 10% Gabon's land area within a National Park (NP) network. In 2007, upon legal adoption of the Law on National Parks (003/2007), the National Agency of National Parks (ANPN) was formed. ANPN is a public institution with administrative and financial autonomy and is tasked to implement the government's NP policy to:

- Protect natural areas and landscapes of national and international significance for scientific, educational, spiritual, recreational or tourist purposes;
- Perpetuate, in as natural a state as possible, representative examples of physiographic regions, biological communities, genetic resources and species, while ensuring stability and ecological diversity;

- Limit the number of visitors, so that the area remains in a natural or near-natural state;
- Eliminate and, subsequently, prevent any form of exploitation or occupation incompatible with the objectives of the conservation status.
- Guarantee respect for the ecological, geomorphological, sacred or aesthetic elements justifying this status;
- Take into account the needs of local populations, and to make these parks an important axis of the fight against poverty (Parcs Gabon 2018).

ANPN has legal policing powers and its activities include management and enforcement of NP policy and conservation of landscapes and species (enacted via the Direction Technique; Figure 1.5). The ANPN Secretariat Executif provides technical and strategic support to the Gabonese government (including The National Advisory Board on Climate Change and the Ministry for Water and Forests) within various multilateral biodiversity and climate change conventions and partnerships (e.g. the Convention on Biological Diversity, CDB and the United Nations Framework Convention on Climate Change, UNFCCC; Figure 1.5). In accordance with the government's national fight against poverty and in line with Gabon's Strategic Plan (Plan Stratégique Gabon Emergent), ANPN engages in various integrated conservation and development initiatives – such as ecotourism and alternative livelihoods - as a means of stimulating economic development in the NP buffer zones (Parcs Gabon 2018; Figure 1.5). Such activities are commonly pursued as conservation outreach tools with the aims of encouraging buy-in from local populations and compensating for real and perceived losses of access to natural resources (Naughton-Treves *et al.* 2005; Struhsaker *et al.* 2005) although there is increasing evidence that their effectiveness may be limited with few win-win scenarios (Wunder 2001; Adams *et al.* 2004). The Gabonese NP system also hosts a wide range of scientific research (coordinated through the ANPN Cellule Scientifique), including its own core research programs (Figure 1.5).

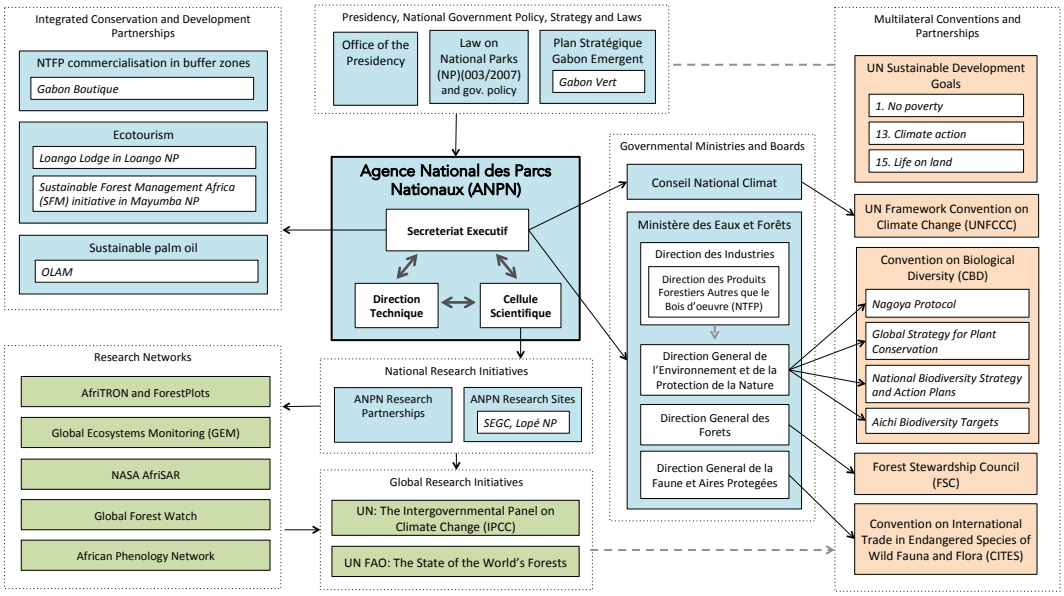

Figure 1.5. ANPN in context.
The role of the National Agency of National Parks (ANPN) in supporting the Gabonese government within multilateral conventions and partnerships, integrated conservation and development initiatives and scientific research.

1.4.2 SEGC and the Lopé Long-Term Phenology Study

Of particular note in ANPN's research portfolio is the field station at Lopé NP (the Station d'Études des Gorilles et des Chimpanzées, SEGC) where scientific research on human health as well as the ecology, environment and climate of the Lopé landscape has taken place since the early 1980s. In 1983 Caroline Tutin and Michael Fernandez, then associated with the University of Stirling's Psychology and later Biological and Environmental Sciences departments, established SEGC as a research station. Tutin and Fernandez settled on the then Lopé-Okanda Wildlife Reserve as the prime site for long-term research of the ecology of the sympatric populations of chimpanzee and gorillas following a nation-wide census of the two species, commissioned by the International Centre for Medical Research in Franceville (CIRMF; Tutin & Fernandez 1987). CIRMF ran the field station from 1984 to 2013 after which ANPN took over responsibility with the University of Stirling continuing as scientific partner. Since its initiation, SEGC's research program has become internationally renowned and has diversified into many aspects of large mammal ecology (including elephants, mandrills, buffalo etc.) as well as the

dynamics of tropical forest floral and faunal communities, the role of tropical forests in the global carbon cycle and the emergence and transmission of zoonotic diseases. Research originating at SEGC has shaped conservation policy and practice (e.g. through the design of Gabon's NP system as well as large mammal census techniques throughout central Africa), directly supported management of the Lopé NP and contributed to regional and international science initiatives and local conservation training and capacity building.

One of the most valuable research assets of ANPN's investment at Lopé is an ongoing study of individual-level plant phenology (leaf, flower and fruits; currently 32 years long from 1986-present). Originated to study resource availability for chimpanzees and gorillas, the Lopé phenology study has contributed to a number of publications (Tutin *et al.* 1991a,b, 1997; Tutin & Fernandez 1993; Tutin 1998; Tutin & White 1998; Voysey *et al.* 1999) and prior theses (Voysey 1995; Momont 2007; White 2007). After just eight years of data collection (1984-1991) Tutin and Fernandez (1993) identified at least eight species which flower after the dry season and are dependent on a critical low temperature (<=19°c), demonstrated by the anomalous flowering of these species when this temperature occurred aseasonally in January. The first two years of phenology data (1984-1986) were removed from subsequent analyses because of the reduced sample size (only five individuals per species) and other inconsistencies related to establishing a new method. Five years after the publication on critical minimum temperature, Tutin and White (1998) presented a review of primates, phenology and frugivory. Using nine years of Lopé phenology observations (1986-1995) they described the dominance of annual flowering modes among the studied species and community-wide flowering peaks in March-April and September-November. While many species (mean number of species >20) were observed to carry unripe fruit through the dry season (June-September), most fruit ripened between September and March (>15 species) with the quantity of fruit showing a similar pattern. Thus Tutin and White concluded that the long dry season (June-September) posed a stark challenge for the fruit-dependent animals of the forest.

From 1999 to 2017 there was a hiatus in publication using this dataset. Now at 32 years long, it is one of the longest continuous phenology-monitoring programs known in the tropics (matched only by one other site, BCI in Panama). While similar work has been undertaken at Kibale, NP, unfortunately there have been gaps in recording due to political instability. Such continuous, long-term phenology data is extremely rare in the tropics and holds unique value to understand the dynamics of tropical forest ecosystems. Seven of 11 species that make up the top 75% of community-wide crown volume at the site are included in the phenology species sample (Chapter 5) meaning that it can be used to monitor the community-wide impacts of global environmental change and the role of tropical forests in global climatic and atmospheric processes. Plant phenology also underpins the availability of resources for animals and people (Butt *et al.* 2015; Morellato *et al.* 2016; Abernethy *et al.* 2018). Of the 80+ plant species monitored at Lopé NP since 1984, seven are recognised as important indigenous fruit trees because they provide non-timber forest products (NTFPs) traditionally used by Gabonese people for cooking, medicine and cultural activities (Iponga *et al.* 2018). The Lopé dataset has relevance not just for resource availability for chimpanzees and gorillas as originally planned, but also for understanding resource availability for other species including humans and the study of forest-wide responses to seasonal and long-term climate variability.

This thesis was jointly funded by ANPN and the University of Stirling as an Impact Collaborative Studentship to analyse the newly available 32-year long Lopé phenology dataset and explore the potential for this resource to contribute to ANPNs aims and activities (park management, research and integrated conservation and development) as well as government policy and relevant multilateral conventions and partnerships such as the UNFCCC and the CDB (Figure 1.5). The main aims of this thesis are to: 1. Describe the cyclical behaviour of vegetative and reproductive phenophases for a diverse community of tropical trees in western equatorial Africa; 2. Improve field and statistical methods to enable evaluation of long-term changes in the tropical forest plant community; 3. Evaluate long-term changes in the weather and

phenology of an African tropical forest and 4. Consider the impacts of phenological regularity and long-term change on the resources available for human users of the forest. Throughout this thesis I trace the realised and potential impact pathways for the work presented.

1.5 INTRODUCTION TO THE THESIS CHAPTERS

Chapter 2: *Fourier analysis to detect phenological cycles using long-term tropical field data and simulations*

⇒ A version of this chapter has been published as: Bush, E.R., Abernethy, K.A., Jeffery, K., Tutin, C., White, L., Dimoto, E., Dikangadissi, J.T., Jump, A.S. & Bunnefeld, N. (2017). Fourier analysis to detect phenological cycles using tropical field data and simulations. Methods in Ecology and Evolution, 8, 530–540.

Due to the complexity of tropical phenological cycles and their explicit circularity (no winter season) we are missing a standardised set of quantitative indicators to describe and compare tropical phenological activity. In chapter 2 I present and demonstrate a novel application of Fourier methods to objectively and quantitatively describe long-term individual-level plant phenology data even when data may be noisy. I use the approach to test the hypothesis that flowering occurs on a regular, synchronised cycle within species using focal crown observations from Lopé and simulated data. Finally I use simulated data to test the hypotheses that cycle regularity, ease of observation and sample size (data length) positively affect cycle detectability using Fourier analysis.

Chapter 3: *Towards effective monitoring of tropical phenology: maximizing returns and reducing uncertainty in long-term studies*

⇒ A version of this chapter has been published as: Bush, E.R., Bunnefeld, N., Dimoto, E., Dikangadissi, J.T., Jeffery, K., Tutin, C., White, L. and Abernethy, K.A., 2018. Towards effective monitoring of tropical

phenology: maximizing returns and reducing uncertainty in long-term studies. Biotropica, 50(3), pp.455-464.

Despite relatively long data observation and a large sample of individuals and species at Lopé we still face challenges of noisy data. In chapter 3 I tease apart the uncertainties associated with both the biological processes and observation biases in long-term phenology studies. I use the Lopé long-term focal crown observations to test the hypotheses that process and observation uncertainty negatively impact cycle detectability using Fourier methods and compare the relative importance of each, making recommendations for the future of our study and other study sites.

Chapter 4: ***Seasonal, inter-annual and long-term weather variability in western equatorial Africa***

Given the context of global environmental change and growing evidence that plant productivity and reproductive cycles are influenced by climate and local weather conditions, in Chapter 4 I analyse the long-term Lopé weather record for the first time. Using Fourier and Wavelet methods as well as Generalised Linear Mixed Models I investigate the hypotheses that seasonal, inter-annual and long-term weather variability at the site is predictably associated with the ITCZ, major oceanic oscillations and long-term climate change.

Chapter 5: ***CO_2 drives long-term reduction in tropical canopy leaf turnover***

Phenology is an Essential Biodiversity Variable vital to our understanding of the ecological impacts of global climatic and atmospheric processes. Yet knowledge of how seasonal, interannual and long-term weather variation impacts tropical leaf turnover is lacking. In Chapter 5 I describe the seasonal patterns of leaf turnover at Lopé NP for a representative sample of species using Fourier analyses and Generalised Linear Mixed Models. I then test the hypotheses that light, moisture, temperature, CO_2 and leaf herbivory are

likely drivers of monthly and interannual variation in canopy leaf production and compare their relative importance.

Chapter 6: ***Is Moabi a reliable source of enterprise for the future?***

Finally, using the knowledge accumulated from the previous chapters I apply our data and methods to a practical problem facing my Impact partner, ANPN. In Chapter 6 I investigate the impacts that raw resource availability may have on successful commercialisation of the non-timber forest product Moabi Oil in the buffer zones of Gabon's NPs. I combine over 15 years' scientific monitoring of the phenology of *Baillonella toxisperma* at Lopé National Park with indigenous knowledge of Moabi Oil producers in rural Gabon, to describe the factors that influence Moabi harvest success and its impacts on the rest of the Moabi oil value chain.

CHAPTER 2

Fourier analysis to detect phenological cycles using long-term tropical field data and simulations

A version of this chapter has been published as:

Bush, E.R., Abernethy, K.A., Jeffery, K., Tutin, C., White, L., Dimoto, E., Dikangadissi, J.T., Jump, A.S. & Bunnefeld, N. (2017). Fourier analysis to detect phenological cycles using tropical field data and simulations. Methods in Ecology and Evolution, 8, 530–540.

EB, KA, AJ and NB conceived the research idea and designed the study. KA, KJ, CT, LW, ED, JTD and EB collected and archived the data and EB performed analyses with advice from KA, AJ and NB. All authors contributed critically to the drafts, and the published version formatted for the thesis is presented here.

2.1 ABSTRACT

Changes in phenology are an inevitable result of climate change, and will have wide-reaching impacts on species, ecosystems, human society and even feedback onto climate. Accurate understanding of phenology is important to adapt to and mitigate such changes. However, analysis of phenology globally has been constrained by lack of data, dependence on geographically limited, non-circular indicators and lack of power in statistical analyses. To address these challenges, especially for the study of tropical phenology, we developed a flexible and robust analytical approach - using Fourier analysis with confidence intervals - to objectively and quantitatively describe long-term observational phenology data even when data may be noisy. We then tested the power of this approach to detect regular cycles under different scenarios of data noise and length using both simulated and field data. We use Fourier analysis to quantify flowering phenology from newly available data for 856 individual plants of 70 species observed monthly since 1986 at Lopé National Park, Gabon. After applying a confidence test, we find that 59% of the individuals have regular flowering cycles, and 88% species flower annually. We find time series length to be a significant predictor of the likelihood of confidently detecting a regular cycle from the data. Using simulated data we find that cycle regularity has a greater impact on detecting phenology than event detectability. Power analysis of the Lopé field data shows that at least six years of data are needed for confident detection of the least noisy species, but this varies and is often greater than 20 years for the most noisy species. There are now a number of large phenology datasets from the tropics, from which insights into current regional and global changes may be gained, if flexible and quantitative analytical approaches are used. However consistent long-term data collection is costly and requires much effort. We provide support for the importance of such research and give suggestions as to how to avoid erroneous interpretation of shorter length datasets and maximize returns from long-term observational studies.

2.2 INTRODUCTION

Phenology concerns the timing of recurring life-cycle events - such as leaf growth, flowering and fruiting in plants - and has long fascinated ecologists and evolutionary scientists. Questions range from understanding the complex environmental cues and internal mechanisms that initiate phenology events (phenophases) to the adaptive significance of their timing and duration and responses to environmental change. Phenology has wide-reaching influence within ecosystems and determines the nature of many inter-specific interactions (Butt *et al.* 2015). Changes in global climate will inevitably have long-term impacts on phenology (Parmesan 2006) with knock-on effects for ecosystems and people (Van Vliet 2010). It is also clear that there will be feedbacks between changing phenology and climate, but they are poorly characterised by current climate models (Pachauri *et al.* 2014).

2.2.1 TROPICAL PHENOLOGY OVERLOOKED IN REVIEWS OF CHANGE

Major reviews of phenological change to date have lent heavily on evidence from temperate, especially Northern hemisphere, regions (Parmesan 2006; Cleland *et al.* 2007; Chambers *et al.* 2013). In these regions more phenology data is available and analyses are arguably simpler. The strong seasonality in temperate regions accompanied by a dormant winter season results in broad synchronisation of phenology on the annual cycle. Years can be treated to some extent as independent repeating events and researchers are able to make use of a relatively simple suite of "spring indicators" (e.g. first appearance, first lay-date, bud-burst measured in days since January 1st).

While tropical climates are often seasonal, annual variation is more limited than in temperate regions and vegetative growth and reproduction are possible at any time of the year resulting in more diverse phenology and cycles other than twelve months (van Schaik *et al.* 1993). Use of simple spring indicators is not appropriate for tropical phenology because of the

circularity of the data (e.g. January 1st is an arbitrarily low value and not meaningfully different from December 31st).

Furthermore, phenology is subject to many conflicting demands, for example an organism may receive an environmental signal to reproduce but fail to do so because it lacks critical resources (Obeso 2002). Inconsistencies and gaps in data collection due to observation error are also common in long-term studies, making quantification in many cases harder still. Thus analytical approaches for tropical phenology need to take account of the circularity of the data, be flexible, quantitative and attribute confidence to conclusions.

2.2.2 ANALYSES OF LONG-TEM TROPICAL PLANT PHENOLOGY

Published analyses of tropical plant phenology range from simple descriptions and correlations with environmental variables to more recent, quantitative analyses of change (Table S2.1). The Newstrom et al. (1994) framework was an important step towards objective inter-site comparisons, however categorisation loses analytical power and visual comparisons lack objective rigour. More computationally intensive methods have included differentiation of species-level reproductive cycles using finite mixture theory and bootstrapping methods (Cannon *et al.* 2007), modelled autocorrelation functions (Norden *et al.* 2007), sinusoid-based regression (Anderson *et al.* 2005), spectral analysis (Chapman *et al.* 1999), circular statistics (Ting et al. 2008; Zimmerman et al. 2007; Wright et al. 1999; Wright & Calderon 1995), generalized linear models (GLMs; Newbery *et al.* 2006; Ting *et al.* 2008) and generalized additive mixed models (GAMMs; Polansky & Robbins 2013). While data has often been collected at the scale of the individual plant (9/18 studies in Table S2.1), this is not always reflected in analysis where individuals are clumped into species, guilds, or a percentage score of a whole community, losing power and precluding vital covariate information. The longest tropical phenology dataset analysed to date is 22 years of flowering data (Pau *et al.* 2013) and 18 years of flowering and fruiting data (Wright & Calderon 2006) from Barro Colorado Island, Panama with many other studies relying on fewer than ten years data (9/18 studies in Table S2.1).

Addressing the challenges of sample size, data quality, circularity and pseudo-replication is of paramount importance to quantify tropical phenology and compare between sites and over time. Consensus as to the most suitable way to analyse these data, what length of data is necessary to identify cycles and how to attribute confidence to results has been missing, although progress is being made (Hudson & Keatley 2010).

In this article, we apply statistical theory to both field and simulated data, to develop and demonstrate objective methods – based on ***Fourier analysis*** - to detect and quantify confidence in regular phenological cycles. We also test the likelihood of detecting cycles under different data noise and length scenarios and discuss opportunities for incorporating the resulting insights into research and policy. Explanations of technical terms related to Fourier analysis used in this paper are given in the glossary in Table 2.1 and their first use in the text is indicated in ***bold italics***.

Table 2.1. Glossary to technical terms

Term	Definition
Bandwidth	The distance at which two peaks in the ***periodogram*** can be distinguished from each other, a quantitative measure of ***resolution***. For example a bandwidth of 0.1 means that cycles can be distinguished from each other when the difference between their frequencies is at least 0.1.
Circular mean	A mean value calculated for ***circular data*** where the arithmetic mean would be inappropriate. For example, the circular mean of 5° and 355° is 0°, in comparison to the arithmetic mean which is 180°.
Circular standard deviation	A measure of dispersion calculated for ***circular data*** where the arithmetic standard deviation would be inappropriate.
Circular data	Data from circular distributions (e.g. months, hours, directions etc.) where there is no true zero and "high" and "low" values are arbitrary (e.g. Figure 2.1A).
Co-Fourier analysis	Simultaneous ***Fourier analysis*** of two ***time series***. Additional outputs include relative ***phase difference*** between the time series at every possible ***cycle*** (Figure 2.1E).
Cycle	A pattern of repeating events in a regular order
Cycle length / Wavelength	The time taken for a whole ***cycle*** to repeat itself (e.g. number of months between repeating flowering events)
Daniell kernel	A moving-average smoother used to eliminate fine detail from the ***raw spectral estimate*** to make the output more ***stable*** and easier to interpret (e.g. ***smoothed spectral estimate*** in Figure 2.1C)

Dominant cycle	The ***cycle length*** associated with the ***dominant peak***.
Dominant peak	The point in the ***spectral estimate*** with highest ***power***
Fourier analysis	Decomposition of a ***time series*** into a series of ***sinusoidal*** functions. The ***power*** of each ***cycle*** in the series can be used to identify ***dominant cycles*** (Figure 2.1C).
Frequency	The rate at which something occurs (e.g. number of flowering cycles per month or per year)
Null continuum	A ***spectral estimate***, derived from the data series, that has been smoothed extensively so that only the underlying shape remains, and no fine detail can be identified (Figure 2.1D).
Periodogram	The visual output of the ***spectral estimate*** derived from ***Fourier analysis*** (Figure 1c-d)
Phase difference	The distance between the peaks in two ***cycles*** of matching ***frequency*** and referenced in time (Figure 2.1E).
Power	The relative tendency of all possible ***cycles*** to appear in the data. Estimated in the ***spectral estimate*** and plotted in the y-axis of a ***periodogram*** (Figure 2.1C). Cycles not well supported by the data have low power, while cycles well supported by the data have high power
Radians	The standard unit of angular measures; 2π radians $=$ $360°$.
Raw spectral estimate	The default output of ***Fourier analysis*** where all fine-scale structure is included, and can be overly influenced by certain segments of the data.
Resolution	The ability to represent fine structure and distinguish between close peaks in the ***spectral estimate*** derived from ***Fourier***, quantified as the ***bandwidth*** (Bloomfield 2000). Spectral estimates with high resolution will show all peaks including minor ones, where as spectral estimates with very low resolution may show no peaks at all, but rather the general shape of the data (e.g. the ***null continuum*** in Figure 2.1D). Increased resolution reduces stability and visa versa.
Sinusoid / Sine wave / Cosine wave	A smooth repeating pattern occurring every 2π radians (or $360°$) (e.g. the simulated curve in Figure 2.1E).
Smoothed spectral estimate	The output of ***Fourier analysis*** after a moving-average smoother is applied to the ***raw spectral estimate*** (Figure 2.1C-D).
Spans	The user-specified widths of the ***Daniell kernel*** smoother, specifically how many data points are used to smooth the ***spectral estimate*** in each local window.
Spectral estimate / Spectrum	The output of ***Fourier analysis*** showing the tendency of all possible ***cycles*** to appear in the data, from twice the observation interval to the full length of the series (Figure 2.1C-D).
Stability	Extent to which small fluctuations in certain segments of the data influence the ***spectral estima***te derived from ***Fourier***. Greater stability reduces ***resolution*** and visa versa. (Bloomfield 2000).
Synchrony	The simultaneous occurrence of two or more events.
Time series	A sequence of data points arranged in time order

2.2.3 Introduction to Fourier analysis for phenology

The Fourier transform is a mathematical method used to identify regular ***cycles*** in ***time series*** data by comparing fluctuations in the data with ***sinusoids*** (Bloomfield 2000) and has been used extensively in disciplines such as engineering and mathematics. The Fourier transform calculates the tendency (hereafter known as ***power***) of all possible cycles to appear in the data and can therefore be used to quantify seasonal phenology data without the need for prior knowledge or hypotheses of ***cycle length***. However it has been rarely used in the context of phenology analysis and never for long-term observational phenology data. Chapman et al. (1999) used Fourier to identify dominant reproductive cycles from six years of data for a tropical tree community, but did not use a confidence test. More recently Zalamea *et al.* (2011) used Fourier to identify flowering cycles from reconstructed 12-month series of herbarium data for a genus of neotropical tree, attributing confidence to cycles using a bootstrapping method.

Compared to other data for which Fourier has been used, phenology data are often comparatively short and collected at low resolution due to the costs and effort incurred. However, in the field of movement ecology, Wittemyer *et al*. (2008) and Polansky *et al.* (2010) successfully used Fourier to confidently identify regular cycles in animal movements by comparing outputs with a null hypothesis of random movement and 95% confidence intervals.

In this paper we build on Wittemyer *et al.'s* (2008) analytical framework to extend the existing uses of Fourier for the field of long-term phenology research. First we demonstrate appropriate application of Fourier to phenology data by quantifying flowering cycle confidence, length, power, timing and ***synchrony*** for individuals of a single species from the Lopé long-term observational study of tropical forest plants (1986 – 2016). Second, we up-scale this Fourier-based approach to analyse flowering phenology using newly available data for all species from the Lopé study (856 individuals, 70 species). Third, we recognize that while the Lopé study is one of the longest

and most consistent of its kind in the tropics, data is still often noisy or short for certain individuals and/or species. In order to apply this framework elsewhere, and to inform best practice for data collection, we test the ability of the Fourier method to detect regular phenology under different scenarios using both simulated data and field data with realistic noise.

2.3 HOW TO DETECT AND DESCRIBE FLOWERING CYCLES USING FOURIER ANALYSIS

The Lopé long-term observational phenology study.

Since 1986, researchers from the Station d'Études des Gorilles and Chimpanzées (SEGC), Lopé National Park, Gabon, have observed individual plants of 88 different species each month and noted the proportion of each canopy covered by new, mature and senescing leaves, flowers, unripe and ripe fruits. Canopy coverage for a particular phenophase is assessed from the ground using binoculars and recorded as a score from 0 to 4. The study area experiences an equatorial climate, where seasonality is determined by movements of the inter-tropical convergence zone to form two dry and two wet seasons annually. See Tutin and White (1998) for detailed site description including local climate and vegetation.

In this first section we demonstrate Fourier analysis using flowering data for tree species *Duboscia macrocarpa* Bocq. (Malvaceae, n=11). Initial observation of species-level data shows no apparent seasonality in flowering (Figure 2.1 A-B). However this is because the true flowering cycle for this species is 18 months long and is not synchronised between individuals. This unusual reproductive phenology is useful to demonstrate the explicitly circular basis of Fourier analysis, and how analysis at the individual-level allows for quantification of complex tropical phenology.

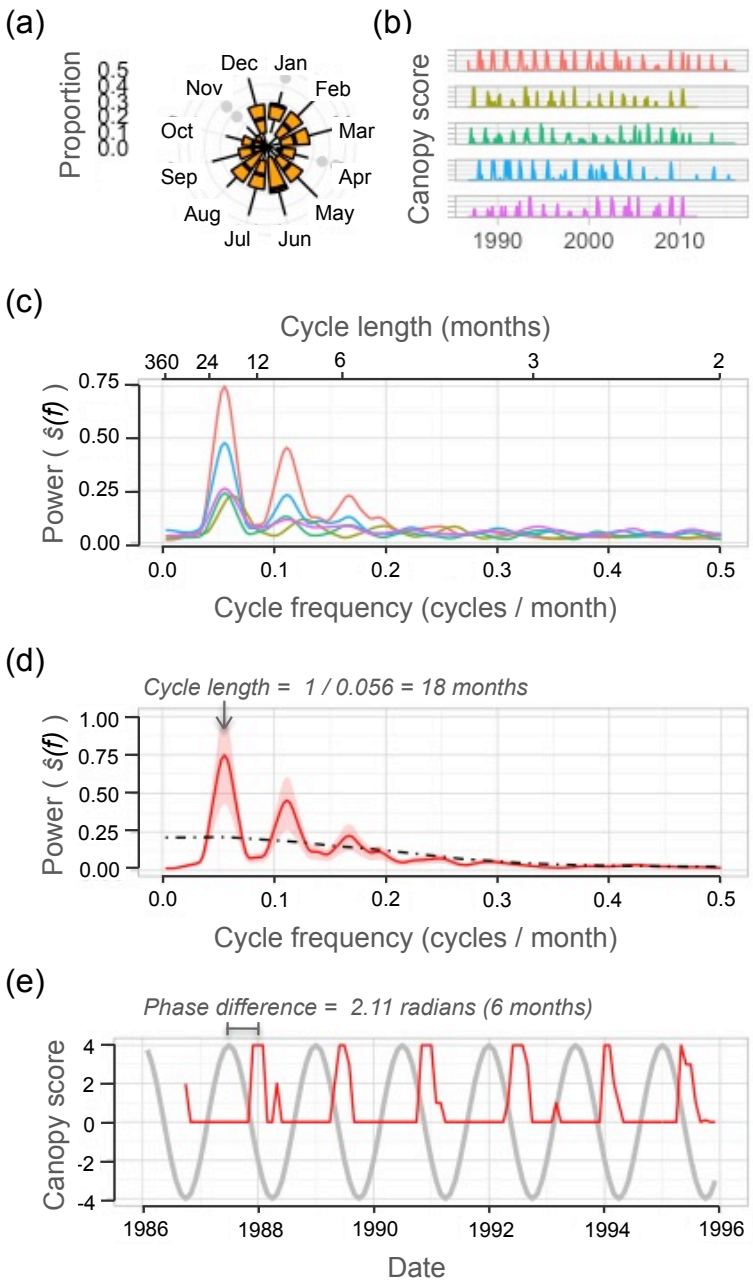

Figure 2.1. Using Fourier analysis to detect flowering phenology for a single species: Duboscia macrocarpa.

a) Boxplots showing the proportion of individuals (n=11) in flower each month from 1986 to 2016. There is no obvious seasonal flowering pattern for this species. b) Time series plots showing flowering canopy scores every month since 1986 to 2016 (five individuals shown as an example). There appears to be some regular flowering cycles for individuals. c) Periodogram displaying the smoothed spectral estimates (bandwidth=0.1) derived from Fourier analysis for each individual flowering time series in (b). The x-axis of the shows all possible cycle frequencies (from one cycle every two months to the full length of the series). The y-axis shows the power of each cycle. The highest peak in each spectrum occurs at a frequency of 0.056 cycles per month (indicating a flowering cycle length of 18 months). d) Periodogram displaying smoothed spectral estimate

(caption for Figure 2.1 continued…) derived from Fourier analysis for the first flowering time series shown in (b) (red line). The 95% confidence intervals for the spectral estimate (red shades) show that the dominant peak (grey arrow) at 0.056 cycles per month is different from the null hypothesis of no cyclicity (the null continuum: black dashed line). We can be confident that the 18-month cycle is different from surrounding noise and represents a real flowering cycle. e) Demonstration of co-Fourier analysis to derive the relative phase of the flowering cycle identified in (d). The flowering time series (red line) is decomposed alongside a regular cosine curve, simulated to have the same cycle length as the flowering data (18 months) and by convention for our data peaking on the 1st January 1986 (grey line). The phase difference (2.11 radians) between the two time series can be converted to time (6 months).

Data input requirements

For all Fourier analyses we used the function *spectrum* from the R base package 'stats' (R Core Team 2015). The method requires regular time intervals between observations, so we interpolated data for gaps up to three data points long using a simple linear estimator, *interpNA* from R package '*timeSeries*' (Rmetrics Core Team *et al.* 2015). For longer gaps we suggest analysing time series in separate parts but more sophisticated forms of interpolation could be used or Lamb normalized periodogram analysis (Press *et al.* 1992) which allows for unevenly spaced data.

The periodogram

The Fourier transform decomposes a time series into a series of ***sine and cosine waves*** of differing ***frequencies***, quantifying the power of each via the ***spectral estimate***, visualised in the ***periodogram*** (Figure 2.1C). The shortest possible cycle for our data is two months long (twice the observation interval) and the longest is the full length of the data available. Cycles not well supported by the data have low power while cycles well supported by the data have high power.

Smoothing the spectral estimate

The ***raw*** (unsmoothed) ***spectral estimate*** shows all fine-scale structure and can be overly influenced by certain segments of data. We smooth all spectral estimates using a moving-average smoother - the modified ***Daniell kernel*** -

available within function spectrum. The width of the Daniell kernel (known as the span) is user-specified and is a compromise between ***resolution*** and ***stability***. The classic text on this method (Bloomfield 2000) recommends a trial and error approach for span-choice relying on visual observation of the periodogram. After much experimentation we found that successively applying the Daniell kernel to achieve a smoothed spectral estimate with a ***bandwidth*** close to 0.1 gave sufficient resolution to identify ***dominant peaks*** in the periodogram. For example, applying a Daniell kernel with a span of seven, followed by a kernel with a span of nine to the first *D. macrocarpa* flowering time series of length 353 months (Figure 2.1B) resulted in a spectral estimate with bandwidth 0.099. ***Smoothed spectral estimates*** derived from Fourier analysis of flowering data for five example D. macrocarpa individuals are shown in Figure 2.1C

Identifying dominant cycles

Interpreting the periodogram begins with observing the general shape of the ***spectrum*** (e.g. is the data influenced by short or long cycles) and then to identify the peaks with highest power, representing ***dominant cycles*** within the data. The smoothed spectral estimates derived from flowering data for *D. macrocarpa* show a similar pattern between individuals (Figure 2.1C). The highest peak for each individual is near to 0.056 cycles per month (equivalent to a cycle length of 18 months).

Assigning confidence to dominant cycles

Tree phenology studies often rely on monthly canopy observations and are subject to both measurement error (observation uncertainty) and natural variation (process uncertainty). Because of these uncertainties a measure of confidence is needed to differentiate real cycles from the surrounding noise. Bloomfield (2000) suggests that spectral estimates approximate a chi-square distribution, and that 95% confidence intervals can be derived as follows,

$$\frac{v\hat{s}(f)}{\mathrm{X}^2_v(0.975)} \leq s(f) \leq \frac{v\hat{s}(f)}{\mathrm{X}^2_v(0.025)}$$

Eqn. 1.

where v is the degrees of freedom (derived from the function output), $\hat{s}(f)$ is the spectral estimate, $s(f)$ is the true spectrum, and $\mathrm{X}^2_v(0.975,0.025)$ are the 2.5% and 97.5% quantiles of the chi square distribution with v degrees of freedom.

There are two credible null hypotheses - representing "no cyclicity" - with which to compare the 95% confidence intervals. The first is the ***null continuum*** of the spectrum, which is an extreme smooth of the spectral estimate such that only the underlying shape remains (dotted line, Figure 2.1D). The second is simply the mean spectrum (otherwise known as the white noise spectrum; Meko 2015). We prefer the null continuum as its use results in fewer false positive results at medium to high noise scenarios (Appendix A).

We found we could achieve sufficient smoothness for the null continuum by successively applying the Daniell kernel to give a bandwidth similar to 1. Where the lower confidence interval for a specified frequency does not overlap with the null hypothesis, the peak at that frequency can objectively be considered as significantly different from the surrounding noise and representing a real cycle. Bloomfield (2000) cautions against general fishing expeditions for significant peaks because the 95% confidence intervals calculated are not simultaneous. We therefore, only recommend using this method to test the dominant peak, not all local peaks. Occasionally we find that when data are highly irregular, the dominant peak is identified at the longest possible cycle length and is likely to score as "significant" against the null continuum. To avoid these false positive results, we screen Fourier outputs and exclude dominant cycles greater than half the data length.

95% confidence intervals for the smoothed spectral estimate derived from one example *D. macrocarpa* time series are shown in Figure 2.1D. We can be confident that the dominant peak at 18 months represents a real flowering cycle because the lower confidence interval doesn't cross the null continuum.

Assessing timing and synchrony

In order to assess timing and synchrony within populations, we developed a method to reference the peak events of tropical phenological cycles in time using a simulated cosine curve within ***co-Fourier analysis***. Co-Fourier allows simultaneous Fourier analysis of any two time series and in addition to normal outputs, gives an estimate for the lag (***phase difference***) between the time series for every possible cycle. Once a dominant cycle has been detected in an empirical time series, we simulate a cosine curve with matching cycle length, by convention for our data peaking on 1st January 1986. After co-Fourier analysis of the empirical time series alongside the matching simulated time series, we then extract the phase difference associated with the dominant cycle.

In figure 2.1E we show flowering data for an example *D. macrocarpa* individual alongside a simulated cosine curve with matching cycle length (18 months) and peaking on January 1st 1986. The phase difference between these two time series at the dominant cycle of 18 months is 2.11 ***radians***.

Phase difference can be converted to time (an estimate of the first flowering peak, in months since January 1st) by the following,

$$if\ \Phi_{radians} > 0, \qquad \Phi_{months} = \frac{\Phi_{radians}}{(2\Pi/\lambda)}$$

$$if\ \Phi_{radians} < 0, \qquad \Phi_{months} = \frac{\Phi_{radians} + 2\Pi}{(2\Pi/\lambda)}$$

Eqn. 2.

where Φ is the phase difference and λ is ***wavelength*** in months.

It is important to consider that radians are a circular unit and there are 2Π radians in a full cycle no matter how many months are in that cycle. Converting phase to months is very simple when the cycle is annual: one month = $2\Pi/12$ and the first peak month will be the only peak month in a given calendar year. However, for cycle lengths other than 12 months, conversion to time will need some careful thought. For a six-month cycle, we

would expect two peaks in each calendar year, and for an 18-month cycle we would expect one peak a calendar year but in different months in alternate years.

For the *D. macrocarpa* time series used as an example in Figure 2.1E, the phase difference of 2.11 radians converts to six months since January 1st, placing the first peak at the beginning of July. The next peak in flowering will occur 18 months later, at the beginning of January. We would expect this individual to have flowers in January and July in alternate years.

Calculating mean timing and synchrony for species

Mean phenophase timing can be computed for a sample with the same dominant cycle by taking the ***circular mean*** of the phase difference (in radians) for each individual, as calculated from co-Fourier analysis. Synchrony can be quantified by taking the ***circular standard deviation*** of the mean phase (all circular values calculated using the R package '*circular';* Agostinelli & Lund 2013). For the *D. macrocarpa* example, mean phase difference for all individuals with significant dominant cycle at 18 months is 0.94± 1.68 SD radians. Converted to time, this references a flowering peak in mid-March and mid-September in alternate years. However synchrony between individuals is so low (SD of peak month is 4.8 months) that "peak flowering" for the population has little biological meaning.

In Appendix B we have included a detailed description of Fourier analysis for the flowering cycles of two additional species (*Antidesma vogelianum* Muell. Arg. flowering on a six-month cycle, and *Pentadesma butyracea* Sabine flowering on an annual cycle) and a comparison of Fourier alongside four other commonly used methods for seasonal phenology analysis – graphical representations, circular statistics, autocorrelation analysis and GAMs.

2.4 SCALING UP – QUANTIFYING FLOWERING PHENOLOGY AMONG MANY INDIVIDUALS AND SPECIES

2.4.1 METHODS

We used the methods developed above to quantitatively describe flowering data for all species monitored as part of the Lopé study. We preselected 856 individuals (70 species of 26 families) with the following criteria; greater than five years continuous data, at least one flowering event and no persistent records of disease (species list given in Table S2.2). Where we found isolated gaps longer than three months, we excluded data before or after (whichever was shorter) from further analysis. Linear interpolation for gaps shorter than three months was necessary for 95% of the individuals in the sample. Time series' length ranged from 60 to 353 months (mean = 249 months).

To quantitatively describe regular cycles, we ran Fourier analysis and a confidence test of the dominant flowering cycle for each tree. To allow comparison between individuals for the power of the dominant cycle, we normalised the spectrum so that the mean power across frequencies was equal to one (Polansky *et al.* 2010).

To summarise at the species-level we calculated the modal cycle length for species with more than five individuals with significant dominant cycles. To estimate the level of synchrony at the species-level, we ran co-Fourier analysis for each individual with a significant dominant cycle equal to the modal cycle length for that species (only including species with more than five such individuals). From the co-Fourier outputs we calculated the standard deviation of mean phase difference in radians and converted to months using Eqn 2. for each species.

We present whole sample summaries for time series length and sample size per species and compare these between all individuals and those for which we could detect significant cycles. We then present the most common

flowering cycles and level of synchrony (standard deviation of mean phase difference) per species. We also tested the impact of time series length as a predictor of detecting significant regular phenology using a binomial Generalized Linear Mixed Model (GLMM) with species as a random effect.

2.4.2 RESULTS

We detected significant regular flowering cycles for 509 out of 856 individuals in our sample, 79% of which were annual. Of those for which we could not confidently detect regular cycles, 22 came from five species for which no significant cycles were detected (e.g. *Baillonella toxisperma* Pierre and *Dacryodes normandii nornandii* Aubr. & Pell., Table S2.3).

When only trees with significant cycles were included, the sample distribution shifted toward longer time series (Figure 2.2A), and mean sample size per species for all trees (12 individuals $\pm$ 8.1 SD) was reduced (seven individuals $\pm$ 5.8 SD) (Figure 2.2B). We found time series' length to be a significant positive predictor (Z value = 6.42, $p<0.001$) of the likelihood of detecting a significant regular cycle from the data (GLM outputs in Table S2.4).

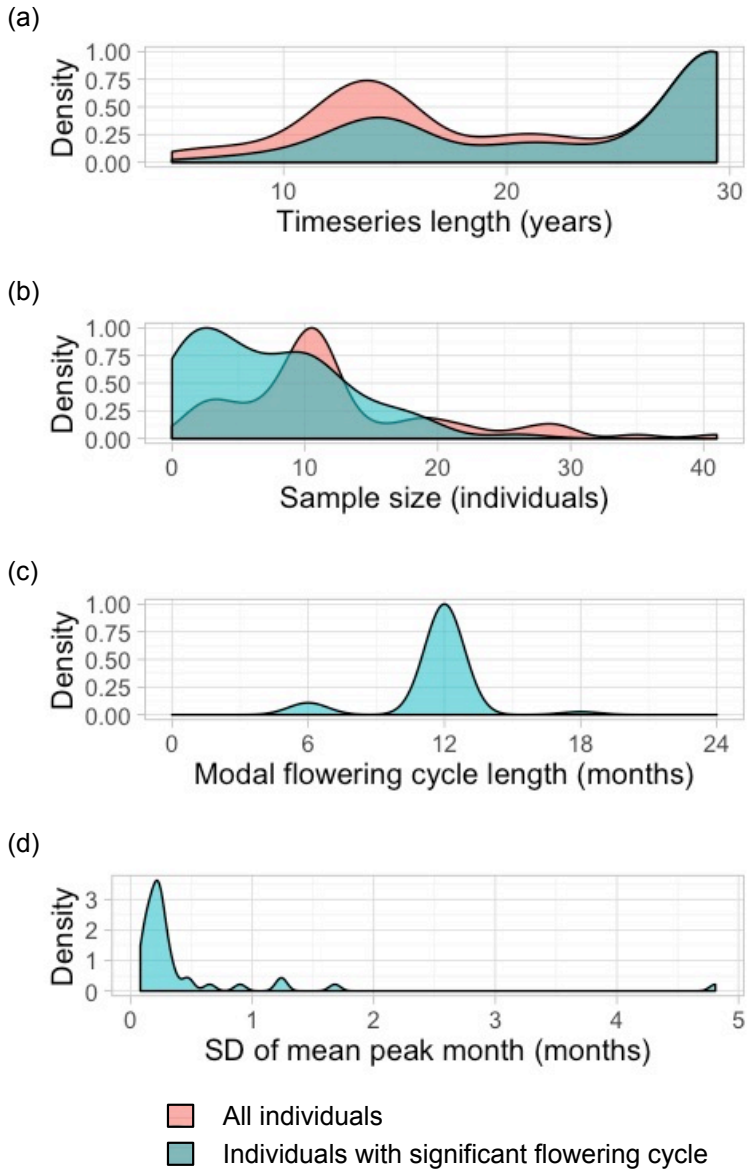

Figure 2.2. Summary of flowering phenology for all tree species monitored at Lopé NP, Gabon.

a) Density plot of time series' length for all individuals analysed (red, 856 individuals) compared to individuals with significant flowering cycles (blue, 509 individuals). b)Density plot of number of individuals per species for all individuals (red, 856 individuals, 70 species) compared to individuals with significant flowering cycles (blue, 509 individuals, 65 species). c) Density plot of most common flowering ***cycle length*** *(mode) per species, for a subsample of 42 species, each more than five individuals with significant flowering cycles (458 individuals). d) Density plot of* ***synchrony*** *(standard deviation of mean peak month) per species, for a subsample of 39 species, each with more than five individuals with significant dominant cycle equal to the species modal cycle length (402 individuals).*

To assess modal cycle length we used a subsample of 42 species (458 individuals). The modal flowering cycle for most species was annual (37 species, e.g. *P. butyracea,* Table S2.3), with others flowering on a 6-month (4 species, e.g. *A. vogelianum,* Table S2.3) and an 18-month basis (1 species, *D. macrocarpa;* Figures 2.2C and 2.3 and Table S2.3).

To assess modal level of synchrony between species we used a subsample of 39 species (402 individuals). The majority of species had flowering cycles well synchronised between individuals, (38 species with standard deviation of mean peak less than one month; Figure 2.2D, Table S2.3).

Species showed considerable inter- and intra-specific variation in flowering phenology (Figure 2.3). Some species were split between different cycle length strategies; e.g. for a sample of 19 *Uapaca guieensis Muell. Arg.* trees, the dominant flowering cycle was annual for 13 trees and six months for six trees. Species also varied in the power of their dominant flowering cycles. Despite all individuals shown in Figure 2.3 having significant flowering cycles, some species such as *Maranthes glabra (Oliv.) Prance* (mean power = 9.3$\pm$1.6 S.D.) and *Xylopia aethiopica (Dunal) A. Richard* (mean power = 8.1$\pm$2.6 S.D.) tended to have much stronger, less noisy cycles than others such as *Klainedoxa gabonensis Baill.* (mean power = 2.1$\pm$0.4 S.D.) and *Pseudospondias microcarpa (A Rich.) Engl.* (mean power = 2.4 $\pm$0.7 S.D.).

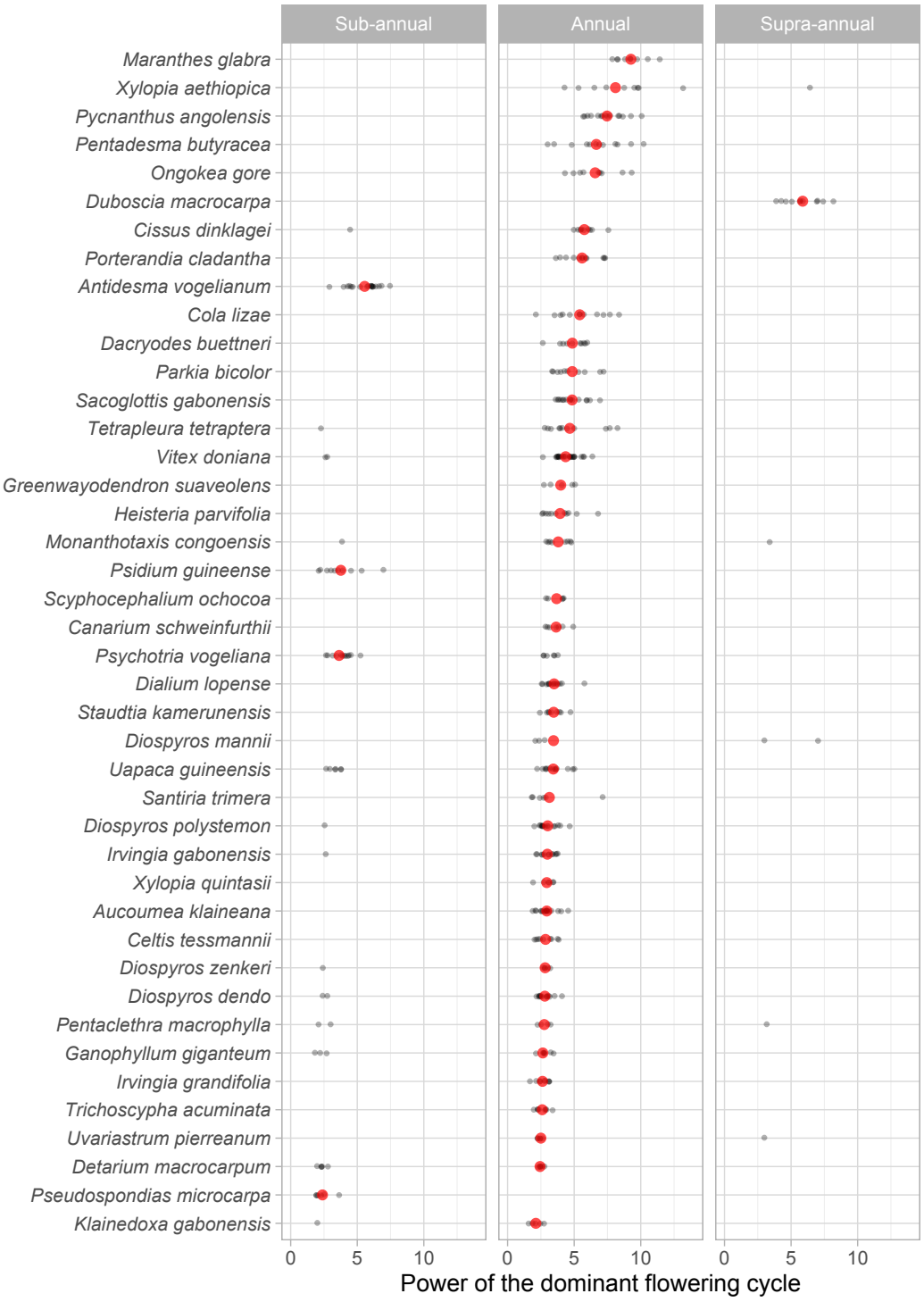

Figure 2.3: Inter- and intra-specific variation in flowering phenology for tree species monitored at Lopé NP, Gabon.
Cycle length *(sub-annual, annual and supra-annual) and* ***power*** *for each individual (grey dots) and modal cycle length and mean power per species (red dots) from a sub-sample of 42 species with more than five individuals with significant flowering cycles (458 individuals).*

2.5 TESTING FOURIER UNDER DIFFERENT SCENARIOS USING BOTH SIMULATED AND FIELD DATA

2.5.1 METHODS

To test the impact of noise and sample length on cycle detectability, we undertook a power analysis of simulated phenology data. We simulated 10,000 individual time series representing an annually repeating flowering cycle peaking in June, with three key parameters allowed to vary between "individuals"; 1) the regularity of the peak month (representing process uncertainty), 2) the detectability of flowering events (representing observation uncertainty) and 3) the length of data recorded. For each year of data, we generated monthly flowering scores of zero and a peak of three-months duration with positive scores randomly chosen from a distribution similar to that found in our field data. We varied levels of regularity by randomly choosing the peak flowering month each year from a truncated normal distribution (ranging from two to 11, with mean six and standard deviation randomly selected from 0.1 to six). The standard deviation of the distribution was consistent between years but allowed to vary between individuals. We then varied levels of detectability by replacing a certain percentage of randomly chosen positive flowering scores with zeros (from zero to 60%). Finally, a window of data (five, ten or 15 years) was randomly cut from each full-length time series prior to Fourier analysis (example simulated data are plotted in Appendix A). We assessed the dominant cycle using a 95% confidence test and whether it fell within the expected interval for an annual cycle (11-13 months).

To demonstrate the impact of data length with realistic noise we also conducted a power analysis using all individual time series from the Lopé study longer than 20 years, from which we had previously detected significant annual flowering cycles and for species with more than five such individuals (233 individuals of 30 different species). We randomly chose individual time series from this sub-sample and cut shorter windows of data (window length randomly selected from the range 2:20 years with randomly

selected start date), repeating 10,000 times. We analysed the windowed time series with Fourier as described above and recorded if the dominant cycle was significant and fell within the expected interval for an annual cycle (11-13 months). We fitted binomial GLMs to compare the effect of time series' length between species.

2.5.2 RESULTS

The power analysis of simulated phenology data (Figure 2.4) showed that as time series' length increased, from 5 to 15 years, so did likelihood of confidently detecting the annual cycle. For example, for a mid-level noise scenario (cycle regularity 2SD; zero replacement 20%) the proportion of the sample with a significant annual cycle was zero after 5 years, 57% after 10 years and 81% after 15 years. However, at relatively low- noise scenarios, (highly regular cycles <1SD; low zero replacement < 20%), the effect of time series length saturated quickly, with 100% likelihood of detecting a significant annual cycle after just five years. In contrast at high-noise scenarios (highly irregular cycles >4SD; zero replacement > 60%), likelihood of detecting a significant annual cycle never rose above 20% even after 15 years. For highly regular cycles (SD<2), even poor event detectability (zero replacement 40 – 60%) had little impact on likelihood of detecting the cycle.

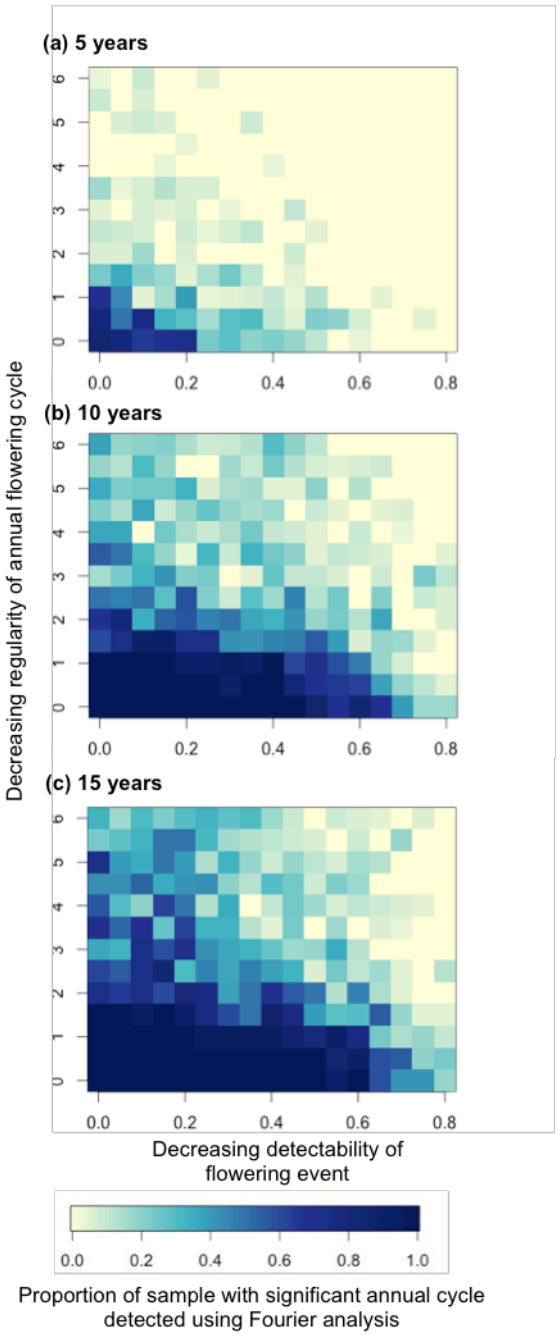

Figure 2.4. Power analysis of simulated phenology data (n=10,000) to show the impact of data noise and length on likelihood of detecting cycles using Fourier analysis.
Noise simulated as cycle regularity (y-axis: standard deviation - 0.1: 6 - of mean month of annual flowering event) and event detectability (x-axis: proportion – 0: 60% - of positive flowering events replaced by zeros).

Similar to the simulated data, we found that as time series' length increased, so did likelihood of detecting regular cyclic behaviour for our field data

(Figure 2.5). We found that for the species in our sample with the most positive slope estimates for time series length (*M. glabra* and *Pycnanthus angolensis* Welw. Warb., S2.5), just six and seven years of data respectively were required before the annual flowering cycle could be detected with greater than 95% likelihood. However species ranged widely, with 19 species not reaching this 95% threshold until after 20 years. The species with the least positive slope estimates were *Detarium macrocarpum Harms* and *Greenwaydodendron suaveolens Engl. & Diels.* (Table S2.5).

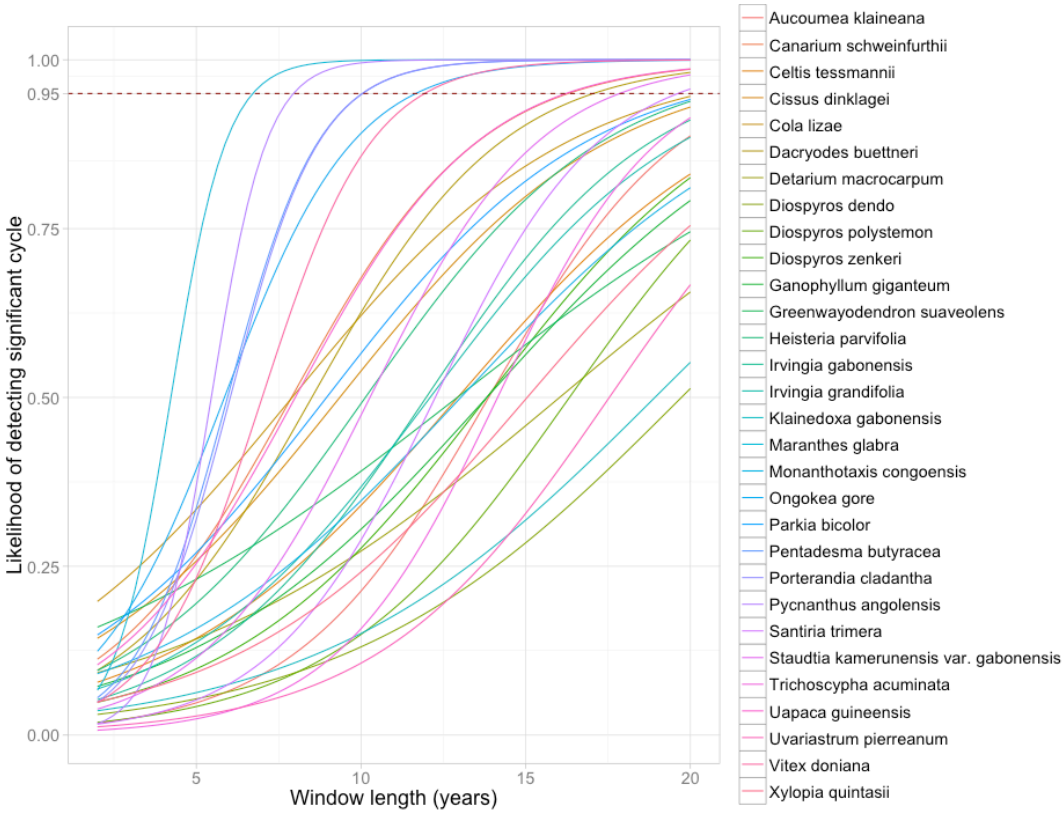

Figure 2.5: Power analysis of annually flowering phenology data from Lopé NP to show the impact of time series length on cycle detection using Fourier analysis.

Generalised linear model (GLM) predictions (family=binomial, link=logit) for each species. Window length varied from 2-20 years and results are from 10,0000 random samples from 233 individuals of 30 species.

2.6 DISCUSSION

2.6.1 DETECTABILITY AND POWER

The flowering phenology of trees observed at Lopé National Park, Gabon, is dominated by annual cycles (88% species), in contrast with forests from the neotropics that appear to be dominated by sub-annual reproductive cycles and the Dipterocarp forests of South-East Asia that are dominated by supra-annual reproductive cycles (Sakai 2001). We could not confidently describe regular cycles for many individuals in our sample (41%), where either flowering is regular but the data were too noisy or too short for detection or glowering is irregular. Observation length was shown to be a significant positive predictor of detecting regular cycles in both field data and simulations. Even when cycles were confidently described, we found that the power attributed to cycles ranged widely, meaning that the flowering phenology of some species is much noisier than others. However the source of this noise is difficult to differentiate for field data. To explore this further we simulated two forms of noise associated with both process and observation uncertainty and found that cycle regularity has a greater effect on ability to detect a significant cycle than event detectability: Fourier analysis can be used to detect the cycle even if the observer misidentifies 60% of flowering months. There are likely to be additional sources of noise in the field, such as false recording of non-existent phenophases, however we consider these to occur less often.

We attributed cycle characteristics to the species-level when we had five or more individuals with significant cycles, under the biological assumption that phenology is an evolutionarily adaptive trait and likely to be constraining con-specifics in a similar way. However, true levels of intraspecific variation are unknown. We find considerable intraspecific variation for some species (i.e. *Uapaca guineensis*) and further research may reveal that phenology is not necessarily a stable trait within a species or an individual's lifetime

Our results can be used to inform effective collection, processing and analysis of phenological data. We have shown that where suitable data is available,

objective analyses can be used to confidently detect regular phenology and that frequency-based outputs – cycle length, power, timing and level of synchrony – give a suite of indicators that could be used to quantitatively describe and compare phenology globally.

2.6.2 Development for causation and change research

The indicators derived from Fourier analysis can be used to address research questions such as the proximate and ultimate causes of adaptive phenology and detection of change. Where data is available, analysis at the individual-level allows for inclusion of covariates (e.g. location, age, size of individuals etc.) in subsequent statistical models, either in combination with random effects and best linear unbiased predictors (BLUPs) to account for variation (for example between different sites, genera or functional groups) or as fixed effects to test hypotheses of the causes of variation between individuals' phenology. Co-Fourier analysis would allow testing of other cyclic factors (such as climate data) alongside phenology to measure synchrony. The advantage of these spectral approaches is that they explicitly model the circular nature of phenology and weather data without losing power by clumping data points into arbitrary time periods or pseudo-replication.

Detecting long-term changes in phenology is challenging and field observations (Plumptre 2011) are vital to stimulate hypotheses and further analysis. However it will be increasingly important to measure the statistical confidence of detected changes. To date, studies of change in tropical phenology are few (Table S2.1), due to the paucity of long-term data. Wavelet analysis is the natural extension of Fourier into the time-frequency domain *(Hudson et al. 2010; Polansky et al. 2010; Wittemyer et al.* 2008), overcoming assumptions of stationarity, to estimate the spectrum as a function of time (Cazelles *et al.* 2008). For phenology research, this could enable analysis of whether individuals or species reproduce more or less frequently (e.g. change in dominant cycle length), reproduce at the same frequency but with more or less certainty (e.g. change in the power of the dominant cycle) or shift phase and become more or less synchronised over time. The power of a

cycle may be a more subtle and effective indicator for change than frequency to track increasing uncertainty over time, especially in the shorter term.

In a formal comparison of this Fourier-based method with other commonly used methods for quantifying phenology (Appendix B), we found Fourier is flexible to diverse phenology and provides a suite of quantitative information to describe seasonal activity with attribution of variance and confidence.

2.6.3 STEPS FORWARD

We have shown that at least six years of data are necessary to confidently detect reproductive cycles amongst our species sample. For data-collection scenarios resulting in noisier data – those with high likelihood of measurement error (e.g. inconspicuous flowers), systematic error (e.g. high inter-observer uncertainty) or natural variation that cannot be controlled for (e.g. diverse array of phenological responses within a population) – it will be necessary to invest in large samples of individuals over a longer time period to detect cycles confidently. To effectively monitor the response of tropical forests to global change, it will be necessary to focus efforts on suitable indicator species – those with good signal to noise ratios - to maximise analytical power over relatively short time periods.

For many phenology research questions, collecting sufficient data will be a challenge and require significant research effort. Ways to achieve this include: formation of research networks and greater coordination of methods and objectives between sites, internet-based citizen-science data collection networks and technical solutions to data collection, such as automated canopy photography and GIS.

2.6.4 CONCLUSIONS

Phenology is a key adaptive trait shown to determine species distributions (Chuine 2010) and as such will shape how ecosystems respond to rapidly increasing regional and global changes including human pressure. With the emergence of long-term tropical phenology data, the need also emerges for appropriate analytical methods to improve our understanding of the

functioning of ecosystems. We present a Fourier-based method that can be further developed and tested, to give simple, flexible and quantifiable indicators for phenology activity, and demonstrate the importance of consistent long-term investment in phenological research.

2.7 ACKNOWLEDGEMENTS:

Phenology research at SEGC, Lopé National Park was funded by the International Centre for Medical Research in Franceville (CIRMF; 1986-2010) and by Gabon's National Parks Agency (ANPN; 2010 – present). We acknowledge significant periods of independent data collection undertaken by Richard Parnell, Liz Williamson, Rebecca Ham, Patricia Peignot and Ludovic Momont. Permission to conduct this research in Gabon was granted by the CIRMF Scientific Council and the Ministry of Water and Forests (1986 – 2010), and by ANPN and the National Centre for Research in Science and Technology (CENAREST; 2010 – present.) We thank Daisy Dent, Tim Paine, Ed Mitchard whose comments in preparation of this chapter significantly improved it.

S2 SUPPORTING INFORMATION

Table S2.1 Summary of the key literature analysing long-term tropical phenology (as of 2016).

	Reference	Site	Pheno-phase[1]	Data length (yrs)	Analytical methods	Scale		Attribute confidence to results?	Indicators[4]
						Data[2]	Analysis[3]		
Describing phenology	Newstrom et al (1994)	La Selva, Costa Rica	FL	11	Graphical representation Categorisation	Inds	Comm (Inds)	No	Frequency (categorical) / Regularity / Duration / Amplitude / Timing
	Wright & Calderon (1995)	BCI, Panama	FL	5	Circular statistics	Spp	Comm (Spp)	Yes	Duration / Timing / Temporal concentration
	Sakai (1999)	Lambir, Malaysia	FL / FR	4.4	Categorisation Morisita's Index of aggregation	Spp	Comm (Guild (Inds)	Yes	Frequency (categorical) / Temporal distribution
	Sakai (2001)	La Selva, Costa Rica / Lambir, Malaysia	FL	11 / 4	Graphical representation	Spp	Comm (Inds) / (Spp)	No	Frequency (categorical)
Correlating phenology with weather	Chapman et al (1999)	Kibale, Uganda	FL / FR	6.34	Fourier analysis Coefficient of Dispersion (CD)	Inds	Comm (Spp)	No	Frequency CD
	Wright et al (1999)	BCI and Gigante, Panama	FR	8.5	Circular statistics Circular correlation analyses	Spp	Comm (Spp)	Yes	Productivity /Timing / Temporal concentration
	Anderson et al (2005)	Taï National Park, Côte d'Ivoire	L / FL / FR	3.9	Sinusoid-based regression Graphical representation	Inds	Comm Comm (Spp)	Yes	Frequency / Duration / Timing
	Sakai et al (2006)	Lambir, Malaysia	FL / FR	10	Spearman's rank correlation coefficient	Inds	Comm (Inds)	Yes	Productivity
	Cannon et al. (2007)	Gunung Palung, Indonesia	FR	5.7	Bootstrapping Finite mixture theory	Inds	Comm (Genera (Inds))	Yes	Productivity
	Norden et al (2007)	Nouragues, French Guiana	FR	5	Modeled autocorrelation functions	Spp	Comm (Spp)	Yes	Frequency (categorical)
	Ting et al (2008)	Global (48 studies)	FR	1+	Circular statistics, GLMs, Circular correlations	Spp	Comm (Comms)	Yes	Duration / Timing
	Zimmerman et al (2007)	EL Verde, Puerto Rico / BCI, Panama	FL / FR	10 / 15	Circular statistics Cross-correlation analysis	Spp	Comm (Spp)	Yes	Timing / Temporal concentration / Productivity
	Newbery et al (2013)	Korup, Cameroon	L / FL / FR	16	Logistic regression with GLMs	Inds	Spp (Inds)	Yes	Productivity
	Pau et al (2013)	BCI, Panama / Luquillo, Puerto Rico	FL	22 / 15	Regression analysis	Spp	Comm	Yes	Productivity
Detecting change	Chapman et al (2005)	Kibale, Uganda	FR	12	Graphical representation Regression analysis	Inds	Comm (Spp)	Yes	Productivity Coefficient of Variation
	Wright and Calderon (2006)	BCI, Panama	FL / FR	18	Cross-correlations Repeated one-way ANOVA	Spp	Comm (Guild)	Yes	Productivity
	Polansky and Boesch (2013)	Taï National Park, Côte d'Ivoire	FR	12	Semi-parametric generalized additive model (GAM) framework	Inds	Comm (Spp (Inds))	Yes	Probability of phenophase
	Polansky and Robbins (2013)	Bwindi, Uganda	FR	7.9	Semi-parametric GAM framework	Inds	Comm (Spp (Inds))	Yes	Probability of phenophase

[1]Phenophase: L = leafing, FL = flowering, FR = fruiting; [2]Scale at which data was collected: Inds = individuals, Spp = species; [3]Scale at which data was analysed including hierarchical structure: Comm = community, Spp = species, Inds = individuals; [4]Indicators derived from analysis with potential to be used more widely, for example to compare between sites or over time. Productivity refers to number of phenology events over a certain time period.

Literature cited in Table S2.1:

Anderson, D.P., Nordhelm, E.V., Moermond, T., Bi, Z.B.G. & Boesch, C. (2005) Factors Influencing Tree Phenology in Taï National Park , Côte d'Ivoire. Biotropica, 37(4), pp.631–640.

Cannon, C.H., Curran, L.M., Marshall, A.J. & Leighton, M. (2007) Long-term reproductive behaviour of woody plants across seven Bornean forest types in the Gunung Palung National Park (Indonesia): Suprannual synchrony, temporal productivity and fruiting diversity. Ecology Letters, 10(10), pp.956–969.

Chapman, C., Wrangham, R. W., Chapman, L. J., Kennard, D. K & Zanne, A.E. (1999) Fruit and flower phenology at two sites in Kibale National Park, Uganda. Journal of Tropical Ecology, 15, pp.189–211.

Chapman, C., Chapman, L.J., Struhsaker, T.T., Zanne, A.E., Clark, C.J. & Poulsen, J.R. (2005) A long-term evaluation of fruiting phenology: importance of climate change. Journal of Tropical Ecology, 21(1), pp. 31-45.

Newbery, D.M., Chuyong, G.B. & Zimmermann, L. (2013) Mast fruiting of large ectomycorrhizal African rain forest trees: importance of dry season intensity, and the resource-limitation hypothesis. New phytologist, 170(3), pp.561–579.

Newstrom, L., Frankie, G. & Baker, H. (1994) A new classification for plant phenology based on flowering patterns in lowland tropical rain forest trees at La Selva, Costa Rica. Biotropica, 26(2), pp.141–159.

Norden, N., Chave, J., Belbenoit, P., Caubère, A., Châtelet, P., Forget, Pierre M., & Thébaud, C. (2007) Mast fruiting is a frequent strategy in woody species of eastern South America. PLoS ONE, 2(10).

Pau, S., Wolkovich, E.M., Cook, B.I., Nytch, C.J., Regetz, J., Zimmerman, J. & Wright, S Joseph (2013). Clouds and temperature drive dynamic changes in tropical flower production. Nature Climate Change, 3. p.838

Polanksy, L. & Boesch, C. (2013) Long-term changes in fruit phenology in a west African lowland tropical rain forest are not explained by rainfall. Biotropica, 45(4), pp.434-440.

Polanksy, L. and Robbins, M.M. (2013) Generalized additive mixed models for disentangling long-term trends, local anomalies, and seasonality in fruit tree phenology. Ecology and Evolution, 3(9), pp.3141-3151.

Sakai, S. (2001) Phenological diversity in tropical forests. Population Ecology, 43(1), pp.77–86.

Sakai. S., Harrison, R.D., Momose, K., Kuraji, K., Nagamasu, H., Yasunari, T., Chong, L. & Nakashizuka, T. (2006) Irregular droughts trigger mass flowering in aseasonal tropical forests in Asia. American Journal of Botany, 93(80), pp. 1134-1139.

Ting, S., Hartley, S. & Burns, K.C. (2008) Global patterns in fruiting seasons. Global Ecology and Biogeography, 17(5), pp.648–657.

Wright, S. (1996) Phenological responses to seasonality in tropical forest plants. In Tropical forest plant ecophysiology. Springer US, pp.440-460..

Wright S.J., Carrasco, C., Calderón, O. and Paton, S. (1999) The El Niño Southern Oscillation, variable fruit production, and famine in a tropical forest. Ecology, 80(5), pp1632-1647.

Wright, J.S. & Calderon, O. (2006) Seasonal, El Niño and longer term changes in flower and seed production in a moist tropical forest. Ecology letters, 9, pp.35–44.

Zimmerman, J.K., Wright, S.J., Calderón, O., Aponte Pagan, M. and Paton, S. (2007) Flowering and fruiting phenologies of seasonal and aseasonal neotropical forests: the role of annual changes in irradiance. Journal of Tropical Ecology 23(02), pp231 – 25

Table S2.2. List of Families (n=26), species (n=70) and individuals (n=856) included in Fourier analysis.

Selected according to the following criteria; greater than five years continuous data, no data gaps greater than three months, at least one flowering event and no records of disease or death.

Family	Species	N
ANAC	Mangifera indica	5
	Pseudospondias longifolia	2
	Pseudospondias microcarpa	12
	Trichoscypha acuminata	11
ANNO	Annickia chlorantha	10
	Greenwayodendron suaveolens	12
	Monanthotaxis congoensis	10
	Uvariastrum pierreanum	12
	Xylopia aethiopica	11
	Xylopia hypolampra	10
	Xylopia quintasii	12
	Xylopia sp593	3
BURS	Aucoumea klaineana	41
	Canarium schweinfurthii	10
	Dacryodes buettneri	11
	Dacryodes normandii	5
	Santiria trimera	9
CALO	Mammea africana	8
CHRY	Maranthes glabra	9
CLUS	Pentadesma butyracea	14
EBEN	Diospyros dendo	27
	Diospyros mannii	7
	Diospyros polystemon	18
	Diospyros zenkeri	8
EUPH	Antidesma rufescens	1
	Antidesma vogelianum	21
	Uapaca guineensis	29
FABA	Bobgunnia fistuloides	11
	Detarium macrocarpum	16
	Dialium lopense	35
	Guibourtia tessmannii	4
	Parkia bicolor	10
	Pentaclethra macrophylla	26
	Pterocarpus soyauxii	10
	Tetrapleura tetraptera	20
HUMI	Sacoglottis gabonensis	19
IRVI	Irvingia gabonensis	23
	Irvingia grandifolia	22
	Klainedoxa gabonensis	10
LAUR	Beilschmeidia fulva	8

Family	Species	N
MORA	Ficus 97	3
	Ficus mucuso	2
	Ficus recurvata	4
	Milicia excelsa	11
	Myrianthus arboreus	12
	Treculia africana	2
MYRI	Pycnanthus angolensis	15
	Scyphocephalium ochocoa	9
	Staudtia kamerunensis	11
MYRT	Psidium guineense	19
OLAC	Heisteria parvifolia	11
	Ongokea gore	10
PAND	Panda oleosa	12
RUBI	Massularia acuminata	10
	Nauclea diderrichii	18
	Nauclea vanderguchtii	6
	Porterandia cladantha	12
	Psychotria vogeliana	29
SAPI	Ganophyllum giganteum	10
	Lecaniodiscus cupaniodes	5
SAPO	Baillonella toxisperma	8
	Chrysophyllus africanum	10
	Chrysophyllus subnudum	3
	Omphalocarpum procerum	7
SCYT	Scytopetalum spp	2
STER	Cola lizae	12
TILI	Duboscia macrocarpa	11
ULMA	Celtis tessmannii	10
VERB	Vitex doniana	29
VITA	Cissus dinklagei	11

Table S2.3. List of species with key outputs from Fourier analysis summarised at the species level.

Ordered according to mean power.

A. Species with >5 individuals with significant dominant cycles (included in further analysis)

Species	Individuals	Significant cycles	Modal cycle length (months)	Mean power	Synchrony - sd phase (months)
Maranthes glabra	9	9	12	9.3	0.32
Xylopia aethiopica	11	10	12	8.1	1.24
Pycnanthus angolensis	15	15	12	7.5	0.17
Pentadesma butyracea	14	12	12	6.7	0.46
Ongokea gore	10	9	12	6.6	0.23
Duboscia macrocarpa	11	11	18	5.9	4.81
Cissus dinklagei	11	10	12	5.8	0.25
Antidesma vogelianum	21	19	6	5.6	0.2
Porterandia cladantha	12	12	12	5.6	0.13
Cola lizae	12	12	12	5.4	0.25
Dacryodes buettneri	11	10	12	4.9	0.13
Parkia bicolor	10	10	12	4.9	1.24
Sacoglottis gabonensis	19	15	12	4.8	0.25
Tetrapleura tetraptera	20	12	12	4.7	0.9
Vitex doniana	29	26	12	4.4	0.48
Greenwayodendron suaveolens	12	5	12	4	0.36
Heisteria parvifolia	11	11	12	3.9	0.27
Psidium guineense	19	10	6	3.8	0.11
Monanthotaxis congoensis	10	10	12	3.8	0.19
Scyphocephalium ochocoa	9	5	12	3.7	0.15
Psychotria vogeliana	29	18	6	3.6	0.11
Canarium schweinfurthii	10	7	12	3.6	0.65
Dialium lopense	35	14	12	3.5	0.19
Staudtia kamerunensis var. gab	11	9	12	3.5	0.31
Diospyros mannii	7	5	12	3.5	0.5
Uapaca guineensis	29	19	12	3.4	0.31
Santiria trimera	9	6	12	3.1	1.68
Diospyros polystemon	18	16	12	3	0.15
Irvingia gabonensis	23	13	12	3	0.25
Aucoumea klaineana	41	18	12	2.9	0.23
Xylopia quintasii	12	6	12	2.9	0.21
Diospyros dendo	27	16	12	2.8	0.23
Celtis tessmannii	10	9	12	2.8	0.1
Pentaclethra macrophylla	26	7	12	2.8	0.52
Diospyros zenkeri	8	6	12	2.8	0.08
Ganophyllum giganteum	10	10	12	2.6	0.11
Irvingia grandifolia	22	9	12	2.6	0.17
Trichoscypha acuminata	11	8	12	2.6	0.19
Uvariastrum pierreanum	12	6	12	2.5	0.23
Detarium macrocarpum	16	11	12	2.4	0.23
Pseudospondias microcarpa	12	6	6	2.4	0.17
Klainedoxa gabonensis	10	6	12	2.1	0.25

Total (only species in A)	664	458

B. Species with <5 individuals with significant cycles (excluded from further analysis)

Species	Individuals	Significant cycles	Modal cycle length (months)	Mean power	Synchrony - sd phase (months)
Mangifera indica	5	3	12	5.5	0.13
Guibourtia tessmannii	4	3	12	4.1	0
Omphalocarpum procerum	7	2	6	3.5	0
Antidesma rufescens	1	1	6	3.5	0
Bobgunnia fistuloides	11	3	11	3.2	0
Treculia africana	2	1	12	3.2	0
Chrysophyllus subnudum	3	3	12	3.1	0.21
Myrianthus arboreus	12	4	12	3	0.86
Mammea africana	8	3	12	2.9	0.06
Nauclea diderrichii	18	3	12	2.8	0.1
Xylopia sp593	3	3	12	2.8	0.38
Massularia acuminata	10	1	32	2.7	0
Annickia chlorantha	10	3	12	2.6	0.21
Beilschmeidia fulva	8	1	12	2.6	0
Xylopia hypolampra	10	4	12	2.5	0.04
Panda oleosa	12	3	2	2.5	0
Chrysophyllus africanum	10	1	12	2.4	0
Nauclea vanderguchtii	6	1	12	2.4	0
Milicia excelsa	11	3	6	2.2	0
Pseudospondias longifolia	2	2	4	2.2	0
Pterocarpus soyauxii	10	1	12	2	0
Ficus mucuso	2	1	2	2	0
Lecaniodiscus cupaniodes	5	1	12	1.8	0
Scytopetalum spp	2	0	NA	NA	NA
Baillonella toxisperma	8	0	NA	NA	NA
Ficus recurvata	4	0	NA	NA	NA
Ficus 97	3	0	NA	NA	NA
Dacryodes normandii	5	0	NA	NA	NA

Total (all species in A + B)	856	509
Mean (all species in A + B)	12.0	7.0
SD (all species in A + B)	8.1	5.8

Table S2.4. Outputs from a model for the likelihood of detecting significant regular cycles using all available field data.

Estimates are from a Generalised Linear Mixed-effects Model (family=Binomial). The predictors are the length of the time series (Years) and Species are included as random intercepts; SE = standard error.

	Estimate	SE	Z value	P value
Fixed effects:				
Years	0.10	0.02	6.42	<0.001
Random effects:				
Pycnanthus angolensis	2.11			
Porterandia cladantha	1.62			
Cissus dinklagei	1.39			
Cola lizae	1.39			
Duboscia macrocarpa	1.36			
Ganophyllum giganteum	1.12			
Heisteria parvifolia	1.11			
Monanthotaxis congoensis	1.10			
Chrysophyllus subnudum	1.05			
Parkia bicolor	1.05			
Maranthes glabra	0.98			
Xylopia aethiopica	0.73			
Antidesma rufescens	0.66			
Xylopia sp593	0.51			
Pseudospondias longifolia	0.48			
Antidesma vogelianum	0.46			
Vitex doniana	0.44			
Diospyros polystemon	0.08			
Sacoglottis gabonensis	-0.13			
Pentadesma butyracea	-0.29			
Dacryodes buettneri	-0.40			
Ongokea gore	-0.46			
Diospyros zenkeri	-0.54			
Celtis tessmannii	-0.66			
Tetrapleura tetraptera	-0.92			

Staudtia kamerunensis var. gabonensis	-0.95
Guibourtia tessmannii	-0.95
Mangifera indica	-1.04
Psychotria vogeliana	-1.05
Diospyros mannii	-1.08
Santiria trimera	-1.09
Omphalocarpum procerum	-1.11
Uapaca guineensis	-1.13
Canarium schweinfurthii	-1.26
Detarium macrocarpum	-1.30
Trichoscypha acuminata	-1.39
Diospyros dendo	-1.49
Scyphocephalium ochocoa	-1.61
Psidium guineense	-1.63
Irvingia gabonensis	-1.68
Xylopia hypolampra	-1.75
Dialium lopense	-2.02
Ficus mucuso	-2.05
Mammea africana	-2.05
Aucoumea klaineana	-2.08
Bobgunnia fistuloides	-2.10
Treculia africana	-2.10
Xylopia quintasii	-2.13
Irvingia grandifolia	-2.21
Uvariastrum pierreanum	-2.25
Pseudospondias microcarpa	-2.32
Panda oleosa	-2.32
Klainedoxa gabonensis	-2.41
Greenwayodendron suaveolens	-2.49
Pentaclethra macrophylla	-2.59
Myrianthus arboreus	-2.61
Beilschmeidia fulva	-2.66
Massularia acuminata	-2.71
Annickia chlorantha	-3.19

Chrysophyllus africanum	-3.23
Lecaniodiscus cupaniodes	-3.24
Scytopetalum spp	-3.25
Milicia excelsa	-3.52
Ficus 97	-3.55
Nauclea diderrichii	-3.57
Dacryodes normandii	-3.57
Baillonella toxisperma	-3.58
Nauclea vanderguchtii	-3.87
Ficus recurvata	-3.97
Pterocarpus soyauxii	-4.53

Table S2.5. Outputs from a model for the likelihood of detecting significant annual cycles after power analysis of annually cycling field data.

Estimates are from a Generalised Linear Model (family=Binomial). The predictors are the length of the time series (Months) and Species derived from a power analysis to show the impact of time series length (2-20 years window length) for detecting periodicity (10,000 samples from 233 individuals of 30 species); SE = standard error.

	Estimate	SE	Z value	P value
Months	0.03	0.00	12.54	<0.001
Cola lizae	-1.87	0.27	-7.05	<0.001
Greenwayodendron suaveolens	-1.96	0.39	-5.00	<0.001
Parkia bicolor	-2.25	0.28	-8.08	<0.001
Cissus dinklagei	-2.27	0.31	-7.37	<0.001
Detarium macrocarpum	-2.61	0.37	-7.03	<0.001
Monanthotaxis congoensis	-2.72	0.31	-8.82	<0.001
Canarium schweinfurthii	-2.77	0.39	-7.04	<0.001
Heisteria parvifolia	-2.80	0.27	-10.28	<0.001
Uapaca guineensis	-2.87	0.38	-7.52	<0.001
Celtis tessmannii	-2.92	0.32	-9.06	<0.001
Dacryodes buettneri	-2.93	0.31	-9.38	<0.001
Ongokea gore	-2.97	0.41	-7.28	<0.001
Ganophyllum giganteum	-2.98	0.38	-7.86	<0.001
Irvingia grandifolia	-3.13	0.37	-8.57	<0.001
Xylopia quintasii	-3.41	0.45	-7.55	<0.001
Irvingia gabonensis	-3.47	0.50	-6.91	<0.001
Diospyros zenkeri	-3.48	0.48	-7.23	<0.001
Klainedoxa gabonensis	-3.67	0.53	-6.94	<0.001
Diospyros dendo	-3.84	0.52	-7.34	<0.001
Staudtia kamerunensis var. gabonensis	-3.99	0.41	-9.78	<0.001
Vitex doniana	-4.18	0.52	-8.03	<0.001
Pentadesma butyracea	-4.27	0.59	-7.19	<0.001
Porterandia cladantha	-4.43	0.61	-7.24	<0.001
Diospyros polystemon	-4.49	0.49	-9.27	<0.001
Aucoumea klaineana	-4.68	0.36	-12.82	<0.001
Santiria trimera	-4.90	0.62	-7.85	<0.001
Uvariastrum pierreanum	-4.95	0.73	-6.82	<0.001
Maranthes glabra	-5.01	0.88	-5.72	<0.001

Trichoscypha acuminata	-5.72	0.62	-9.20	<0.001
Pycnanthus angolensis	-6.44	1.19	-5.43	<0.001
Months *Maranthes glabra	0.07	0.02	4.41	<0.001
Months *Pycnanthus angolensis	0.07	0.02	4.08	<0.001
Months *Porterandia cladantha	0.03	0.01	4.19	<0.001
Months *Pentadesma butyracea	0.03	0.01	4.17	<0.001
Months *Vitex doniana	0.02	0.01	3.56	<0.001
Months *Ongokea gore	0.01	0.01	2.73	<0.01
Months *Trichoscypha acuminata	0.01	0.00	1.30	0.19
Months *Santiria trimera	0.01	0.00	1.10	0.27
Months *Staudtia kamerunensis var. gabonensis	0.00	0.00	1.14	0.26
Months *Uapaca guineensis	0.00	0.00	0.44	0.66
Months *Canarium schweinfurthii	0.00	0.00	0.28	0.78
Months *Dacryodes buettneri	0.00	0.00	0.18	0.85
Months *Irvingia gabonensis	0.00	0.00	-0.98	0.33
Months *Uvariastrum pierreanum	0.00	0.00	-1.00	0.32
Months *Heisteria parvifolia	-0.01	0.00	-1.68	0.09
Months *Diospyros polystemon	-0.01	0.00	-1.45	0.15
Months *Irvingia grandifolia	-0.01	0.00	-1.95	0.05
Months *Diospyros zenkeri	-0.01	0.00	-1.94	0.05
Months *Parkia bicolor	-0.01	0.00	-2.32	<0.05
Months *Cissus dinklagei	-0.01	0.00	-2.42	<0.05
Months *Cola lizae	-0.01	0.00	-2.72	<0.01
Months *Xylopia quintasii	-0.01	0.00	-2.57	<0.05
Months *Celtis tessmannii	-0.01	0.00	-3.04	<0.01
Months *Ganophyllum giganteum	-0.01	0.00	-3.07	<0.01
Months *Monanthotaxis congoensis	-0.01	0.00	-3.51	<0.001
Months *Diospyros dendo	-0.01	0.00	-3.18	<0.01
Months *Klainedoxa gabonensis	-0.01	0.00	-3.15	<0.01
Months *Detarium macrocarpum	-0.01	0.00	-4.50	<0.001
Months*Greenwayodendron suaveolens	-0.02	0.00	-4.58	<0.001

CHAPTER 3

Towards effective monitoring of tropical phenology: maximizing returns and reducing uncertainty in long-term studies

A version of this chapter has been published as:

Bush, E.R., Bunnefeld, N., Dimoto, E., Dikangadissi, J.T., Jeffery, K., Tutin, C., White, L. and Abernethy, K.A., 2018. Towards effective monitoring of tropical phenology: maximizing returns and reducing uncertainty in long-term studies. Biotropica, 50(3), pp.455-464.

EB, NB and KA formulated the research idea. KA, KJ, CT, LW, ED, JTD and EB collected and archived the data and EB performed analyses with advice from KA and NB. All authors commented on draft versions of this manuscript, and the published version formatted for the thesis is presented here.

3.1 ABSTRACT

Phenology is a key component of ecosystem function and is increasingly included in assessments of ecological change. We consider how existing, and emerging, tropical phenology monitoring programs can be made most effective by investigating major sources of noise in data collection at a long-term study site. Researchers at Lopé NP, Gabon, have recorded monthly crown observations of leaf, flower and fruit phenology for 88 plant species since 1984. For a subset of these data, we first identified dominant regular phenological cycles, using Fourier analysis, and then tested the impact of observation uncertainty on cycle detectability, using expert knowledge and generalized linear mixed modelling (827 individual plants of 61 species). We show that experienced field observers can provide important information on major sources of noise in data collection and that observation length, phenophase visibility and duration are all positive predictors of cycle detectability. We find that when a phenological event lasts > four weeks, an additional 10 years of data increases cycle detectability by 114 percent and that cycle detectability is 92 percent higher for the most visible events compared to the least. We also find that cycle detectability is four times as high for flowers compared to ripe fruits after 10 years. To maximise returns in the short-term, resources for long-term monitoring of phenology should be targeted towards highly visible phenophases and events that last longer than the observation interval. In addition, programs that monitor flowering phenology are likely to accurately detect regular cycles more quickly than those monitoring fruits, thus providing a baseline for future assessments of change.

3.2 INTRODUCTION

While the impacts of climate change on phenology are widely acknowledged (Cleland *et al.* 2007; Chambers *et al.* 2013), most of the evidence is geographically and taxonomically biased towards temperate regions and vertebrates (Feeley *et al.* 2017). There is little data available to assess change in tropical plant phenology and, to date, few relevant published studies (but

see Pau *et al.* 2013 and Chapman *et al.* 2018 for recent examples). The lack of evidence for phenological change in the tropics should not be taken as evidence of no change, but instead reflects the paucity of long-term data records and the complexity of monitoring highly diverse tropical ecosystems. The question remains as to how to fill this evidence-gap and assess both stability and change in phenological function.

Phenology datasets that have already supported effective statistical tests of change have been either very long - for example Japanese cherry blossom records began in the 9th century (Aono & Kazui 2008; Primack *et al.* 2009) - or very widespread - for example The International Phenology Gardens network, initiated in 1957, includes 89 European sites across 28 latitudes (Humboldt-University of Berlin 2012). The most widespread contemporary phenology monitoring programs are those that involve citizen scientists, make use of accessible technology - such as smartphones apps - and observations made in everyday life (e.g. the USA National Phenology Network's "Nature's Notebook", USA-NPN 2017). From these successful temperate examples we learn that to achieve phenology datasets with strong *statistical power* (long-term, widespread etc.), data collection methods need to have real *sticking power* (cultural importance, familiarity, appeal to a large spread of people and ease of recording).

It is apparent that such "sticking power" remains a challenge in the tropics. Even among science-led monitoring programs, there is little coordination of recording effort across multiple sites (Adole *et al.* 2016; Morellato *et al.* 2016), fieldwork is often remote and logistically challenging and financial resources for long-term monitoring are extremely limited meaning that few sites can be considered long-term (e.g. >10 years continuous moniroting; Mendoza *et al.* 2017; Adamescu *et al.* 2018). In addition, many of the tropical phenology studies that are now invaluable to assess global change were originally conceived for the study of resource availability and are not necessarily optimised to study climate-change impacts on plants (e.g. phenology monitoring at Lopé NP was originally set up in 1984 to study Gorilla and Chimpanzee foraging: Tutin *et al.* 1991).

While a complete redesign of tropical phenology monitoring programs within tightly coordinated networks would be ideal, we do not consider it to be feasible immediately, nor can it can reach into the past. Instead we ask: How can we ensure that existing science-led phenology monitoring programs are allocating limited resources most effectively for their research aims?

There are two ways to improve statistical power in analyses of data from phenology monitoring programs: (1) increase sample size; and (2) reduce noise. Sample size can be restrictive both spatially (e.g. the number of sites recording phenology data or the area / number of individuals monitored) and temporally (e.g. the length of the study). The spatial sample determines the scope of potential research questions while the length of study positively affects the detectability of regular phenological cycles (Bush et al. 2017) and phenological shifts (Chambers *et al.* 2013). Noise can be introduced to phenology data through both "process uncertainty" (how well we can predict ecological processes e.g. the regularity of phenological cycles) and "observation uncertainty" (how easily we can observe and record ecological events). Different life-cycle events and stages such as development of leaves, flower and fruits, even from the same species, may differ in regularity and/or ease of observation, leading to systematic biases in phenology recording related to the frequency and type of observations (see Regan *et al.* 2008 for a full description and "taxonomy" of the different uncertainties associated with ecological data).

To explore this further, we present hypothetical scenarios of crown phenology observations subject to different combinations of process and observation uncertainty and demonstrate how interpretation of the data without careful consideration of the source of noise could lead to erroneous conclusions. For species where a phenological event is easy to see (e.g. large, brightly coloured flowers that contrast with the leaf canopy or cauliflorous flowers on the trunk of the tree), most observations will be accurate and it will be straightforward to tell from the recorded data if the actual cycle is regular or irregular (Figure 3.1A-C, Observation uncertainty = Low, Process uncertainty = Low: High). On the other hand, if for another species the same

phenological event is difficult to see (e.g. flowers that are very small, held high in the canopy or persist for just a few days), data are likely to be recorded imperfectly and the cycle may appear irregular (Figure 3.1G-H, Observation uncertainty = High, Process uncertainty = Low: High). Without quantifying the observation biases for these species, it will be impossible to differentiate if their actual cycles are regular or irregular as an inaccurately recorded regular cycle will look similar to an accurately recorded irregular cycle (Figure 3.1G compared to Figure 3.1C). This distinction is important as adaptive features of the phenological cycle itself and changes in predictability or synchrony will be of great interest to the global change community, whereas apparent irregularity derived from inaccurate observation will not. In this paper, we seek to quantify observation biases between species and phenophases at our study site, Lopé NP, Gabon, in order to direct precious resources where they are likely to give robust data and to include important sources of variation in future explanatory models of plant phenology and ecological change.

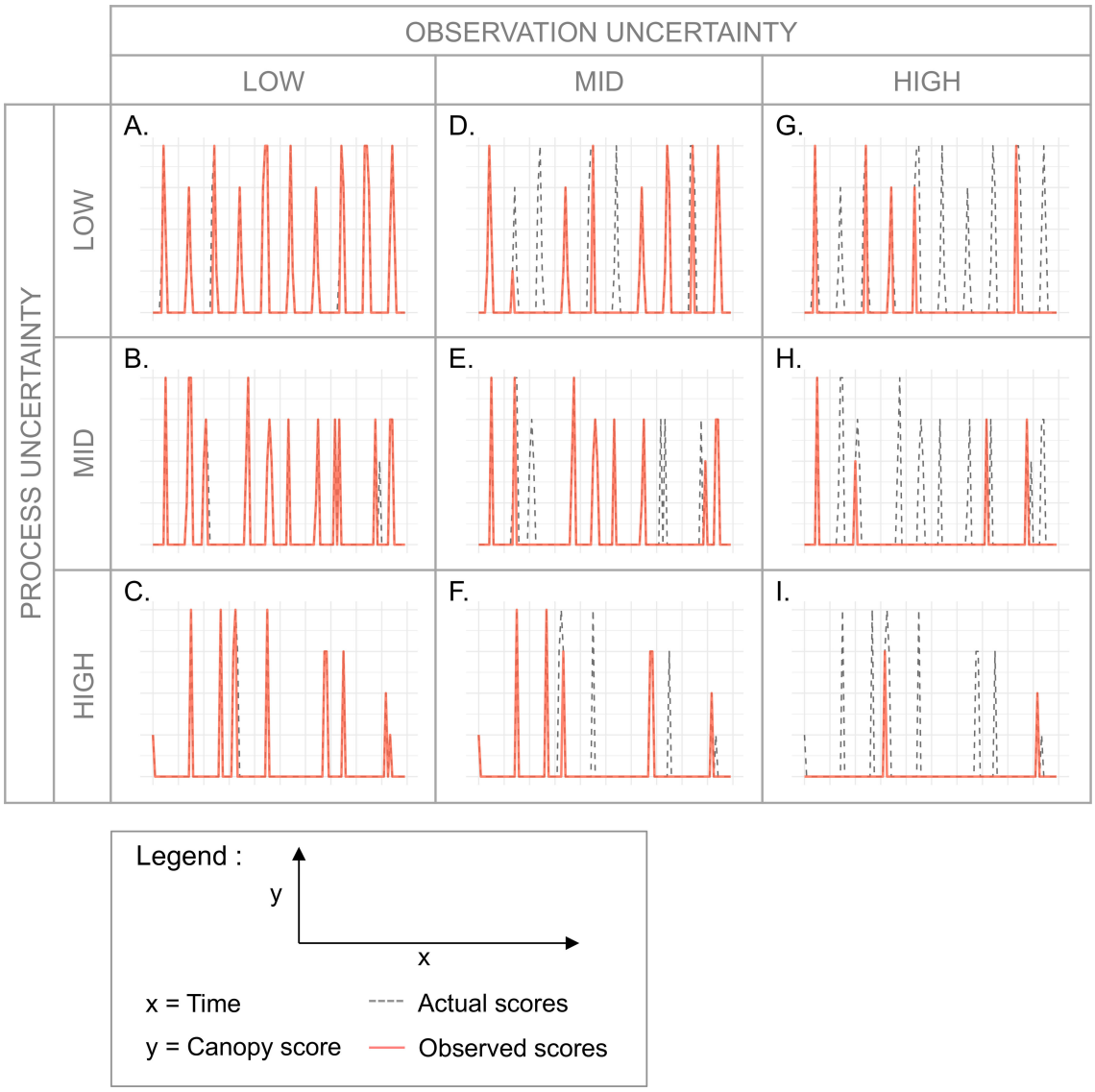

Figure 3.1. Simulated data scenarios to show the impacts of both observation and process uncertainty on recorded time series compared to real time series.

Red solid lines indicate observed scores where as grey dashed lines indicate actual scores. Observation uncertainty is "low" when a phenological event is easy to see and the recorded time series closely matches the real time series and "high" when a phenological event is difficult to see leading to many missing observations and a recorded time series that does not closely match the real time series. Process uncertainty is "low" when phenological events occur in clean, regular cycles and are easy to predict and is "high" when phenological events occur in noisy, irregular cycles and are difficult to predict. From the recorded time series alone, it is impossible to differentiate between a record with high process uncertainty but low observation uncertainty (bottom left) and a record with low process uncertainty but high observation uncertainty (top right).

Quantifying observation uncertainty for different phenological events is not easy as there are multiple sources of variation - specific to the phenology sampling method in question - that lead to systematic observation biases. At Lopé, phenology monitoring takes the form of crown observations, and variation in the "visibility" of phenological events and their "duration" are likely to be key factors contributing to uncertainty. Visibility, however, is inherently subjective from the point of view of the observers. For example, the size of a flower or fruit is likely to influence how visible it is, but so will its colour, or the distance it is held from the observer (e.g. a large green flower high up in the canopy may be less "visible" than a small, red flower lower in the canopy or a cauliflorous flower growing from the tree trunk). In order to capture this information many multiple axes of variation would need to be measured and then calibrated with the observer experience. Such empirical data is not readily available and so instead, we sought to describe the visibility and duration of phenology events using expert knowledge elicited from long-term phenology observers at our site. These experts hold substantive knowledge of the ecosystem based on their personal experience over many years of fieldwork at the site (Martin *et al.* 2012).

Considering data for all species and phenological events (leaf, flower and fruit cycles, hereafter "phenophases") recorded as part of the Lopé long-term phenology study, alongside expert knowledge for observation uncertainty, we ask the following questions: (1) Can observation uncertainty be quantified? (2) Does observation uncertainty impact detectability of regular cycles among different species and phenophases? (3) What are the relative contributions of different sources of observation uncertainty to cycle detectability? We believe that the analysis presented here, using rare, long-term data, will help to improve resource allocation and sample design at other existing and emerging tropical phenology programs and aid robust assessments of phenological change in the future.

3.3 METHODS

3.3.1 THE LOPÉ LONG-TERM PHENOLOGY STUDY

Since 1984, researchers at the Station d'Études des Gorilles and Chimpanzées (SEGC) in Lopé National Park, Gabon have recorded leaf, flower and fruit phenology monthly for 88 species of tropical trees and shrubs (>1000 individuals) spread over an area of 33km^2. The SEGC study area is situated in a tropical forest-savanna matrix with an equatorial climate characterised by two dry and two wet seasons annually (see Tutin & White 1998 for detailed site description). At the beginning of every month (usually completed within the first seven working days), SEGC researchers examine the crowns of each plant from the ground with 10 x 42 binoculars and record the proportion of the canopy covered by each phenophase (new and senescent leaves, flowers, unripe and ripe fruits) as a scale from zero to four (including half points; Tutin & Fernandez 1993; Tutin & White 1998). The data recorded for each phenophase form multiple continuous time series for each individual tree. Data are only recorded autonomously by observers with more than one years experience with the plant species involved and working under another observer. Data have been recorded by a total of only ten observers throughout the 387 months (32 years) of continuous observations, with individual observers making continuous contributions of 2-20 years. Thus this dataset is likely to have minimal (but not zero) inter-observer biases.

3.3.2 DETECTING PHENOLOGY CYCLES USING FOURIER ANALYSIS

We excluded data collected before 1986 when the project was being established and made selections for further analysis according to the following criteria; more than five years continuous data for each individual plant, no data gaps greater than three months, and no persistent records of disease (e.g. field comments referring to the ill-health of a tree consistently for more than a year). The resulting sample consisted of 4280 continuous time series for new and senescent leaves, flowers, unripe and ripe fruits from 856 individual plants of 70 species. The number of individuals per species ranged from one to 41, with a mean of 12, while the length of time individual

plants were monitored ranged from 60 to 353 months, with a mean of 249 months.

To identify the dominant regular cycle for each time series in this sample we used Fourier analysis; Fourier is a form of spectral analysis based on sine and cosine waves that can be used to quantitatively describe the cyclic nature of any time series data (Bloomfield 2000). We used a confidence test, based on 95% confidence intervals and a null hypothesis of "no cyclicity", to determine if the dominant cycle was objectively different to surrounding noise. We refer to a "detected cycle" as one that can be quantified and considered significant according to this method. A full explanation of the Fourier methods used and our data selection criteria is given in Chapter 2 (Bush *et al.* 2017).

3.3.3 Eliciting expert-knowledge on two major sources of observation uncertainty.

We gathered expert knowledge to describe the observation uncertainty associated with each phenophase for every species in our study. Following the recommendations of Martin et al. (2012) the authors of this study were assigned different (sometimes multiple) roles in the process of expert elicitation; EB, NB and KA acted as the "problem owners" defining the questions and design of the expert survey, while KA, LW, ED and CT were the "experts", each of whom had recorded phenology data at SEGC for more than 15 years. EB and NB were the "analysts" and independently processed the expert responses and analysed the data.

EB and the station manager at SEGC facilitated the process of expert elicitation in February 2016. For ease of interpretation by all experts we chose to elicit knowledge on observation uncertainty in the form of categorical measures (Kuhnert *et al.* 2010). The experts were independently presented with a survey listing all species monitored at SEGC and five phenophases (new and senescent leaves, flowers, unripe and ripe fruits) and asked to record their perception of both the visibility and duration for each. Phenophase visibility was presented as a score from one to three, representing events that are "Difficult to see", "Easy to see" and "Very

obvious". Phenophase duration was presented as a binary category: "events lasting <= 4 weeks" or "events lasting >4 weeks" (the four week interval corresponding to the field observation frequency). The observers were informed that they were allowed to leave an answer blank if they were unsure.

A correlation matrix for phenophase visibility showed that scores were positively correlated between all observer pairs, ranging from 0.13 to 0.38 (mean = 0.27; Figure S3.1). To combine the expert judgements we took group averages (Martin *et al.* 2012) by calculating mean event visibility and modal duration category for each species-phenophase. We excluded 15% of species-phenophase visibility scores because fewer than three observers provided an answer, and 31% of species-phenophase duration scores because either fewer than three observers provided an answer or there was no clear majority (e.g. if two observers considered an event to last <= 4 weeks and two observers considered an event to last > 4 weeks). This may occur when the true event duration is around four weeks and thus the phenophase cannot be easily assigned to either category.

3.3.4 Modelling the impact of observation uncertainty on cycle detection among phenology data.

To compare how different sources of observation uncertainty contribute to variation in cycle detectability we combined the data derived from the 4280 times series used in Fourier analysis with the observer scores for phenophase visibility and duration. We only included species with more than three observed individuals and complete information on phenophase visibility and duration, resulting in a final sample of 3083 time series from 827 individuals (61 species). Before analysis, we standardized predictors by scaling them to mean = 0 and standard deviation = 2 to allow meaningful comparison of effect sizes (Schielzeth 2010; Table 3.1).

Table 3.1. Key summary statistics and definitions of all predictors included in the maximal model.

Variable	Definition	Level [a]	Summary statistics [b]	Predictor [c]
Time series length	Length of continuous observation of tree in months.	ID	Continuous (Mean = 251; SD = 93.9; Min = 60.0; Max = 353)	Length $_{Scaled}$
Phenophase visibility	Mean observer score for visibility, 1 (Difficult to see) to 3 (Very obvious).	Sp-Ph	Continuous (Mean = 2.27; SD = 0.43; Min = 1.0; Max = 3.0)	Visibility $_{Scaled}$
Phenophase duration	Modal observer score for duration, 0: <= 4 wks, 1: > 4 wks.	Sp-Ph	Categorical (0 = 59%)	Duration

[a] *Level of data-collection for variable (ID = Tree ID; Sp-Ph = Species-phenophase)*

[b] *Summary statistics for variables included in binomial GLMM pre-scaling*

[c] *Code for scaled predictor included in binomial GLMM*

To test the effects of phenophase visibility (**Visibility $_{Scaled}$**) and phenophase duration (**Duration**) on the likelihood of detecting a cycle we used a Generalized Linear Mixed Model (GLMM, family = binomial, link = logit). As we already know time series length is an important positive predictor of cycle detection (Chapter 2; Bush et al. 2017) we included it as a fixed effect in the model (**Length $_{Scaled}$**).

In our mixed model we included the grouping factors tree **ID**, **Species** and **Phenophase** as random intercepts and all continuous predictors as random slopes by **Phenophase**. First, this reflected the hierarchical nature of the data (multiple phenophases simultaneously recorded per individual tree; duration and visibility scored at the level of the species-phenophase) and second, it

allowed us to take account of the biological differences (process uncertainties) between species and phenophases.

We followed a model simplification process starting with the maximal model for both fixed effects (all possible pair-wise interactions between predictors) and random effects (random slope by **Phenophase** for all continuous predictors), removing each term in a step-wise fashion and then comparing resulting models using AIC values. We used the standardised effect sizes derived from the final, most parsimonious model to compare between predictors. We temporarily modified the final model by removing terms for the intercept and the main effect of continuous predictors involved in interactions to determine if predictor effect sizes were different to zero (95% confidence intervals derived from standard errors; Schielzeth 2010).

3.4 RESULTS

3.4.1 Overview of dominant phenology cycles

Using all available phenology time series from the Lopé long-term study after selection criteria, we confidently detected regular cycles from 36% of the sample (total number of time series = 4280, five different phenophases from 856 individuals). However, detection differed among phenophases, being highest for flowers (59%), unripe fruit (54%) and new leaves (51%) and lowest for ripe fruit (29%) and senescing leaves (25%). Annual cycles were most commonly detected among reproductive data (75% all detected cycles for flowers, unripe and ripe fruits were annual), while sub-annual cycles were most commonly detected from vegetative data (51% all detected cycles for new and senescing leaves were sub-annual).

3.4.2 Observation uncertainty scores

The inter-quartile ranges for the visibility scores of all phenophases overlapped (Figure 3.2A) but on average, new leaves were considered the most visible (mean score = 2.42) and flowers the least visible (mean score = 2.08). In contrast, event duration scores were not evenly distributed among phenophases (Figure 3.2B); Unripe fruit events were perceived as lasting > 4 weeks for almost all species (65 out of 66 species) while new leaf events were perceived as lasting <= 4 weeks for all species.

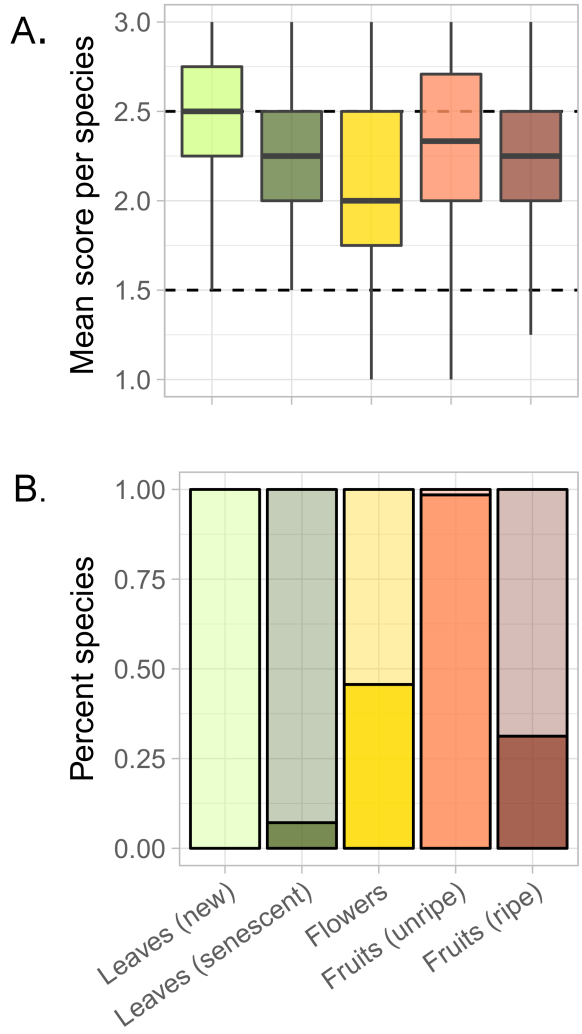

Figure 3.2. Summary of mean scores calculated for phenophase event visibility and duration by phenophase.
(A) Distribution of mean phenophase visibility scores for each species showing median scores (bold horizontal lines), the interquartile range (coloured boxes) and the 95% range (vertical lines) and the breaks between each score (horizontal dashed lines). (B) Percentage of species categorised according to phenophase duration: events lasting <= 4 weeks (light shading) and events lasting > 4 weeks (dark shading).

3.4.3 Effects of observation uncertainty on cycle detection.

After model simplification, all of the main predictors and an interaction between **Length** $_{\text{Scaled}}$ and **Duration** were retained in the most parsimonious model (Table 3.2). We found both **Length** $_{\text{Scaled}}$ and **Visibility** $_{\text{Scaled}}$ to have significant positive effects (95% confidence intervals different to zero; Figure 3.3A and Table S3.1) on the likelihood of detecting a cycle from our phenology data. The relative effect of **Visibility** $_{\text{Scaled}}$ (standardised effect size = 0.79) was almost half that of **Length** $_{\text{Scaled}}$ when **Duration** <= 4 weeks (standardised effect size = 1.51), and a third of **Length** $_{\text{Scaled}}$ when **Duration** > 4 weeks (standardised effect size = 2.31; Figure 3.3A). Model predictions from the final model showed that when a phenophase event lasted <= 4 weeks, the likelihood of detecting a regular cycle was 0.23 after 10 years of data collection and 0.39 after 20 years. If the phenophase event lasted > 4 weeks, the likelihood of detecting a regular cycle after 20 years of data collection increased to 0.47 (Figure 3.3B). We also found that for the least visible phenophase events (score = 1) the likelihood of detecting a regular cycle was 0.26 when the phenophase event lasted <= 4 weeks and 0.34 when the phenophase event lasted > 4 wks. For the most visible phenophase events (score = 3), this increased to 0.5 when the phenophase event lasted <= 4 weeks and 0.58 when the phenophase event lasted > 4 weeks (Figure 3.3C).

Table 3.2. Results of model simplification starting with the maximal model for both fixed and random effects.

Fixed effects included all possible pair-wise interactions between main effects and random effects included random slope by ***Phenophase*** *for all continuous main effects. The best most parsimonious model is considered that with the least degrees of freedom (DF) within two AIC values of the model with the lowest AIC value, indicated by an asterisk.*

Fixed effects structure:		**Random effects structure:**		**Model statistics:**	
Main effects	**Interaction effects**	**Random intercepts**	**Random slopes**	**DF**	**AIC**
Length $_{scaled}$ Visibility $_{scaled}$ Duration	Length $_{scaled}$: Duration	ID Phenophase Species	Length $_{scaled}$ by Phenophase	10	3319.14*
Length $_{scaled}$ Visibility $_{scaled}$ Duration	Length $_{scaled}$: Duration Visibility $_{scaled}$: Duration	ID Phenophase Species	Length $_{scaled}$ by Phenophase	11	3320.06
Length $_{scaled}$ Visibility $_{scaled}$ Duration	Length $_{scaled}$: Visibility $_{scaled}$ Length $_{scaled}$: Duration Visibility $_{scaled}$: Duration	ID Phenophase Species	Length $_{scaled}$ by Phenophase	12	3320.11
Length $_{scaled}$ Visibility $_{scaled}$ Duration	Length $_{scaled}$: Visibility $_{scaled}$ Length $_{scaled}$: Duration Visibility $_{scaled}$: Duration	ID Phenophase Species	Length $_{scaled}$ by Phenophase Visibility $_{scaled}$ by Phenophase	15	3321.67
Length $_{scaled}$ Visibility $_{scaled}$ Duration		ID Phenophase Species	Length $_{scaled}$ by Phenophase	10	3323.57
Length $_{scaled}$ Visibility $_{scaled}$ Duration	Length $_{scaled}$: Visibility $_{scaled}$ Length $_{scaled}$: Duration Visibility $_{scaled}$: Duration	ID Phenophase Species	Visibility $_{scaled}$ by Phenophase	12	3334.95

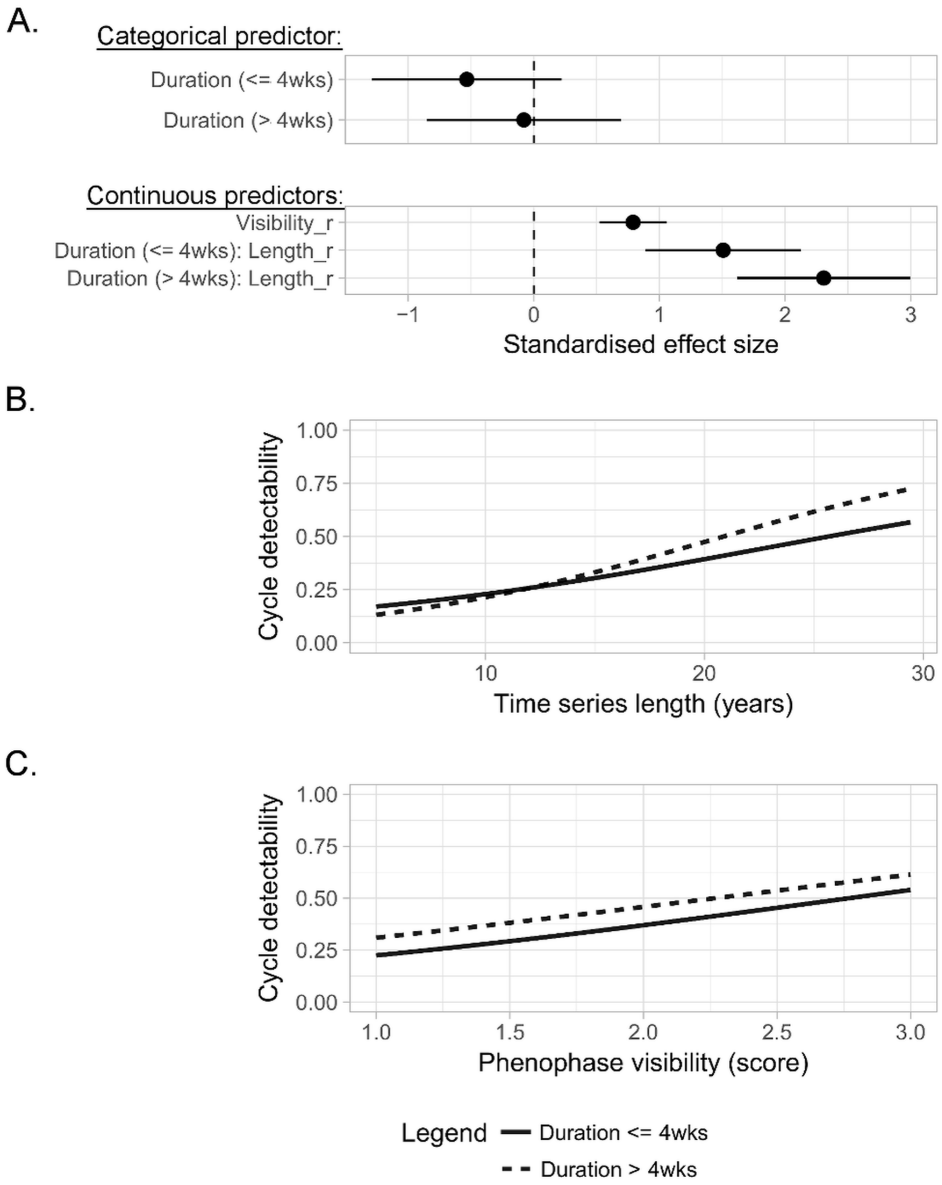

Figure 3.3. Standardised effect sizes and predictions for all predictors retained in the final model.

(A) The standardised effect of each predictor on the likelihood of detecting a regular cycle (filled black circles) and 95% confidence intervals (horizontal black lines) to show whether effect is significantly different to zero (derived from a modified final model with intercept and main effect for Length $_{Scaled}$ *temporarily removed). (B-C) Model predictions for the relationship between the significant predictors - time series length, phenophase visibility (both continuous) and phenophase duration (binary) - and the likelihood of detecting a significant cycle from phenology data.*

3.4.5 Effects of process uncertainty on cycle detection

The random intercepts for **Phenophase** and **Species** accounted for most of the variance in the data (23% and 25%, respectively) while tree **ID** accounted for the least (<0.04%; see Table S3.1 for variance and standard deviation). The likelihood of detecting a cycle varied by **Phenophase**, being most likely for flowers and least likely for senescing leaves and ripe fruits. While for unripe fruits and new leaves, likelihood of detecting a cycle was greater than, but very similar to, the intercept for the fixed effects model (Figure 3.4 and Table S3.1). In the most parsimonious model, a random slope term by **Phenophase** was retained for **Length** $_{\textbf{Scaled}}$. The effect of **Length** $_{\textbf{Scaled}}$ as a predictor of cycle detectability was positive for all phenophases (Figure 3.4A), however, the effect was more positive than the general trend for new leaf, and flower cycles and less positive than the general trend for unripe fruit cycles (Table S3.1).

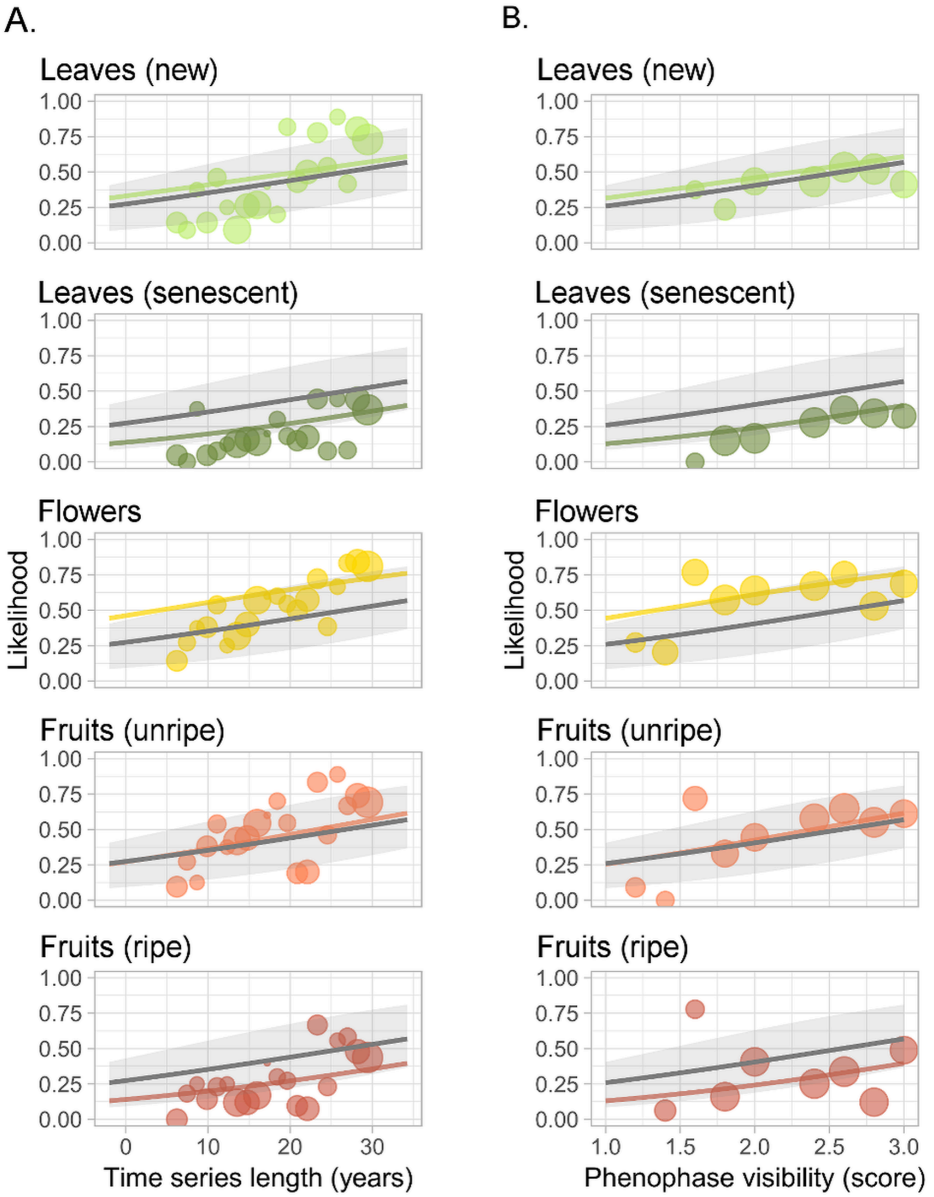

Figure 3.4. Predictions from the final model by phenophase.
General model predictions (grey lines) and 95% confidence intervals (grey shades) show the relationship between both significant continuous predictors (A) time series length and (B) visibility and the likelihood of detecting a significant cycle from phenology data when phenophase events last <= 4 weeks. Predictions from the random intercept and slope terms show how model predictions vary by phenophase (coloured lines). The mean probability of detecting a cycle from binned raw data demonstrates the model fit (coloured dots, scaled by number of observations in each bin).

3.5 DISCUSSION

We have shown that experienced field observers can provide important information on major sources of noise in phenology monitoring and that this can improve explanatory power for analyses of complex phenological data. For data derived from crown observations, we found that time series length, phenophase event visibility and duration are all good, positive predictors of finding regular phenological cycles. However, a relative increase in time series length has up to three times as large an effect on likelihood of detecting a cycle as a similar increase in phenophase visibility (comparison of standardised effect sizes).

The hierarchical nature of our modelling approach, including both species and phenophases, also allowed us to investigate variation in cycle detectability due to biological differences (process uncertainty). Species is an important predictor of cycle detectability, with some species - such as *Duboscia macrocarpa, Detarium macrocarpum* and *Saccoglottis gabonensis* - much more likely to have highly regular cycles among all phenophases than the general trend. We also found that cycle detectability varies among phenophases and is highest for flowers, followed by new leaves and unripe fruits and lowest for senescing leaves and ripe fruit. It is interesting to note, that among reproductive phenophases, detectability is highest for flowers, then unripe fruits, then ripe fruits. The fact that flowers occur first in a chain of linked events is likely to contribute to this pattern, as there are fewer accumulated opportunities for ecological processes to contribute noise at this stage. For instance more regular flowering than fruiting could arise because trees may abort their reproductive efforts after poor pollination or unfavourable weather conditions, or because of widespread removal of flowers by florivores (e.g. red colobus monkeys, *Procolobus rufomitratus,* in Uganda; Chapman *et al.* 2013).

3.5.1 LESSSONS LEARNED FOR EFFECTIVE ANALYSIS OF LONG-TERM TROPICAL PHENOLOGY DATA

The information gained from this study can help guide us to more effective data collection and more robust statistical analyses of tropical phenology; namely the best ways to increase sample size and reduce noise. Our first conclusion is that differences in observation uncertainty among species for the same phenophase should be accounted for in explanatory models of phenology data, otherwise the error associated with observational differences may lead to misleading conclusions. For example, it would be possible to erroneously link some aspect of leafing phenology to the functional group of the species (e.g. shade-tolerant, long-lived species) when in reality it could have arisen from an observation bias, such as visibility, associated with those traits (Figure 3.1). There have been a number of calls for more quantitative assessment of the impacts of climate on tropical phenology (Butt *et al.* 2015; Mendoza *et al.* 2017) and to correct the temperate (Northern hemisphere) bias of current climate change studies (Feeley *et al.* 2017). We have shown that even a simple assessment of observation uncertainty, undertaken by experienced field observers, can provide important information and be incorporated into and improve quantitative analyses of existing tropical phenology data.

3.5.2 LESSONS LEARNED FOR THE DESIGN OF TROPICAL PHENOLOGY MONITORING PROGRAMS

Going forward, we propose that both established and new programs seek to minimise sources of noise in phenology sampling design. We have shown that the length of study is the most important predictor of cycle detectability; thus it is vitally important that resources be directed towards maintaining existing and emerging long-term monitoring programs. For all phenophases, an additional 10 years of data collection (from 10 to 20 years) increases likelihood of detecting a cycle by 70% for phenology events lasting less than or equal to four weeks and by 114% for events lasting greater than four weeks. Observation length is a source of uncertainty relevant to all phenology

sampling methods (e.g. both crown observations and traps) and clearly, the elusive "sticking power" necessary to ensure long-term data collection needs to be addressed in the tropics. This can be achieved either through recognition of the importance of phenology research and allocation of substantial long-term resources from tropical nations and international funders, or through relevant and innovative, citizen-based initiatives.

While increasing the length of observation has the largest relative effect on cycle detectability, it is not always practicable. Often the duration of monitoring programs is outside of scientists' control, or assessments are necessary in the short-term and cannot wait an additional ten years. Therefore, for new monitoring programs looking to make meaningful assessments of cycle regularity through canopy observations over a short time, we recommend that they target species with highly visible phenological events that last longer than the monitoring interval (in our case, monthly). For example, at Lopé, flowers from species *Beilschmedia fulva*, *Milica excela* and *Mammea africana* are difficult to see (visibility score <1.5) and last greater than four weeks, whereas flowers from species *Antidesma vogelianum, Mangifera indica* and *Omphalocarpum procerum* are very easy to see (visibility score >2.5) and persist in the canopy for less than four weeks. Data from the latter species are more likely to be robust and free from observation error (similar to the scenarios for "low" observation uncertainty from Figure 3.1). After a period of initial monitoring (at least five years) it will be possible for data collectors at study sites to assess the amount of noise associated with specific species and phenophases in their sample. This information would allow project managers to select directly for the most easily observed species and target limited resources towards them by increasing sample sizes and including such species in inter-site comparisons.

Inevitably there will be occasions when it is important to monitor a noisy species or phenophase. For example, Moabi (*Baillonella toxisperma*) nuts are an important source of oil for cooking, cosmetics and rural enterprises in central Africa (Plenderleith & Brown 2004) but Moabi trees exhibit irregular phenology (random intercept for cycle detectability = -0.50) and its flowers

are difficult to see, as they are small and held very high in the canopy (similar to scenarios for "high" process uncertainty and "high" observation uncertainty, Figure 3.1). In such cases it will be important to tailor observation programs accordingly, by investing in alternative forms of monitoring (e.g. installing cameras in tree canopies opposed to observations from the ground), increasing number of trees monitored or increasing the frequency of observations.

Any systematic biases in recording phenology data will of course be related to the sampling method, "visibility" and "duration" being key sources of uncertainty identified for crown observation sampling protocols. The duration of a phenophase may be of less concern for trapping methods, although different biases are likely to arise such as rate of decomposition and trap-checking frequency, or the relative influence of weather conditions such as strong winds on the deposition of plant material. If used concurrently, crown observations and trapping methods could prove to be complimentary, accounting for different sources of uncertainty particular to each. In particular, seed traps employed alongside canopy monitoring could be used to further quantify the duration of phenological events.

The scientific community hopes to assess climate-induced changes in tropical ecological processes with only decades-long data at their disposal (for example, the data analysed here represents the longest published continuous phenology dataset in the tropics). This expectation has been raised by the rate of change observed in temperate systems (Schwartz *et al.* 2006). However, with such limited data it is essential that variation associated with processes outside of the focal question be kept to a minimum. When allocating resources for new and ongoing research, phenologists should aim to maintain monitoring programmes for as long as possible and target species and phenophases with least inherent noise to maximise statistical power and therefore ability to assess change in future analyses.

3.6 ACKNOWLEDGEMENTS

Phenology research at SEGC, Lopé National Park was funded by the International Centre for Medical Research in Franceville (CIRMF; 1986-2010) and by Gabon's National Parks Agency (ANPN; 2010 – present). We acknowledge significant periods of independent data collection undertaken by Richard Parnell, Liz Williamson, Rebecca Ham, Patricia Peignot and Ludovic Momont. Permission to conduct this research in Gabon was granted by the CIRMF Scientific Council and the Ministry of Water and Forests (1986 – 2010), and by ANPN and the National Centre for Research in Science and Technology (CENAREST; 2010 – present). We thank Alistair Jump, Daisy Dent, Isabel Jones, Jeremy Cusack and Irene Mendoza whose comments in preparation significantly improved the chapter.

S3 SUPPORTING INFORMATION

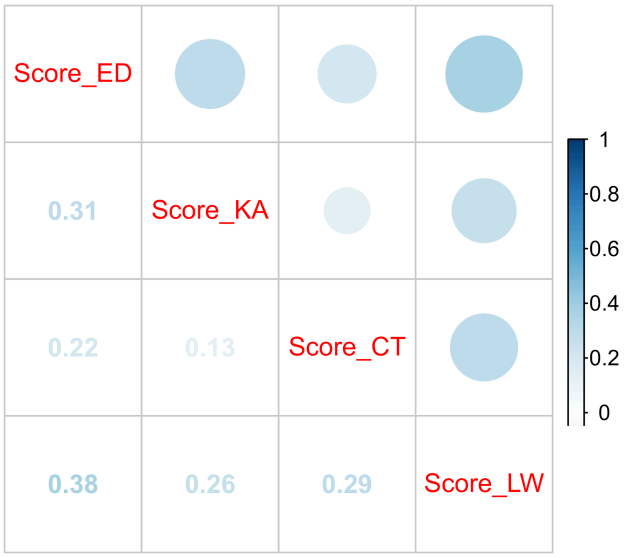

Figure S3.1.Correlation matrix of phenophase event visibility scores given by each observer for each species-phenophase.
The size of the dot indicates the magnitude of the correlation and the colour of the dot indicates the direction of the correlation. Observers are ED, KA, CT and LW.

Table S3.1 Outputs from the best model for the likelihood of detecting significant regular cycles.

Estimates for the fixed effects (A) and random effects (B and C) from a Generalised Linear Mixed-effects Model (GLMM; family= Binomial) with time series (Length $_{Scaled}$), phenophase visibility (Visibility $_{Scaled}$) and phenophase duration (Duration <= 4 weeks vs. > 4 weeks) as predictors. Phenophase, Species and ID are included as random grouping factors in the hierarchical model (number of observations = 3083; Groups: Phenophase = 5, Species = 61, ID = 827). Residual variance for binomial models is by default equal to 1 (B). Random intercept and slope show how the model for each level of phenophase differs from the fixed effects model (C). SE=Standard Error. SD = Standard Deviation.

A.

Predictor	**Estimate**	**SE**	**Z value**	**P value**
Intercept	-0.54	0.39	-1.39	0.16
Length $_{Scaled}$	1.51	0.32	4.78	<0.001
Visibility$_{Scaled}$	0.79	0.14	5.77	<0.001
Duration $_{(>4wks)}$	0.46	0.17	2.67	<0.01
Duration$_{(>4wks)}$ * Length $_{Scaled}$	0.80	0.34	2.38	0.02

B.

Group	**Random effect**	**Variance**	**SD**	**% Variance**
ID	Intercept	<0.001	<0.001	<0.04
Species	Intercept	0.59	0.77	22.77
Phenophase	Intercept	0.66	0.81	25.47
	LengthScaled	0.34	0.58	13.12

C.

Phenophase	**Intercept**	**Length$_{Scaled}$**
Flowers	1.19	0.16
Leaves (new)	0.33	0.84
Fruits (unripe)	0.23	-0.79
Leaves (senescent)	-0.84	-0.31
Fruits (ripe)	-0.88	-0.07

CHAPTER 4

Seasonal, inter-annual and long-term weather variability in western equatorial Africa.

4.1 ABSTRACT

Central Africa is a major convective region influencing weather worldwide and plays a global role in the carbon cycle. However meteorological data are notoriously sparse and incomplete and there are substantial issues with satellite-derived data because of cloudiness and inability to ground-truth estimates. We have the rare opportunity to analyse a 34-year dataset of rainfall and temperature (and shorter periods of relative humidity, wind speed, solar radiation and aerosol optical depth) from a long-term ecological research site in western equatorial Africa (Lopé National Park, Gabon) that has not contributed to the regional climate products available, thus able to act as an independent control. Using Generalised Linear Mixed Models and Wavelet methods we analysed seasonal and interannual variation and long-term trends using this data. Weather at Lopé has changed significantly over the last three decades, warming at a rate of 0.23°C per decade (minimum daily temperature) and drying at a rate of -78mm per decade (total annual

rainfall). Interannual weather variability at Lopé is highly influenced by global weather patterns; Rainfall significantly correlates with large-scale sea surface temperature (SST) patterns of the Pacific, Atlantic and Indian oceans, providing some but not conclusive support for the mechanisms behind the "dry" climate change-models for western equatorial Africa. The warm phase of the El Niño Southern Oscillation is significantly correlated with above average temperatures at Lopé although this association is in addition to and doesn't explain the long-term warming trend. The long-term observations we present here have not previously been made public and are of great value in such a data-poor region.

4.2 INTRODUCTION

The humid forests of central Africa make up 30% of the world's tropical forests (Malhi *et al.* 2013), are a globally important carbon store (Lewis *et al.* 2013) and form a major convective region, influencing weather globally (Bonan 2008; Washington *et al.* 2013). Long-term changes to climate and climatic variability in the region (James *et al.* 2013) are likely to have far-reaching impacts on the functioning of African tropical forests (Asefi-najafabady & Saatchi 2013; Zhou *et al.* 2014) with knock-on effects for the global carbon cycle (Mitchard 2018) and local human livelihoods (Niang et al., 2014). However, evidence for changes in forest function linked to weather conditions in Africa is extremely rare, mainly due to missing long-term data.

Empirical data for the region is notoriously sparse and incomplete. The number of rain gauge stations reporting data across central Africa has fallen from a peak of more than 50 between 1950 and 1980 to fewer than ten in 2010 (Washington et al. 2013). A similar land area (3 million km^2) in North America is monitored by thousands of gauges (NOAA 2018). The low density of observations in central Africa and poor understanding of local landscape and climatic processes (Nicholson & Grist 2003) limits the accuracy of gridded observational data products (Asefi-najafabady & Saatchi 2013; Suggitt *et al.* 2017) particularly for rainfall where estimates are poorly conserved spatially (Habib *et al.* 2001; Kidd *et al.* 2017). As a result, climate and ecological models in the region rely heavily on satellite data despite major issues due to cloudiness (Washington *et al.* 2013; Maidment *et al.* 2014). This is especially pertinent in the western Congo-Ogooué Basin where warm moisture-rich air rises from the gulf of Guinea (Hansen et al. 2008; Ju & Roy 2008). There is an urgent need for long-term and large-scale climate observations to verify regional climate and vegetation models and shed light on the mechanisms that drive seasonal and long-term climatic changes in tropical Africa (Guan *et al.* 2013; Abernethy *et al.* 2016).

We have the rare opportunity to analyse a 34-year record rainfall and temperature (and shorter periods of relative humidity, aerosol optical depth, wind speed and solar radiation) from a long-term ecological research site in

western equatorial Africa. This local weather data has not contributed to the regional climate products available and is thus able to act as an independent control. In this paper we aim to:

1. Review the published literature on drivers of seasonality, inter-annual variability and long-term trends in central African weather, with a focus on the changes documented for western equatorial Africa (WEA; covering Cameroon, Republic of Congo, Central African Republic, Equatorial Guinea and Gabon, the location of our long-term study site).
2. Analyse seasonal, inter-annual and long-term variability at our site using local weather observations
3. Test the influence of global oceanic SSTs on interanuual weather variation at our site.
4. Compare our results with the literature, with particular focus on rainfall for which uncertainty in regional products is high.

4.2.1 Seasonal weather variation driven by the ITCZ

Seasonality in central African weather is driven by the Inter Tropical Convergence Zone (ITCZ), a band of clouds and high precipitation caused by converging trade winds around the equator that moves periodically with the position of the sun throughout the year (National Weather Service 2018). The ITCZ reaches its Northern limit in July and its southern limit in January (Figure 4.1; Barlow et al. 2018). Rainfall peaks in the Congo-Ogooué Basin during the transitional seasons as the ITCZ passes the equator (Farnsworth *et al.* 2011; Suzuki 2011; Preethi *et al.* 2015). Most regional climate estimates show the September-November rainy season to be more intense than March-May (Washington et al. 2013). Region-wide, just 3% total annual rainfall falls during the major dry season from June to August when the ITCZ is furthest North, while around 25% total annual rainfall falls during the secondary dry season from December to February (Balas et al. 2007). Monthly runoff data (averaged over the last century) for the two major rivers in the region – the Congo and Ogooué - show that river flow peaks in May and November and is

lowest in August, lagging the rainfall pattern (Laraque *et al.* 2001; Mahe *et al.* 2013).

Whilst day length is constant at the equator and varies little throughout the tropics (Borchert *et al.* 2005), surface solar radiation can be highly seasonal (Wright 1996) and vary regionally. In the light deficient WEA region, there is a distinctive drop in irradiance during the long dry season (due to cloud cover) and peaks as the ITCZ passes the equator (Philippon *et al.* 2019). In these transitional seasons the sky is usually clear in the morning with convection clouds developing into storms late in the day or night (Gond *et al.* 2013). The seasonal synchrony between light and moisture availability in WEA is in contrast to central equatorial Africa (DRC) and the American tropics where the dry season coincides with peaks in irradiance (Wright & Calderón 2018; Philippon *et al.* 2019). The situation is more complex in the Asian tropics where climatic seasonality is extremely limited near the equator (Sakai 2001; Nagai *et al.* 2016) but becomes more pronounced away from the equator. For example in the northern Asian tropics, insolation peaks during the end of the dry season and the beginning of the rainy season (dropping during the late rainy season and "foggy" early dry season; Zhang et al. 2010).

Temperature varies relatively little throughout the year in WEA but the coolest period south of the equator occurs during the long dry season (June-September; Munzimi et al. 2015; Tutin & Fernandez 1993) when the ITCZ is at its most Northerly peak and cloud cover is highest. It is in the long dry-season also that surface winds are strongest (Tutin & Fernandez 1993; Preethi *et al.* 2015).

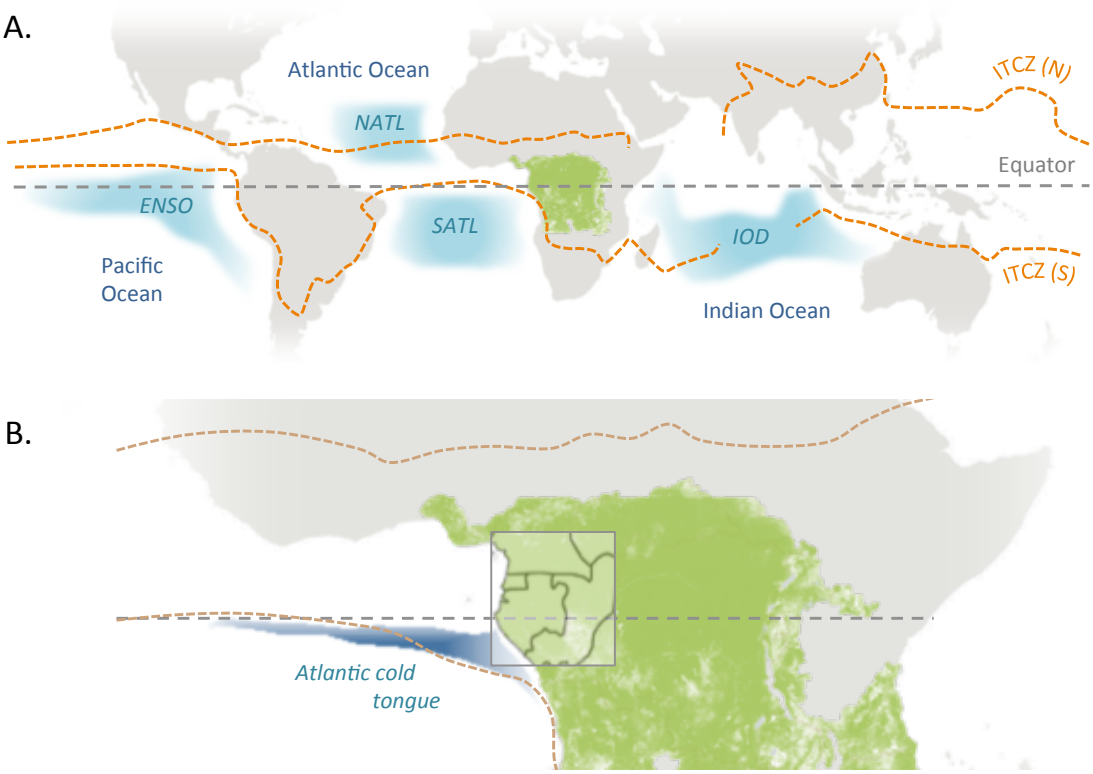

Figure 4.1: Global climatic influences on western equatorial Africa.
A. The forested region of central Africa is indicated by a layer of green pixels (>30% tree cover in 2010 from Hansen et al. 2013). The Northern (July) and Southern limits (January) of the Inter Tropical Convergence Zone (ITCZ) are drawn from Barlow et al. (2018). The blue zones indicate patterns in oceanic sea surface temperatures (SSTs) known to influence weather in Western Equatorial Africa (WEA): the Pacific Ocean El Niño Southern Oscillation (ENSO); North and South Tropical Atlantic SSTs (NATL and SATL) and the Indian Ocean Dipole (IOD). B. The limits of WEA as defined in this paper are indicated by the grey rectangle (including the humid forests of Gabon, Equatorial Guinea, Cameroon and the Republic of Congo). Also the location of the seasonal Atlantic cold tongue, a pool of cool surface water that develops in the eastern tropical Atlantic during the boreal summer (Tokinaga & Xie 2011). Tree cover data are available from http://earthenginepartners.appspot.com/science-2013-global-forest. The world map was created by Layerace at Freepik.com

4.2.2 INTER-ANNUAL WEATHER VARIABILITY DRIVEN BY THE OCEANS

Large-scale patterns in sea surface temperatures (SSTs) caused by ocean currents and upwellings- such as the El Niño Southern Oscillation (ENSO), North and South tropical Atlantic SSTs and the Indian Ocean Dipole (IOD) – are known to influence local weather conditions across the tropics (Camberlin et al. 2001; Figure 4.1). ENSO refers to the state of the atmosphere and SSTs of the tropical Pacific Ocean. Conventional (canonical) ENSO phases switch periodically every two to seven years between El Niño conditions when SSTs of the tropical eastern Pacific are above average (usually developing in December and January) and La Niña conditions when SSTs are below average (Behera *et al.* 2013). El Niño Modoki differs from the canonical oscillation and in these events warming occurs in the central Pacific with cooler waters on the east and west side of the basin (Behera *et al.* 2013). The IOD is the difference between the SSTs of the western and eastern tropical Indian ocean with positive phases representing cool anomalies in the south east and warm anomalies in the west (Behera *et al.* 2013).

ENSO has a relatively straightforward, instantaneous, effect on temperature throughout the African continent, with greater warming when the ENSO index is above average (commonly referred to as El Niño years) but only significantly so from December-February in WEA (Collins 2011; Table 4.1). No evidence was found for the effects of other SST phenomena on temperature in the central African region. While inter-annual variation in central African precipitation is strongly connected to SSTs of all major oceans (Otto *et al.* 2013), the interactions are highly complex and seasonally specific. In Table 4.1 we summarise results from five major studies of oceanic influences on rainfall in the region (Camberlin *et al.* 2001; Todd & Washington 2004; Balas *et al.* 2007; Otto *et al.* 2013; Preethi *et al.* 2015). The main agreements between these studies for WEA are that (1) in El Niño years (canonical) rainfall is below average from February to August (Camberlin *et al.* 2001; Todd & Washington 2004; Balas *et al.* 2007; Preethi *et al.* 2015), (2) Indian Ocean SSTs positively correlate with rainfall in January and February

(Balas *et al.* 2007; Preethi *et al.* 2015) and (3) warm tropical South Atlantic SSTs enhance rainfall from June-September (Camberlin *et al.* 2001; Balas *et al.* 2007; Otto *et al.* 2013). We found no evidence in the literature for how large-scale climate oscillations impact other weather variables such as light availability or wind speeds in the region.

Table 4.1: The influences of major oceanic drivers on temperature and rainfall in western equatorial Africa.

CEA= Central equatorial Africa (centred on the Democratic Republic of Congo); WEA = Western equatorial Africa (covering Cameroon, Republic of Congo, Central African Republic, Equatorial Guinea and Gabon); SST= Sea Surface Temperature; ENSO= El Niño Southern Oscillation; IOD= Indian Ocean Dipole.

	Reference	Data	Major Oceanic Drivers		
			Pacific SSTs	Indian Ocean SSTs	Atlantic SSTs
Temperature	Collins 2011	Africa-wide. Satellite and reanalysis data. 1979-2010.	Positive relationship between ENSO and temperature in the dry seasons (Dec-Feb and June-Aug; other seasons not tested).	Not tested	Not tested
Rainfall	Preethi et al 2015	Africa-wide. Satellite and gridded obs. 1979-2010.	Negative relationship between ENSO and rainfall Jan- Sep. Positive relationship between ENSO Modoki and rainfall Mar-May.	Positive relathionship between basin-wide SSTs Jan-Feb. No relationship to IOD.	Not tested.
	Camberlin et al. 2001	Sub-Sahara. Gridded obs. 1951-1997.	Negative relationship between ENSO and rainfall Apr-Jun.	Not tested.	Positive relationship between South Atlantic SSTs and rainfall Apr-Sep.
	Balas et al. 2007	WEA. Precip. gauge dataset. 1950-1998.	Negative relationship between ENSO and rainfall in all seasons, (strongest Mar-May).	Weak positive relationship between Indian Ocean SSTs and rainfall in all seasons except Mar-May where it is reversed.	Positive relationship between South Atlantic SSTs and rainfall Jun-Nov, negative relationship Dec-Feb. Rainfall most closely linked to SST along Benguela coast Mar-May.
	Todd & Washington 2004	CEA (but data also shown for WEA). Gridded obs. and disharge. 1901-1998.	Weak negative relatioship between ENSO and rainfall (Feb-Apr tested only).	Not tested.	Negative correlation between NAO and rainfall from Feb-Apr (mediated by Tropical North Atlantic SSTs and anomolous mid-trophospheric westerly winds).
	Otto et al. 2013	CEA (but data also shown for WEA). Simulated data for dry season rainfall.	Strong influence of ENSO on rainfall in the dry seasons (Dec-Feb and June-Aug; other seasons not tested).	Strong influence of IOD on rainfall in the dry seasons (Dec-Feb and June-Aug; other seasons not tested). IOD negatively associated with rainfall in both dry seasons (strongest Dec-Feb).	Positive correlation between North and South tropical Atlantic SSTs with rainfall in both dry seasons (strongest Dec-Feb).

4.2.3 HIGH CONFIDENCE IN INCREASED WARMING BUT UNCERTAINTY IN PRECIPITATION CHANGES

There is high confidence in warming over African land regions. Near surface temperatures have increased by at least 0.5°C over the last century across most of the continent, with most rapid change in minimum daily temperature (Niang *et al.* 2014). Satellite estimates for tropical Africa show an annual

mean temperature increase of 0.15°c per decade from 1979-2010 (Collins 2011). A recent multi-model ensemble showed that mean temperature for the whole African continent is likely to continue to increase more than the global average (1.1 °C at 1 °C globally, 2.3 °C at 2 °C, 3.4 °C at 3 °C, and 4.3 °C at 4 °C), especially in the long dry season (James & Washington 2013).

Tropical land areas globally have seen no overall change in precipitation over the last century, with a recent increase in precipitation (2003-2013) reversing a drying trend from the 1970s to the 1990s (Hartmann *et al.* 2013). Observational datasets (gauge networks and merged-satellite data; 1983-2010) show strong disagreement in the sign and magnitude of the rainfall trend for central Africa (not including WEA; Maidment et al. 2015), probably due to insufficient observations (Niang *et al.* 2014). However, when gridded gauge-observations (from the Climate Research Unit, CRU dataset) are examined for the Gabon/Cameroon WEA region, a decline in total annual precipitation of 1% per decade is evident from 1968-1998 (Malhi & Wright 2004). Flow data for the Ogooué river indicates that runoff in the same region has declined since the 1960s, including the most recent decade for which data is available (2000-2010) and that the flood peak has moved from May to April (Mahe *et al.* 2013). As land-cover change has been minimal in the watershed (Abernethy *et al.* 2016) it is likely that reduced rainfall has been the biggest determinant of this change in runoff, supporting the trend observed directly from gauge data.

Predicted changes for future rainfall vary widely across the African continent, with good model support for a drying trend (increase in dry season water deficit) in Western and Southern Africa, a wetting trend in East Africa, and high uncertainty in the direction of change centrally, probably due to the sparse network of observations and poor understanding of local climate forcing (James & Washington 2013). However when Central Africa is examined more closely, model projections for precipitation (and therefore water deficit) mostly show no change or a weak wet signal centrally, and a dry signal in the western region in climate scenarios where warming is greater than 2°C (James et al. 2013). Models that predict the drying trend in

WEA show strong associations with Atlantic and Indian (but not Pacific) Ocean SSTs. The construction of these models suggests that projected reductions in rainfall in WEA are caused by a northward displacement of the ITCZ associated with cool SSTs in the Gulf of Guinea (the Atlantic cold tongue; Figure 4.1B) and an eastward shift in convection caused by contrasts between Indian and Atlantic SSTs (James et al. 2013).

As for surface solar radiation, once again the picture varies spatially within central Africa. In the central Congo Basin (14E-30E; no data presented for WEA) there has been a recent widespread decline in cloud optical thickness and no change in aerosol optical thickness (MODIS, 2000 -2012) leading to an increase in downward photosynthetically available radiation (CERES, 2003-2012; Zhou et al. 2014). While for sunshine duration, there has been no change in the central region but a weak decline (2-4 hours per decade) in WEA from 1983-2015 (SARAH-2, Kothe et al. 2017). We found no evidence for or against long-term changes in relative humidity or wind speed in the region.

4.3 METHODS

4.3.1 DESCRIPTION OF THE STUDY AREA AND WEATHER DATA RECORDING SINCE 1984

The Station d'Études des Gorilles et Chimpanzées (SEGC) research station is situated at the northern end of Lopé National Park, in the heart of Gabon (-0.2N, 11.6E). The station sits within a tropical forest-savanna matrix, at an elevation of 280m and within 10.5 km of the River Ogooué (the second largest river in the Congo-Ogooué basin). Ecological research activities, including weather, plant and animal observations, have taken place at SEGC continuously from 1984 until the present (>300 publications; 1983-2018).

Weather data has been recorded at Lopé since 1984 using various different types of equipment split between two locations: a savanna site (the research station; 11.605E, -0.201N) and a forest site (800m from the research station and approximately 10m from the savanna/forest edge; 11.605E, -0.206N). From 1984 to the present, a manual rain gauge was situated in the savanna

(50cm above ground >5m from any tree or building) and used to record daily rainfall totals at 8am each morning. There was a gap in data recording in 2013 and occasional missing days due to logistical constraints (e.g. availability of personnel). Since 1984 daily maximum and minimum temperatures and relative humidity were recorded using a manual thermometer and wet/dry bulb located in the forest (1.5m aboveground under closed canopy), which was checked daily when logistics permitted, or whenever researchers from SEGC passed it. In 2002 all temperature recording at the forest site was transferred to continuous automatic units (ONSET HOBO® Data Loggers refhttps://www.onsetcomp.com/, these units also recorded relative humidity) and temperature recording using the same units also began in the savanna. Due to technical failures these units were replaced in 2006 with the original manual max/min thermometer in the forest and a digital max/min thermometer (Taylor 1441) in the savanna. These were in turn replaced by another type of automated unit (TinyTag Plus 2, Gemini DataLoggers https://www.geminidataloggers.com/data-loggers/tinytag-plus-2, some of which could record both temperature and relative humidity), deployed in the forest from 2007 and in the savanna from 2008 and used until the present (with a gap at the forest site from mid-2015 to mid-2016 and intermittent recording throughout 2017 partly due to termite infestation). In addition two weather stations were installed in the savanna (sited near the research station, on a rock 4m from the ground) between 2012 and 2016. A Davis VantagePro2 (https://www.davisinstruments.com/solution/vantage-pro2/) was installed in January 2012 and recorded rainfall, temperature, relative humidity, pressure, wind speed and direction, UV index and solar radiation every 30 minutes for two years until the equipment was struck by lightning in January 2014 and stopped functioning. A SKYE MINIMET weather station (https://www.skyeinstruments.com/minimet-automatic-weather-station/) was installed at the same location in 2013 and collected temperature, relative humidity, wind speed and direction and solar radiation (and was also programmed to collect rainfall but this never worked). It ran intermittently until 2016 when the equipment was also struck by lightning. Data recorded

between January 2014 and November 2014 was also lost. Finally, a sun photometer was installed at the research station in April 2014 and used to record Aerosol Optical Depth (AOD) up to the present as part of the NASA Aerosol Robotic Network (Aeronet; https://aeronet.gsfc.nasa.gov/; Holben et al. 1998).

The remote and challenging environment at Lopé has led to a patchy weather data record. This is especially true since the introduction of automated loggers, due to unreliable performance combined with difficulties and time delays in replacing or repairing malfunctioning equipment and respecting annual calibration schedules with manufacturers based in Europe or the USA. In addition, new equipment was often introduced out of necessity when previous equipment failed, precluding the opportunity of collecting simultaneous data for standardisation. This situation is far from unique and is replicated across many other similar field stations in Africa (Maidment *et al.* 2017). In Appendix C we show daily records for all weather observations at Lopé since 1984 and explain in detail how we selected and standardised data in order to reduce systematic biases between recording equipment.

In brief, we constructed a long-term record of daily rainfall (1984-2018) by combining two sources of rainfall data (rain gauge and weather station), calibrating them using simultaneous records and where possible filling missing daily values (3% observations) using the ten-day running mean for the time series however 11 months in three different years remained incomplete.

Temperature was recorded at Lopé using six different pieces of equipment across two sites (forest and savanna). We used both maximum and minimum daily data to demonstrate seasonality and periodicity. However to avoid the erroneous impacts of direct solar radiation on air temperature estimation related to different equipment (Appendix C) we constructed a long-term temperature record using minimum daily temperature observations only (1984-2018) for analyses of trends and inter-annual variation. 36 months are missing from this record because there were fewer than five observations from which to calculate the monthly mean.

Finally we used shorter (and/or patchier) periods of data for relative humidity (2002-2018), solar radiation (2012-2016), wind speed (2012-2016) and aerosol optical depth (2014-2017) to assess seasonality and periodicity for these climate variables.

4.3.2 Gridded regional temperature datasets

Because of the lack of simultaneous recording between temperature equipment we also downloaded two widely used gridded regional data products with which to compare the Lopé data: daily minimum air temperature from the Gridded Berkeley Earth Surface Temperature Anomaly Field (1° resolution; Rohde *et al.* 2013) and monthly mean daily minimum temperature from the Climate Research Unit's Time-Series v4.01 of high-resolution gridded data (CRU TS4.01; 0.5° resolution; University of East Anglia Climatic Research Unit et al. 2017; Harris et al. 2014). Both were downloaded from http://climexp.knmi.nl/start.cgi for the grid-cell overlapping the SEGC location (0.2N, 11.6E).

4.3.3 Ocean sea surface temperatures (SSTs)

We downloaded data for four oceanic SSTs from commonly used data sources: the Multivariate ENSO Index (MEI; Wolter & Timlin 1993; Wolter & Timlin 1998) sourced from the NOAA website (https://www.esrl.noaa.gov/psd/enso/mei/index.html), the Indian Ocean Dipole (IOD) Dipole Mode Index (Saji & Yamagata 2003) sourced from the NOAA website (https://www.esrl.noaa.gov/psd/gcos_wgsp/Timeseries/DMI/) and SST anomalies for the tropical north Atlantic (NATL, 5°–20°N, 60°–30°W) and the south equatorial Atlantic (SATL ,0°–20°S, 30°W–10°E) sourced from the NOAA National Weather Service Climate Prediction Center (http://www.cpc.ncep.noaa.gov/data/indices/). We rescaled all four SST indices by subtracting the mean and dividing by one standard deviation to allow direct comparison of modelled effect sizes. Positive values for MEI indicate El Niño conditions; positive values for NATL and SATL indicate warm SSTs in those regions while positive values for IOD indicate cool SSTs

in South Eastern equatorial Indian Ocean and warm SSTs in the Western equatorial Indian Ocean.

4.3.4 ANALYSES

Seasonality

To describe the seasonality of each weather variable, we calculated the mean value for each day of the year (DOY), the ten-day running mean of DOY and the monthly mean from empirical daily data. This allowed us to summarise the data while retaining fine-scale variation where available.

To assess the periodicity of each weather variable, we created standardised time series by calculating the mean value for each month in the record and filling missing months using the mean value for the corresponding calendar month for the whole time series. We then scaled the data by subtracting the mean and dividing by its standard deviation. We computed the Fourier transform for each of these time series and inspected the spectra for peaks that represent strong regular cycles in the data (Chapter 2; Bush et al. 2017)

Long-term trends

We assessed whether total annual rainfall and temperature had changed over the observation period (1984-2018) by fitting generalized linear models (GLMs, family=Poisson) for rainfall and linear mixed models (LMMs) for temperature to account for the data distribution and hierarchical structure. We fitted models with Year (continuous, rescaled) as the predictor (representing long-term change) and compared them to intercept-only models (representing no long-term change) using AIC values. We preferred simple models (few parameters) with lowest AIC (significantly different if delta AIC >2). We repeated the same procedure with gridded data for Lopé from the daily Berkeley dataset and the monthly CRU dataset to compare with our Lopé recorded temperature trends. Inspection of the autocorrelation function for total annual rainfall and the median autocorrelation function of residuals for daily temperature (autocorrelation calculated for each DOY) showed no significant temporal autocorrelation.

We then investigated whether trends in daily rainfall and minimum temperature varied seasonally. Various seasonal definitions are used throughout the tropics, usually related to the annual rainfall cycle. We defined our seasons according to Lopé rainfall climatology where the long dry season extends into September, i.e. October-November (ON), December-February (DJF, the "short" dry season), March-May (MAM) and June-September (JJAS, the "long" dry season; Figure 4.2A). We fitted an initial model that included Year (continuous, rescaled), Season (factor with four levels as above) and their interaction as predictors (representing long-term change varying by season), a second model without the interaction term (representing long-term change not varying by season) and a third model excluding Year altogether (representing no long-term change, seasonal effects only). We compared the three models using AIC values to test if the interaction between Year and Season improved the model. We fitted models without the global intercept to estimate the magnitude of the trend in each season rather than comparing each season trend to the global intercept. All models included Year and DOY as random intercepts to account for pseudoreplication.

Periodicity over time

We also used wavelet analyses to assess if and how periodicity varied over time for rainfall and temperature explicitly taking account of the circular nature of the data (Adamowski *et al.* 2009). We computed the wavelet transform for the standardised monthly timeseries for each variable using the R function *wt* from the package *biwavelet* (Gouhier *et al.* 2018) and plotted the power (higher power denotes greater fidelity to a certain cycle), significance (a cycle is significant if >0.95, X^2 test) and cone of influence (denoting the unreliable region at the beginning and end of the time series due to edge effects). We then extracted the power of the biannual, annual and multiannual (mean of the 2-4 year periods) components to assess how these dominant cycles varied over time. The multiannual component was limited to four years because lower frequency cycles were heavily influenced by edge effects.

Influence of oceanic SSTs on interannual variability

We tested the seasonal influence of oceanic SSTs for the three major oceans hypothesized to influence weather in the Gabon region (Pacific: MEI, Indian Ocean: IOD and Atlantic Ocean: NATL and SATL) within a linear regression framework (GLMMs, family=Poisson, for rainfall, LMMs for temperature).

For the monthly time series for each weather variable we fitted an initial model including each Oceanic Index (MEI, NATL, SATL and IOD), Season and the interaction between each Index and Season as predictor variables. For those weather variables that had previously shown to be changing linearly over time, we included Year (continuous, rescaled) and its interaction with Season as predictors. We modified these initial models by removing terms, starting with the interactions between each Oceanic Index and Season and ending with the Oceanic Index main effects, comparing models using AIC values to find the simplest model with the lowest AIC. As before, we fitted models without the global intercept to estimate the magnitude of the effect in each season rather than comparing each season effect to the global intercept. All models included Year and Season as random intercepts to account for pseudoreplication.

4.4 RESULTS

4.4.1 SEASONALITY

Mean total annual rainfall at Lopé from 1984-2018 was 1465mm ± 203 sd. Rainfall at Lopé occurs in a biannual cycle (Figure. 4.2), with broad peaks in MAM and ON where mean daily rainfall is always greater than 5mm (Figure 4.3A). The long dry season (JJAS) is very consistent, with a 60-day period (mid-June to mid-August) in which the ten-day running mean is never greater than 1mm. The DJF rainy season is much more variable and the ten-day running mean is always greater than 1mm.

Mean daily maximum and minimum temperatures at Lopé were 28.1°C and 21.9°C at the forest site (1984-2018) and 31.6°C and 22.0°C at the savanna site (2002-2018), meaning that the daily temperature range in the savanna is greater than the forest (Figure 4.3C and D). Maximum daily temperature in the forest has strong annual and bi-annual cycles while in the savanna the annual cycle is dominant (Figure 4.2). The difference between the two sites occurs during the short dry season where temperatures are maintained in the savanna at similar levels to the rainy seasons (ten-day running mean always greater than 31.7°c from October to May in the savanna; Figure 4.3C). In the forest, the highest peaks in maximum daily temperature occur in April and September (mean monthly maximum daily temperatures are 29.5°c and 28.6°c respectively; Figure 4.3D). Annual cycles dominate the minimum daily temperature record for both the forest and the savanna (Figure 4.2). Minimum daily temperatures are relatively constant from September to June (~22.5°c) followed by a cool period during the long dry season reaching an annual trough in July (mean monthly minimum daily temperature is 20.6°c in both the savanna and forest; Figure 4.3C and D).

Overall mean humidity is greater in the forest than the savanna throughout the year (mean humidity is 98.2% and 92.7% respectively; Figure 4.3E and F) but cycles biannually in both (Figure 4.2). Relative humidity drops at the end of both the long and dry seasons in the savanna to a similar value (89.7% and 90.1% in February and September respectively) but is much more

asymmetrical in the forest, where high humidity is maintained throughout the short dry season (10-day running mean for DJF always greater than 98.7%). Relative humidity in both the savanna and the forest lags the rainfall cycle by one month with the annual minima occurring in February and September and the maxima occurring in May/June and November/December (Figure 4.3E and F).

Both surface solar radiation and wind speed are dominated by annual cycles at Lopé (Figure. 4.2), with the long dry season coinciding with low irradiance (mean monthly solar radiation for July = 129.3 W/m2; Figure 4.3G) and increasing wind speeds (mean monthly wind speeds for August and September are 1.3 m/s and 1.4m/s respectively; Figure 4.3B). Aerosol optical depth cycles twice yearly (Figure 4.2), peaking during the dry seasons and dropping during the rainy seasons (AOD at 500nm is shown in Figure 4.3H, AOD at 440 and 675nm is shown in Figure S4.1). In contrast to the solar radiation cycle, which drops to its minima during the long dry season (JJAS), the strongest peak in AOD occurs in the short dry season (mean monthly AOD for February = 0.97).

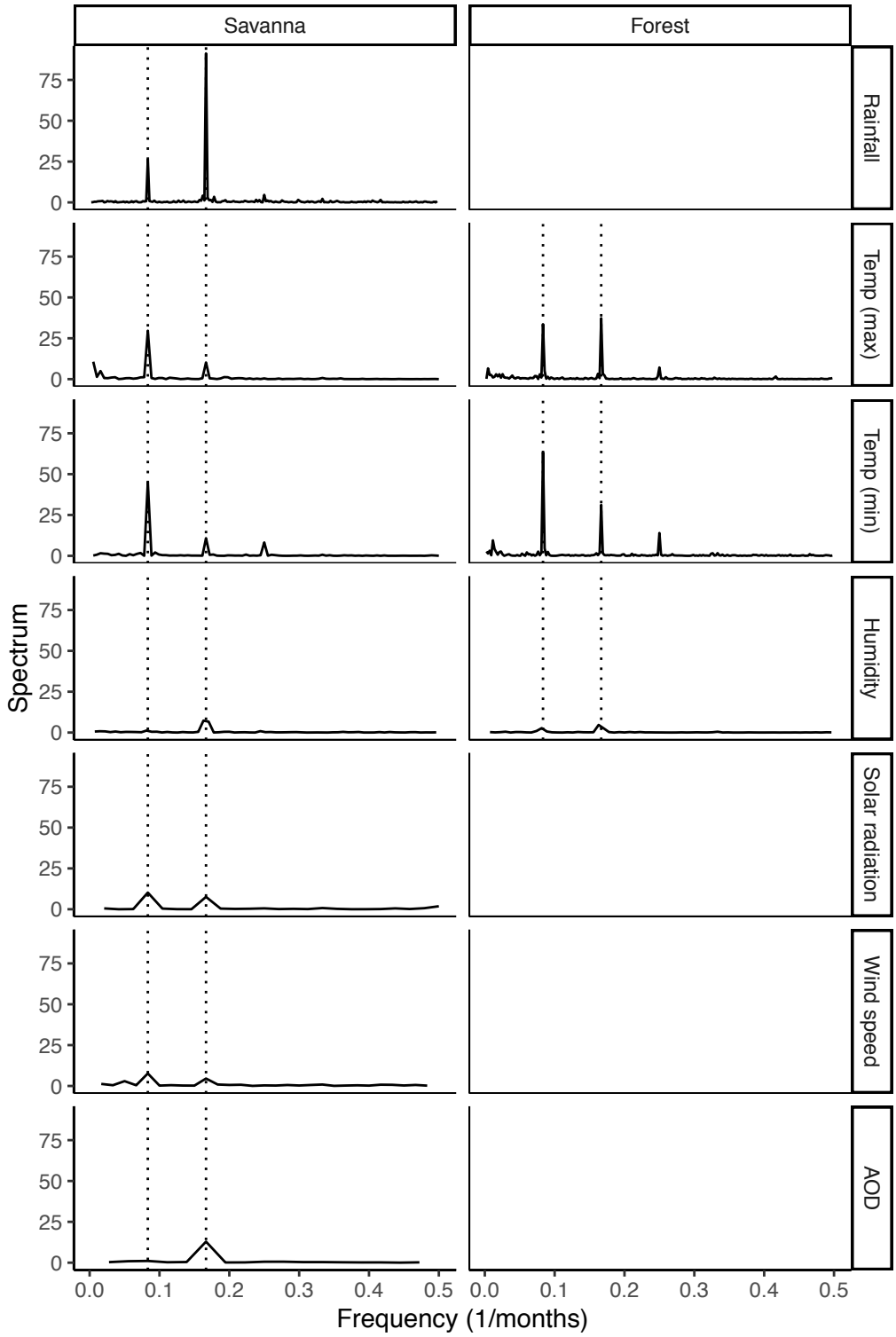

Figure 4.2. Fourier spectra for Lopé weather data.
The spectrum represents the power of the cycle at that particular frequency and peaks in the spectra indicate dominant cycles. The dotted vertical lines indicate the position of annual (0.083 cycles per month) and biannual (0.167) cycles. Timeseries were standardised but observation lengths differ.

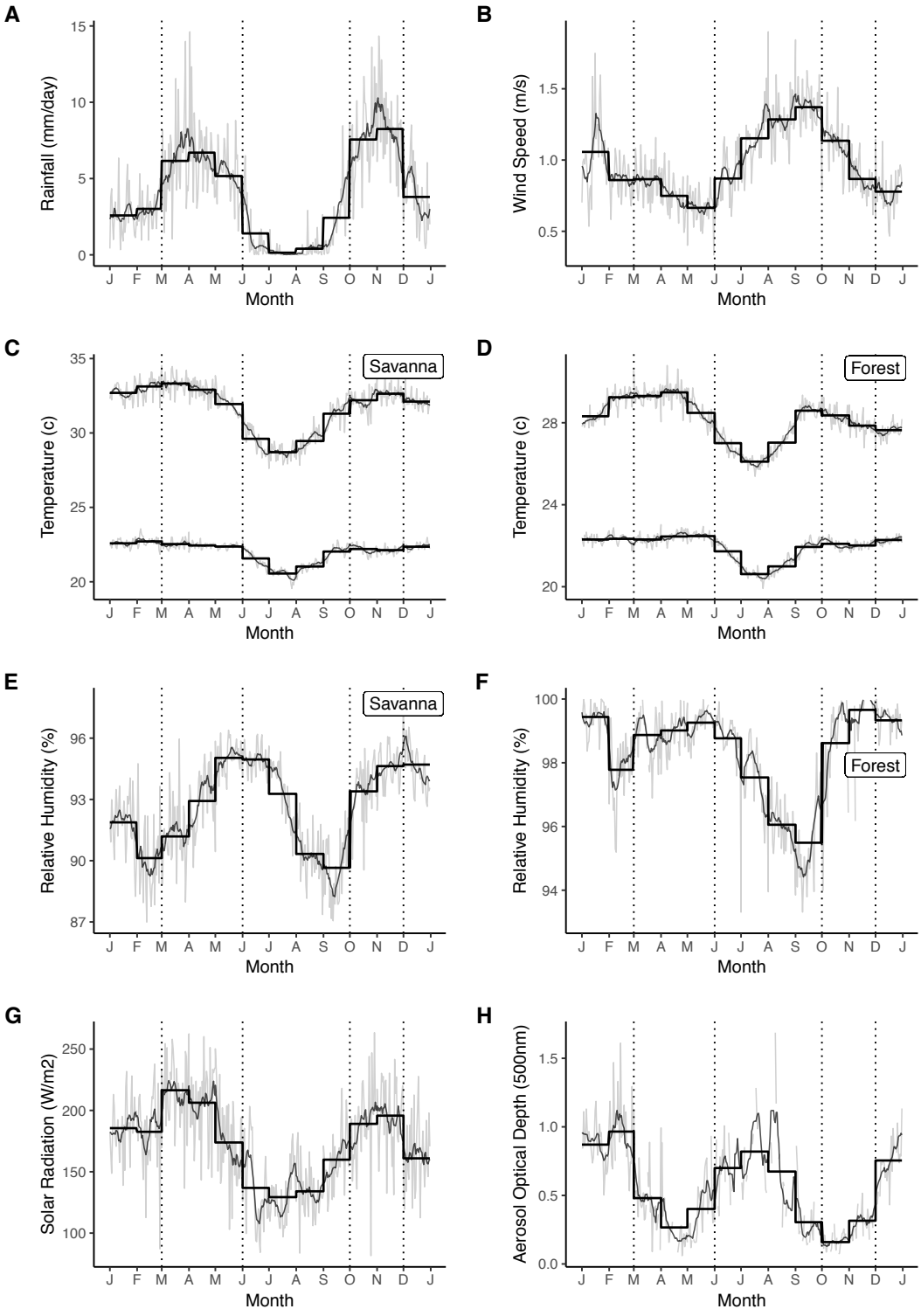

Figure 4.4: Seasonal weather variability at Lopé, Gabon.
Shown are the day of year means (thin grey line), seven-day running means (thin black line) and monthly means (bold black line) for daily rainfall (1984-2018), maximum and minimum daily temperature (1984-2017), relative humidity (2007-2015), surface solar radiation (2012-2014) , wind speed (2012-2014) and aerosol optical depth at 500nm (2014-2017). Vertical dotted lines indicate the alternating rainy and dry seasons.

4.4.2 LONG-TERM TRENDS

Total annual rainfall decreased by 52mm per decade, a change of -3.5% relative to mean annual rainfall for the time period (GLM, family=Poisson, Estimate = -0.036, SE= 0.005, Z= -7.21, P<0.0001; Tables 4.2A and Figure 4.4A). However the slope of the decline is seasonally dependent (Tables 4.2B and 4.3) with no change in daily rainfall in DJF and ON and most rapid decline in JJAS (-0.26 mm per day per decade, equating to 23.6% of mean JJAS daily rainfall) followed by MAM (-0.19 mm per day per decade, equating to 3.2% of mean MAM rainfall).

Minimum daily temperature at Lopé has increased at a rate of 0.23°c per decade, equivalent to 1.1% relative to mean minimum temperature for the time period (LMM, Estimate = 0.24; SE = 0.05; T = 5.2; Table 4.2A and Figure 4.4B). Berkeley minimum daily temperature for the interpolated Lopé grid square (1° resolution) increased at a rate of 0.16°c per decade (LMM, Estimate = 0.34, SE = 0.09, T = 3.9) while the CRU interpolated record (0.5° resolution) increased by 0.18°c per decade (LMM, Estimate = 0.18, SE = 0.03, T = 5.4; Fig S4.2 and S4.3). The rate of warming at Lopé also varied by season (Tables 4.2B and 4.3) with minimum temperature increasing most quickly in ON and DJF (0.30°c and 0.29°c per decade respectively) and most slowly in JJAS (0.16°c per decade).

Table 4.2. Model comparisons to test for long-term change in rainfall and minimum temperature.

A. Comparison of models for long-term change in total annual rainfall (generalised linear model, family=Poisson) and mean minimum daily temperature (linear mixed model). B. Comparison of models for long-term change varying by season for daily rainfall (generalised linear mixed model, family=Poisson) and mean minimum daily temperature (linear mixed model). Year and Day of Year (DOY) were included as grouping factors in the random effects of all mixed models. AIC = Akaike Information Criterion, DF = degrees of freedom. Asterisks indicate the simplest model with lowest AIC.

A.

Response	Long-term change (~Year)		No long-term change (~1)	
	AIC	DF	AIC	DF
Rainfall	1068.8 **	2	1119.0	1
Min temp	22595.1**	5	22608.3	4

B.

Response	Long-term change varying by season (~Year * Season)		Long-term change not varying by season (~Year + Season)	
	AIC	DF	AIC	DF
Rainfall	151049.8**	10	151261.8	7
Min temp	22260.5**	11	22274.3	8

Table 4.3. Outputs from the best models for seasonal changes in rainfall and minimum daily temperature.

Estimates from generalised linear mixed models (family = Poisson) for daily rainfall and linear mixed models for minimum daily temperature. SE = Standard Error. Day of Year (DOY) and Year were included as random effects. P values are not available for LMM so 95% confidence intervals were calculated instead. Asterisks indicate predictors where 95% CI doesn't overlap zero and thus are considered significantly different to zero.

Response	Predictor	Estimate	SE	T/Z value	P value / 95% CI	
Rainfall	DJF	0.69	0.12	5.64	<0.0001	**
	JJAS	-0.02	0.11	-0.22	0.83	
	MAM	1.12	0.11	9.93	<0.0001	**
	ON	0.71	0.13	5.38	<0.0001	**
	Year: DJF	0.02	0.03	0.79	0.43	
	Year: JJAS	-0.25	0.03	-8.68	<0.0001	**
	Year: MAM	-0.06	0.03	-2.45	<0.05	**
	Year: ON	-0.03	0.03	-1.36	0.17	
Min Temp	DJF	22.34	0.06	368.60	(22.23, 22.46)	**
	JJAS	21.25	0.06	375.47	(21.14, 21.36)	**
	MAM	22.36	0.06	371.86	(22.25, 22.48)	**
	ON	22.02	0.07	328.67	(21.89, 22.15)	**
	Year: DJF	0.30	0.05	6.05	(0.20, 0.39)	**
	Year: JJAS	0.16	0.05	3.41	(0.07, 0.26)	**
	Year: MAM	0.25	0.05	5.06	(0.15, 0.34)	**
	Year: ON	0.31	0.05	6.05	(0.21, 0.41)	**

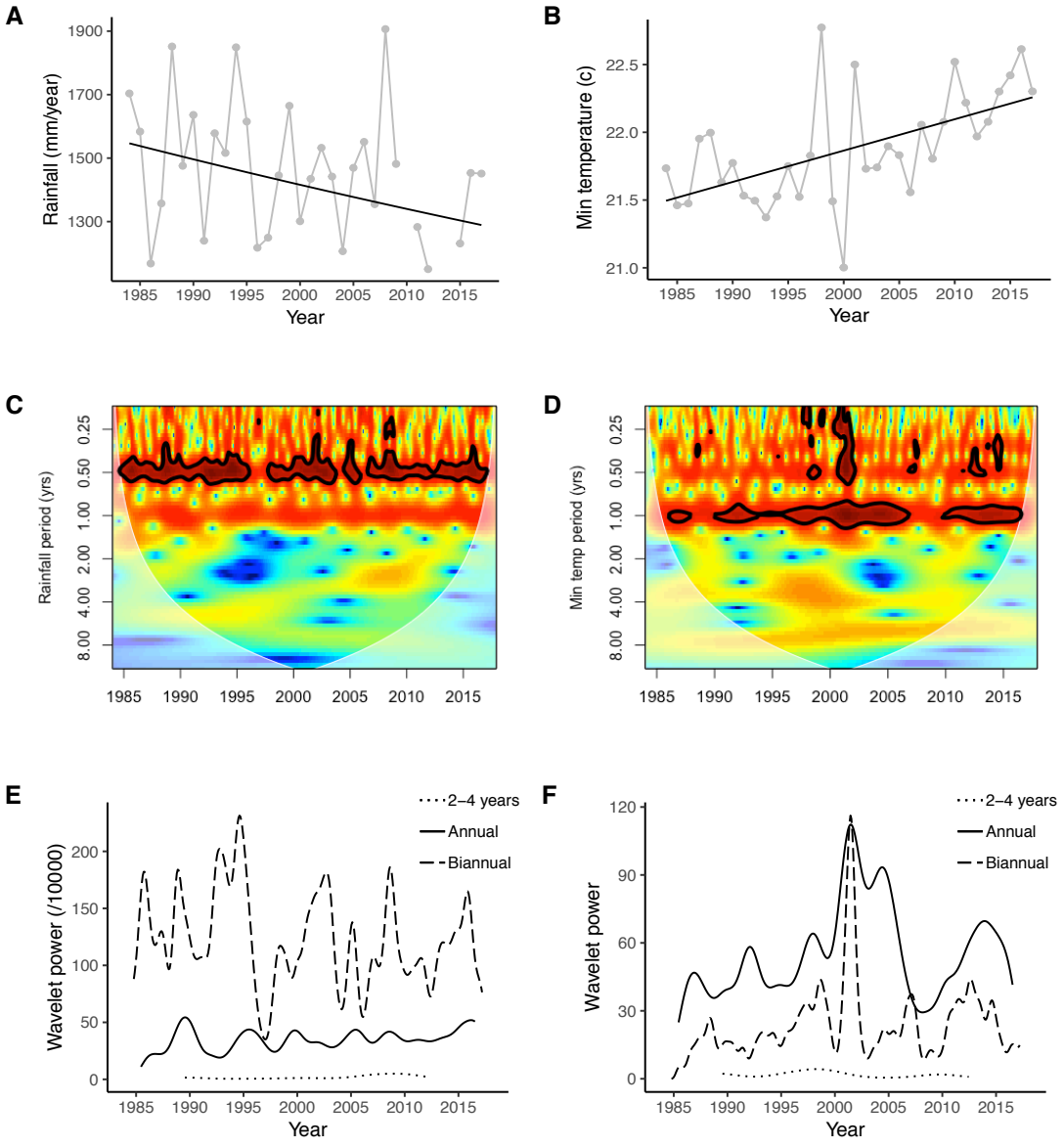

Figure 4.4. Inter-annual variation, long-term trends and periodicity for rainfall and temperature at Lopé NP, Gabon.

A-B: Inter-annual variation (grey line) and long-term trends (black line) for total annual rainfall (1984-2018; generalised linear mixed model, family=Poisson) and mean minimum daily temperature (1984-2017; linear mixed model). C-D: Wavelet transforms of the monthly time-series for rainfall and minimum temperature data at Lopé The faded region indicates the "cone of influence" where end effects made the data unreliable. The colour indicates the power of the cycle at each time period, red= high power and blue = low power. Bold black lines indicate cycles with significant power (Chi-sq test). E-F: Extracted wavelet components for the biannual, annual and multi-annual (mean of 2-4 years) periods from C-D respectively adjusted for edge effects.

4.4.3 PERIODICITY OVER TIME

Wavelet analysis gave further indication of the nature of these changes. The dominant six-month cycle for rainfall was, on average, 3.5 times as powerful as the annual component and 65 times as powerful as the multi-annual component (Figure 4.4E) and remained significant for most of the time period (Figure 4.4C). However the biannual cycle did lose power on three occasions, 1996-97, 2004 and 2006 (Figure 4.4C). The biannual cycle in rainfall appears to be losing power over time while the annual cycle is getting stronger (Figure 4.4E).

The annual cycle for minimum temperature was more than twice as powerful as the biannual component and 30 times as powerful as the multi-annual component (Figure 4.4F) and remained dominant throughout most of the time period with patches of lost power at the end of the 1980s and between 2005 and 2010 (Figure 4.4D). There are also periods of high power in the minimum temperature wavelet at the 2-4 years scale and some significant high frequency cycles around 2003 when the biannual cycle matches the power of the annual cycle. Both annual and semiannual components may be increasing in strength over time (Figure 4.4F).

4.4.4 Influence of sea surface temperatures (SSTs) on interannual variability

Rainfall was significantly correlated with the SSTs of all three oceans while minimum temperature was significantly associated with the Pacific Ocean only (Table 4.4). There were weak positive correlations between IOD and MEI, IOD and NATL and between NATL and SATL (all <0.27, Figure S4.3).

The best model for rainfall incorporated all oceanic indices and each of their interactions with Season, meaning that all three oceans impact rainfall at Lopé in seasonally specific ways (Figure 4.5A and Table 4.4). El Niño conditions reduced rainfall in the months between June and February and increased rainfall in MAM (Figure 4.5G and Table 4.5). The El Niño effect was strongest in DJF and ON where a 1-point decrease in the ENSO index resulted in a predicted reduction of 32mm and 41mm rainfall per month respectively. In MAM a 1-point increase in the ENSO index resulted in a predicted increase of 7mm rainfall per month.

Warm North and South Atlantic SSTs coincided with greater than average rainfall in all seasons (all significantly different from zero apart from the effect of NATL in MAM; Figure 4.5A, B and D and Table 4.5). The South Atlantic had a greater impact on Lopé rainfall than the North Atlantic (size of the estimates; Table 4.5) and was especially strong in the months from March to September (Figure 4D,E and Table 4.5); A 1°C increase in the South Atlantic SST anomaly increased predicted monthly rainfall in MAM by 80mm and in JJAS by 16mm. Positive Indian Ocean Dipole modes coincided with enhanced rainfall in all seasons but were strongest in JJAS (Figure 4.5I and Table 4.5) where a 1-point increase in the IOD resulted in an increase of 11mm monthly predicted rainfall.

The best model for minimum daily temperature retained the interaction with season for MEI only (Tables 4.4 and 4.5 and Figure 4.5A). El Niño conditions significantly increased minimum daily temperature from December to May (Figure 4.5C and Table 4.6). A 1-point increase in ENSO index in these

months resulted in a 0.19°C and a 0.18°C increase in predicted minimum temperature in DJF and MAM respectively.

Table 4.4. Model comparisons to test for the effects of oceanic indices on rainfall and minimum temperature at Lopé.

We used Generalised Linear Mixed Models (family=Poisson) for rainfall and Linear Mixed Models for temperature.. NATL=North Tropical Atlantic SST; SATL = South Tropical Atlantic SST; MEI = Multivariate ENSO Index; IOD = Indian Ocean Dipole; AIC = Akaike Information Criterion, DF = degrees of freedom. Asterisks indicate the simplest model with lowest AIC.

Response	Predictors	DF	AIC	
Rainfall	Season + NATL: Season + SATL: Season + MEI: Season + IOD: Season + Year: Season	26	12233.8	**
	Season + NATL: Season + SATL: Season + MEI: Season + IOD + Year: Season	23	12325.9	
	Season + NATL: Season + SATL: Season + MEI + IOD: Season + Year: Season	23	12847.0	
	Season + NATL: Season + SATL + MEI: Season + IOD: Season + Year: Season	23	12374.5	
	Season + NATL + SATL: Season + MEI: Season + IOD: Season + Year: Season	23	12249.2	
Min. Temp.	Season + NATL: Season + SATL: Season + MEI: Season + IOD: Season + Year: Season	27	500.1	
	Season + NATL: Season + SATL: Season + MEI: Season + IOD:+ Year: Season	24	483.8	
	Season + NATL: Season + SATL: Season + MEI: Season + Year: Season	23	476.6	
	Season + NATL: Season + SATL: Season + MEI+ Year: Season	24	487.3	
	Season + NATL: Season + SATL + MEI: Season + Year: Season	20	464.2	
	Season + NATL: Season + MEI: Season + Year: Season	19	457.2	
	Season + NATL + MEI: Season + Year: Season	16	443.6	
	Season + MEI: Season + Year: Season	15	442.1	**

Table 4.5. Outputs from the best model for the effects of oceanic indices on rainfall at Lopé NP.

The estimates are from generalized linear mixed models (family=Poisson) and are from modified models with the global intercept removed to allow comparison between effect sizes. Asterisks indicate predictors that are significantly different to zero. NATL=North Tropical Atlantic SST; SATL = South Tropical Atlantic SST; MEI = Multivariate ENSO Index; IOD = Indian Ocean Dipole.

Predictor	Estimate	SE	Z Value	P Value	
DJF	4.45	0.37	11.89	<0.0001	**
JJAS	2.89	0.33	8.89	<0.0001	**
MAM	5.18	0.37	13.85	<0.0001	**
ON	5.43	0.46	11.87	<0.0001	**
NATL: DJF	0.06	0.02	4.18	<0.0001	**
NATL: JJAS	0.05	0.02	2.41	<0.05	**
NATL: MAM	0.01	0.01	0.68	0.49	
NATL: ON	0.09	0.02	4.87	<0.0001	**
SATL: DJF	0.12	0.01	10.47	<0.0001	**
SATL: JJAS	0.31	0.02	15.52	<0.0001	**
SATL: MAM	0.15	0.01	15.45	<0.0001	**
SATL: ON	0.05	0.01	4.09	<0.0001	**
MEI: DJF	-0.32	0.01	-24.72	<0.0001	**
MEI: JJAS	-0.11	0.02	-5.29	<0.0001	**
MEI: MAM	0.03	0.01	3.04	<0.01	**
MEI: ON	-0.16	0.01	-11.33	<0.0001	**
IOD: DJF	0.08	0.02	4.66	<0.0001	**
IOD: JJAS	0.22	0.02	12.32	<0.0001	**
IOD: MAM	0.03	0.01	2.63	<0.01	
IOD: ON	0.05	0.01	4.76	<0.0001	**
Year: DJF	-0.05	0.04	-1.31	0.19	
Year: JJAS	-0.34	0.04	-8.68	<0.0001	**
Year: MAM	-0.09	0.04	-2.65	<0.01	**
Year: ON	-0.09	0.04	-2.44	<0.05	**

Table 4.6. Outputs from the best model for the effects of oceanic indices on minimum temperature at Lopé NP.

The estimates are from linear mixed models for temperature and are from modified models with the global intercept removed to allow comparison between effect sizes. Asterisks indicate predictors that are significantly different to zero. MEI = Multivariate ENSO Index.

Predictor	Estimate	SE	T Value	Lower 95% CI	Upper 95% CI	
DJF	22.29	0.21	105.32	21.92	22.66	**
JJAS	21.19	0.18	115.12	20.87	21.51	**
MAM	22.29	0.21	105.45	21.92	22.66	**
ON	21.95	0.26	85.17	21.50	22.40	**
MEI: DJF	0.19	0.04	4.71	0.11	0.26	**
MEI: JJAS	0.05	0.04	1.29	-0.03	0.13	
MEI: MAM	0.18	0.05	3.93	0.09	0.27	**
MEI: ON	0.05	0.05	1.02	-0.05	0.15	
Year: DJF	0.31	0.05	5.79	0.21	0.42	**
Year: JJAS	0.16	0.05	3.21	0.06	0.26	**
Year: MAM	0.26	0.05	4.81	0.15	0.36	**
Year: ON	0.32	0.06	5.13	0.20	0.44	**

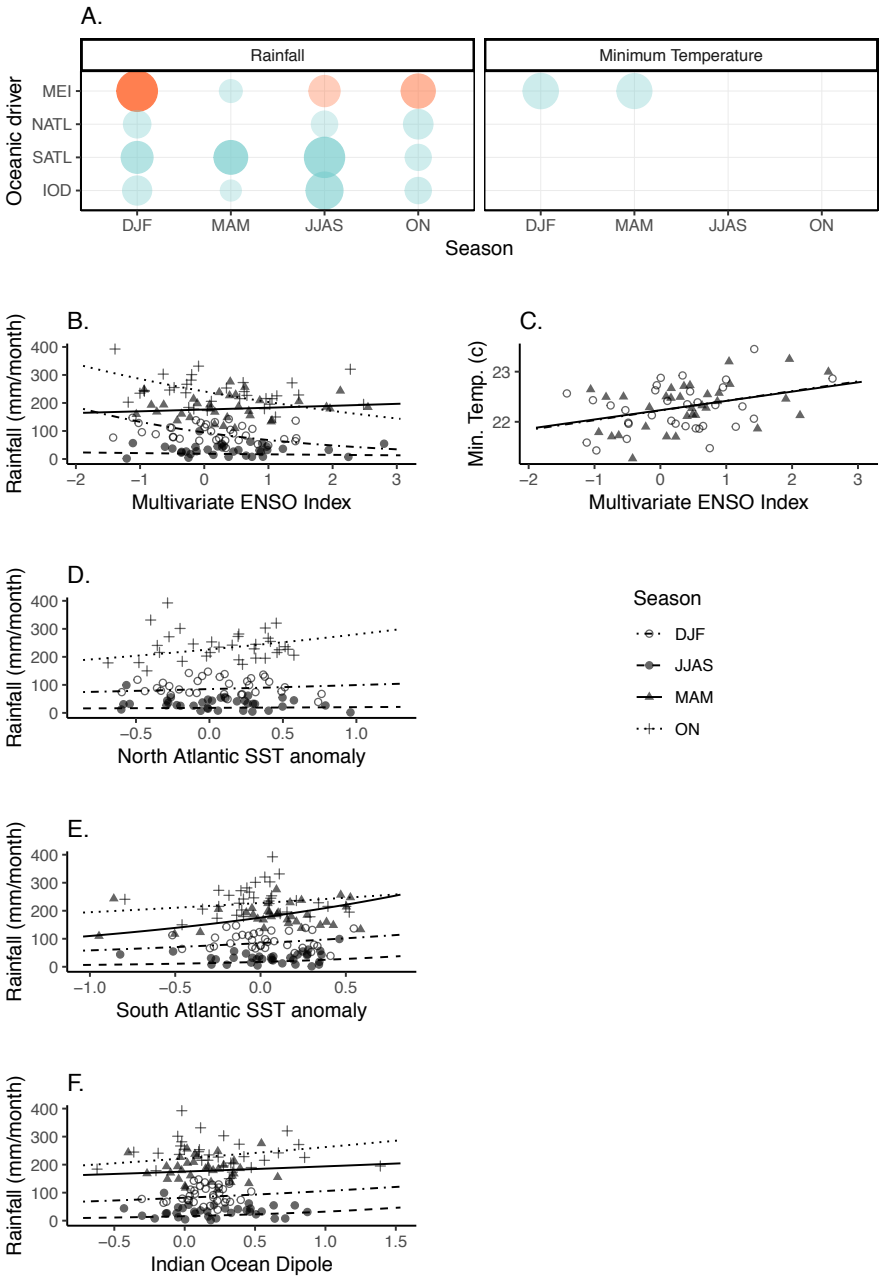

Figure 4.5. The influence of oceanic Sea Surface Temperatures (SSTs) on Lopé rainfall and temperature.

A. Standardised effect sizes for significant correlations between each oceanic index (NATL = northern tropical Atlantic SST, SATL= southern equatorial Atlantic SST, MEI = Multivariate ENSO Index, IOD = Indian Ocean Dipole) and both total monthly rainfall and mean minimum daily temperate. Colour indicates the direction of the correlation (blue= positive, red=negative). The size of the circle indicates the relative size of the effect and the transparency of the circle indicates the uncertainty (low transparency = low T/Z value = high uncertainty, high transparency = high T/Z value = low uncertainty). B-F The raw data (summarised to seasonal means) and model predictions (linear mixed

models for temperature, generalised linear models, family=Poisson, for rainfall) from the best-fit models for the effects of each oceanic index.

4.5 DISCUSSION

4.5.1 OUR RESULTS

Lopé weather has changed significantly over the last three decades, warming at a rate of 0.23°c per decade (minimum daily temperature) and drying at a rate of -52mm per decade (total annual rainfall). Both trends are seasonally dependent: warming was significant in all seasons, but most rapid from October to February and most gentle in the long dry season, while rainfall showed significant decline between March and September only, incorporating both the long rainy season and the long dry season.

The drying trend at Lopé supports observations of reduced flow from March to September (which includes the long rains and the long dry season) for the Ogooué river (to which the Lopé watershed drains; Mahe et al. 2013) and precipitation declines evident from gridded gauge-data for the Gabon/Cameroon region (-1% total annual rainfall, 1968-1998; Malhi & Wright 2004). However, the Lopé total annual rainfall decline of -3.6% per decade exceeds the trend estimated from the regional gauge-data. While the biannual wavelet component for rainfall appears to be declining at Lopé along with the overall interannual trend, the annual component is getting more powerful. Declines in rainfall in the long but not the short dry season are likely to be further differentiating the two seasons and enhancing an overall annual rainfall cycle.

The warming trend recorded at Lopé is greater than that estimated for the location over the same time period using the Berkeley and CRU gridded datasets (+0.16°C and +0.18°C respectively). It is also greater than that identified using satellite data for mean annual temperature for all tropical Africa (0.15°c , 1979-2010; Collins 2011), but is lower than the change estimated from gridded observational data (CRU) for mean annual temperature specifically for African tropical forests (+0.29°c per decade, 1976-1998; Malhi & Wright 2004). This latter analysis showed African

tropical forests to be warming faster than those in both America and Asia (0.26 and 0.22°c per decade, respectively. While we haven't been able to calibrate the data recorded between different equipment over time at Lopé there is good evidence that the warming trend observed there since 1984 is real. The slower warming trend in the already cool long dry season is likely to account for the apparent increase in the power of the annual wavelet component for Lopé minimum temperature.

In addition to these directional trends in climatological averages, interannual weather variability is highly influenced by global weather patterns at our site. Our analysis shows that interannual variation in rainfall at Lopé is linked to the SST patterns of all three oceans while temperature variation is only significantly associated with the Pacific. The SSTs of the North and South tropical Atlantic regions positively influence Lopé rainfall in all seasons and the influence was especially strong in the southern equatorial Atlantic from March to September. This association between Atlantic SSTs and rainfall is supported by other analyses of interannual rainfall variation for WEA; Camberlin et al. (2001) found that the Atlantic dipole (cool temperatures in the North Atlantic and warm temperatures in the South Tropical Atlantic) is associated with higher than average rainfall in March-May, while Balas *et al*. (2007) found that positive temperature anomalies in the southern equatorial Atlantic (especially the Benguela coast) enhanced rainfall in the long dry season. In another study, warm southern Atlantic anomalies were shown to correlate positively with rainfall in both dry seasons (Otto *et al.* 2013). South Tropical Atlantic SST and circulation patterns have been an important influence on Congo Basin precipitation for the past 20,000 years (Schefuss *et al.* 2005).

Lopé rainfall is positively correlated with ENSO from March to May and negatively correlated from June to February, influencing the rainfall contrast between seasons. In La Niña years, rainfall is above average from December-February, making it much more similar to the March-May rainy season (where rainfall is reduced). In El Niño years, rainfall is below average in December-February increasing the contrast with the rainy seasons which are

also much more similar to each other at these times (Figure 4.3G). While these findings support the conclusion that ENSO influences rainfall in the region, there are disagreements between our study and other analyses as to the direction of influence. Three major analyses of the effects of ENSO on rainfall in central Africa using satellite and gridded data concluded that El Niño reduces rainfall from December to September (including both dry seasons and the March-May rainy season; Preethi et al. 2015; Camberlin et al. 2001; Balas et al. 2007). We observed reduced rainfall at Lopé in El Niño years from December-February and June-September, but found the opposite interaction between ENSO and rainfall in March-May. Finally, we found that positive dipole modes for the Indian Ocean (above average SSTs along the east African coast) led to increased rainfall in all seasons at Lopé. The IOD was similarly found to influence rainfall in the long dry season in another study focussing on the central equatorial region just to the east of Gabon, although the sign of the correlation was not made known (Otto *et al.* 2013). Overall, our work supports the idea that the drivers of rainfall variability in WEA are highly complex, with strong local and seasonal influence from the major oceans. Land topography (e.g. the highlands of Gabon, Cameroon and East Africa) is also likely to be a major influence on the highly localised expressions of rainfall and rainfall variability in the region (Balas *et al.* 2007; Dezfuli *et al.* 2015).

Model projections for rainfall remain broad for WEA and as a result, averaged model trends are close to zero. Those models that predict drying in WEA do so due to a northward shift of the ITCZ, related to cool SSTs in the Gulf of Guinea in in all seasons, but most markedly in March-May (The Atlantic cold tongue; James et al. 2013). We found strong reductions in rainfall in these months associated with a cool southern equatorial Atlantic (0°- 20°S) and thus our data provides some support for the mechanisms behind the “dry” models for WEA.

Anomalously warm Pacific Ocean conditions (El Niño) are associated with above average minimum temperatures at Lopé from December to May. This result is supported by a continent-wide study showing increased warming in

El Niño years throughout Africa (Collins 2011). As the long-term trend in minimum temperature was retained in our final model, alongside ENSO, it is likely that the El Niño effect is not the main influence on long-term warming in the region (as in Collins 2011). The Atlantic and Indian Oceans had no significant effects on temperature at Lopé once the general warming trend was accounted for in our model. This means that both Lopé and the Atlantic oceans are warming, but that we find no evidence that one causes the other, above and beyond the established global warming trend. This strong association between ENSO and Lopé minimum temperature is likely to account for the periodicity evident in the wavelet transform at ENSO scales (two to eight-year window).

Another question that arises from our analysis and merits further investigation is: What causes seasonal variability in surface solar radiation in WEA? We know from our data that aerosols are not the main driver of seasonal radiation variability as the highest aerosol load at Lopé occurs during the short dry season while surface solar radiation is lowest during the long dry season. Seasonal and inter-annual variation in coarse and fine dust concentrations, as well as cloud, will be important in understanding the availability of photosynthetically active radiation for vegetation in the region. Of further interest to us at Lopé is the role of Saharan dust and smoke mass in aerosol loads in WEA (Yang *et al.* 2013) and its impact on irradiance. Various studies have commented on the links between the tropical rain belt and African easterly jets (including anomalous westerly winds; Nicholson & Grist 2003), suggesting that variability in rainfall may be related to wind speeds and to a decoupling of the ITCZ and the tropical rainbelt. Further observations of wind speed at Lopé and use of data from other weather stations in the region, alongside regional atmospheric models, may shed light on these issues.

4.5.2 Data quality and availability

One of the major issues with climate analysis in central Africa is the limited and declining publicly available data from weather stations in the region: The nearest weather stations to Lopé listed on the Global Historical Climatology

Network (GCHN) Daily Database (Menne et al. 2012) are between 136 and 185km away and there is no public data available since 1980. The World Meteorological Organisation (WMO) has a minimum recommended density of weather stations eight times higher than the modern density of weather stations in Africa (Collins 2011). This lack of data has direct impacts on the quality of gridded climate data products (Suggitt et al. 2017) and ability to calculate daily climatic indices for the extremes (Niang *et al.* 2014). Gabon is also one of the cloudiest places on earth (http://www.acgeospatial.co.uk/the-cloudiest-place/) which leads to large uncertainties in satellite estimates, with some satellite algorithms overestimating rainfall in the region by at least a factor of two (Balas *et al.* 2007). Finally, poor correlation between the rainfall of central Africa and neighbouring regions and variability between individual stations suggests much local influence (Balas *et al.* 2007), further confounding the challenges of sparse data.

The importance of maintaining long-term tropical study sites and improving the quality and type of weather measurements has been known for some time (Clark 2007). However, the region is remote and there are many financial, logistical and political challenges to face when servicing field stations to address this. One such issue is that WEA has the highest frequency of lightning strike in the world (Balas *et al.* 2007) leading to difficulties and great expense maintaining equipment. Lightning is an issue we regularly confront at Lopé and that has led to major gaps in the data record. While automatic continuous measurements can provide vast amounts of detailed data relevant for ecological studies they are also inherently more susceptible to technical failures that need expert fixes and in our experience data gaps are more likely to go unnoticed than for manual data collection. Whilst we welcome new automatic data methods, we recommend maintaining long-term manual records alongside for consistency.

4.5.3 Conclusions for the tropical forest biome

We have shown that while there are many agreements between our data and regional analyses, particularly for seasonal norms and long-term warming,

there are also surprises, including the positive influence of ENSO on rainfall from March to May. While there remains uncertainty in the direction of precipitation change in the region more widely, the reduction in rainfall observed at Lopé lends support to the drying trend evident from other observational data (both gridded gauge data and river run-off) for WEA and its association with the Atlantic cold tongue.

It is only 4000 years ago that the forests of the Congo-Ogooué basin are likely to have retreated due to climate change (Willis *et al.* 2013), raising the strong possibility that such ecosystem-wide changes might happen again. Extreme mean temperature increases are most likely to result in reduced photosynthetic capacity of tropical forests via reduced enzyme activity (Cusack *et al.* 2013). Increasing minimum daily temperature (which reflects night-time temperatures) are likely to reduce plant growth through increased loss of CO_2 and moisture due to respiration and transpiration (Cusack *et al.* 2013). While CO_2 enrichment may act to override the influence of temperature by increasing plant water use efficiency (James *et al.* 2013), drought has been shown to lead to increased deciduousness, shorter trees, simplified canopy structure and decreased leaf-area index (van Schaik *et al.* 1993). It has been suggested that African tropical forest species may be relatively drought-adapted compared to those found elsewhere because of the extreme climatic cycles (Asefi-najafabady & Saatchi 2013). However James et al (2013) emphasise that precipitation levels in African forests are already near to the hydrological limit for closed canopy forest, and that drier conditions are likely to lead to water stress.

Our seasonal analysis of weather variability at Lopé further serves to emphasise the ecological importance of the long dry season in the western equatorial African tropics; Three-four months that are anomalously dry (almost no rainfall for 60 consecutive days) and getting drier, cool (mean maximum daily temperature is 2.5°C lower in July compared to April), and that experience high wind speeds, low humidity and limited light availability (although light quality might be high; Philippon *et al.* 2019). Such a defined season poses specific challenges to the biota and is likely to act as a temporal

marker for ecological events, similar to a winter event in temperate regions. The long dry season is highly likely to be an unfavourable period for photosynthesis and for most reproductive events that require high energy and moisture availability. The response of the biota to this recurrent and predictable seasonal drought could be used to estimate their long-term response to drying over multi-annual time scales (Detto *et al.* 2018). In addition, the seasonal synchrony between moisture and light in western equatorial Africa gives an opportunity to test the relative importance of each for adaptive plant phenology, when compared to other tropical regions where these factors are asynchronous. In contrast to the Asian and American tropics, the vegetation of western equatorial Africa "has it all" in the rainy seasons with both moisture and light in abundance.

The long-term observations we presented here have not previously been made public and, while they are derived from a single site, are of great value in such a data-poor region. The co-occurrence of this local weather record alongside long-term vegetation and animal monitoring at Lopé is well situated to elucidate the mechanisms of tropical forest adaptation to climate change in western equatorial Africa. Will warming occur slowly enough for plants to acclimate? Can individual plants adapt to new rainfall regimes within their lifetime through changes in deciduousness and leaf chemistry? Or will the new climate regime lead to increased mortality and long-term compositional shifts in the forest biome? These are all vital questions that require urgent investigation and to which end this accurate local data can be used.

4.6 ACKNOWLEDGEMENTS

Weather research at SEGC, Lopé National Park was funded by the International Centre for Medical Research in Franceville (CIRM; 1986-2010) and by Gabon's National Parks Agency (ANPN; 2010 – present). We acknowledge significant periods of independent data collection undertaken by Richard Parnell, Ruth Starkey, Edomond Dimoto and Lee White.

Permission to conduct this research in Gabon was granted by the CIRMF Scientific Council and the Ministry of Water and Forests (1986 – 2010), and by ANPN and the National Centre for Research in Science and Technology (CENAREST; 2010 – present).

S4 SUPPORTING INFORMATION

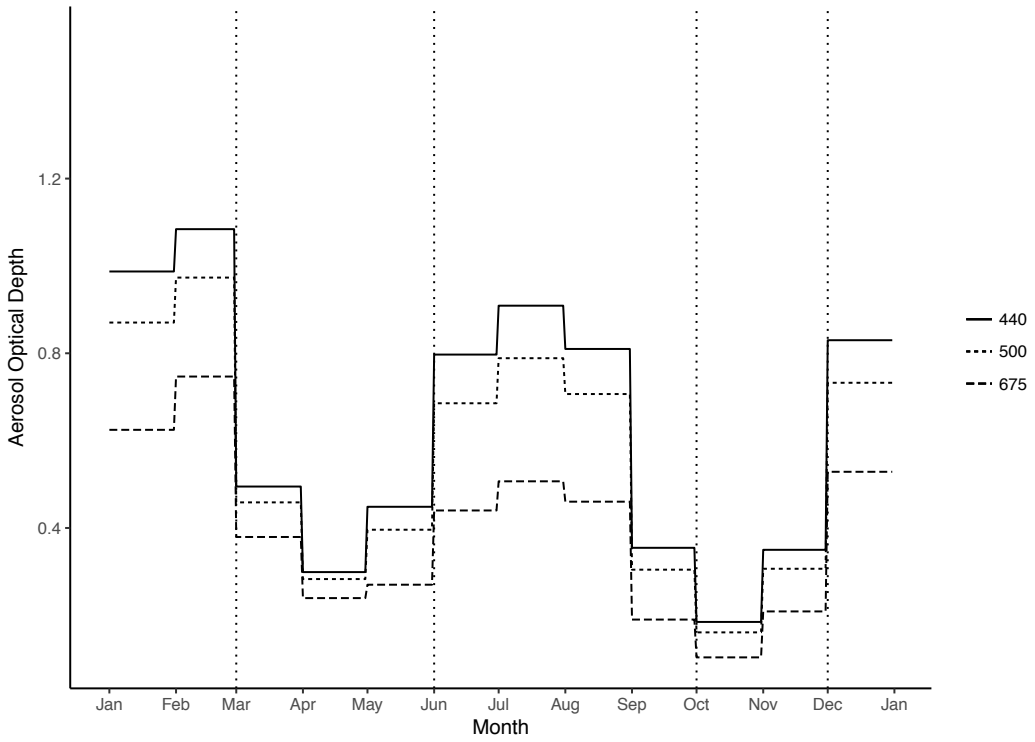

Figure S4.1: Seasonality of aerosol optical depth at three different wavelengths (440nm, 500nm and 675nm) relevant for photosynthetically active radiation.

Shown are monthly means of daily data 2014-2017 from Lopé NP.

Figure S4.2. Time series of annual mean minimum daily temperature for two gridded data products for Lopé NP, Gabon.
The black line represents temperature data recorded at Lopé and the coloured lines are from gridded regional data products: daily minimum air temperature from the Gridded Berkeley Earth Surface Temperature Anomaly Field (Rohde et al. 2013) and monthly mean daily minimum temperature from the Climate Research Unit's Time-Series v4.01 of high-resolution gridded data (CRU TS4.01; University of East Anglia Climatic Research Unit et al. 2017; Harris et al. 2014). The annual mean is calculated from deseasonalised monthly means.

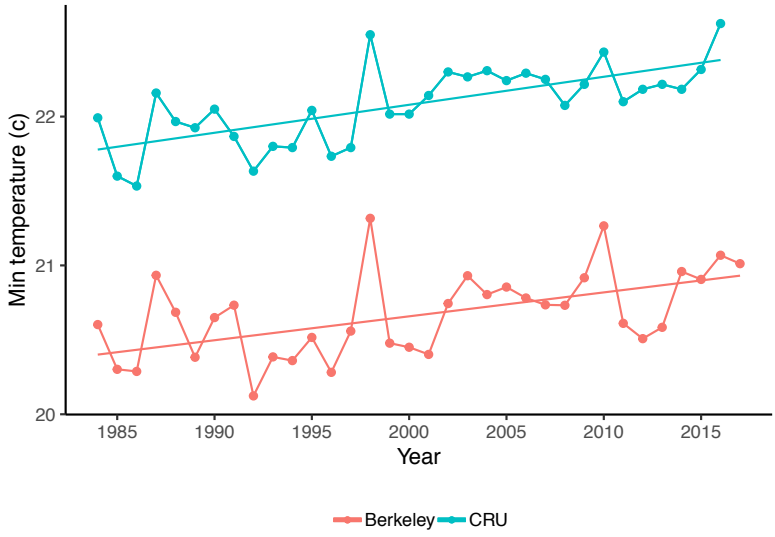

Figure S4.3. Trend in annual mean minimum daily temperature for two gridded data products for Lopé NP, Gabon.
The dots and lines represent the data (annual means of monthly means) and the thin lines represent the trend derived from a linear mixed model

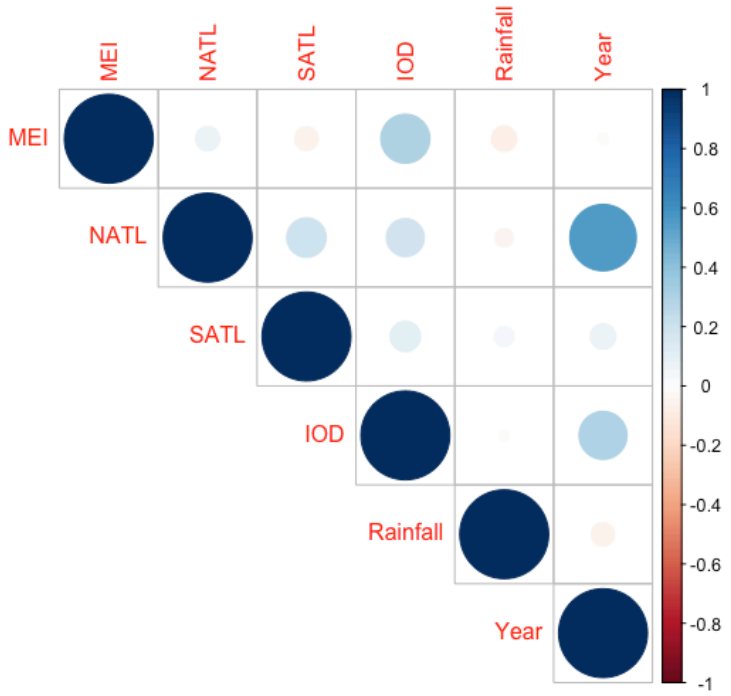

Figure S4.4. Plot showing matrix of Pearson correlation coefficients for four oceanic indices and rainfall.

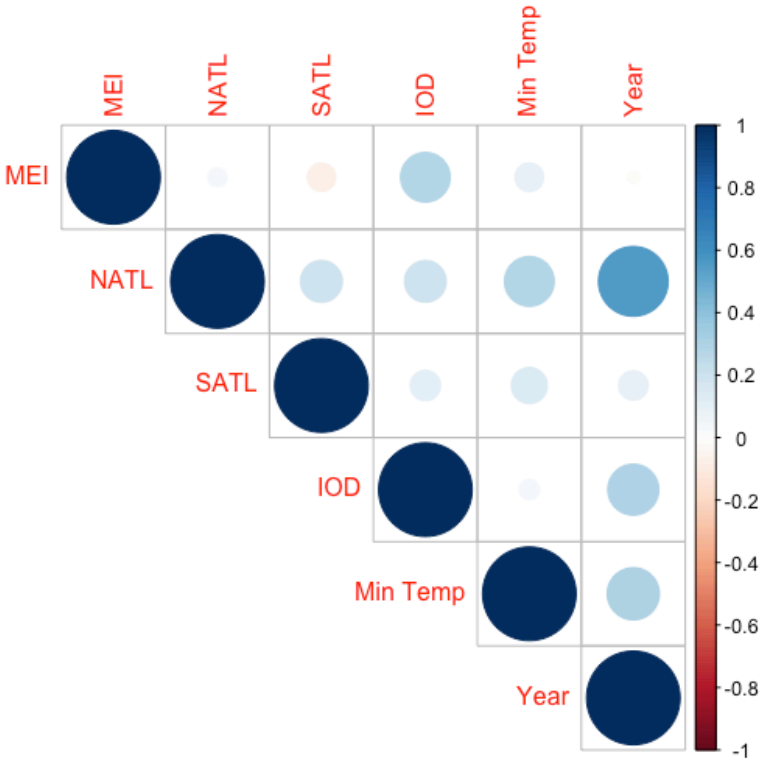

Figure S4.5. Plot showing matrix of Pearson correlation coefficients for four oceanic indices and minimum temperature.

CHAPTER 5

CO_2 drives long-term reduction in tropical canopy leaf turnover

5.1 ABSTRACT

Phenological cycles in leaf turnover and leaf photosynthetic activity are tightly coupled with both local and global climatic and atmospheric processes. However there are very few observational studies of leaf phenology in the tropics and most uncertainty over tropical land areas in recent earth system models is due to poorly characterised impacts of climate and CO_2 on primary productivity. In this analysis we present newly available leaf phenology data from long-term focal-crown observations at Lopé National Park, Gabon (1986-2018). For a sample of 108 individual trees, representative of the most common canopy species in the region, we use a range of methods (including Fourier analyses and Generalised Linear Mixed Models) to test for seasonality and long-term trends in leaf phenology and to evaluate the relative importance of light, moisture, temperature, CO_2 and leaf herbivory as drivers of monthly and interannual variation in tropical forest leaf production. We found that despite relatively low annual rainfall and strong rainfall seasonality, the Lopé forested region is dominated by evergreen leaf phenology with mature leaf canopies maintained throughout

the long dry season. New leaf production is common all year round except for the long dry season when leaf development is supressed due to reduced light availability. Moisture, light and leaf herbivory are all positive predictors of new leaf production at seasonal scales. A long-term decline in the probability of leaf flush for all species is strongly associated with the rise in CO_2. While the mechanism for this remains unclear, we propose a theory based on delayed senescence and increased leaf longevity related to improved water use efficiency and a slower decline of photosynthetic rate with leaf age. This is the first time a reduction in leaf turnover has been shown for a tropical forest and our results challenge the idea that the warming and drying trend predicted for western equatorial Africa will lead to increased deciduousness. Such predictions refer to species turnover in the long-term and few studies have assessed the likely impacts of environmental change within the lifetime of long-lived canopy trees.

5.2 INTRODUCTION

Leaves are highly specialised, transitory organs adapted for optimal carbon capture and sunlight absorbance. They pass through a series of developmental stages from leaf bud and emergence (birth) to maturation, senescence and eventually abscission (death) and these phenophases will be apparent many times in a tree's lifetime. Vegetative phenology concerns not only the physical development of leaf cohorts but also their physiological activity (photosynthesis, evapotranspiration etc.) and is tightly coupled with climatic and atmospheric processes on local and global scales (Richardson *et al.* 2013). Leaves and leafy canopies alter climate and atmospheric composition through absorption of sunlight, evaporative cooling, carbon sequestration and oxygen production and are themselves impacted by these processes (Mitchard 2018; Bonan 2008).

Extensive evidence for the impacts of global environmental change on vegetative phenology points towards elongated growing seasons driven by global warming and elevated CO_2 in temperate regions (Menzel *et al.* 2006; Cleland *et al.* 2007; Chambers *et al.* 2013). However the picture is much less clear for the tropics where phenological controls on leaf emergence, leaf

longevity and photosynthetic activity are highly complex and often poorly understood. Moisture and light availability are thought to be much more likely candidates than temperature as drivers of seasonal leaf phenology in the tropics (Cleland *et al.* 2007; Cook *et al.* 2012). Changes to precipitation regimes, CO_2 concentration, temperature and cloudiness are all hypothesised to influence tropical foliar development and tree growth on interannual scales (Reich 1995; Lewis *et al.* 2009; Richardson *et al.* 2013).

Despite the importance of tropical forests for the global carbon cycle (Mitchard 2018), there are very few ground-based observational studies of leaf phenology in the tropics and even fewer that have monitored phenological activity over long time frames. Remote sensing has great potential for sampling leaf phenology across landscapes but there have been controversies over the biological interpretation of canopy reflectance data at the plant-level and the impacts of non-leaf artefacts such as solar zenith angle (Huete & Saleska 2010; Morton *et al.* 2014; Wu *et al.* 2018). Remote sensing is thus far unable to contribute widely to our quantitative understanding of species or individual-level plant responses to global environmental change. Most of the uncertainty over tropical land areas in the most recent earth system models is due to disagreement on the modelled impacts of climate and CO_2 on primary productivity (Mitchard 2018).

In this chapter we present an economic theory of leaf exchange and review the evidence for seasonal and interannual controls on tropical tree leaf phenology before presenting and discussing newly available data from focal-crown observations at Lopé National Park, Gabon (1986-2018). Long-term ground-based phenology data are a rare but highly valuable resource in global change research and can be used to evaluate the mechanisms behind tropical leafing strategies to ground-truth and interpret the biological basis for large-scale canopy observations.

5.2.1 Leaf phenology as an economic process

The major axes of variation in the leaf phenology of perennial plants are leaf habit, individual leaf lifespan and the timing and patterning of leaf

emergence. Leaf turnover is essentially an economic process and phenology should be organised in a way that maximises carbon gain for the plant, taking account of leaf construction costs, photosynthetic rate and its decline with leaf age due to damage, dirt, accumulation of epiphylls and redistribution of nitrogen within the plant (Kikuzawa & Ackerly 1999; Kitajima *et al.* 2002; Toomey *et al.* 2009).

Plants with leaf-exchanging or (semi-) evergreen habits replace leaves sequentially and are never leafless for more than a very short period (Singh & Kushwaha 2005). These species are found most frequently in equatorial and boreal latitudes (Kikuzawa 1995). Deciduous plants by contrast undertake complete canopy turnover with a distinct leafless period and are most common in temperate regions where leaflessness during the winter is an adaptation to low temperatures and limited light availability and also to avoid frost and snow damage. Deciduousness in the tropics is usually a response to water stress and is determined by a combination of seasonal drought and geology (Singh & Kushwaha 2005; Ouédraogo *et al.* 2016).

Leaf longevity has been described as the "duration of the revenue stream from each leaf constructed" (Wright *et al.* 2004) and among tropical evergreen trees ranges from as short as ten days to greater than ten years (Kikuzawa & Ackerly 1999). Leaf lifespan strongly co-varies with the costs of leaf construction and maintenance (leaf mass per area) as well as the biomechanical and transport costs associated with plant size and life form (Kikuzawa & Ackerly 1999; Wright *et al.* 2004; Osnas *et al.* 2013). As a tree grows, the cost of supporting leaves in the upper canopy increases and may be compensated by increased leaf lifespan; Adult broadleaf deciduous trees in Japan have longer-lived leaves than seedlings of the same species (Kikuzawa & Ackerly 1999). However, there is little evidence for an impact of plant size on leaf lifespan in trees post-seedling stage, especially when compared to other factors. Increased leaf longevity among mature plants is more often associated with shading and nutrient-poor soils (Reich et al. 2004). In temperate regions elevated CO_2 is thought to reduce the rate of photosynthetic decline with leaf age, making it economical for some plant

species to delay autumnal senescence, increasing leaf longevity and extending the growing season (Cleland *et al.* 2007; Taylor *et al.* 2008). Reich (1995) hypothesised a similar effect of elevated CO_2 on leaf longevity in dry tropical forests, where improved water use efficiency could reduce water stress and delay leaf fall in the dry season, although extreme warming could act against this by enhancing water stress via increased evapotranspiration. In addition they considered the possibility that elevated CO_2 could in fact accelerate leaf development, leading to leaf shedding in seemingly unstressful conditions and reduce leaf lifespan.

5.2.2 Seasonal controls on tropical leaf phenology

In the neotropics there is seasonal asynchrony between light and moisture leading to light-limited rainy seasons and bright dry seasons (e.g. Barro Colorado Island, Panama; Wright & Calderón 2018). Leaf phenology is key to understanding the on-going debate as to whether the tropical forests that experience this climate are water-limited (with evidence for dry season declines in productivity mainly originating from modelling studies) or light-limited (evidence for dry season increases in productivity mainly originating from *in situ* and satellite studies; reviewed in Wu et al. 2016). Young and senescing leaves tend to have reduced infra-red reflectance compared to mature leaves due to less chlorophyll per unit area (Wu *et al.* 2017a, 2018). Leaf demography (the distribution of leaf ages within the canopy) is the dominant factor accounting for remotely-sensed seasonality in reflectance (Lopes 2016). At their study site in the Brazilian Amazon, Lopes (2016) observed that leaf flush occurs at the start of the dry season, 3-5 months before the seasonal peak in reflectance. Wu *et. al.* (2017b) found that while environmental variation is the dominant driver of ecosystem productivity at hourly to daily timescales (i.e. water availability limits photosynthetic function in a given assemblage of leaves), it is biotic variation (associated with leaf phenology) that dominates productivity at seasonal scales (i.e. light availability limits new leaf production in the canopy).

Long-term observations from Panama show that tree species tended to drop their leaves before the dry season and the leaf area index is lowest from the

beginning to the middle of the dry season, rising towards the end of the dry season and peaking in the rainy season (Detto *et al.* 2018). New leaf development is enhanced during the dry season because of the abundance of light and the reduced leaf area at this time is thought to help relieve water stress and can be achieved without compromising productivity because photosynthesis is more efficient in the bright conditions (Wright & Cornejo 1990). In the Hawaiian Islands, where dry seasons are also bright, leaf phenology is specific to the forest type and rainfall regime (Pau *et al.* 2010). In the water-abundant rainforests, plants can take advantage of increased light availability during the dry season and respond with community-wide green-up, where as the water-limited dry forests become less green during the same season due to water stress.

An analysis of new leaf production and leaf fall along a spectrum of central American tropical forests with different rainfall regimes, showed that leaf phenology is much more highly synchronised in dry forests (<1500mm total annual rainfall) with leaf fall peaking during the dry season and leaf production peaking during the rainy season (Reich 1995). In contrast, leaf phenology in the rain forests (>3500mm total annual rainfall) was much less synchronised and the plant community was also able to produce leaves during the drier (and brighter) period of the year.

In western equatorial Africa, light and moisture are strongly synchronised (Chapter 4 and Philippon *et al.* 2019)) - with high irradiance during the rainy seasons (due to low cloud cover during the day) and low irradiance during the dry seasons (due to high cloud cover and increased aerosol load) - making the rainy seasons optimal for both new leaf development and photosynthetic activity. Remote sensing studies have shown that central African evergreen forests are most green during the rainy seasons and least green during the long dry season (Gond *et al.* 2013; Guan *et al.* 2013; Philippon *et al.* 2014). Canopy structure (leaf biomass and water content of the upper canopy) however is reduced during the rainy seasons because the bright conditions stimulate leaf turnover thus temporarily reducing the leaf area in the canopy (Guan et al. 2013). Canopy structure peaks during the long

dry season when leaf turnover is reduced and the new leaves produced in the dry season have matured. Evergreen forests in central Africa are limited to the light-deficient western region (Gabon), where potential evapotranspiration is reduced in the long dry season (Philippon *et al.* 2019).

Thus it appears that both water and light are important seasonal environmental controls on tropical vegetative phenology with the rainfall regime determining the dominant leaf habitat of the plant community in combination with potential evapotranspiration (lower annual precipitation and more extreme dry seasons leading to deciduous phenology) and seasonal moisture and light availability driving the timing of peak photosynthetic capacity and leaf production respectively.

5.2.3 Interannual controls on tropical leaf phenology

Although mechanistic interpretations of the effects of major climate and atmospheric changes (e.g. to temperature, precipitation and CO_2) on tropical tree leaf exchange remain unclear, there is evidence for directional changes in tropical forest leaf area and function over recent decades. A global analysis of satellite-derived leaf area index (LAI; 1982-2009; Zhu et al. 2016) reported widespread greening across the tropics attributed mainly to elevated CO_2 and "other factors" such as land management and disturbances (e.g. storms and insect attacks). However the picture is more complicated at regional and temporal scales. The global greening described by Zhu *et al.* occurred predominately pre-2000 with seemingly stable or declining LAI observations in most continents since then. In addition, while the authors identified central Africa as one of the strongest regions of greening using combined LAI datasets in the main analysis (1982-2009), an extension to one of the satellite products (GIMMs; 1982-2014) showed recent regional variation, with a continued increase in LAI in western equatorial Africa (northern Gabon and Cameroon) and a newly emerging decline in LAI in the central Congo basin. In the same study, CO_2 was found to have a positive impact on LAI throughout equatorial Africa but climatic changes were shown to negatively impact LAI in the central region, and have marginal positive impacts in the western

region which may explain the local variation in the LAI trend (Zhu *et al.* 2016).

Another analysis of a number of remotely sensed vegetation indices (enhanced vegetation index: EVI, vegetation optical depth: VOD, and canopy backscatter) also uncovered a recent browning of the forest canopy in the central Congo Basin, attributed to the long-term drying trend (2000-2012; Zhou et al. 2014). Water deficit stress causes leaves to become less turgid and eventually to be abscised. The authors argued that while in the short-term, leaves will be replaced when water deficit is alleviated, long-term reductions in rainfall are likely to favour deciduous species and lead to changes in species composition and structure (Fauset *et al.* 2012; Zhou *et al.* 2014).

Large-scale climatic oscillations such as the El Niño Southern Oscillation (ENSO) can also have strong impacts on leaf development in tropical forests. Long-term leaf-litter observations at Barro Colarado Island, Panama from 1987-2017 showed strong coherence between leaf fall and both soil water deficit and solar radiation at ENSO timescales. El Niño years are associated with dry and bright conditions in this region and are preceded by elevated leaf fall, mirroring the seasonal plant response to dry season conditions (Detto *et al.* 2018). In western and central equatorial Africa, ENSO is negatively correlated with canopy greenness (normalised difference vegetation index, NDVI) during the long dry season, related to seasonal reductions in rainfall in El Niño years (and vice versa in La Niña years; Philippon et al. 2014). The authors attributed this effect on canopy greenness in the long dry season to changes in photosynthetic activity not leaf production or senescence.

Lopé is a dry tropical forest in comparison to the neotropical examples mentioned in this introduction (total annual rainfall <1500mm) and has steadily been experiencing drier conditions over the last three decades, especially in the long dry season (Chapter 4). This drying trend combined with increasing temperatures is likely to result in increased evapotranspiration and elevated water stress for plants especially during the long dry season (June-September). In addition, El Niño years are known to

reduce rainfall and increase temperatures in most months at the site (Chapter 4). If reduced precipitation is translated into reduced moisture availability then a community-wide shift towards deciduous species would be expected over the long-term and an increase in water stress for established individuals over the short-term. However it is unclear what mediating effects the cloudiness of the dry seasons and elevated CO_2 may have on evapotranspiration. In the following analysis we test for seasonality and long-term trends in leaf phenology at our equatorial African site and evaluate the relative importance of light, moisture, temperature, CO_2 and leaf herbivory as drivers of monthly and interannual variation in tropical forest leaf production.

5.3 METHODS

5.3.1 SOURCING DATA

Phenology data from the Lopé long-term observational study

Plant phenology observations began at the Station d'Études des Gorilles et Chimpanzées (SEGC) in Lopé National Park, Gabon, in 1986, with the aim of quantifying food resource abundance for primates and other large mammals. Plant species were chosen based on leaf, flower or fruit presence in the diet of gorillas, chimpanzees, mandrills and elephants, with *Aucoumea klaineana* Pierre added in 1996 due its overall abundance in the habitat (highest basal area; White 1995). At the beginning of each month, focal crowns are observed from the ground using 10 x 42 binoculars. Canopy coverage of leaves (new, mature and senescent), flowers and fruit (unripe and ripe) are recorded and noted as a nine-point score representing increments of an eighth of the canopy, from absence of the phenophase to full coverage. Hereafter these scores are converted to percentages from zero to 100%. Leaf damage (i.e. insect herbivory or fungal damage) was recorded as a presence/absence score alongside Lopé phenology observations for each tree each month consistently for all species from 1995 (with some earlier records of exceptionally high leaf damage). Up to the present, there have been >1000 individual plants of 88 different species included in this study.

The SEGC phenology study area is a matrix of habitats and is situated at the northern end of a continuous forest block. The forest bounds an enclosed equatorial savannah that occurs along the mid reaches of the river Ogooué (Figure 5.1). The closed-canopy tropical forest is dominated by *A. klaineana*, a characteristic species of large swathes of forest in western Gabon. Logging occurred in the study area in the late 1960s or early 1970s and *A. klaineana* was extracted at a rate of one tree ha^{-1} (White 1992). Mean total annual rainfall from 1984 to 2018 was 1465mm and has declined at a rate of 78mm per decade (Chapter 4). Mean daily maximum and minimum temperatures in the forest at Lopé over the same period were 28.1°c and 21.9°c respectively and minimum daily temperature has increased at a rate of 0.23°c per decade (Chapter 4).

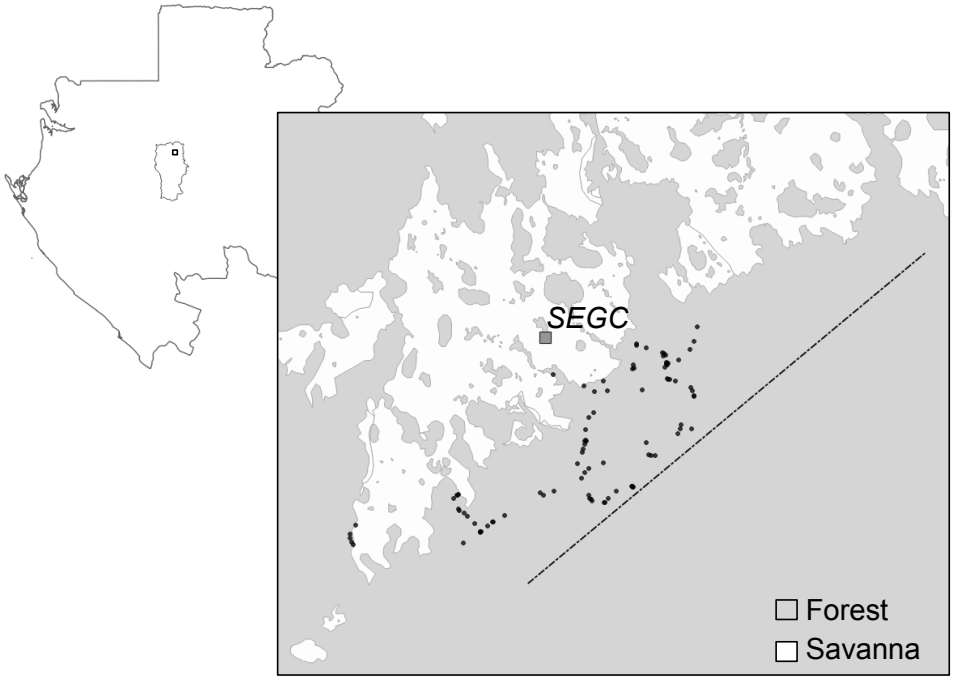

Figure 5.1. Map of the Lopé study area.
The focal trees (black dots) are located on the northern edge of a continuous forest block enclosing an equatorial savannah. A 5km botanical transect (black dashed line) was set up in 1989. The inset map shows the location of study area within the boundaries of Lopé National Park and Gabon. SEGC = Station d'Études des Gorilles et Chimpanzées.

We selected a sample of species from the wider phenology study that are most representative of the surrounding forest canopy in order to assess leaf

turnover at the community level, and allow comparison with remote sensing studies that can only estimate the leaf properties of the upper canopy. To do this we used data for all trees recorded along a 5km botanical transect established in 1989 near to the forested portion of the phenology study area (Figure 5.1; White 1992). All trees and lianas with the centre of their trunks within a 5m strip and $\geq$ 10cm diameter at breast height (DBH) were recorded over a sample area of 2.5ha. We calculated crown volume (CV; which scales with the square of trunk radius, see Shenkin *et al. in review*) for each tree using DBH. We ranked species according to the sum of their CV and calculated cumulative CV as a percentage of total CV for the entire transect. 11 species made up 75% total CV, eight of which - *A. klaineana*, *Cola lizae* N.Hallé, *Dacryodes buettneri* (Engl.) H.J.Lam, *Ganophyllum giganteum* (Engl.) H.J.Lam, *Klainedoxa gabonensis* Pierre, *Pentaclethra macrophylla* Benth., *Pterocarpus soyauxii* Taub. and *Pycnanthus angolensis* (Welw.) Warb. – were included as part of the Lopé phenology study. The eight species account for 63% total CV (Figure 5.2) and are all medium to large trees with crowns in the upper canopy of the forest (Table 5.1).

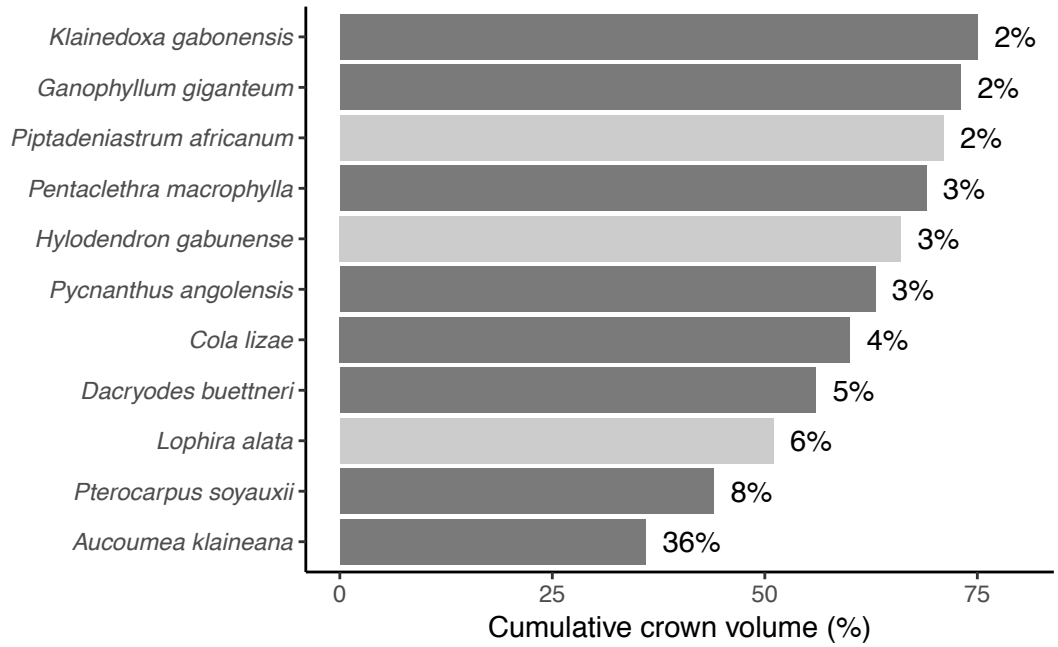

Figure 5.2. All species within 75% crown volume along the 5km botanical transect at Lopé NP.
Shown are the cumulative crown volume for each species in ranked order with their individual contribution written in text to the right of the bars. Dark bars indicate species for which phenology data has been recorded.

We selected leaf phenology data for all individuals of these eight species that had been observed for more than five years and are located within the continuous forest block (Figure 5.1). The resulting sample included 120 individuals with a mean of 15 individuals per species (ranging from 10 to 42) and mean observation length of 293 months (ranging from 65 – 377; Table 5.1).

Table 5.1. Summary of botanical information, leaf phenology and sample sizes of eight species analysed in this study.

Species (Family[1])	**Botanical description[2]**	**Leaf phenology[3]**	**Leaf damage[3]**	**Sample[4]**
Aucoumea klaineana (BURS)	Large tree, 35-40m, 110-240 cm dbh. Nutrients exchanged between individuals. Leaves up to 40cm of 7-13 leaflets. New leaves flush pink. Restricted to Gabon where rainfall >1200mm. Most important timber tree in Gabon.	**Incremental leaf exchange with some seasonality.** New leaves occur at low level (CC<50%) all year, most common Nov-Aug. Strong flushing in certain years after leaf damage in Dec-Feb.	Foliage targeted by leaf-rolling caterpillars Dec-Jan, can result in total defoliation.	n= 42; o = 235 (65-275)
Cola lizae (STER)	Medium tree, 40-50cm dbh. Huge leaves, typically 40-50cm across (in young trees can reach 100cm x 120cm). Very restricted - exclusive to Lopé.	**Incremental leaf exchange with some seasonality.** New leaves occur at low level (CC<25%) all year, most common Apr-Sept.	Leaf warts (cause unknown) occur any time of year.	n= 12; o= 347 (192-377)
Dacryodes buettneri (BURS)	Tall tree, 15-20m and 80-150cm dbh. Leaves 10-30cm long of 5-8 leaflets, dark green. Restricted mostly to Gabon. Popular timber tree.	**Incremental leaf exchange with strong seasonality.** New leaves can occur at low level any time of year (CC<50%) but most common Dec-Jul.	Foliage targeted by same caterpillar as *A. klaineana.*	n = 11; o= 354 (244-377)
Ganophyllum giganteum (SAPI)	Large tree, 40m and >1m dbh. Leaves 25cm long of 11 leaflets. New leaves shiny from resin. Occurs throughout western C. Africa	**Incremental leaf exchange with no seasonality.** New leaves occur at low-level (CC<50%) throughout the year. Occasionally completely defoliated.	Low-level leaf damage (cause unknown) throughout year.	n = 10; o= 353 (317-377)
Klainedoxa gabonensis (IRVI)	Large tree 45m and 120cm dbh in closed canopy forest. Leaves of mature individuals (15cm x 5cm) turn yellow as senesce. Wide ecological tolerance occurring across west and central Africa.	**Incremental leaf exchange with some seasonality.** New leaves occur at low-level (CC<50%) throughout the year, most common Nov-May. Occasionally completely defoliated.	Little leaf damage observed.	n= 10; o = 375 (357-377)
Pentaclethra macrophylla (FABA)	Medium to large tree 30m and 40cm dbh. Large compound leaves 20-45cm long. Young leaves coppery. Wide range across W. and C. Africa.	**Full canopy leaf exchange with some seasonality.** New leaves can occur any time of year but most often Dec-Feb (CC often>50%).	Little leaf damage observed.	n = 10; o = 257 (222-261)
Pterocarpus soyauxi (FABA)	Large tree, >50m and 2m dbh. Compound leaf with 11-17 leaflets (6 x 2.5cm). Mature leaves dark green, young leaves emerald. Wide range across W. and C. Africa.	**Full canopy leaf exchange with some seasonality.** New leaves most common Nov-Dec and Apr-Jun (CC often >50%).	Little leaf damage observed.	n =10; o= 377 (377-377).
Pycnanthus angolensis (MYRI)	Large tree. Leaves 20 x 5cm. New leaf underside rust coloured and hairy. Occurs throughout W. and C. Africa.	**Incremental leaf exchange with no seasonality.** New leaves common (>50% inds) all year (CC<50%). Occasionally completely defoliated.	Circular holes (cause known) in leaves throughout the year.	n =15; o = 242 (67-377)

[1]Families: BURS = Burseraceae; STER = Sterculiaceae; SAPI = Sapindaceae; IRVI = Irvingiaceae; FABA = Fabaceae; MYRI = Myristicaceae.

[2]Botanical description summarised from (Le Thomas 1969; van der Vossen & Mkamilo 2018)

[3]Lopé leaf phenology and nature of leaf damage summarised from (White & Abernethy 1996) and Figures XX. CC = Canopy coverage

[4]Description of the phenology sample used in this study: n=number of individuals; o=mean observation period (range) in months.

In a previous analysis, long-term phenology recorders at SEGC estimated the observation uncertainties associated with the phenophases of all species recorded at Lopé (Chapter 3 and Bush et al. 2018). In general, new leaves were considered highly visible (more visible than senescing leaves) but of short duration (always lasting less than four weeks). New leaf events for the eight focal species of this study were categorised as either "easy to see" or "very obvious". Thus new leaves are considered a good, visible, indicator of leaf flushing, but the short duration of new leaf events means that some are likely to be undetected. However the SEGC observers recorded comments alongside the monthly canopy scores such as "newish" when leaves had matured but had clearly been refreshed since the last observation. We were able to include this information in the analyses below and thus reduce the number of missed new leaf events.

Environmental data from Lopé and downloaded sources

Rainfall and temperature data have been collected at SEGC since 1984 with shorter periods of data collection for relative humidity, solar radiation, wind speed and aerosol depth (detailed description of collection methods in Chapter 4). The rainfall cycle at Lopé is biannual with a long dry season from June-September and a shorter dry season from December-February. These rainfall patterns have been used to determine seasons in the following analyses. Minimum and maximum daily temperature drop during the long dry season alongside surface solar radiation and relative humidity. As described in Chapter 4, the Lopé minimum daily temperature record is more reliable than maximum daily temperature due to impacts of direct solar radiation on the latter dataset. We therefore used minimum daily temperature (combined from both forest and savanna sites) in further analyses in this chapter.

In addition to empirical measures from SEGC, we sourced mean monthly Potential Evapo-Transpiration (PET; mm per month) for Lopé (-0.2N, 11.6E) from the Global Potential Evapo-Transpiration (Global-PET) and Global Aridity Index (Global-Aridity) Geo-Database (1950-2000; 1km resolution; Trabucco & Zomer 2009). We downloaded timeseries at the monthly time

step for solar radiation (downward shortwave flux, 0.05° resolution) from the Surface Solar Radiation Data Set - Heliosat version 2 (1985-2015; SARAHv2; Pfeifroth et al. 2017; Kothe et al. 2017) and equatorial atmospheric CO_2 concentration (14.5N – 14.5S) from the NOAA Earth System Research Laboratory (1980-2017; Dlugokencky et al. 2017).

5.3.2 GENERATING RESPONSE AND PREDICTOR VARIABLES

Generating monthly response and predictor variables to assess seasonality

For linear analyses of monthly variation in leaf phenology we calculated binomial response variables as follows. For each calendar month and individual tree we summed the number of years with and without 1) new leaves (new leaf canopy coverage >0% or new leaf comment; NL), (2) senescing leaves (senescing leaf canopy coverage >0%; SL), (3) a full leaf canopy (mature leaves canopy coverage >75%; ML) and (4) leaf damage (Table 5.2A).

We generated predictor variables for analyses of leaf seasonality as follows (Table 5.2B and Figure 5.3). For each calendar month we calculated the long-term mean for total monthly rainfall, solar radiation and minimum daily temperature. As described in Chapter 4, 3% daily rainfall values are missing from the Lopé record, 1984-2018. Where possible we filled these values using the 10-day running mean before summarising to monthly totals. However 11 months (spread over the years 2009, 2010 and 2013) are missing from the monthly timeseries because they were incomplete and therefore did not contribute to the long-term monthly means. Also, 34% daily minimum temperature values are missing from the Lopé record, 1984-2018. As these values are spread throughout the time period and the calendar year (the number of daily records of minimum temperature available for each calendar month ranged from 80 to 91) we used all available data to directly calculate long-term means for each calendar month.

To estimate moisture availability we calculated the mean cumulative water deficit (CWD; Figure 5.3B) for each calendar month following James *et. al.* (2013). First water deficit (WD) was calculated as the difference between

mean *Rainfall* from the Lopé record and *PET* from the Global-PET database (Figure 5.3A) for each calendar month *m,* as:

$$WD_m = PET_m - Rainfall_m.$$

For the month with most positive WD (in this case November; Figure 5.3A), we assumed the soil was saturated and set CWD to zero. We then computed the CWD for subsequent months as the sum of that month's WD and the previous month's CWD:

$$CWD_{\max(WD_1, WD_2 \ldots, WD_{12})} = 0;$$

$$CWD_m = CWD_{m-1} + WD_m.$$

Finally leaf damage was summarised as the long-term mean probability of leaf damage each calendar month for each individual tree.

Weather data was recorded for the entirety of each month (and monthly means are assigned to the middle of the month) whereas phenology data was recorded at the start of each month and indicative of phenological activity since the last observation. Thus we lagged all environmental predictors by one month in monthly analyses, including leaf damage as we were interested in the new leaf response following leaf damage not the co-occurrence of leaf damage on new leaves.

Table 5.2. Monthly response, predictor and grouping variables for linear seasonal analyses of leaf phenology

A. Response variables

Variable	Description	Data points	Code
Probability of new leaf presence	Binomial; c(Yearspresent, Yearsabsent)	12 calendar months x 120 inds	NL
Probability of senescent leaf presence	Binomial; c(Yearspresent, Yearsabsent)	12 calendar months x 120 inds	SL
Probability of full canopy of mature leaves	Binomial; c(Yearspresent, Yearsabsent)	12 calendar months x 120 inds	ML
Probability of leaf damage	Binomial; c(Yearspresent, Yearsabsent)	12 calendar months x 120 inds	LeafDamage

B. Predictor variables

Variable	Description	Data points	Code
Calendar month	Factor; Jan:Dec	12 calendar months	Month
Lagged rainfall	Continuous; Long-term mean total monthly rainfall lagged by 1 month	12 calendar months	Rain1
Lagged cumulative water deficit (CWD)	Continuous; Long-term mean CWD lagged by 1 month	12 calendar months	CWD1
Lagged minimum daily temperature	Continuous; Long-term mean minimum daily temperature lagged by 1 month	12 calendar months	MinTemp1
Lagged solar radiation	Continuous; Long-term mean radiation lagged by 1 month	12 calendar months	Solar1
Lagged probability of leaf damage	Probability; Long-term mean probability of leaf damage lagged by 1 month	12 calendar months x 120 inds	LeafDamage1

C. Grouping factors

Variable	Description	Data points	Code
Calendar month	Factor; Jan:Dec	12 calendar months	Month
Species	Factor	8 species	Species
Individual	Factor	120 inds	TreeID

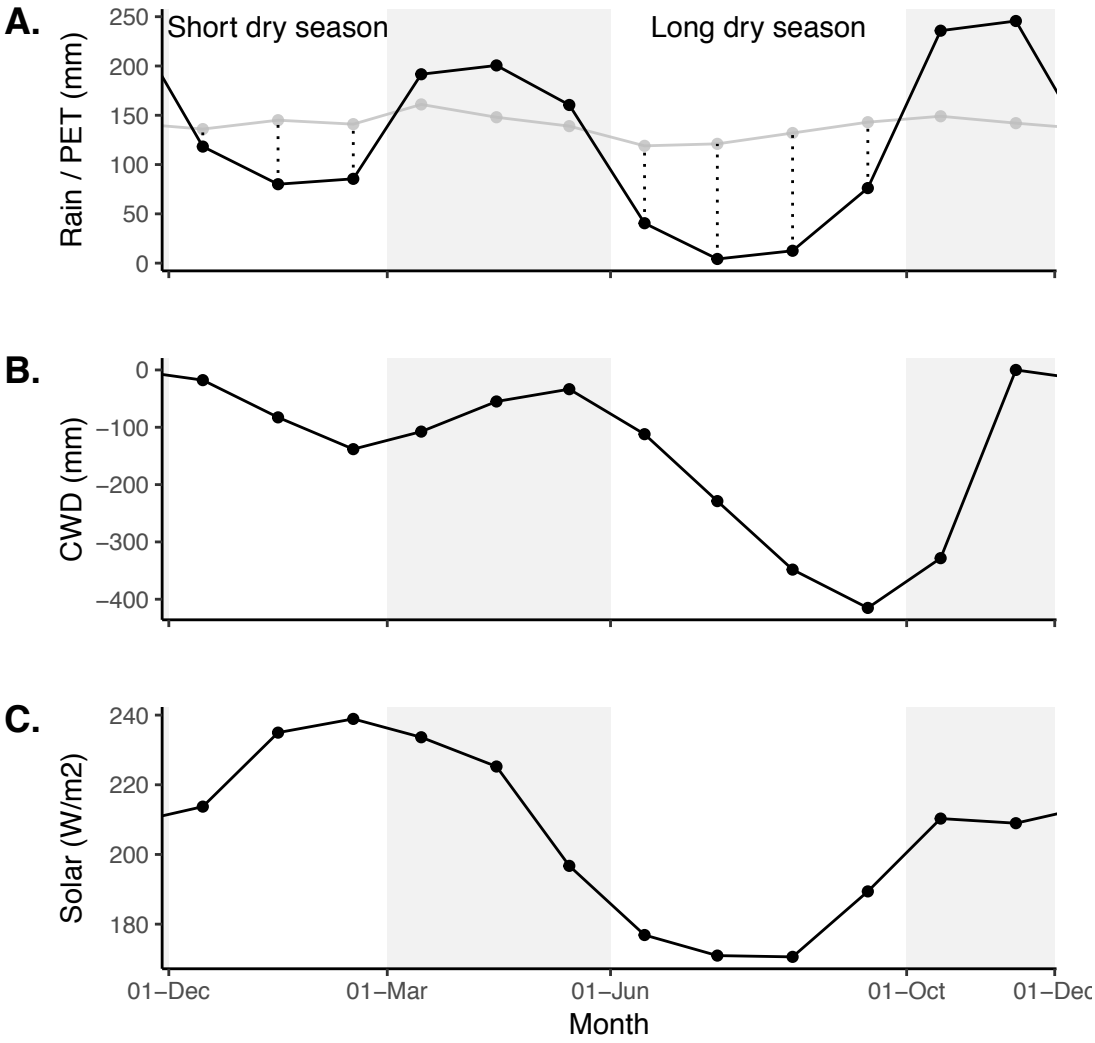

Figure 5.3. Seasonal variation in rainfall, water deficit and solar radiation at Lopé National Park, Gabon.

A. Mean monthly rainfall from the long-term Lopé record (1984-2018; black line), mean monthly potential evapo-transpiration (PET) from the Global-PET database (1950-2000; grey line) and mean monthly water deficit (WD) during the dry seasons (vertical dashed lines). B. Cumulative water deficit derived from WD shown in A (method described in text). C. Mean monthly surface solar radiation from the SARAHv2 dataset (1984-2015).

Generating annualised response and predictor variables' to assess inter-annual variation and long-term trends

For linear analyses of interannual variation in the probability of (1) all leaf-flushing events (number of months per year with new or senescing leaves present or mature leaf canopy coverage ≤75%) and (2) major leaf flushing events (number of months per year with new or senescing leaf canopy coverage ≥50% or mature leaf canopy coverage ≤50%) we calculated

binomial response variables by summing the number of months with and without (major) leaf flushing events for each tree (Table 5.3A). Years for leaf phenology data were defined from mid-October to mid-October mirroring the relief of negative water deficit following the long dry season (Figure 5.3). This means that phenology records taken at the beginning of October were assigned to the previous biological year and the first phenology observations in a biological year are recorded at the beginning of November.

For the predictor variables, we annualised environmental data (total annual rainfall, mean minimum temperature, mean surface solar radiation, mean CO_2 concentration) according to the biological year (starting from mid-October as before; Table 5.3B and Figure 5.4). Due to missing rainfall data, we were unable to calculate total annual rainfall (and dependent variables) for the years 2009, 2010 and 2013. To overcome data gaps in the minimum temperature record we first calculated deseasonalised minimum daily temperature (minimum daily temperature for each date recorded in the time series minus the long-term mean minimum daily temperature for that day of the year) and then calculated the mean temperature for each year using all data available. The number of deseasonalised minimum temperature data points contributing to each yearly mean ranged from 33 to 366. To estimate the maximum climatological water deficit (MCWD) of the long dry season each year we calculated the WD for each month in the rainfall timeseries as for the monthly predictor values above and took the sum of all months with negative WD between May and October (Ouédraogo et al. 2016). Leaf damage data was annualised as the mean probability of leaf damage each biological year (for each individual tree in the phenology sample.

Table 5.3. Annualised response, predictor and grouping variables for linear analyses of leaf interannual variation and trends.

A. Response variables

Variable	Description	Data points	Code
Probability of all leaf flushing events	Binomial; c($Months_{present}$, $Months_{absent}$)	2978 ind-years	Flush
Probability of major leaf flushing events	Binomial; c($Months_{present}$, $Months_{absent}$)	2978 ind-years	MajorFlush

B. Predictor variables

Variable	Description	Data points	Code
Year	Factor; Biological year (mid-Oct to mid-Oct; 1987-2017)	30 years	Year
Atmospheric CO_2	Continuous; Annual mean CO_2 (ppm)	30 years	Rain
Solar radiation	Continuous; Annual mean solar radiation (W/m^2)	29 years	Solar
Minimum daily temperature	Continuous; Annual mean deseasonalised minimum temperature (C)	30 years	MinTemp
Rainfall	Continuous; Total annual rainfall (mm)	27 years	Rain
Maximum cumulative water deficit (MCWD)	Continuous; Long dry-season MCWD (mm)	27 years	MCWD
Lagged maximum cumulative water deficit (MCWD)	Continuous; Long dry-season MCWD of the previous year (mm)	26 years	MCWD1
Probability of leaf damage	Probability; Annual mean probability of leaf damage per individual	2464 ind-years	LeafDamage

C. Grouping factors

Variable	Description	Data points	Code
Year	Factor; Biological year (mid-Oct to mid-Oct; 1987-2017)	30 years	Year
Species	Factor	8 species	Species
Individual	Factor	120 inds.	TreeID

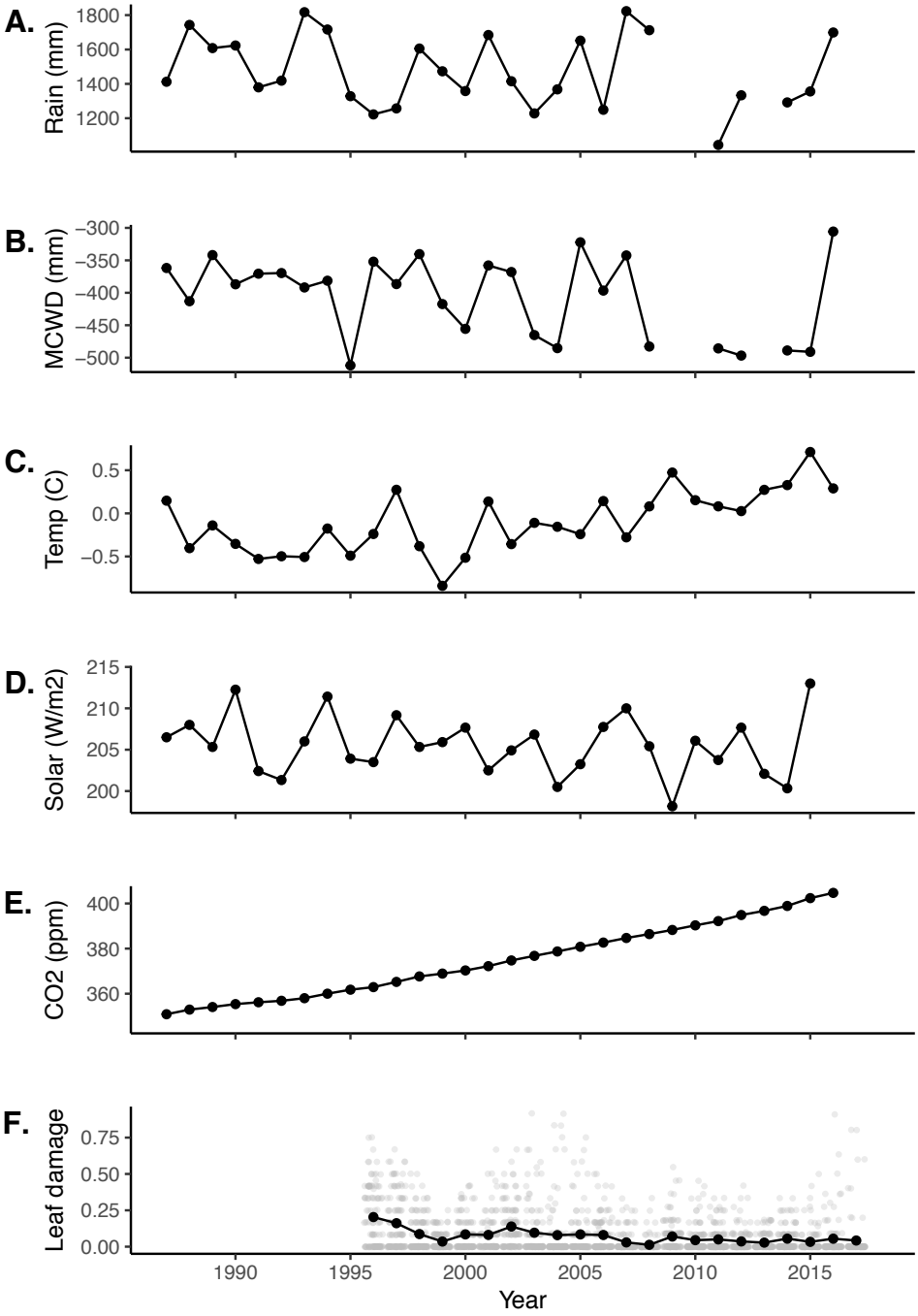

Figure 5.4. Interannual variation in environmental conditions and probability of leaf damage at Lopé National Park, Gabon.

A. Total annual rainfall from Lopé (1987-2018). B. MCWD calculated using Lopé rainfall and mean monthly PET from the Global-PET dataset. C. Mean deseasonalised minimum daily temperature from Lopé (1987-2018). D. Mean surface solar radiation from SARAHv2 (1987-2016). E. Mean annual equatorial CO_2 concentration from NOAA (1987-2018). F. Annual mean probability of leaf damage for all individuals and species observed at Lopé (1995-2018). Black dots indicate the mean probability for the whole sample (n=120 individuals) per year and grey dots indicate mean for each individual per year.

5.3.3 ANALYSES

Seasonality in leaf flushing

We assessed the general character of leaf phenology for each species using Fourier analyses to identify periodicity within the new leaf time series for each individual tree (Bush *et al.* 2017). We then assessed seasonality and synchrony for each species using circular boxplots to show the mean, interquartile range and 95th centiles of the proportion of individuals with new leaves and leaf damage each calendar month between years. Finally we plotted histograms of new leaf canopy coverage (%) to show the distribution of the magnitude of leaf exchange events per species.

We used generalized linear mixed models (GLMMs; family=Binomial) to estimate the monthly probability of (1) new leaves (NL), (2) senescing leaves (SL), (3) a full leaf canopy (ML) and (4) leaf damage (LeafDamage) as described above and in Table 5.2A. We included Month as the fixed effect predictor variable and to reflect the hierarchical nature of our data, we incorporated random slopes for Month by Species (Table 5.2C). We included a random intercept for each individual tree (TreeID) to account for pseudoreplication (Table 5.2C). Inspection of model residuals for each individual timeseries (split by TreeID) using the R packagae "itsadug" (van Rij *et al.* 2017) showed no significant lags in the median autocorrelation function.

We were able to predict the population-level mean probability for each phenophase (from the fixed effect estimates, equal to the arithmetic mean of the species-level random effects) and the species-level probabilities for each phenophase (from the random effect estimates) directly from these models. For this and all following analyses we also calculated a community-wide probability for each phenophase by taking the mean of the species-level predictions weighted according to each species' CV (Figure 5.2).

Drivers of seasonal variation in leaf flushing

We tested the lagged monthly effects of moisture availability (CWD1), sunlight (Solar1) and leaf damage (LeafDamage1) on the probability of new leaf events (NL; response variable created as above) using a GLMM (family=Binomial). We chose not to include mean minimum daily temperature as it is strongly collinear with solar radiation on the monthly scale (r=0.86) and there is greater evidence for the influence of solar radiation than temperature on leaf flush. We also rescaled the predictors (mean=0 and standard deviation=1) to allow direct comparison between the slope estimates. We included random slopes by species (Species) for all other predictors and random intercepts for each individual tree (TreeID) and month of data collection (Month; Table 5.2C). After inspection of models residuals as before, we included the lagged response variable (with lags 1 and 2; NL1 and NL2) as random slopes by individual (TreeID) to reduce autocorrelation (no significant lags in the median autocorrelation function after inclusion of the lagged variables). We removed predictors sequentially and compared models using AIC values, preferring simple models with lower AIC (delta AIC>2).

Trends in leaf flushing

We assessed whether leaf flushing had changed linearly over time using GLMMs (family=Binomial) to predict the probability of (1) all leaf-flushing events and (2) major leaf flushing events. A reduction in the probability of leaf flushing could occur if leaf flush became more concentrated in time and were spread over fewer months each year. The latter model was designed to test this whether such concentrated large-scale deciduous events were becoming more or less likely. The random effects structure for both models included random slopes for Year by Species and individual tree (TreeID) and random intercepts for Year to account for pseudoreplication (Table 5.3C). Inspection of model residuals revealed no significant lags in the median autocorrelation functions.

We tested the effects of rainfall (Rain), drought intensity of the long dry season in the current (MCWD) and previous year (MCWD1), minimum temperature (MinTemp), sunlight (Solar), carbon dioxide concentration (CO_2) and leaf damage (LeafDamage) on the probability of all leaf-flushing events within a GLMM (family=Binomial; Table 3B). The strongest correlations between predictors were between leaf damage and CO_2 (r=-0.59), leaf damage and rainfall (r=-0.56), minimum temperature and CO_2 (r=0.56) and MCWD and Rain (0.42), the remainder being below 0.4 (absolute values; Table S5). We included all predictors as random slopes by Species and random intercepts for individual tree (TreeID) and Year to account for pseudoreplication (Table 5.3C). We removed predictors sequentially and compared models using AIC. As leaf damage data was only consistently recorded since 1995, we undertook two simultaneous model comparisons to find the important drivers of interannual variation in leaf flushing; one using a shorter dataset, inclusive of leaf damage data (1995-2018; m1) and one using the complete dataset without leaf damage as a predictor (1986-2018; m2). Model residuals were inspected and there were no significant lags in the median autocorrelation functions.

5.4 RESULTS

5.4.1 SEASONALITY IN LEAF FLUSHING

Most new leaf events at Lopé occurred on a small scale (median canopy coverage ranged from 2.5% for *C. lizae and G. giganteum* to 38% for *P. soyauxii;* Figure 5.5C). However large-scale canopy turnover events were recorded for some species (95th centile canopy coverage is 50% for *A. klaineana* and 100% for *P. macrophylla* and *P. soyauxii*). While new leaves have been observed in every calendar month for all species (Figure 5.5B), dominant peaks at annual frequencies in the mean Fourier spectra (Figure 5.5A) for all species except *G. giganteum* and *P. soyauxii* indicate some seasonality. Leaf damage has been recorded for all species but most often for *P. angolensis*, *C. lizae*, *G. giganteum* and *A. klaineana* (probability of leaf

damage for any individual in any month is 28%, 13%, 9% and 7% respectively; Figure 5.5D).

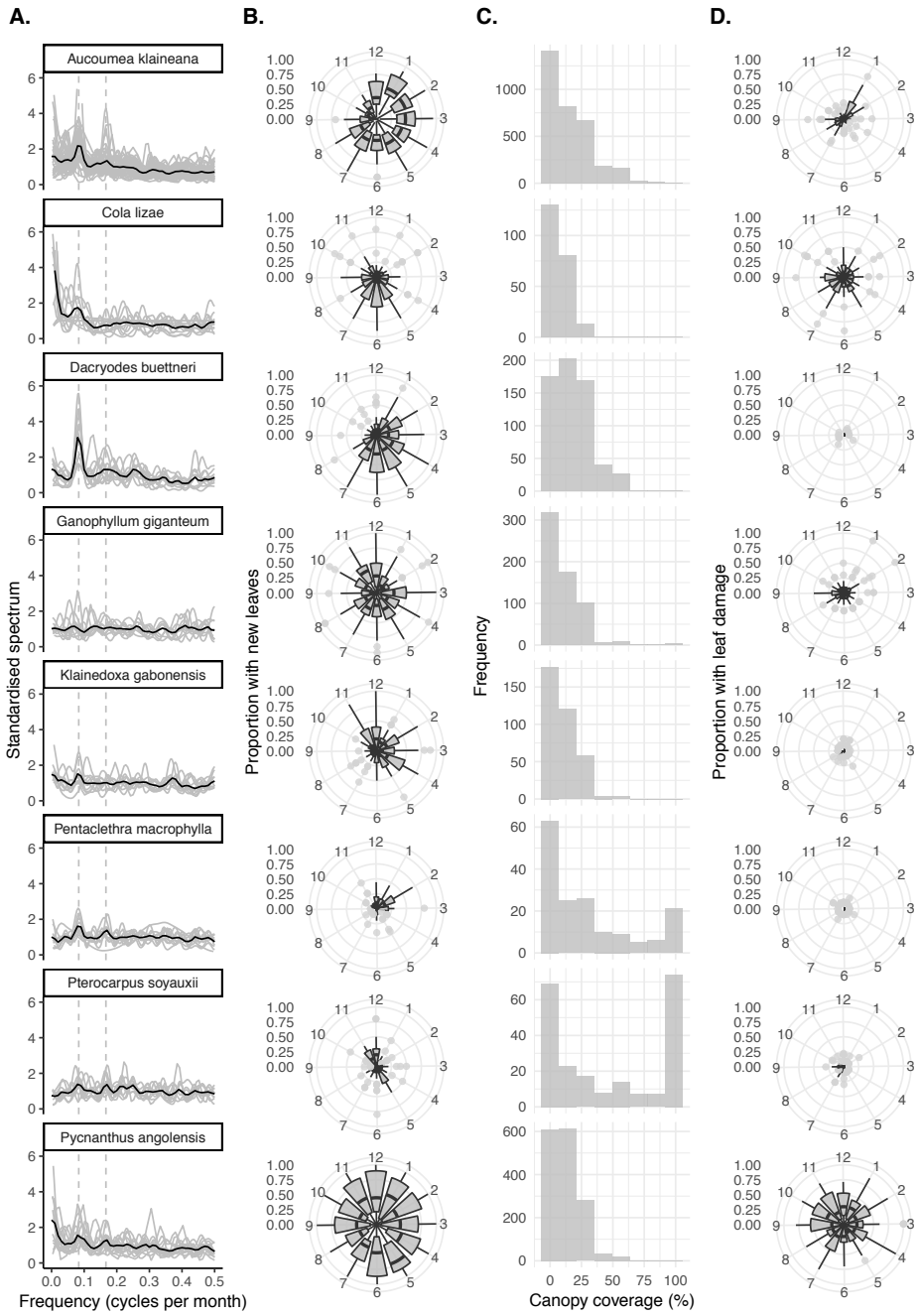

Figure 5.5. Summary of new leaf phenology and leaf damage for each species.

A. These plots show the Fourier spectra for each individual tree (grey lines) and the mean spectra for each species (bold lines). Dashed vertical lines indicate periodicities of 12 months and 6 months. B. Circular boxplots show the mean (bold horizontal lines), interquartile range (shaded grey boxes) and 95th centile range (horizontal black lines) of proportion of individuals with new leaves each calendar month between years. C. Histograms of all canopy coverage scores greater than zero recorded for each species. D. Circular boxplots show the mean (bold horizontal lines), interquartile range (shaded grey boxes) and 95th centile range (horizontal black lines) of proportion of individuals with leaf damage each calendar month between years

Community-wide, new leaves were most likely to occur from November to June (weighted mean probability = 0.28-0.43) and least likely towards the end of the dry season (Figure 5.6A), while senescent leaves were most common in August, in the later dry season (weighted mean probability = 0.21;Figure 5.6C). The community-wide probability of a tree having a full canopy of mature leaves was high for most of the year (>0.74) but dropped in January (weighted mean probability =0.63; Figure 5.6E). Leaf damage was most likely in the dry seasons, peaking in January and September (weighted mean probabilities = 0.21 and 017 respectively, Figure 5.6G). These community-wide patterns were strongly influenced by *A. klaineana* - which makes up 36% CV – and peaks in the leaf phenophases and damage differed for each species (Figure 5.6B, D, F and H). The community-wide pattern for new leaves and mature canopies differed most strongly from the species mean between January and May (Figure 5.6A and E). In these months new leaves were more likely and full mature leaf canopies were thus less likely among *A. klaineana* than most other species (Figure 5.6B and F). GLMM outputs including fixed effects estimates and the variance of random effects are show in supporting information (Tables S5.1-5.4).

The maximum probability of new leaves ranged from 0.26 for *P. macrophylla* to 0.62 for *P. angolensis* but always occurred between November and May (i.e. not in the long dry season, Figure 5.6B). New leaves for species *P. soyauxii, P. angolensis* and *G. giganteum* peaked twice yearly in May and November/December (Figure 5.6B). The minimum probability of new leaves ranged from 0.02 for *P. macrophylla* to 0.42 for *P. angolensis* and occurred in August/September/October for all species except for *C. lizae* for which the new leaf minima was in December (Figure 5.6B). Leaf damage was most seasonal for *A. klaineana* with peaks in January and September during both dry seasons (Figure 5.6H).

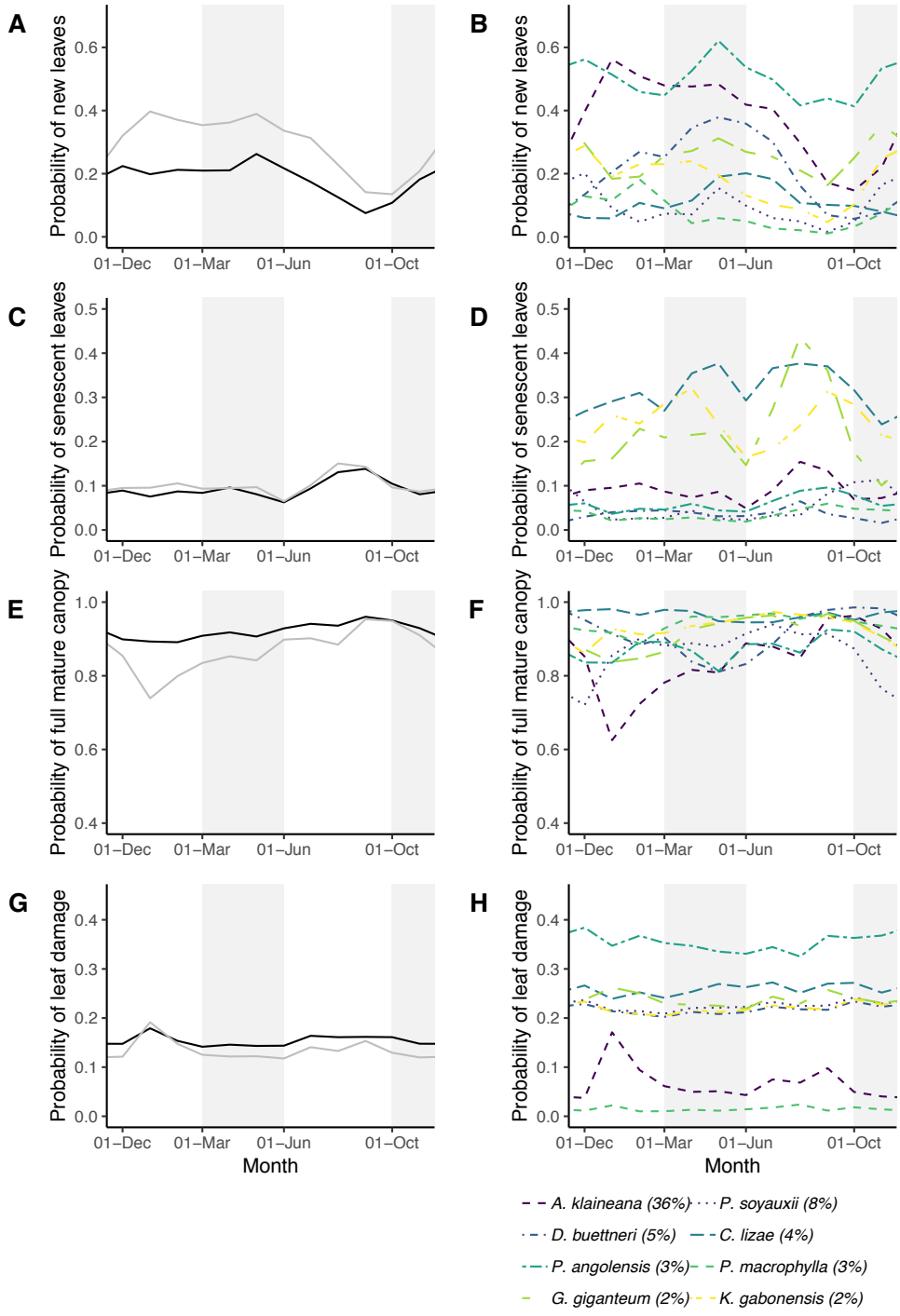

Figure 5.6. Monthly variation in leaf phenology and leaf damage at Lopé National Park, Gabon.

These plots show the predictions from GLMMs (family=binomial) for the mean probability of leaf phenology and damage derived from the fixed effects (black solid line; A,C,E,G), the community-wide probability of leaf phenology and damage derived as a weighted mean of the species-level predictions according to crown volume (grey solid line; A,C,E,G) and the species-level probabilities derived from the species-level predictions (coloured lines; B,D,F,H). The percentage scores in the key refer to the crown volume of each species in the surrounding forest.

5.4.2 DRIVERS OF SEASONAL VARIATION OF LEAF FLUSHING

Moisture availability (CWD1), light (Solar1) and leaf damage (LeafDamage1) were all important predictors of leaf flush and retained as fixed effects in the best model for seasonal drivers of new leaf events (Table 5.4). Moisture availability had a more positive effect on the probability of new leaf occurrence than both light availability and leaf damage (fixed effects estimates = 0.27 and 0.17 and 0.21 respectively, Table 5.5A and Figure 5.7A). However, the relative effects of these drivers varied by species; random slope estimates for cumulative water deficit were more positive than the fixed effect estimate for *A. klaineana* and *D. buettneri* and more negative for *G. giganteum, C. lizae* and *P. angolensis* (95% confidence intervals don't cross zero; Table 5.9C and Figure 5.7B). Similarly, the random slope estimates for solar radiation were more positive than the fixed effect estimate for *K. gabonesis* and *P. macrophylla* and more negative for *C. lizae, G. giganteum* and *P. angolensis* (95% confidence intervals don't cross zero; Table 5.9C and Figure 5.6B). Leaf flushing was most positively impacted by leaf damage for *P. macrophylla*, *P. soyauxii* and *K. gabonesis* and least impacted for *P. angolensis*, G*. giganteum* and *A. klaineana* (Table 5.5C and Figure 5.7C).

Table 5.4. Model comparison for the drivers of seasonal variation in probability of new leaves.

We used generalised linear mixed effects models (family=Binomial). The random effects structure included random slopes for all predictors listed for each model by Species and random slopes for the lagged response variable by each individual tree (TreeID) and month. Asterisks indicate the simplest model with lowest AIC.

Predictors	Obs.	DF	AIC	
CWD1 + Solar1 + LeafDamage1	1440	21	9356.7	*
CWD1 + Solar1	1440	13	9483.5	
CWD1 + LeafDamage1	1440	16	9438.3	
Solar1 + LeafDamage1	1440	16	9489.5	

Table 5.5. Outputs from the best model for the drivers of seasonal variation in probability of new leaves.

Estimates are from a generalised linear mixed effects model (family=Binomial). The random effects structure included random slopes for all predictors listed for each model by Species and random slopes for the lagged response variable by each individual tree (TreeID) and month. The predictors CWD1 and Solar1 were all rescaled by removing the mean and dividing by 1SD. A. Estimates for the fixed effects. B. Variance of the random effects. C. Conditional means of the random effects.

A.

Predictor	**Estimate**	**SE**	**Z value**	**P value**
Intercept	-1.55	0.29	-5.37	<0.0001
CWD1	0.27	0.07	3.70	<0.001
Solar1	0.17	0.07	2.38	<0.05
LeafDamage1	0.21	0.07	2.97	<0.01

B.

Group	**Random effect**	**Variance**	**SD**
TreeID	Intercept	0.74	0.86
	NL1	4.01	2.00
	NL2	4.62	2.15
Month	Intercept	0.02	0.12
Species	Intercept	0.62	0.79
	CWD1	0.02	0.15
	Solar1	0.03	0.18
	LeafDamage1	0.01	0.11

C.

Species	**Random intercept**	**Random slope**		
		CWD1	**Solar1**	**LeafDamage1**
A. klaineana	0.83	0.22	-0.05	-0.09
C. lizae	-0.44	-0.14	-0.24	-0.02
D. buettneri	0.44	0.14	0.09	-0.02
G. giganteum	0.50	-0.23	-0.14	-0.10
K. gabonensis	-0.16	-0.01	0.22	0.07
P. macrophylla	-1.13	0.12	0.28	0.20
P. soyauxii	-0.99	0.00	-0.03	0.10
P. angolensis	1.05	-0.12	-0.14	-0.16

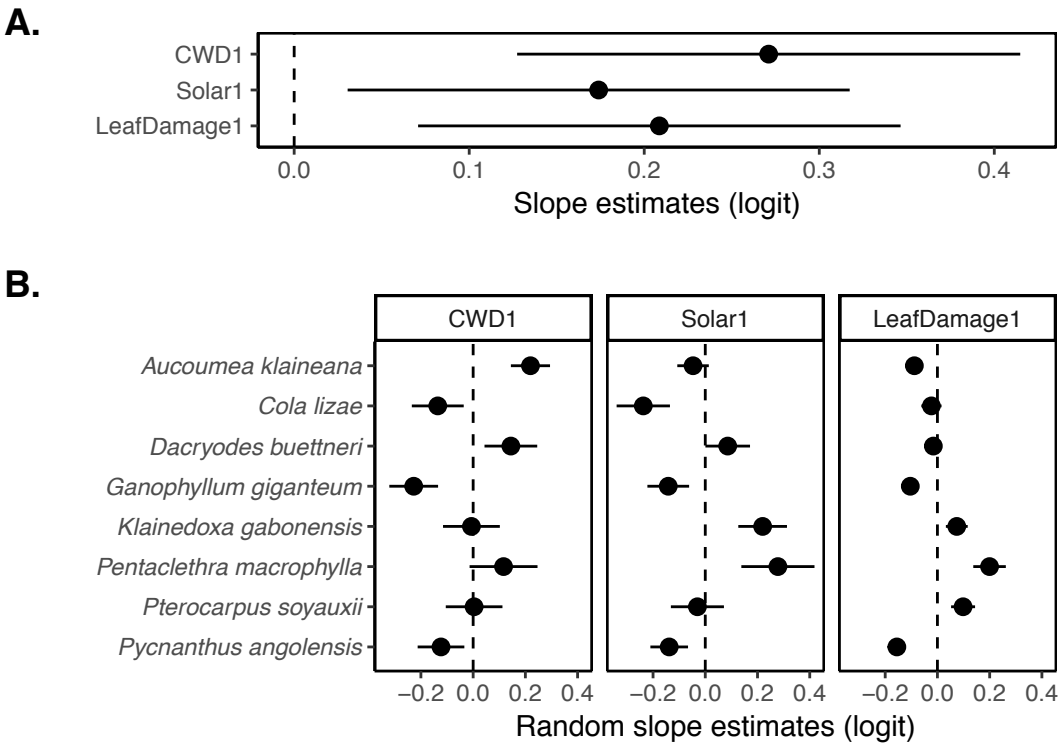

Figure 5.5. Model estimates for the drivers of seasonal variation in new leaf events.
Estimates (dots) and 95% confidence intervals (horizontal lines) for the fixed effects (A) and random slopes by species (B) from the best model (GLMM; family=binomial) for probability of new leaf events. Predictors in the best model are: cumulative water deficit (CWD1), surface solar radiation (Solar1) and leaf damage (LeafDamage1).

5.4.3 TRENDS IN LEAF FLUSHING

Year was retained as a fixed-effect in the best model for the probability of all leaf flushing events but not for major flushing events where it was retained only at the species-level (Table 5.6). The mean probability of all leaf flushing events has declined over time from a peak of 0.57 in 1987 to 0.09 in 2017 (fixed effect estimate = -0.90; Table 5.7A and Figure 5.8A). The community-wide probability of leaf flushing has declined at a slower rate than the species mean (Figure 5.8A) because the very dominant species, *A. klaineana,* has declined less rapidly than the mean for all species (conditional mode of the random slope =0.14; Table 5.7C and Figure 5.8B). Leaf flushing among *P. angolensis* trees has declined most rapidly, while flushing among *P.*

macrophylla has declined most weakly (conditional mode of the random slopes = -0.35 and 0.28 respectively; Table 5.7C and Figure 5.8B). As for the probability of major flushing events, the slope of the trend over time varied between Species but there was no significant population-level trend (Table 5.8). Predicted probability of major flushing events remained low for all incremental leaf exchanging species and appeared to reduce over time for *A. klaineana* and *P. soyauxxi* (Figure 5.8C-D).

Table 5.6. Model comparison for change over time in leaf flushing.
We used generalised linear mixed effects models (family=Binomial). The random effects structure. The random effects for all models also included random slopes for Year by TreeID . Asterisks indicate the simplest model with lowest AIC in each case. A. Probability of all leaf flushing events and B. Probability of major leaf flushing events.

A.

Model	Predictors	Random slope by Species	DF	AIC	
Population-level change over time	Year	Year	9	11465.4	*
Species-level change over time	Intercept only	Year	8	11482.5	

B.

Model	Predictors	Random slope by Species	DF	AIC	
Population-level change over time	Year	Year	9	3911.6	
Species-level change over time	Intercept only	Year	8	3911.3	*
Individual-level change over time	Intercept only	Intercept only	6	3932.1	

Table 5.7. Outputs from the best model for the trend in probability of leaf flushing events.

Estimates are from a generalised linear mixed effects model (family=Binomial). A. Coefficient estimates of the fixed effects including standard error (SE). B. Variance and standard deviation (SD) of the random effects. C. Conditional modes of the random effects. Year indicated the biological year starting in mid-October and the continuous variable was rescaled by removing the mean and dividing by 1SD.

A.

Predictor	Estimate	SE	Z value	P value
Intercept	-0.90	0.26	-3.45	<0.001
Year	-0.83	0.12	-7.05	<0.0001

B.

Group	Random effect	Variance	SD
TreeID	Intercept	0.17	0.41
	Year	0.04	0.20
Year	Intercept	0.19	0.44
Species	Intercept	0.48	0.69
	Year	0.06	0.24

C.

Species	Random intercept	Random slope
		Year
A. klaineana	0.87	0.14
C. lizae	0.37	-0.09
D. buettneri	-0.66	-0.18
G. giganteum	0.54	0.21
K. gabonensis	-0.03	-0.18
P. macrophylla	-0.97	0.28
P. soyauxii	-0.76	0.21
P. angolensis	0.69	-0.35

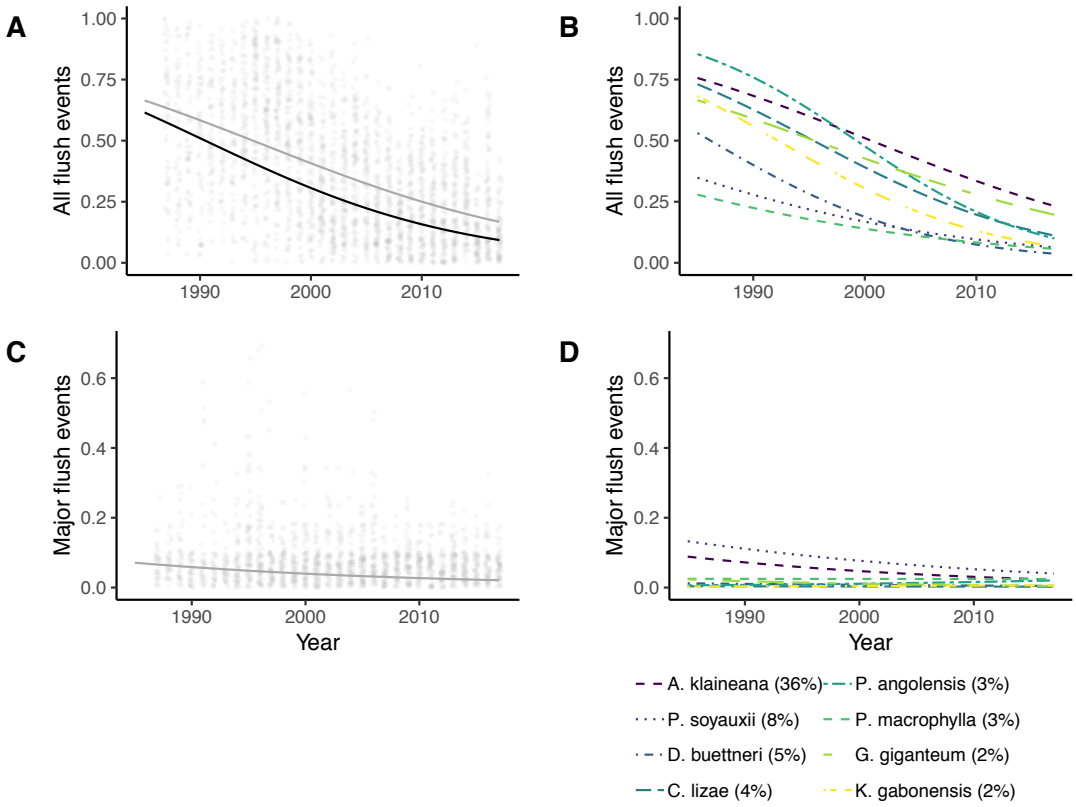

Figure 5.8. Probability of leaf flush over time at Lopé National Park, Gabon 1987-2017.

A+C: Mean probability (fixed effects prediction; black solid line) and community-wide probability (weighted mean of species predictions by crown volume; grey solid line) of all leaf flushing events and major leaf flushing events each year derived from GLMMs (family=binomial). Also shown are the probabilities of (major) leaf flushing for each individual each year (n=120; grey dots).B+D: Species-level predictions (random slope of Year by Species; coloured lines) from the random effects of the GLMMs (family=binomial) of (major) leaf flushing each year.

Table 5.8. . Outputs from the best model for the trend in probability of major leaf flushing events.

Estimates are from a generalised linear mixed effects model (family=Binomial). A. Estimates for the fixed effects. B. Variance of the random effects. C. Estimates for the random effects. Year was rescaled by removing the mean and dividing by 1SD.

A.

Predictor	Estimate	SE	Z value	P value
Intercept	-4.38	0.41	-10.60	<0.0001
Year	-0.24	0.16	-1.44	0.15

B.

Group	Random effect	Variance	SD
TreeID	Intercept	0.16	0.40
	Year	0.04	0.19
Year	Intercept	0.28	0.53
Species	Intercept	1.25	1.12
	Year	0.11	0.33

C.

Species	Random intercept	Random slope
		Year
A. klaineana	1.33	-0.27
C. lizae	-1.43	-0.01
D. buettneri	-0.52	-0.15
G. giganteum	-0.17	-0.33
K. gabonensis	-1.04	0.35
P. macrophylla	0.71	0.12
P. soyauxii	1.85	-0.22
P. angolensis	-0.08	0.47

5.4.4 Drivers of interannual variation in leaf flushing

For the shorter dataset inclusive of leaf damage (1995-2018), all predictors except for current year's rainfall and drought intensity (MCWD) were retained in the best model of interannual variation in leaf flushing events (m1; Table 5.9A). However only the fixed effects estimates for atmospheric CO_2 and the drought intensity of the previous year's long dry season (MCWD1) were significantly different to zero (95% confidence intervals don't cross zero; Figure 5.9A and Table S5.6). Both predictors had negative correlations with the probability of leaf flush although the impact of CO_2 was six times greater than drought intensity (fixed effects estimates = -1.24 and -0.20 respectively; Figure 5.9A, B and C and Table S5.6). For the longer dataset exclusive of leaf damage (1986-2018), all predictors except current year drought intensity (MCWD) were retained in the best model (m2; Table 5.9B). In this latter model, only CO_2 and annual rainfall were significantly different to zero as fixed effects (95% confidence intervals don't cross zero; Figure 5.9A and Table S5.7). The effect of CO_2 was reduced in this model compared to the best model for the shorter period (fixed effect estimate = -1.02; Figure 5.9A).

Table 5.9. Model comparison to find important drivers of interannual variation in probability of leaf flushing.

We used generalised linear mixed models (family=Binomial) for (A) a shorter dataset inclusive of leaf damage (m1; 1995-2018) and (B) a longer dataset exclusive of leaf damage (m2; 1984-2018). Predictors include: atmospheric CO_2, previous year's drought intensity (MCWD1), surface solar radiation (Solar), total annual rainfall (Rain), annual mean deseasoned minimum daily temperature (MinTemp) and leaf damage (LeafDamage1). The random effects structure for all models included random slopes for all predictors listed by species and random intercepts for each tree and year. Asterisks indicate the simplest model with lowest AIC.

A.

Predictors	**Obs.**	**DF**	**AIC**	
CO2 + Solar + MinTemp + Rain + MCWD + MCWD1 + LeafDamage	1820	46	7146.9	
CO2 + Solar + MinTemp + Rain + MCWD + MCWD1	1820	37	7173.4	
CO2 + Solar + MinTemp + Rain + MCWD + LeafDamage	1820	37	7177.6	
CO2 + Solar + MinTemp + Rain + MCWD1 + LeafDamage	1820	37	7137.6	
CO2 + Solar + MinTemp + MCWD1 + LeafDamage	1820	29	7139.2	*
CO2 + Solar + MinTemp + MCWD1 + LeafDamage	2038	29	7910.9	*
CO2 + Solar + MCWD1 + LeafDamage	2038	22	7914.3	
CO2 + MinTemp + MCWD1 + LeafDamage	2038	22	7924.8	
Solar + MinTemp + MCWD1 + LeafDamage	2038	22	8026.5	

B.

Predictors	**Obs.**	**DF**	**AIC**	
CO2 + Solar + MinTemp + Rain + MCWD + MCWD1	2235	37	8883.0	
CO2 + Solar + MinTemp + Rain + MCWD	2235	29	8914.0	
CO2 + Solar + MinTemp + Rain + MCWD1	2235	29	8877.6	*
CO2 + Solar + MinTemp + MCWD1	2235	22	8894.8	
CO2 + Solar + Rain + MCWD1	2235	22	8893.4	
CO2 + MinTemp + Rain + MCWD1	2235	22	8900.6	
Solar + MinTemp + Rain + MCWD1	2235	22	9047.4	

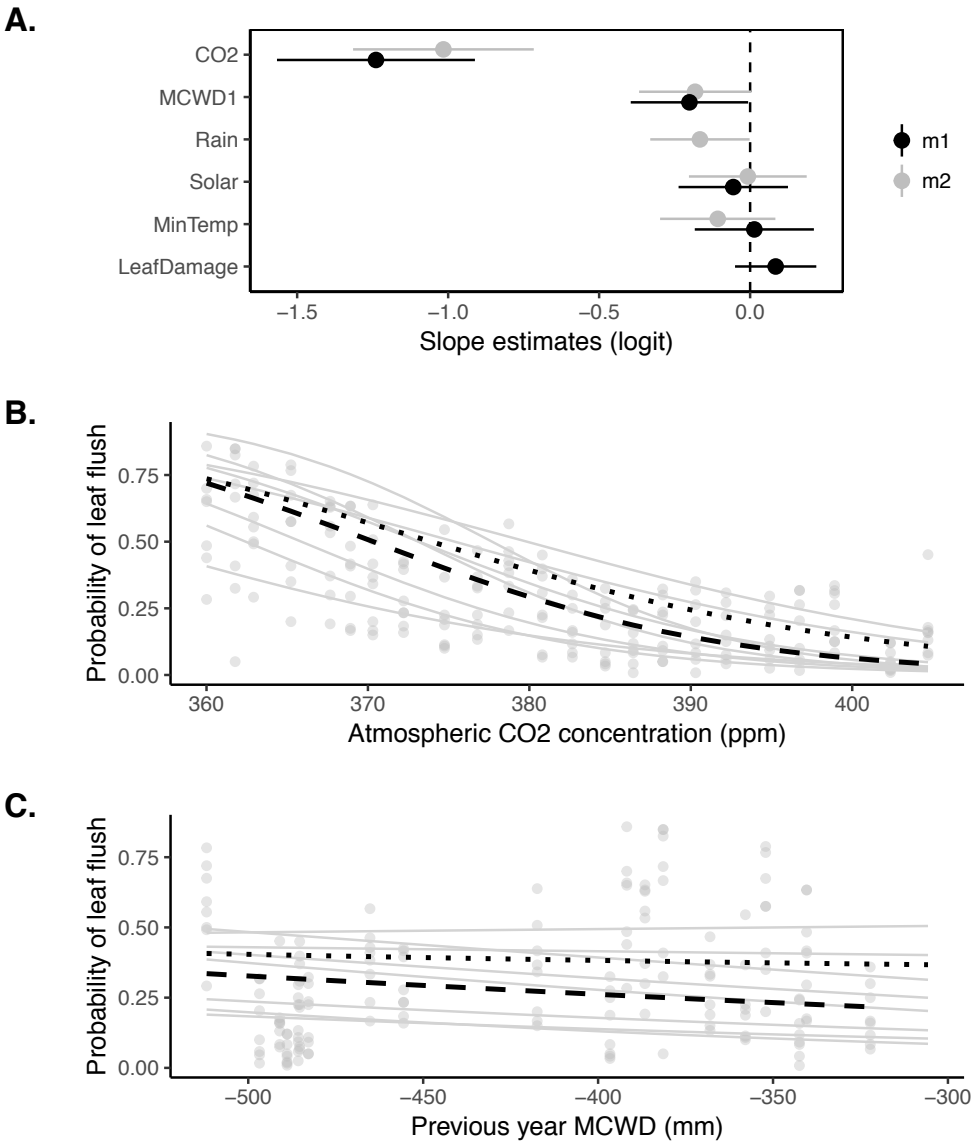

Figure 5.9. Model estimates and predictions for the drivers of interannual variation in leaf flushing events.

A. Model estimates (dots) and 95% confidence intervals (horizontal lines) from the best models (GLMM; family=binomial) for the probability of leaf flushing from a shorter dataset inclusive of leaf damage (m1; 1995-2018) and a longer dataset exclusive of leaf damage (m2; 1986-2018). B-C. Model predictions for the impacts of CO_2 concentration and previous year dry season water deficit (MCWD1) on the probability of leaf flushing from the best model for the shorter dataset (m1; GLMM; family=binomial). Shown are the global (predictions from the fixed effects estimate; black dashed line), species-level (predictions from the random slopes; grey solid lines) and canopy-wide (mean of species predictions weighted by CV; black dotted line,) probabilities of leaf flushing and the raw data for each species binned at different levels of the predictor variables (grey dots).

Random slopes for CO_2 by species showed that in both models (m1 and m2) the effect of CO_2 was more negative than the fixed effect estimate for *K. gabonesis* and *P. angolensis* and more positive than the fixed effect estimate for *P. macrophylla* and *G. giganteum* (Figure 5.10 and Tables S5.6C and S5.7C). The random slopes for MCWD1 by species showed that the effect of MCWD1 was more negative than the fixed effect estimate for *P. soyauxii* and less negative for *A. klaineana* and *G. giganteum* (Figure 5.10 and Tables S5.6C and S5.7C). Surface solar radiation, total annual rainfall, minimum temperature and leaf damage were not significantly different to zero as fixed effects in either model but did vary by species (Figure 5.10 and Tables S5.6C and S5.7C).

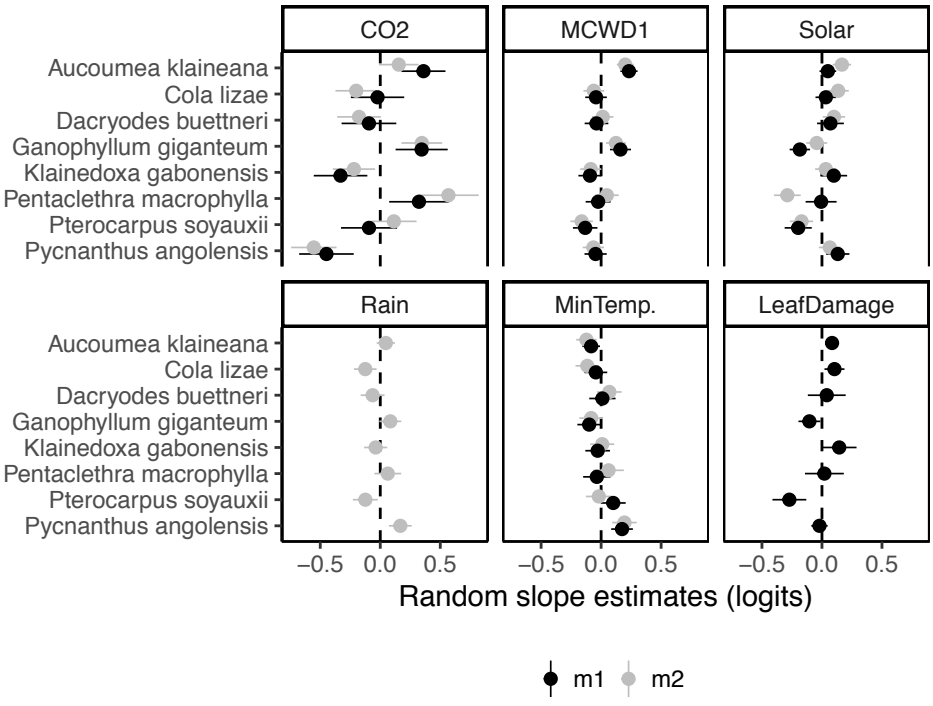

Figure 5.10. Random slope estimates for the drivers of interannual variation in leaf flushing.

Random slope estimates (dots) and 95% confidence intervals (horizontal lines) by species from the best models (GLMM; family=binomial) for the probability of leaf flushing from a shorter dataset including leaf damage (m1; 1995-2018) and a longer dataset excluding leaf damage (m2; 1984-2018). Random slopes include: atmospheric CO_2, previous year's drought intensity (MCWD1), surface solar radiation (Solar), total annual rainfall (Rain), annual mean deseasoned minimum daily temperature (MinTemp) and leaf damage (LeafDamage1).

5.5 DISCUSSION

5.5.1 SEASONAL PHENOLOGY

All eight species demonstrated evergreen, not deciduous, phenology. Two of the species – *P. macrophylla* and *P. soyauxii* - regularly undertook leaf exchange events covering more than 50% of the canopy but leafless periods were minimal. The remaining species were incremental leaf exchangers with most new leaf events involving less than 25% of the canopy. New leaf flush at Lopé is maintained throughout the year at a fairly constant level but drops during the long dry season when the probability of senescing leaves peaks. Mature leaves are most likely to dominate tree canopies by the end of the long dry season. We found that both moisture and light are important positive predictors of intra-annual timing and quantity of leaf flush at Lopé although their effects are difficult to tease apart as they are seasonally synchronised at the site.

The dominance of leaf-exchanging rather than deciduous leaf habits and the maintenance of mature leaf canopies during the long dry season indicates that soil moisture must be high enough during those months to maintain leaf function. This is somewhat of a surprise considering the relatively low annual rainfall at the site (which would be considered a "dry site" by Reich 1995) and the strong seasonality in rainfall. Elevated daytime cloud cover during the dry seasons blocks sunlight, maintaining fairly high relative humidity (monthly mean humidity is always >95% in the forest) and causing a drop in maximum daily temperature in both dry seasons and minimum daily temperatures in the long dry season only (weather seasonality described in Chapter 4). These factors are likely to reduce evapotranspiration and increase water–use efficiency, meaning that forest plants in the Gabon region may not be as water-limited as they appear from the rainfall regime (Philippon *et al.* 2019). In addition the negative association between total annual rainfall and deciduousness established across a spectrum of dry to wet neotropical forests appears to be less strong when there is more than one dry season per year, as is common in the African tropics (Reich 1995).

The peak in full mature-leaf canopies during the long dry season corroborates the peak in leaf biomass and canopy structure observed at this time from remote sensing observations of central African evergreen forests (Guan *et al.* 2013). However, remote sensing has also shown peaks in reflectance during the rainy seasons differentiating them from both dry seasons where reflectance is diminished (Gond *et al.* 2013; Guan *et al.* 2013; Philippon *et al.* 2014). While the increase in senescent leaves (usually brown or yellow) and reduction in supply of newly mature (bright green) leaves in the long dry season is likely to contribute to this seasonality in reflectance it is more difficult to make the same interpretation for the short dry season where leaf demography at Lopé is indistinguishable from the rainy seasons. Instead the elevated reflectance in the rainy seasons compared to the short dry season is likely to be due to elevated light and moisture increasing photosynthetic capacity rather than altering the demography of the leaf cohort or leaf area.

Leaf production at Lopé appears to be light limited (in agreement with recent analyses of leaf demography in the Amazon; Wu et al. 2018), but new leaf production is only supressed during the long dry season (Jun-Sep) indicating that the shallower seasonal trough in solar radiation during the short dry season (Dec-Feb) is not enough to reduce leaf flush, although it is enough to reduce photosynthetic capacity (Guan *et al.* 2013). While these patterns are true for the canopy as a whole, they mask the diversity at the species level revealed here. For example, *C. lizae* has a peak of new leaf production just before the long dry season when light and water levels are dropping leading to seemingly sub-optimal conditions for photosynthesis and leaf development. Species specific associations between leaf phenology and climate have been shown previously at BCI (Wright & Cornejo 1990) while Reich (1995) emphasised that individual trees even of the same species may experience climatic conditions differently dependent on their leaf demography (e.g. variation in water potential dependent on mean leaf age among unsynchronised conspecifics).

Leaf damage at Lopé peaks during the dry months in contrast to that observed in the neotropics (e.g. BCI, Panama; Reich 1995). Leaf damage (mainly to mature leaves, Table 5.1) in the previous month is a positive predictor of new leaf production at seasonal scales, having the most positive impact on *P. macrophylla*, despite leaf damage rarely being observed for this species. *A. klaineana*, which makes up 36% crown volume at Lopé, is targeted by a leaf-rolling caterpillar (*Patania balteata* moth; White & Abernethy 1997; PlantUse English Contributors 2015) which results in total defoliation in some years. In any given month, there is a 7% chance that an *Aucoumea* tree will be suffering from leaf damage at Lopé. However this leaf damage is strongly seasonal, occurring most often at the turn of the year (December-January; the short dry season). It would be interesting to examine more closely what impact this biological intermediary has on overall forest productivity and how the effect is interpreted from remote sensing studies, especially as *Aucoumea* is the dominant tree species in this region.

5.5.2 INTERANNUAL PHENOLOGY

The probability of leaf flush among canopy tree species has declined at Lopé since 1986. This change does not represent a shift away from incremental leaf flush towards more synchronised deciduous phenology, as there was no concurrent increase in major leaf flushing events. Instead this suggests a reduction in all flushing activity and thus increased longevity of individual leaves. The trend was observed for all species at varying rates. Leaf flush for the most common species (*A. klaineana*) declined at a slower rate than the global mean, reducing leaf flush decline for the canopy as a whole. The strongest predictor of this decline is elevated CO_2. While there has been a lot written about the impacts of elevated CO_2 on plant growth there are few studies that have focussed on its impacts on phenology and especially of closed-canopy mature trees. However a recent analysis of a similar length tropical dataset from BCI, Panama showed increased flowering duration (especially for canopy trees) associated with rising CO_2 (Pau *et al.* 2017).

In temperate regions, autumnal senescence was shown to be delayed (increasing leaf longevity) under elevated CO_2 conditions for a young

population of *Populus* (individuals 6-7 years old; Taylor et al. 2008) as well as for a closed-canopy population of the same genus (Tricker *et al.* 2004). However growth and leaf phenology of mature temperate forest trees of various species (individuals ~100 years old) showed inconsistent and species-specific responses to elevated CO_2 (Asshoff *et al.* 2006). According to leaf economics, leaf longevity should be related to the rate of photosynthetic decline as well as leaf construction costs etc. (Kikuzawa & Ackerly 1999). Elevated CO_2 may reduce the rate of photosynthetic decline allowing leaves to be maintained for longer. An alternative explanation for the decline in observations of leaf flush could be that elevated CO_2 enhances the rate of leaf expansion (Pritchard *et al.* 1999; Tricker *et al.* 2004) and that new leaf events are occurring at the same rate but being detected less often as they occur more quickly.

Another factor to consider is that the rise in CO_2 is almost perfectly linear, and that its correlation with the decline in leaf flush may be related to another linear trend in the data not accounted for, such as an effect related to time. Leaf longevity has been shown to be a plastic trait and can vary within the lifetime of individuals however there is no evidence for individual tree age effects on leaf longevity beyond the seedling stage (Kikuzawa & Ackerly 1999; Seiwa 1999). It has also been shown that increased shading can lead to longer leaf longevity within the lifetime of individual trees (Reich *et al.* 2004). However, the species considered here are medium to large canopy trees (Table 5.1) and 88% individuals were found to be receiving at least some but mostly full overhead light in their positions in the canopy during a field campaign in 2015 towards the end of the dataset (Figure S5.1). It seems therefore unlikely that an increase in shading has caused this change in leaf flush.

Elevated CO_2 is known to alter stomatal density (Beerling & Kelly 1997) and to increase the thickness of the mesophyll layer and number of chloroplasts (Pritchard *et al.* 1999; Tricker *et al.* 2004), while leaf thickness is also positively associated with leaf longevity (Wright *et al.* 2004). A traits analysis of historical leaf collections in the region could prove a powerful way of

testing the theory that elevated CO_2 has impacted leaf-longevity over the last three decades, or more. Consideration of wood density may also prove useful, with *K. gabonesis* and *P. angolensis*, two hard-wooded trees - showing most negative associations with CO_2.

In contrast to the relationship at seasonal scales, variation in light and water availability at Lopé have weak negative or no impacts on leaf flushing on interannual scales. The analysis of the shorter dataset indicated that leaf flush is elevated in years following unusually negative cumulative water deficits indicative of intense long dry season drought. This effect was no longer significant in the analysis of the longer dataset, which instead indicated that leaf flush is suppressed in years following above average rainfall. Total annual rainfall is more strongly correlated with rainfall in the short than the long dry season so it is possible that these two effects could occur simultaneously. However, leaf damage is highly correlated with rainfall and it is unclear which one may be the most important factor as one or the other are retained in either model.

Another determinant of leaf longevity that we haven't considered in this analysis is Nitrogen availability. In temperate regions it has been shown that trees at N-poor sites have longer leaf longevity than sites with high N (Del Arco *et al.* 1991). However organic N deposition in central African forests is already high and is driven by anthropogenic savannah burns (Bauters *et al.* 2018) which have a long history throughout Africa (Archibald *et al.* 2011). Therefore N deposition is unlikely to be contributing to the increase in leaf longevity witnessed at Lopé.

Finally, leaf damage was a positive (but not significant) predictor of leaf flush at interannual scales. It is well established that leaf longevity is strongly correlated with many other leaf attributes, and that short-lived leaves have higher photosynthetic rates per leaf area, higher nutrient content and leaf area but are also more fragile and a target for herbivory (Reich 1995). On interannual scales, three of the species with the highest probabilities of leaf flush (thus shorter leaf lifespans) – *A. klaineana*, *P. angolensis, G. giganeteum* and *C. lizae* (random intercepts for leaf flush all >0, Table S5.6C) – also suffer

the most leaf damage. The effect of leaf damage on leaf flush at interannual scales is either no different to the population-level effect or more positive for all four of these species. Frequency of leaf damage has clearly declined since 1995 although the reasons for this remain unclear. Could it be that a reduction in insect activity has resulted in less leaf damage over time and reduced stimulation of leaf turnover? Or the opposite, that a reduction in leaf turnover has made leaves less susceptible to leaf damage, as older leaves are less palatable? Whatever the mechanism might be for increased leaf longevity, the long-term trend in reduced leaf flush witnessed at Lopé is likely to explain the increases in leaf area observed since 1982 in the region (Zhu *et al.* 2016) with mature leaves persisting for longer and fewer leaves being dropped from the canopy.

Earth system models still cannot agree whether tropical land areas are likely to be carbon sinks or sources under different climate scenarios and this is mostly down to uncertainty in the effects of climate and CO_2 concentration on productivity and vegetation turnover (Mitchard 2018). It is more important than ever to gain a mechanistic understanding of leaf phenology across spatial and temporal scales and the likely directions that leafy canopies will take under future environmental conditions. It has been suggested that African tropical forest species are relatively drought-adapted compared to species found elsewhere in the tropics because of the climatic cycles experienced over the past 3000 years (Asefi-najafabady & Saatchi 2013). However, James et al (2013) emphasise that current precipitation levels in the African closed-canopy forests are already near to the hydrological limits for moist forest persistence, and that drier conditions are likely to lead to water stress. Rising temperatures are likely to increase transpiration (further enhancing water stress) and directly impact plants by inhibiting photosynthesis. However we provide further evidence, that at least in the short-term, CO_2 enrichment may act to compensate the influence of temperature and drought by increasing plant water use efficiency.

5.6 ACKNOWLEDGEMENTS

Phenology and weather research at SEGC, Lopé National Park was funded by the International Centre for Medical Research in Franceville (CIRM; 1986-2010) and by Gabon's National Parks Agency (ANPN; 2010 – present). We acknowledge significant periods of independent data collection undertaken by Richard Parnell, Liz Williamson, Rebecca Ham, Patricia Peignot and Ludovic Momont, Ruth Starkey, Edomond Dimoto, Jean-Thoussaint Dikangadissi and Lee White. Permission to conduct this research in Gabon was granted by the CIRMF Scientific Council and the Ministry of Water and Forests (1986 – 2010), and by ANPN and the National Centre for Research in Science and Technology (CENAREST; 2010 – present).

S5 SUPPORTING INFORMATION

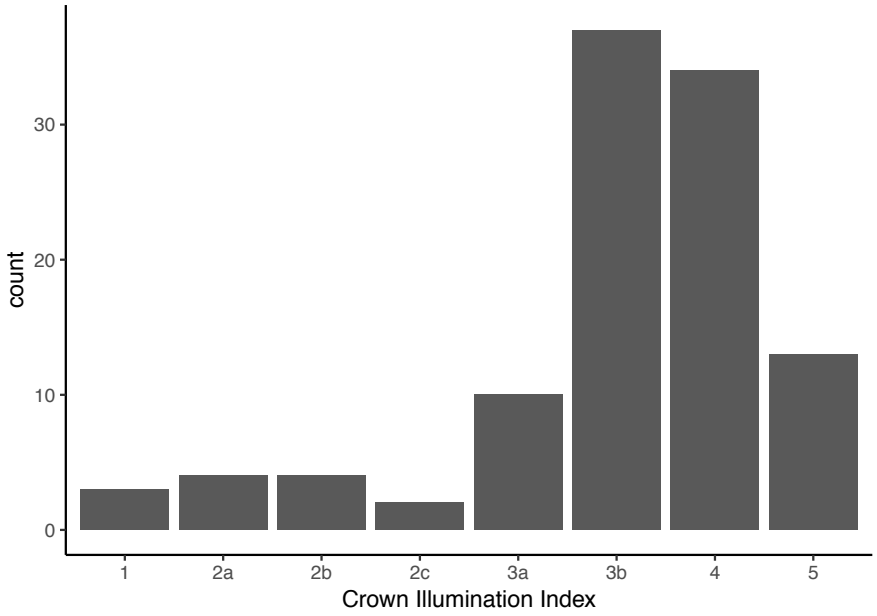

Figure S5.1. Histogram of crown illumination for trees included in the leaf flush analysis.

Scores were assigned in 2015 upon visual assessment of the canopy using binoculars from the ground according to the RAINFOR network guidelines. 1: Lower understorey with no direct light; 2: Upper understorey with some lateral light (a=low, b=medium, c=high); 3: Lower canopy with some overhead light (a=<50% vertical projection exposed, b=>50%); 4: Canopy with full overhead light and 5: Emergent with crown completely exposed

Table S5.1. Model outputs for monthly variation in probability of new leaves.

Generalised linear mixed effects models (family=Binomial). A. Estimates for the fixed effects from a model with the global intercept removed to estimate the magnitude of each monthly intercept. B. Variance of the random effects.

A.

Predictor	Estimate	SE	Z value
Month:Apr	-1.32	0.40	-3.27
Month:Aug	-1.94	0.40	-4.88
Month:Dec	-1.24	0.33	-3.74
Month:Feb	-1.31	0.34	-3.81
Month:Jan	-1.40	0.37	-3.76
Month:Jul	-1.56	0.42	-3.67
Month:Jun	-1.28	0.36	-3.55
Month:Mar	-1.33	0.32	-4.12
Month:May	-1.03	0.36	-2.90
Month:Nov	-1.50	0.34	-4.41
Month:Oct	-2.11	0.36	-5.92
Month:Sep	-2.51	0.49	-5.08

B.

Group	Random effect	Variance	SD
TreeID	Intercept	0.29	0.54
Species	Month:Apr	1.24	1.11
	Month:Aug	1.20	1.09
	Month:Dec	0.83	0.91
	Month:Feb	0.90	0.95
	Month:Jan	1.05	1.03
	Month:Jul	1.38	1.17
	Month:Jun	0.99	0.99
	Month:Mar	0.78	0.88
	Month:May	0.97	0.99
	Month:Nov	0.88	0.94
	Month:Oct	0.95	0.97
	Month:Sep	1.84	1.35

Table S5.2. Model outputs for monthly variation in probability of senescent leaves.

Generalised linear mixed effects models (family=Binomial). A. Estimates for the fixed effects from a model with the global intercept removed to estimate the magnitude of each monthly intercept. B. Variance of the random effects.

A.

Predictor	Estimate	SE	Z value
Month:Apr	-2.24	0.41	-5.51
Month:Aug	-1.89	0.40	-4.70
Month:Dec	-2.32	0.31	-7.50
Month:Feb	-2.35	0.40	-5.81
Month:Jan	-2.50	0.42	-6.00
Month:Jul	-2.27	0.39	-5.78
Month:Jun	-2.71	0.40	-6.83
Month:Mar	-2.39	0.40	-5.94
Month:May	-2.43	0.45	-5.44
Month:Nov	-2.43	0.35	-7.00
Month:Oct	-2.15	0.35	-6.14
Month:Sep	-1.83	0.37	-4.91

B.

Group	Random effect	Variance	SD
TreeID	Intercept	0.27	0.52
Species	Month:Apr	1.25	1.12
	Month:Aug	1.24	1.11
	Month:Dec	0.70	0.84
	Month:Feb	1.23	1.11
	Month:Jan	1.31	1.14
	Month:Jul	1.16	1.08
	Month:Jun	1.16	1.08
	Month:Mar	1.22	1.10
	Month:May	1.52	1.23
	Month:Nov	0.89	0.94
	Month:Oct	0.92	0.96
	Month:Sep	1.05	1.03

Table S5.3. Model outputs for monthly variation in probability of a full mature leaf canopy.

Generalised linear mixed effects models (family=Binomial). A. Estimates for the fixed effects from a model with the global intercept removed to estimate the magnitude of each monthly intercept. B. Variance of the random effects.

A.

Predictor	Estimate	SE	Z value
Month:Apr	2.41	0.28	8.55
Month:Aug	2.68	0.24	11.06
Month:Dec	2.19	0.32	6.89
Month:Feb	2.10	0.24	8.77
Month:Jan	2.12	0.35	6.09
Month:Jul	2.77	0.25	11.07
Month:Jun	2.57	0.23	11.00
Month:Mar	2.30	0.27	8.59
Month:May	2.27	0.27	8.40
Month:Nov	2.57	0.32	7.97
Month:Oct	2.95	0.25	11.89
Month:Sep	3.18	0.21	15.27

B.

Group	Random effect	Variance	SD
TreeID	Intercept	0.19	0.44
Species	Month:Apr	0.56	0.75
	Month:Aug	0.39	0.63
	Month:Dec	0.74	0.86
	Month:Feb	0.41	0.64
	Month:Jan	0.91	0.95
	Month:Jul	0.42	0.65
	Month:Jun	0.36	0.60
	Month:Mar	0.51	0.71
	Month:May	0.52	0.72
	Month:Nov	0.76	0.87
	Month:Oct	0.41	0.64
	Month:Sep	0.25	0.50

Table S5.4. Model outputs for monthly variation in probability of leaf damage.

Generalised linear mixed effects models (family=Binomial). A. Estimates for the fixed effects from a model with the global intercept removed to estimate the magnitude of each monthly intercept. B. Variance of the random effects.

A.

Predictor	Estimate	SE	Z value
Month:Apr	-1.74	0.40	-4.37
Month:Aug	-1.68	0.37	-4.57
Month:Dec	-1.75	0.46	-3.79
Month:Feb	-1.71	0.44	-3.89
Month:Jan	-1.53	0.34	-4.53
Month:Jul	-1.63	0.38	-4.26
Month:Jun	-1.79	0.42	-4.24
Month:Mar	-1.80	0.44	-4.14
Month:May	-1.80	0.44	-4.06
Month:Nov	-1.75	0.43	-4.08
Month:Oct	-1.65	0.40	-4.12
Month:Sep	-1.66	0.43	-3.83

B.

Group	Random effect	Variance	SD
TreeID	Intercept	0.10	0.31
Species	Month:Apr	1.22	1.10
	Month:Aug	1.04	1.02
	Month:Dec	1.65	1.29
	Month:Feb	1.50	1.22
	Month:Jan	0.87	0.93
	Month:Jul	1.14	1.07
	Month:Jun	1.38	1.17
	Month:Mar	1.47	1.21
	Month:May	1.52	1.23
	Month:Nov	1.42	1.19
	Month:Oct	1.24	1.11
	Month:Sep	1.44	1.20

Table S5.5. Correlation matrix for all predictors of interannual variation in probability of leaf flushing.

	Year	Rain	MinTemp	Solar	CO2	MCWD	MCWD1	Leaf Damage
Year	1.00	0.04	0.54	0.27	1.00	-0.34	-0.26	-0.59
Rain		1.00	-0.12	0.04	0.03	0.42	0.04	-0.56
MinTemp			1.00	0.38	0.56	-0.18	-0.25	-0.16
Solar				1.00	0.29	-0.08	0.18	-0.40
CO2					1.00	-0.35	-0.27	-0.59
MCWD						1.00	0.00	0.13
MCWD1							1.00	-0.06
Leaf Damage								1.00

Table S5.6. Model outputs from the best model for interannual variation in leaf flushing (m1).

Generalised linear mixed effects models (family=Binomial). A. Estimates for the fixed effects. B. Variance of the random effects. C. Estimates for the random effects. The predictors were all rescaled by removing the mean and dividing by 1SD.

A.

Predictor	**Estimate**	**SE**	**Z value**	**P value**
Intercept	-0.97	0.25	-3.84	<0.001
CO2	-1.24	0.17	-7.41	<0.0001
MinTemp	0.01	0.10	0.14	0.89
MCWD1	-0.20	0.10	-2.03	<0.05
LeafDamage	0.08	0.07	1.23	0.22
Solar	-0.06	0.09	-0.60	0.55

B.

Group	**Random effect**	**Varian**	SD
TreeID	Intercept	0.19	0.43
Year	Intercept	0.10	0.32
Species	Intercept	0.44	0.67
	CO2	0.10	0.32
	MinTemp	0.01	0.11
	MCWD1	0.02	0.13
	LeafDamage	0.02	0.14
	Solar	0.02	0.13

C.

Species	**Random intercept**	**Random slope**				
		CO2	**MinTemp**	**MCWD1**	**LeafDamage**	**Solar**
A. klaineana	0.90	0.36	-0.08	0.23	0.08	0.05
C. lizae	0.23	-0.02	-0.04	-0.04	0.10	0.03
D. buettneri	-0.54	-0.09	0.01	-0.04	0.04	0.07
G. giganteum	0.60	0.34	-0.10	0.16	-0.10	-0.18
K. gabonensis	0.05	-0.33	-0.03	-0.09	0.14	0.10
P. macrophylla	-0.85	0.32	-0.04	-0.02	0.02	-0.01
P. soyauxii	-0.89	-0.09	0.10	-0.13	-0.27	-0.20
P. angolensis	0.56	-0.45	0.17	-0.05	-0.02	0.13

Table S5.7. Model outputs from the best model for interannual variation in leaf flushing with leaf damage removed allowing for extended data period (m2).

Generalised linear mixed effects models (family=Binomial). A. Estimates for the fixed effects. B. Variance of the random effects. C. Estimates for the random effects. The predictors were all rescaled by removing the mean and dividing by 1SD.

A.

Predictor	Estimate	SE	Z value	P value
Intercept	-1.06	0.24	-4.41	<0.001
CO2	-1.02	0.15	-6.65	<0.001
MinTemp	-0.11	0.10	-1.10	0.27
Rain	-0.17	0.08	-1.98	<0.05
MCWD1	-0.18	0.09	-1.93	0.05
Solar	-0.01	0.10	-0.08	0.94

B.

Group	Random effect	Varianc	SD
TreeID	Intercept	0.19	0.44
Year	Intercept	0.09	0.31
Species	Intercept	0.40	0.63
	CO2	0.13	0.36
	MinTemp	0.01	0.12
	Rain	0.01	0.11
	MCWD1	0.01	0.12
	Solar	0.02	0.16

C.

Species	Random intercept	Random slope				
		CO2	MinTemp	Rain	MCWD1	Solar
A. klaineana	0.81	0.15	-0.12	0.05	0.20	0.17
C. lizae	0.19	-0.20	-0.12	-0.12	-0.06	0.14
D. buettneri	-0.57	-0.18	0.07	-0.06	0.01	0.10
G. giganteum	0.54	0.35	-0.08	0.08	0.12	-0.04
K. gabonensis	0.01	-0.22	0.01	-0.04	-0.09	0.03
P. macrophylla	-0.77	0.57	0.06	0.06	0.05	-0.29
P. soyauxii	-0.82	0.11	-0.02	-0.12	-0.16	-0.17
P. angolensis	0.65	-0.55	0.19	0.17	-0.06	0.07

CHAPTER 6

Is Moabi a reliable source of enterprise for the future?

6.1 ABSTRACT

Moabi oil is highly valued in rural communities in west central Africa for its culinary, cosmetic and medicinal properties. The closely related Argan, Shea or Karité nut oils have become internationally popular since the late 1990s resulting in multi billion dollar industries dependent on wild harvest. In Gabon most Moabi oil is kept for domestic use or traded locally and there are no international markets. Commercialisation of Moabi oil as a non-timber forest product (NTFP) could improve income generation for the rural poor and aid biodiversity conservation because the NTFP-value of the slow-growing, threatened Moabi tree is greater than its timber-value over the long-term. Until the present, Moabi commercialisation efforts have focused on quality control and access to markets with little consideration of raw resource availability, despite large fluctuations in Moabi fruit production between years. In this study, we combined over 15 years' scientific monitoring of Moabi phenology at Lopé National Park with indigenous knowledge from Moabi oil producers in rural Gabon, to describe the factors that influence harvest success and explore the potential impacts on the rest of the Moabi oil value chain. Moabi fruit production is highly variable

between years and regions while Moabi harvest requires a lot of effort (time and physical strength) and harvesters face competition for fruits from a range of forest animals. Currently we consider that the effort required to extract the oil exerts a limit on the amount of fruits collected meaning that producers are unlikely to be harvesting to the limit of the environmental resource. However the Moabi supply chain is moving towards direct purchase of nuts from participants and more centralised, mechanised oil production. In this case it is likely that harvest will increase and be more closely impacted by fluctuations in raw resource availability. To improve income security for rural producers we recommend that current Moabi commercialisation partnerships incorporate either an insurance-type scheme to compensate participants or develop other NTFPs alongside Moabi to form a diverse "safety-net" and reduce economic shocks when Moabi fruits are scarce.

6.2 INTRODUCTION

Before the 1990s, Argan Oil and Shea Butter were practically unknown outside of their native ranges (Morocco and the west African Sahel respectively) where they have long been revered by indigenous peoples for their culinary, cosmetic and medicinal properties (Lybbert *et al.* 2002, 2011; Elias & Carney 2007). Successful commercialisation of these non-timber forest products (NTFPs) has transformed them into multi-billion dollar international industries (Lybbert *et al.* 2011; FAO 2016). In fact, Argan is now the most expensive oil in the world.

A similar nut oil extracted from the closely related Moabi tree (*Baillonella toxisperma* Pierre., also a member of the Sapotaceae family) is highly valued for its culinary and cosmetic properties in its native range in west central Africa (Louppe 2005; Iponga *et al.* 2018). As of yet, most Moabi oil is kept for domestic use or traded locally and there are no international markets (Ingram & Schure 2010). Moabi is listed as vulnerable by the IUCN due to over exploitation for timber which has led to serious declines in large parts of its range (White 1998). However the NTFP value of a Moabi tree is greater than its timber value over the long-term (after at least 7.5 years; Plenderleith

& Brown 2004) suggesting that NTFP commercialisation could contribute to its conservation.

Gabon is a heavily forested country (> 85% land area in 2010; Blaser *et al.* 2011) at the heart of the Moabi native range. The country has a rapidly urbanising population, yet 13% of the population (~260,000 people) remain in rural forest villages where unemployment is high (countrywide unemployment in 2015 = 28%) and a third live under the poverty line (Central Intelligence Agency 2018). More than 10% Gabon's land area is designated within a National Park (NP) network and the National Agency of National Parks (ANPN) is tasked with implementing the government's policy: to protect a representative network of natural areas and landscapes in as natural state as possible, eliminate and prevent exploitation and occupation at odds with the parks' conservation status and to take into account the needs of local populations in the national fight against poverty (Parcs Gabon 2018). In accordance with this mission, ANPN has engaged in various conservation outreach activities – such as ecotourism and alternative livelihoods - as a means of stimulating economic development in NP buffer zones. Under this banner, ANPN partnered with a national cooperative of artisanal craftspeople and producers (Gabon Boutique) in 2010 to pilot Moabi oil production around Lopé NP. Since then the Moabi oil partnership has expanded to the buffer zones of a number of NPs with a focus on establishing markets and securing income for rural Moabi producers, as well as improving production and storage techniques. However, Moabi trees are known to have highly variable fruit production between years (Plenderleith & Brown 2004; Louppe 2005) and thus far there has been little consideration of the impacts raw resource availability may have on successful Moabi harvest and oil production.

In this study we seek to understand and quantify the impacts that raw resource variability has on Moabi oil production. And also whether improved ability to predict Moabi fruiting events could increase income generation and security for rural producers and improve market uptake of Moabi oil. To this end, we combine over 15 years' scientific monitoring of Moabi phenology at

Lopé National Park with interviews to determine indigenous knowledge of rural forest dwelling communities. We use these data to describe Moabi phenology, quantify the factors that influence Moabi harvest success and discuss the possible impacts of harvest success on the rest of the Moabi oil value chain.

6.2.1 NTFP COMMERCIALIZATION AS AN ALTERNATIVE LIVELIHOOD STRATEGY

NTFPs play important nutritional, cultural and commercial roles for forest-dwelling people around the globe. The diet of rural children improves with proximity to forest in low-income countries (Rasolofoson *et al.* 2018) and NTFPs form a diverse "safety net" for the rural poor, contributing to household income and helping to reduce vulnerability to economic shocks (Shackleton & Sheona 2004; Awono & Levang 2018). Commercialisation of NTFP harvests has been a popular conservation and poverty alleviation initiative since the 1980s (Belcher & Schreckenberg 2007). The dual aims of NTFP commercialisation are to improve rural incomes through product development and access to markets and to protect intact forests by providing an economic alternative to timber extraction and clear felling for conventional agriculture (Arnold & Pérez 2001). However these aims are often at odds with each other and common problems associated with NTFP commercialisation include degradation of the natural resource and unrealised or unequal distribution of the benefits in rural communities (reviewed in Arnold & Pérez 2001). Evaluation of the effectiveness of integrated conservation and development projects (ICDPs) in west and central Africa is still in its infancy and the focus so far has been mainly on projects to reduce the impacts of wild meat hunting (e.g. Wicander & Coad 2018) not NTFPs.

The potential that NTFP commercialisation has for biodiversity conservation depends on the extent of harvest, the tolerance of the targeted species (which varies between species and resource type; Ticktin 2004) and how much competition is created between humans and animals who also require access to the resource. In addition, market forces are selective and the supply of

natural resources is inelastic, meaning that successful markets tend to drive production towards intense management, large-scale domestication or synthetic alternatives, which are at odds with the goals of maintaining biodiversity in forest ecosystems (Arnold & Pérez 2001).

How well NTFP commercialization contributes to poverty alleviation is also highly influenced by market forces. NTFPs can both fall out of favour or become more desirable (e.g. wooden furniture) as household incomes rise, while others may face competition from industrial alternatives. Within rural communities, the benefits of NTFP commercialisation are often distributed unequally with many of the benefits captured by the wealthier, more powerful households (Heubach *et al.* 2011). Commercialisation itself can put increased pressure on traditional systems of managing common forest property (Arnold & Pérez 2001).

The harvest of forest fruits presents particular opportunities and challenges. Fruit collection is non-destructive and the local abundance of fruits at particular times facilitates targeted harvesting expeditions. However fruits are usually perishable meaning that storage and transport to market from remote areas can be problematic (Arnold & Pérez 2001; Belcher & Schreckenberg 2007). Removal of fruits from the forest could impact recruitment and genetic diversity of the targeted population, ultimately impacting forest structure and composition, and can lead to heightened competition between people and forest animals for food (Kinnaird 1992; Hall & Bawa 1993).

One of the major differences between NTFPs and agricultural products comes from the very nature of wild harvesting. Wild fruit may be produced far from home and on land without secure tenure (Belcher & Schreckenberg 2007). In addition, indigenous fruits trees have not been subjected to the same selective pressures as domesticated species. Of the NTFP case-studies considered by Newton et al. (2006), limited resource availability and variable yields were two major factors limiting commercialization in 68% and 58% of cases respectively. Complex fruit production contributes a large amount of uncertainty and variability to income generated from NTFP-based

livelihoods. We have shown previously that the phenological cycles of wild tropical tree species are highly complex with reproductive events occurring both regularly and irregularly, on sub-annual, annual and multi-annual time scales and often not synchronised between or within species (Chapter 2 and Bush *et al.* 2017).

Without significant investment, scientific knowledge of the biology of tropical NTFP species is likely to be poor making it difficult to assess whether a species is suitable for successful NTFP commercialisation or whether harvests can be managed sustainably. Indigenous ecological knowledge, on the other hand, can be a rich source of information on plant biology (Wezel & Lykke 2006; Neto *et al.* 2013; Campos *et al.* 2018). The potential for relatively rapid collation of information on species fruiting patterns via indigenous knowledge is particularly attractive because of the long observation periods required for robust phenological analyses (Bush *et al.* 2017). However knowledge acquired by forest-dwelling people will be specific to their requirements and may not cover all areas of a species' biology required for assessment of NTFP commercialization.

62.2 MOABI OIL AS AN NTFP

Moabi, or African pearwood, is a large canopy tree, >60m tall at maturity, found at low densities (one adult tree per 20ha) throughout the lowland rainforests of west central Africa (Louppe 2005). It is a popular hardwood timber species and its bark and fruit are important to rural communities for many culinary, cosmetic, medicinal and ritual uses (Plenderleith & Brown 2004). Moabi seeds can be processed to extract a viscous oil - similar to the closely related Argan, Shea or Karité nut oils - and is highly valued in rural communities (Veuthey & Gerber 2010). Due to the laborious processing required, most Moabi oil is kept for domestic use but some surplus is traded locally for cash income (Endamana *et al.* 2016). Moabi oil has been identified as having the potential to be a high value NTFP (Plenderleith & Brown 2004) and has been promoted for commercialisation by various NGOs (e.g. at the Dja Biosphere Reserve, Cameroon; Veuthey & Gerber 2010; 'Man & Nature' 2017). However markets remain local with little or no international trade

(Ingram & Schure 2010) and there is little accessible information on the commercialisation process.

The factors that favour Moabi oil commercialization are that the flavour of the oil is preferred locally when people have access to it, the oil is highly priced due to its scarcity and the NTFP value of a Moabi tree is greater than its timber value over the long-term (Plenderleith & Brown 2004). An analysis in 1995 for Moabi oil production in Cameroon showed that a Moabi tree's timber value after 140 years was CFA 462,500 (~ US $1850, equivalent to US $3070 in 2018), while the oil revenue at an extraction rate of 135-165l every three years was CFA 300,000 (~ US$ 1200, equivalent to US$ 1990 in 2018). Applying a discount value of 10% the authors found that revenues from oil extraction would be higher than the equivalent timber value after 7.5 years (Plenderleith & Brown 2004).

Moabi fruits also fall to the ground when ripe, rather than remaining on the tree (White & Edwards 2000), making them easy to collect. Finally there is evidence of political will to protect this species in its native range: Moabi is currently protected in Cameroon and was accorded 25 years of protection from logging in Gabon in 2009, awaiting more data on declines and potential for sustainable harvests (Iponga *et al.* 2018). However as timber cutting renders Moabi trees increasingly rare (White 1998), unfamiliarity may lead to people losing their preference for the oil and replacing it with other cheaper alternatives, thus diminishing its value. The process of extraction is laborious and could benefit from increased mechanisation to ensure appropriate quantity and quality of oil for international markets (as for Argan oil; Lybbert *et al.* 2002). In addition, the habit of Moabi is that it is slow to grow, with incremental growth of 1mm per year when diameter at breast height (DBH) is 10cm increasing to 9.5mm per year when DBH is at least 1m (Louppe 2005). It is also slow to mature with flowering only starting after 50—70 years once the canopy has reached the upper storey and regular fruiting beginning even later once the bole has reached 70cm (Louppe 2005). Fruiting is variable between years (one or two fruiting events every three

years, only one of which is likely to be abundant; Plenderleith & Brown 2004; Louppe 2005).

In Figure 6.1 we have sketched a theoretical value chain for Moabi oil production from the perspective of participating harvesters and producers. Stage one in this value chain is "Harvest success" which is defined as the number of fruits harvested by a producer and is dependent on the number of fruits available in the natural environment, the effort put into harvesting and competition from other Moabi producers and forest animals. Harvest success directly determines the maximum performance possible in the next stage of the value chain: "Production success". Production describes the quantity and quality of oil that is produced and is influenced by the number of people-hours dedicated to processing the nuts, the skill of Moabi producers and the availability of specialist equipment. Finally the last stage of the value chain is "Income" which is determined not only by the quantity and quality of oil produced but also by price per unit, access to markets, transport, storage and marketing costs and taxation levels. This latter stage of Moabi oil production is the key element on which the dual aims of Moabi commercialisation rest; poverty reduction via increased income and biodiversity conservation via increased value of standing versus felled Moabi trees.

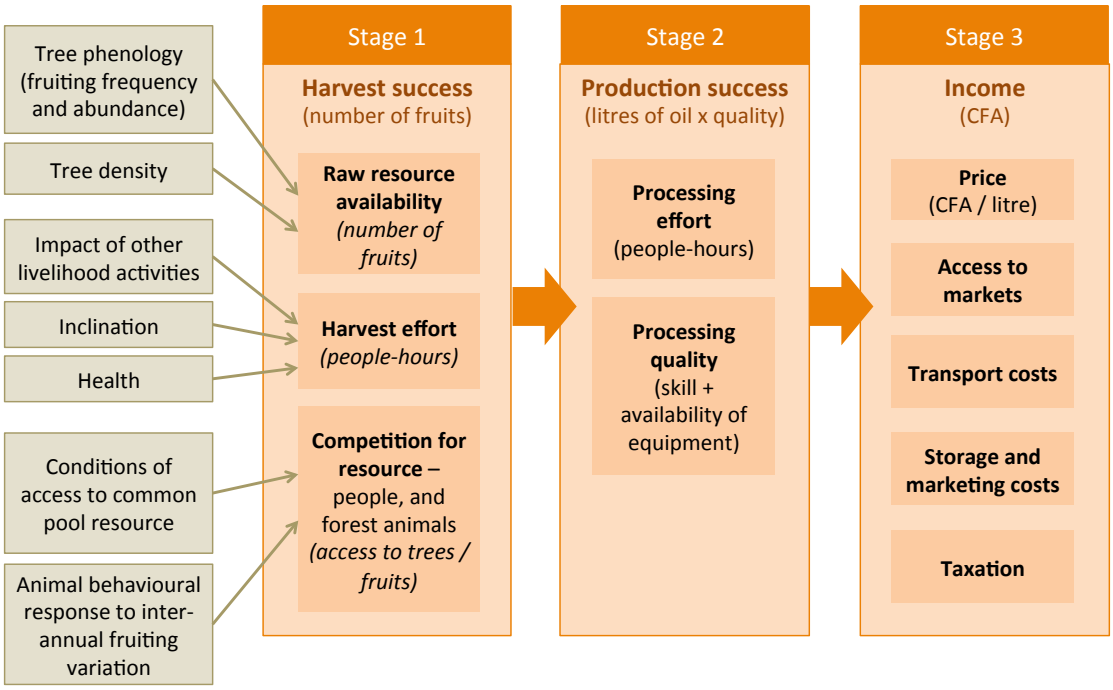

Figure 6.1. Value chain for Moabi Oil commercialisation from the perspective of the producers.

6.2.3 CASE STUDY: GABONESE MOABI OIL IN THE BUFFER ZONES OF NATIONAL PARKS

In the first year that ANPN partnered with Gabon Boutique, 694kg of raw nuts and a small amount of oil (7l) were collected from just five different villages around Lopé NP in an initial pilot to establish the processing and storage systems required to mobilise the product from the villages to market (Figure 6.2). Although the participants were familiar with traditional techniques to extract Moabi oil on a small scale, it was necessary to standardise processes to try and ensure a quality-controlled approach for commercialized oil production. Thus in the second and third years, after standardised production techniques were shared with the participants, oil was purchased directly and production branched out to the surrounding areas of Lopé, Birougou and Waka NPs (362l purchased from 114 producers from 26 villages in 2011 and 334l purchased from 88 producers from 15 villages in 2012). However, despite best efforts, quality (e.g. contamination and deterioration) remained highly variable between producers and an economic assessment by Gabon Boutique established that, particularly for small-scale producers, the time involved in the laborious process of oil

production was not well compensated by the higher price per unit for oil over nuts. In 2013, producers were given the option to sell nuts directly to Gabon Boutique with subsequent oil production organized centrally. In this year 1747kg of nuts and 227l of oil was purchased from 117 producers (23 villages). Production data for the years 2014-2017 are currently unavailable but during this time production groups were formed in certain regions (e.g. Mayengue) with the aims of organising oil production regionally and allowing producers to autonomously negotiate prices. Recent funding has enabled Gabon Boutique to expand the marketing end and develop high value-added products (soap, face creams) as well as raw oil. The amount purchased from any one producer in years 2010-2013 ranged from 0.1 to 16l of oil (median= 2l) and 5 to 87kg of nuts (median = 16kg). The median price paid per unit for oil was CFA 5000 per litre (on the 1st December 2018, CFA 656 = 1 Euro).

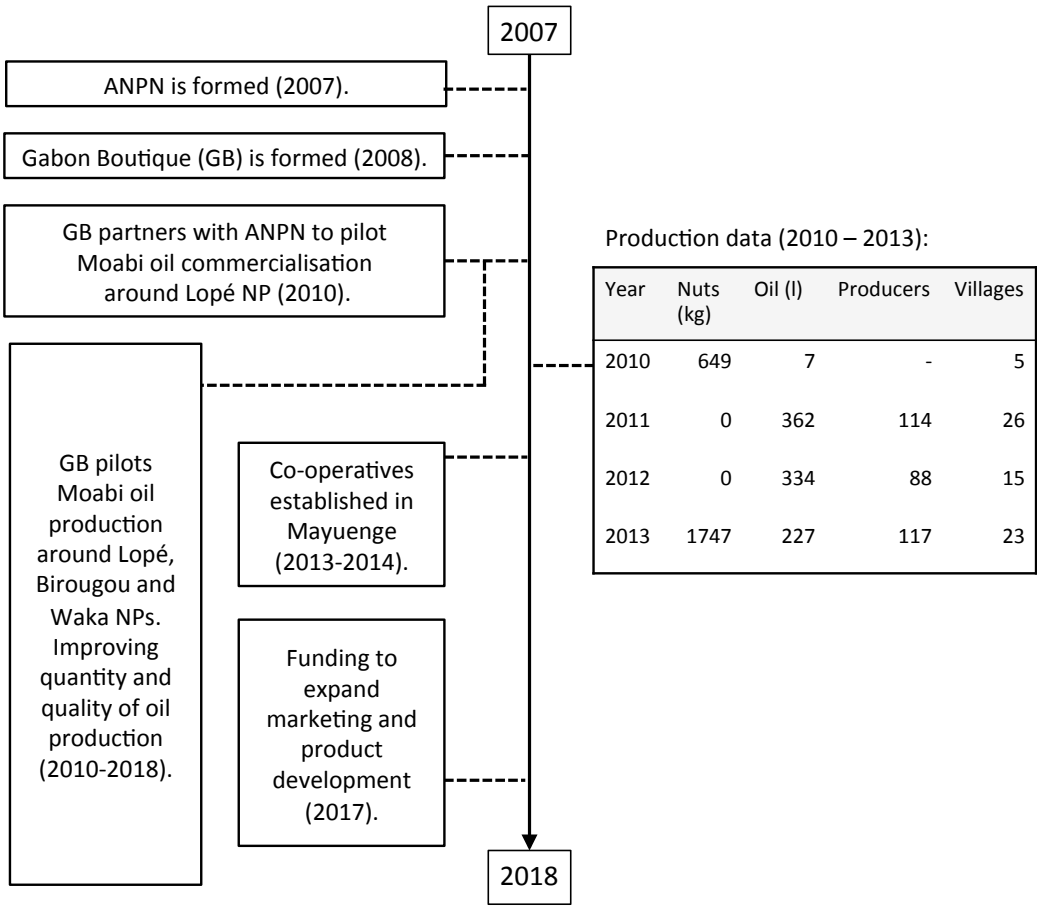

Figure 6.2. Timeline of the National Agency of National Parks (ANPN) and Gabon Boutique partnership to pilot Moabi Oil commercialisation activities in the buffer zones of national parks from 2007 to 2018.

Until now the focus of Gabon Boutique's activities has been on improving the latter two stages of the value chain described in Figure 6.1: production success and income. However, we have established that Moabi fruits are a variable resource between years and that most buyers of value-added products require some guarantee of minimum production per year to allow them to plan investments and marketing. It is also essential that if NTFP commercialisation is presented as an alternative livelihood activity that it is sustainable and doesn't contribute to poverty or insecurity. With these issues in mind, in this study we focus on the first stage of the Moabi value chain - harvest success – and the potential impacts raw resource variability may have on successful Moabi commercialisation. Harvest success is not simply a function of raw resource availability, and so it is also necessary to take account of harvest effort (and competition for resources; Figure 6.1). For example, there could be a bumper crop of Moabi fruits in a particular year, but a poor harvest due to illness or pre-occupation with other activities. Similarly, another year with little fruit available could be masked by strong harvest effort and/or little competition with forest animals. It may be that producers never harvest to the limit of the fruit available and that raw resource availability has little or no impact on harvest success at current levels of harvest and production.

6.3 METHODS

6.3.1 BOTANICAL DESCRIPTION OF *BAILLONELLA TOXISPERMA*

Moabi is a very large canopy tree reaching 60 (-70) m tall with a trunk bole up to 300 (-500) cm in diameter (Louppe 2005). Moabi can germinate in the shade but afterwards only thrives in the direct sunlight created in forest openings (Doucet *et al.* 2009). Trees begin to flower after 50-70 years once the canopy has reached the upper storey but regular fruiting doesn't occur until the bole is at least 70cm diameter, after 90-100 years (Louppe 2005). The canopy is recognisable from the air, and is fully deciduous, producing flowers after the leaves have dropped (Plenderleith & Brown 2004). There is a phenologic inversion either side of the equator with records of flowers

occurring from February to April north of the equator (Cameroon) and from September to October south of the equator (central Gabon; Plenderleith & Brown 2004).

Moabi fruits are large and globose, 5-8cm in diameter and contain 1-3 ellipsoid seeds c. 4cm long (Louppe 2005). Many animals consume the fruits (elephants, wild pigs, porcupines, duikers and gorillas), but it is only elephants and gorillas that are able to consume and excrete the large seeds whole while wild pigs and porcupines are known to eat the seeds (Plenderleith & Brown 2004). People are also important seed dispersers of Moabi, inadvertently when gathering fruits for oil production and intentionally by planting Moabi trees near human settlements (Veuthey & Gerber 2010). Extensive gene flow in Moabi populations indicates unusually high dispersal distances, both of pollen and seeds by animal dispersers, including humans (Ndiade-Bourobou *et al.* 2010).

6.3.2 Long-term Moabi phenology monitoring at Lopé NP

Since 2003, the leaf, flower and fruit phenology of a sample of eight Moabi trees (*Baillonella toxisperma*) has been monitored by researchers at Lopé National Park as part of a long-term phenology study dating back to 1986. At the beginning of every month (usually completed within the first seven working days), researchers examine the crowns of each tree from the ground with 10 x 42 binoculars and record the proportion of the canopy covered by each phenophase (new, mature and senescent leaves, flowers, unripe and ripe fruits) as a 9-point scale from 0 to 100% coverage. In a recent analysis of the observation uncertainties associated with this method, long-term researchers at SEGC scored Moabi flowers as "difficult to see", whereas leaf changes and fruits were much more obvious (Chapter 3; Bush *et al.* 2018). This is because the flowers are small, inconspicuous and held very high in the canopy. Because of this systematic bias in the sampling methodology it is difficult to determine if flower observations are accurate, whereas we have greater confidence in leaf and fruit observations.

The Lopé study area is a tropical forest-savanna matrix with an equatorial climate characterised by two dry and two wet seasons (Chapter 4). The Moabi sample is fairly young - mean diameter in 2015 was 103cm (ranging from 75 to 168 cm) - but all individuals are reproductively mature. One tree was removed from the sample in 2013 after it died; three more were removed in 2016 due to a change to fieldwork protocol. The mean length of canopy observation is 158 months (ranging from 121 to 176) and the time series are on average, 96% complete, with no data gaps greater than three months long. We filled these gaps using simple linear interpolations (Chapter 2; Bush et al., 2017).

6.3.3 Indigenous ecological knowledge of Moabi phenology

Rural forest-dwelling people in Gabon are highly dependent on forest resources and practice a hunter-gatherer lifestyle combined with small-scale shifting agriculture. Families take daily trips into the forest to visit small slash and burn farmed plots and gather resources such as fruits, bark, bushmeat and firewood. In February 2016 we visited 22 different communities (villages/ quartiers) in the rural interior of Gabon participating in Moabi Oil production with ANPN and Gabon Boutique (Figure 6.3). We conducted interviews in 11 locations, but were unable to interview in the remaining communities because the inhabitants were already occupied in the forest when we visited, or didn't want to participate. Following local cultural protocols at each interview, we gave an introduction to all the gathered community members and then directed the survey questions to a select group of elders (e.g. Chef de Village and his wife). As a result, the questions weren't always answered directly by the current fruit collectors although they often contributed. Elders are almost certain to have participated in harvests in their youth.

Our aims for the interviews were to: (1) Gather indigenous ecological knowledge on the phenological cycles of Moabi, (2) Record Moabi fruit productivity for the most recent years, (3) Establish which factors influence Moabi harvest effort and how this has varied in the most recent years, (4)

Describe the competition (from other people and wild animals) Moabi oil producers face when harvesting fruit.

In each interview we asked the following questions.

1. How many Moabi trees do you (as a family) visit to collect fruit? Can you mark them on this map (sketched map of house and key features in neighboring forest).

2a. How long does it take to walk to the closest Moabi tree?

2b. How long does it take to walk to the furthest Moabi tree?

3. What size are the Moabi trees you visit (estimate in cm or indicate with your arms, mark on the map)?

4. How many trips do you make to collect Moabi fruits each year?

5. Can you describe fruit availability in recent years for each tree? (No fruits, few, a lot of fruits etc…)

6. Do you know if it will be a good year for Moabi fruit before you see the fruit? How?

7. What stops you from collecting more fruit?

8. Which animals eat Moabi fruits?

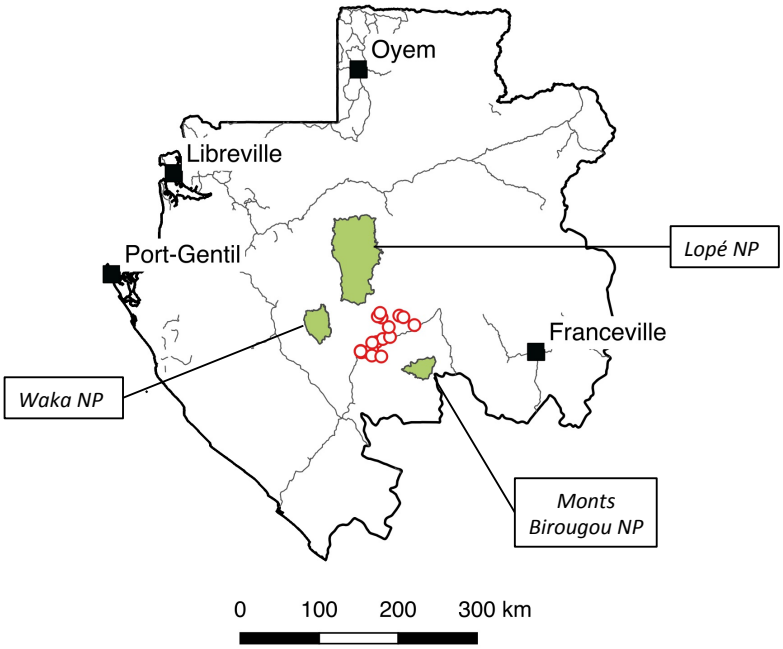

Figure 6.3. Location of communities participating in Moabi Oil production with Gabon Boutique in 2016.
Shown are the four largest cities in Gabon by population (black squares) and the major roads grey lines). Green shaded areas indicate NPs near to the project area and the red circles indicate villages visited for this project in February 2016.

6.3.4 ANALYSES

We calculated the proportion of trees in each phenophase in each month throughout the observation period, and plotted circular boxplots to show both the mean and variation in phenophase synchrony between years. We also calculated the mean canopy score for each calendar month for all individuals and years and displayed this on the same plots to show phenophase intensity. We plotted the time series for mature leaf, flower, unripe fruits and ripe fruit canopy scores for each individual throughout the time period to identify highly synchronous events. Finally we calculated the Fourier spectra for each phenophase for each individual tree in order to identify dominant patterns of cyclicity in the data. Fourier is a form of spectral analysis based on sine and cosine waves that can be used to quantitatively describe the cyclic nature of any time series data (Bloomfield

2000). We used a confidence test, based on 95% confidence intervals and a null hypothesis of 'no cyclicity,' to determine whether the dominant cycle in each spectrum was objectively different to surrounding noise. A full explanation of the Fourier methods used is given in Chapter 2 (Bush et al. 2017). Qualitative responses from the interviews were coded and described using simple summary statistics (means and percentages).

6.4 RESULTS

6.4.1 LONG-TERM MONITORING OF MOABI PHENOLOGY

Moabi leaf phenology at Lopé is seasonally predictable but not regular. Between 2003 and 2018 new leaves usually appeared between October and December and mature leaves began to senesce between July and October (Figure 6.4A-C).

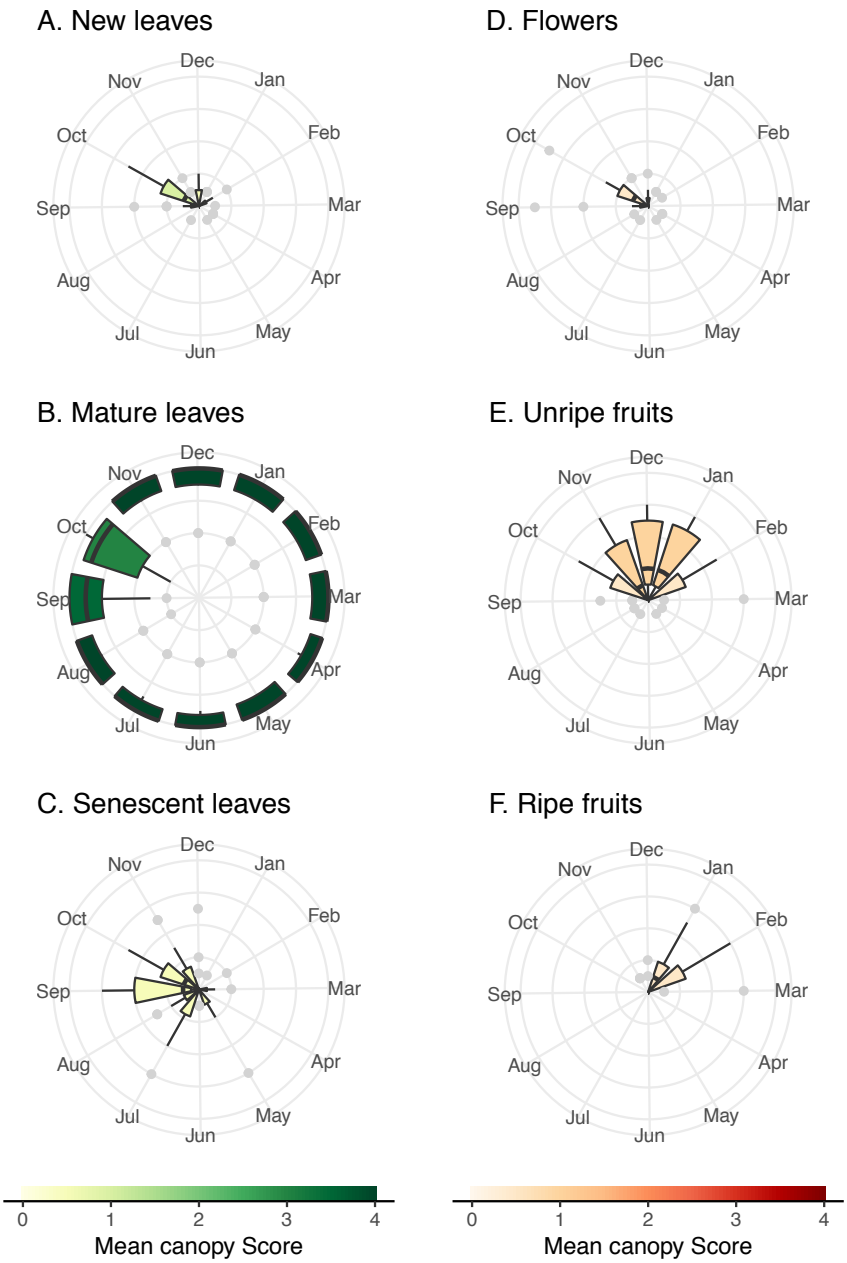

Figure 6.4. Average leaf, flower and fruit phenology of Moabi (Baillonella toxisperma Pierre) at Lopé National Park.

Circular boxplots (A-E) show the proportion of individuals (n=8) in that phenophase each month from 2003 to 2018. The colour of the boxplot represents the mean canopy score (0: no canopy coverage, 4: full canopy coverage) between individuals and years.

Leaf flush did not occur to the same extent every year, for every tree, leading to a leafing phenology with weak cyclicity; the dominant mature leaf cycle was annual for six out of eight individuals but only one of these was considered significantly different to a null spectrum of no cyclicty in the Fourier analysis, while another individual had a significant dominant leafing cycle of six months (Figure 6.5).

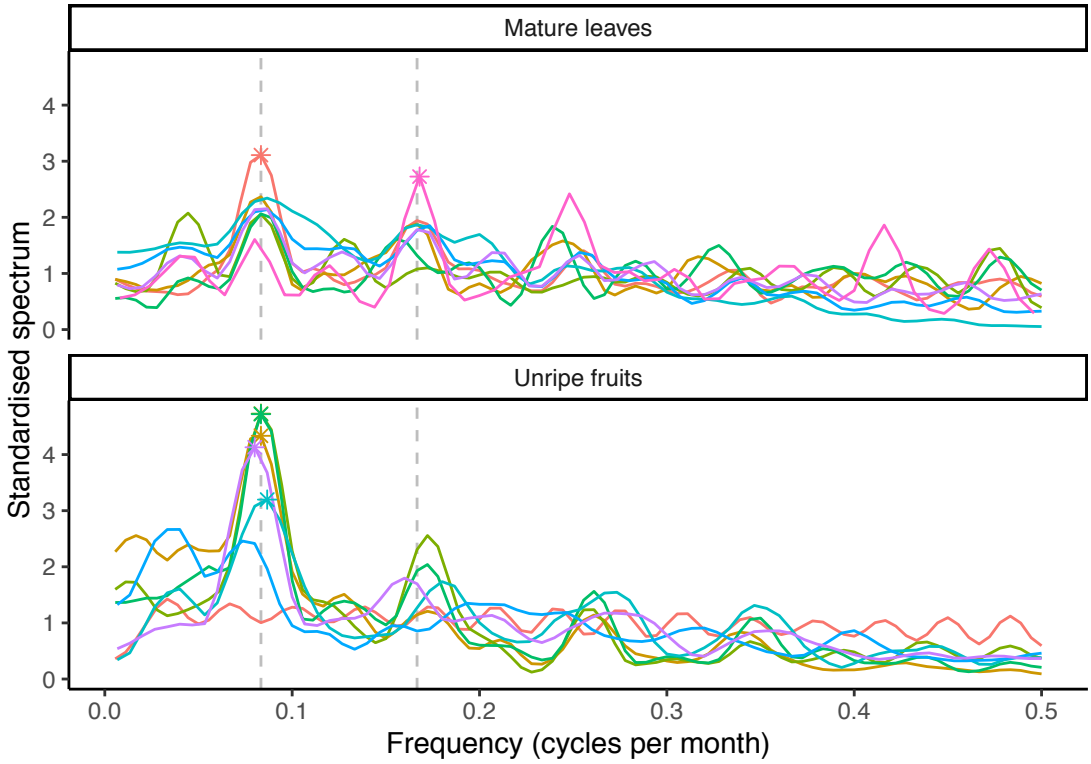

Figure 6.5. Fourier spectra for mature leaf and unripe fruit phenology timeseries for eight Moabi trees (Baillonella toxisperma Pierre) at Lopé National Park, 2003-2018.
Stars indicate dominant cycles significantly different to a null hypothesis of no cyclicity. Horizontal dashed lines indicate the position of peaks in the spectra with 12 month cycles (0.083) and 6 month cycles (0.167).

All of the Lopé Moabi trees were recorded undertaking both full and partial canopy leaf exchange over the 15 years they were observed (Figure 6.6). In certain years (e.g. 2004 and 2010) all individuals underwent a synchronised full canopy deciduous event. In other years, certain individuals (e.g. top and

bottom time series in Figure 6.6) appeared to be more prone to full flushing than others.

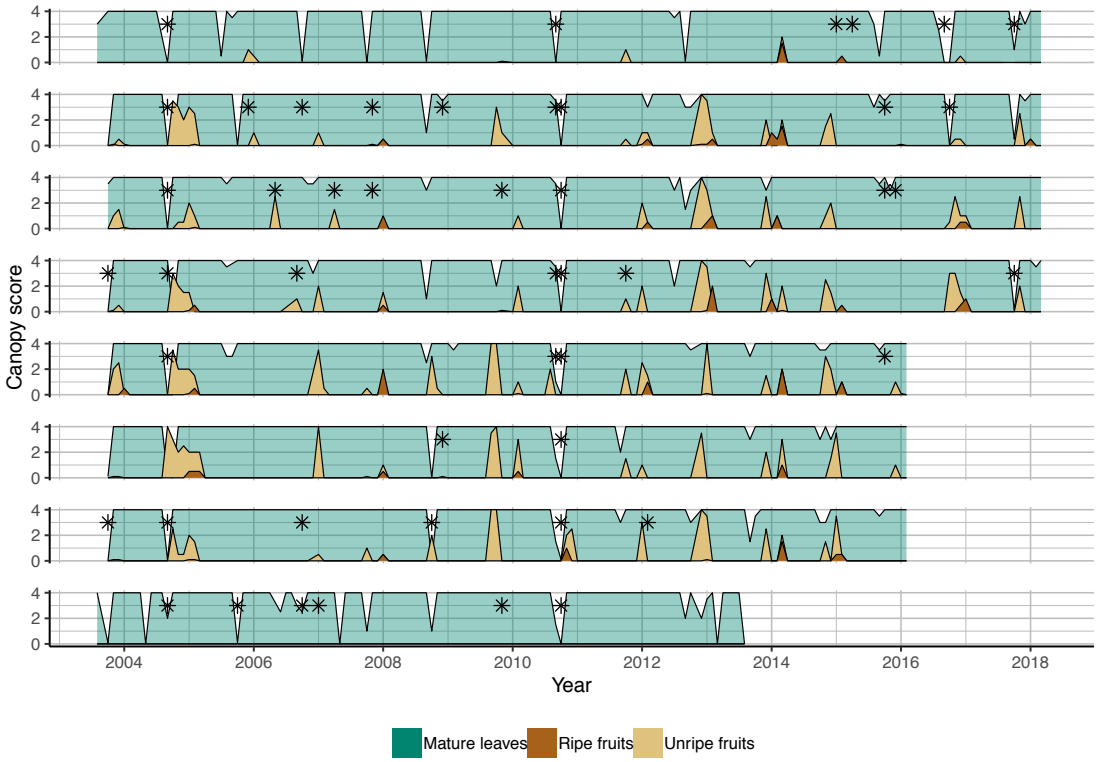

Figure 6.6. Time-series plots of leaf, flower and fruit phenology for eight Moabi trees (Baillonella toxisperma Pierre) at Lopé National Park, 2003-2018.

The canopy score represents canopy coverage for each phenophase (0: no canopy coverage, 4: full canopy coverage). Flower presence is indicated by a star.

Reproductive phenology at Lope showed a similar picture. In years when flowers were present, they usually occurred in October, with fruits developing between October and February and ripening in January and February (Figure 6.4D-F). The dominant reproductive cycle for Moabi was annual (the dominant annual cycle for unripe fruits was significantly different to a null spectrum for five out of eight trees, Figure 6.5). However inter-annual variation was high with fruit abundance differing between individuals and years (Figure 6.6). Excluding the tree that died in 2013, the probability of one of the Lopé trees bearing fruit across all years observed

ranged from 0.33 to 0.92 (mean=0.73, n=7) and the probability of that fruit event covering 50% or more of the canopy (canopy score >=2) ranged from 0.07 to 0.85 (mean=0.50, n=7). In certain years we observed a strong reproductive response from most of the sample (e.g. 2004/5 and 2012/2013; Figure 6.6). In 2010/2011 the entire sample went fully deciduous and then flowered, but fruits were only observed for one individual suggesting an unsuccessful reproductive attempt (Figure 6.6). 64% of fruiting events were recorded with no prior flowering observations (Figure 6.6) indicating the observational uncertainty associated with scoring flowering.

6.4.2 INDIGENOUS KNOWLEDGE

Interviewees described visiting between two and 40 Moabi trees in surrounding forest (mean = 16 trees). The closest trees visited were between five minutes and two hours away (mean = 47 minutes), while the furthest trees were between one hour and 13 hours away (mean=3.9 hours). The interviewees estimated that the trees they visited ranged in size from 60cm to 300cm DBH. Interviewees described making on average 12 trips into the forest to collect Moabi fruits each year, although this question was not very successful with six communities unable to answer. The map exercise was also unsuccessful and was not attempted in most communities after initial failures.

Interviewees were well acquainted with the seasonality of Moabi reproduction through their harvesting activities but also appreciated the variable nature of inter-annual production. All interviewees estimated the amount of fruit available to them in the preceding two years. In 2014/15, seven interviewees considered there to have been no fruit or very few fruits (mostly in the Mimongo area) and only two interviewees considered there to have been “a lot of” fruit (both in the Iboundji area. By contrast, in 2013/14 only one interviewee described there being only a few fruits whereas the rest remembered a normal amount (some) or a lot of fruits and this was across all districts. Only four interviewees attempted to recall fruit availability in years prior to 2014. Interviewees were unable to explain this variability but were able to describe methods they used to predict fruiting events within a season

from other phenological signs. When asked to describe if they knew if Moabi would produce fruit before seeing the fruit, nine out of 11 interviewees described how the trees would lose all their leaves in July –September before a big fruiting year, two out of 11 interviewees referred to the likelihood of Moabi tree producing fruit in the current year if they didn't produce any the previous year. One interviewee described how he could smell Moabi pollen in honey collected from the forest and this let him know if it is likely there will be fruits.

When asked to explain what prevented them from collecting more fruits, six out of 11 interviewees referred to animals eating the fruits before they could access them, five out of 11 interviewees described the effort involved in collecting fruit (time involved, the weight of the baskets full of fruit). When asked which animals eat Moabi fruits, interviewees collectively listed pigs, antelopes, porcupines, elephants, gorillas and rats.

6.5 DISCUSSION

6.5.1 WHAT DETERMINES HARVEST SUCCESS?

From both the scientific monitoring and the interview data it is clear that while Moabi reproduction is seasonal (i.e. when present, flowers and fruit arrive at predictable times of the year), inter-annual variability in flower and fruit production is high. The mean probability of a Moabi tree in Lopé NP reproducing in any year was 0.73 while the mean probability of that event covering at least 50% of the canopy was 0.5. This probability however is higher than the estimates reported in the literature that Moabi trees reproduce in one or two years out of every three (0.33 to 0.66) and that only one of those is likely to be abundant (0.33; Plenderleith & Brown 2004; Louppe 2005). There appears to be much regional variation among the Moabi population as to which years are good or bad for fruit production. 2014/15 was a poor year for fruit production in Mimongo but not Iboundji whereas 2013/14 appeared to be a better than average year across all districts (interviewee data). Our records for the Lopé trees show a relatively strong fruiting response (all trees with fruit >= 50% canopy) in both of these

years. Similarly in 2010/11 fruit was only recorded for one tree at Lopé but 362 litres of Moabi oil were collected by Gabon Boutique in the villages south of the NP indicating that fruit was readily available there.

Harvest requires substantial effort for Moabi producers, who carry fruit back to their dwellings using traditional baskets on their backs, with some interviewees describing visiting trees as far as 13 hours walk away. However effort required is variable between communities with some villages enjoying an abundance of trees (up to 40) with the nearest tree as close as five minutes walk away. Collectively interviewees described a number of animal species eating Moabi fruits, although that depended on their own range with elephant and gorillas largely absent from the southwestern villages. Competition for fruits with forest animals and the effort involved in finding and carrying fruits were the main reasons given by interviewees for why they didn't harvest more. This evidence supports our thesis that without contextual data (number of hours dedicated to harvest and production and competition for resources) it is problematic to assume raw resource availability from the amount of nuts or oil purchased by Gabon Boutique.

We currently do not have the data to establish how closely tied Moabi harvest efforts are to the intensity of fruit production. Under current conditions, we consider it likely that Moabi production is limited by the number of hours required for oil processing, and it is unlikely that producers are harvesting to the maximum of the resource available. However successful international trade in both Argan and Shea oils has been enabled by the development of centralised, mechanised oil processing due to efficiency gains and higher quantity and quality of oil recovered (Lybbert *et al.* 2002; Elias & Carney 2007). In these cases, producers sell their nuts directly to traders and continue artisanal oil production mostly to supply their own requirements and domestic trade. If mechanised production were made more available for Moabi oil production or if traders such as Gabon Boutique continue to buy raw nuts over oil, then the processing limit on production will be lifted and fruit harvest is likely to increase. In this case, harvest may become more closely tied to natural fluctuations and competition between producers and

forest animals may increase and it will be necessary to quantify the impact on the wild population.

6.5.2 How predictable is harvest success?

We have established that Moabi fruit production is highly variable between years. But how predictable is it? Interviewees described a strong connection between leaf phenology and fruiting in Moabi trees. Almost every participant mentioned that in a good fruiting year, Moabi trees lose all their leaves in September before the flowers arrive, while in other years they may lose some leaves but not all. This could form a useful early warning system for fruit productivity in the following September if Gabon Boutique wanted to prepare for oil production ahead of time. However from the scientific monitoring at Lopé we couldn't find a consistent relationship between deciduous events and the strength of the reproductive response. This may be because this relationship does not exist at Lopé, because our sample is too small and trees too young, or because our sampling interval of a month is too long (villagers are likely to check trees more often than that) and flowers are very small and very difficult to see. Shea production is known to be influenced by certain climatic effects, such as an unfavourable wind during flowering or above or below average precipitation (Elias & Carney 2007) while Argan production is susceptible to drought (Zunzunegui *et al.* 2010). Currently we do not know which climatic or other factors influence Moabi fruit production and why this varies between regions, despite the fact that improved ability to predict raw resource availability, especially under long-term projections of climate change in the region, could enable better market preparedness. The data from the scientific study at Lopé is too small (sample size) and too spatially restricted to give robust answers for this research question at present.

6.5.3 Is Moabi suitable for NTFP commercialisation?

Being long-lived and slow to mature, Moabi is an unlikely candidate for intense domestication, favouring Moabi oil's status as a wild product. However, it's unclear if the oil is likely to remain popular enough to justify

the additional expense related to wild harvest compared to other cheaper natural and synthetic alternatives. Other successful NTFP harvests from Sapotaceae species originate from plants with much quicker life habits than Moabi; Argan trees begin to bear fruit after five years although maximum production isn't attained until 60 years (Morton & Voss 1987) while Shea, *Vitellaria paradoxa,* begins flowering after 10–25 years reaching maturity after 20–45 years (Nikiema & Umali 2007). However neither of these species have been domesticated on a large scale and current international trade in their oils comes from naturally regenerated trees within agroforestry systems (Lybbert *et al.* 2002; Elias & Carney 2007). It is unknown what level of harvest is sustainable for the wild population to avoid negative impacts on regeneration.

Shea butter producers also have to accommodate variable quantity and quality of fruit production between years with descriptions in the literature of a repeated three year cycle (good, fair then poor yields; Chalfin 2000) with climate, diseases, parasites and anthropogenic fires known to influence fruit set (Elias & Carney 2007). This means that variability itself does not necessarily preclude successful commercialisation. However there are implications for both marketing and income sustainability. On the marketing end, instability in supply could be accommodated by storing Moabi oil from good years to sell in poor years (if the lifespan of the product allows), or up-scaling production to cover multiple forest zones as Moabi productivity between years appear to be asynchronous spatially. On the supply end, income variability appears to be more of a challenge. In certain years, some households might be unable to produce any oil due to lack of fruit, which could cause hardship if they have become reliant on the income stream. The shocks inherent to this system need to be accounted for in the way the commercialisation scheme is designed. Projects looking to engage villagers in developing NTFPs from fluctuating resources could guarantee some minimum payment for participating households in years when fruit is unavailable (in a similar way to an insurance scheme) paid for by a reduction in price paid per unit at other times. This approach could be organised centrally by the developer or locally via village community funds.

Alternatively, market developers could encourage harvest of other NTFPs (in Gabon this might include Okoumé resin, other edible fruits or woven rattan products) to be bought alongside Moabi, to better mirror the "safety net" already employed by the rural poor to reduce vulnerability to such natural resource fluctuations (Shackleton & Sheona 2004).

6.5.4 Recommendations for future research

There are two avenues for further research to fill the knowledge gaps around Moabi raw resource availability: citizen science monitoring within the Moabi producing villages and a large-scale scientific monitoring program. While the indigenous knowledge of the Moabi system we collated was useful, it was heavily influenced by the way that interviewees used the forest. For example, interviewees found it difficult to answer questions about the number of trips they take into the forest to gather fruit, probably because they access the forest daily for a wide variety of resources and Moabi harvest may not be the sole reason for a forest excursion, even if some Moabi fruit is collected. Training one or two specialised Moabi recorders per village would be a helpful way of combining expert knowledge of the forest with scientific requirements for standardised data collection. The Moabi recorders could make regular observations of the Moabi trees in their surrounding forest (e.g. tree has lost all leaves, some flowers, some fruits) and take note of the harvesting effort of the participants in the village. Remuneration for the time involved in this work would need to be costed. In addition, a separate science-led Moabi Phenology observation network, similar to the Lopé observations but over a larger area, would be highly informative to understand regional variation in fruit availability. Because of the large size of the Moabi canopy and the highly visible nature of deciduous events it is possible that remote sensing could be used to scale-up scientific monitoring in the near future.

Economic development has become a common outreach tool for conservation initiatives with the aims of encouraging buy-in from local populations and compensating for real and perceived losses of access to natural resources. In some cases (e.g. Argan and Shea oils) traditional,

artisanal products can find international appeal and increase income generation especially for the poorest households (Pouliot 2012). However, NTFP commercialisation for both poverty reduction and biodiversity protection – like other ICDP schemes – often fails both objectives. To add to this complexity, tropical phenology is highly complex (Chapter 1; Bush *et al.* 2017) and responds to a wide variety of climatic and other cues (Chapter 5). However hunter-gatherer lifestyles are familiar with these fluctuations and already make use of a wide range of resources to accommodate for natural variability. A well-designed, diverse economic development program, incorporating Moabi oil alongside other commercialised products, is likely to reduce the risks incurred by the rural participants, the trading bodies and partner organisations.

6.6 ACKNOWLEDGEMENTS

This project is the result of a collaboration between ANPN and Stirling University and it would not be possible without the logistical, financial and academic support that both provide. We are grateful to CENAREST for the permission to work at Lopé PN, and to M. Benoit Nziengui, Conservator of PN Lopé, for his support to the project. Many thanks are due to the field assistants who have tirelessly collected the data for the past 30 years, principally M. Edmond Dimoto and M. Jean-Thoussaint Dikangadissi. David Lehmann, Eric Chehoski and Marie-Paule Mboumba provided logistical support while Christian Mboumba, Lambert Vana and Severin Fara were invaluable guides and teachers.

CHAPTER 7

General Discussion

7.1 BACKGROUND

The phenology of tropical forest ecosystems is key to understanding the availability of resources for animal and human users of the forest, the role that tropical vegetation plays in global climatic and atmospheric processes and the direction of change in species communities. Phenology has been repeatedly picked out as an important indicator of environmental change (Rosenzweig *et al.* 2007; Pereira *et al.* 2013) with knock-on consequences for species' interactions within ecosystems (Butt *et al.* 2015; Morellato *et al.* 2016). However tropical phenology is largely missing from global assessments of change due to lack of available data (Feeley *et al.* 2017; Abernethy *et al.* 2018) which is further complicated by the complexity of tropical ecosystems and the diversity of phenological responses among tropical species.

The work contained in this thesis contributes novel insights to tropical phenology research. For the first time in 20 years, we make available one of the longest tropical phenology datasets in the world from Lopé NP in western equatorial Africa, a region containing most of Africa's evergreen tropical forests but for which the climatological context is poorly understood (Philippon *et al.* 2019). We assess both the field and analytical methods at

our long-term site to develop robust indicators of tropical phenological activity and improve the effectiveness of our monitoring design and share these recommendations for others (Chapters 2 and 3; Bush *et al.* 2017, 2018). We analyse the changing environmental (weather) and biological (phenology) context at Lopé for the first time and establish that global climate changes are already impacting this region of western equatorial Africa (Chapter 4) with knock on effects for the phenology of the tropical forest community (Chapter 5). And finally we apply the developments of the previous chapters to a socio-ecological problem: the availability of wild Moabi fruits for NTFP commercialisation. In the following sections we expand on each of these areas and discuss realised and potential opportunities for their impact.

7.2 DEVELOPING ROBUST INDICATORS FOR TROPICAL PHENOLOGY

7.2.1 SUMMARY OF RESULTS

Fourier methods for long-term tropical phenology

In Chapter 2 we address the lack of appropriate circular approaches for tropical phenology analysis by developing a new flexible and robust analytical approach based on Fourier analysis with confidence intervals. We apply this approach to both simulated and long-term field data and present the first analysis of flowering at Lopé (856 individuals, 70 species) since 1998 (Tutin & White 1998). We show that 59% of individuals at Lopé have regular flowering cycles, and annual cycles can be attributed to 88% species. We also show that our ability to detect regular cycles is hampered by observation length (which varies by individual). Using a power analysis we recommended that at least six years of data are required for this method to establish robust estimates of cycle period.

It became apparent in Chapter 2 that cycle detectability differs widely among species with some requiring just six years of data before cycles could be confidently detected and others requiring more than 20 years. In chapter 3 we investigate the source of this noise. First we present a Fourier analysis for leafing and fruiting observations from Lopé (856 individuals, 70 species) in addition to the flowering data presented in Chapter 2. We find that regular cycles are more common among flowers (59% individuals), unripe fruit (54%) and new leaves (51%) than ripe fruit (29%) and senescing leaves (25%). Also that annual cycles are more common among reproductive phenophases (75% all reproductive cycles were annual) while sub-annual cycles are more common among leaf phenophases (51% all vegetative cycles were sub-annual). We gathered expert knowledge from long-term Lopé phenology observers regarding the systematic biases in the observation system and use this information to predict cycle detectability for a subset of 827 individuals from 61 species (each with five or more individuals). We find that in addition to observation length, the visibility and duration of the phenophase being observed are also important positive predictors of cycle detectability. And that in general, cycle detectability among flowering timeseries is four times as high as ripe fruit after ten years of observations.

7.2.2 SYNTHESIS AND APPLICATIONS

We have shown that where suitable data is available, objective, circular analyses can be used to confidently detect regular phenology and that frequency-based outputs – cycle length, power, timing and level of synchrony – give a suite of potential indicators for quantitative comparisons of phenology between species and sites. Particular to our approach is the application of Fourier methods to data from individual trees - enabled by the high resolution of the long-term data at Lopé – and subsequent integration of individual plants to ecosystem level phenology (as recommended by Cleland *et al.* 2007; Adole *et al.* 2016). Since publication in 2017 the methods for individual level plant phenology presented in Chapter 2 have been directly

used in a number of further studies; A pan-African analysis of flowering and fruiting at 12 tropical sites (Adamescu *et al.* 2018), two single site analyses - of flowering and fruiting at Budongo Forest Reserve, Uganda (Babweteera *et al.* 2018) and of leaf phenology at Mount Kiabalu, Borneo (Kitayama *et al.* 2018 PREPRINT) and our own analyses of observation uncertainty in tropical phenology monitoring (Chapter 3: Bush *et al.* 2018), weather variability (Chapter 4), leaf turnover (Chapter 5) and NTFP resource availability (Chapter 6). Phenological analyses using Fourier and associated Wavelet methods at the species and community-level have also been used in a suite of recent publications; two long-term tropical forest fruiting studies (Kibale NP, Uganda: Chapman *et al.* 2018; BCI, Panama: Detto *et al.* 2018), a short-term flowering and fruiting study (Guanica State Forest, Puerto Rico: Lasky *et al.* 2016) and a long-term analysis of lilac blooming dates across the United States (Fu *et al.* 2017).

At Lopé we are fortunate to have access to a relatively long dataset and a large sample of individuals and species, a situation that is rare in the tropics where most datasets are less than ten years long and often target a small set of species (Mendoza *et al.* 2017; Adamescu *et al.* 2018). However, even here, we find that data is noisy and phenophases can be difficult to detect. In Chapter 3 we made recommendations to maximise returns from tropical phenology monitoring efforts. When allocating resources for new and ongoing research into change over time, phenologists should aim to maintain monitoring programmes for as long as possible and target species and phenophases (e.g. flowers) with least inherent biological noise and high visibility to maximise statistical power and therefore ability to assess change in future analyses. We suggest that after a period of initial monitoring (at least five years) it should be possible for data collectors at study sites to assess the amount of noise associated with specific species and phenophases in their sample, allowing project managers to target limited resources.

For many research contexts, collecting sufficient data to allow quantitative analysis of tropical phenology is likely to be challenging. We recommended that ways to achieve this could include: formation of research networks and

greater coordination of methods and objectives between sites, internet-based citizen-science data collection networks and technical solutions to data collection, such as automated canopy photography and GIS. Following these and others' recommendations (Adole *et al.* 2016; Singh & Kushwaha 2016; Mendoza *et al.* 2017), during the course of this thesis we have taken steps to develop an African Phenology Network (www.africanphenologynetwork.online) to facilitate communication and research collaboration between scientists, to promote standardised phenology field methods throughout the continent and to publicise results and publications featuring African phenology. Figure 7.1 shows the phenology sites currently contributing to the metadata inventory.

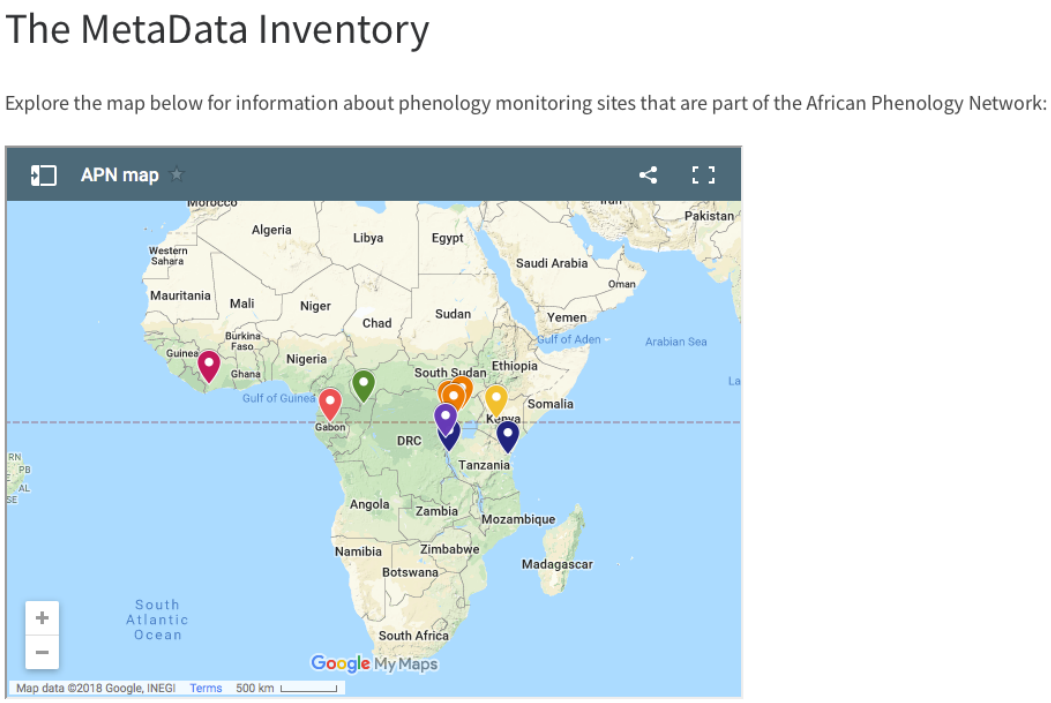

Figure 7.1. The African Phenology Network metadata inventory.
Screenshot from africanphenologynetwork.online showing the sites contributing to the metadata inventory as of December 2018.

The main applications of this research theme have been to improve the effectiveness of ANPNs investment in the Lopé research site and to improve regional and pan-tropical capacity in data collection and analysis so that phenology data can be made available as an Essential Biodiversity Variable to assess biodiversity change.

7.3 TROPICAL PHENOLOGY IN A TIME OF CHANGE

7.3.1 SUMMARY OF RESULTS

Lopé's changing weather context

Despite central Africa being a major convective region (Washington *et al.* 2013) and playing a global role in the carbon cycle (Lewis *et al.* 2013), meteorological data for the region are notoriously sparse and incomplete In Chapter 4 we present a previously unpublished 34-year record of rainfall and temperature from Lopé NP and shorter periods of other weather variables (relative humidity, wind speed, solar radiation, aerosol optical depth). We demonstrate the seasonal context at Lopé, which is characterised by two bright rainy seasons and a cool, cloudy, long dry season and a variable short dry season. We show that Lopé NP has warmed at a rate of 0.23°C per decade (minimum daily temperature) and that total annual precipitation has reduced at a rate of -52mm per decade. We also show that interannual variation in rainfall and temperature is influenced by global weather patterns; El Niño conditions increase the rainfall contrasts between seasons while development of the Indian Ocean Dipole increases rainfall during the long dry season and development of the Atlantic cold tongue reduces rainfall.

Lopé's changing biological context

In chapter 5 we selected seven canopy species (108 individual trees) from the wider Lopé phenology dataset that together make up 63% crown volume of the surrounding forest. Using this subset we test for community-wide seasonality and long-term trends in leaf phenology and evaluate the relative importance of light, moisture, temperature, CO_2 and leaf herbivory as drivers of monthly and interannual variation in tropical forest leaf production. We find that none of these dominant species are deciduous with all maintaining leafy canopies throughout the dry season. Most leaf exchange events are incremental and new leaf development is suppressed during the long dry season. Moisture, light and leaf herbivory are all positive predictors of new

leaf production at seasonal scales while the decline in probability of leaf flush since 1986 is most strongly predicted by rising atmospheric CO_2.

7.3.2 SYNTHESIS AND APPLICATIONS

Despite the lack of weather observations in western equatorial Africa, climatological trends in temperature are spatially conservative and relatively well understood (Niang *et al.* 2014). The warming trend identified at Lopé is as expected from global and regional climate change predictions (Malhi & Wright 2004; Collins 2011; Niang *et al.* 2014). Precipitation however is highly locally variable and lack of observations in central Africa hampers robust estimations of change over time (Niang *et al.* 2014). The drying trend established for Lopé since 1984 lends support to other observations (e.g. precipitation declines for Gabon/Cameroon: Malhi & Wright 2004 and reduced river Ogooué flow: Mahe *et al.* 2013) in a context of opposing model predictions for future rainfall in this region (James & Washington 2013). Our demonstration of the influence of the Atlantic cold tongue on rainfall at Lopé lends weight to the mechanisms behind the "dry" models of climate change impacts in western equatorial Africa (James *et al.* 2013).

The reduction in leaf turnover and postulated concurrent increase in leaf lifespan detected among the dominant canopy species at Lopé in Chapter 5 is a novel result and has not previously been reported in any tropical forest. However the mechanism for the proposed correlation with CO_2 is unclear although improved water use efficiency and a slower decline of photosynthetic rate are possibilities (Tricker *et al.* 2004; Taylor *et al.* 2008). This result clearly needs further investigation to understand potential mechanistic links. Our results do however challenge the idea that the warming and drying trend witnessed in western equatorial Africa will inevitably lead to increased deciduousness (van Schaik *et al.* 1993; Fauset *et al.* 2012; Zhou *et al.* 2014). Such predictions refer to species turnover in the long-term and few studies have assessed the likely impacts of environmental change within the lifetime of long-lived canopy trees (which can be several centuries; Lindenmayer & Laurance 2017).The implications of a reduced supply of new leaves into the canopy and longer leaf longevity among the leaf

cohort for climate feedbacks such as carbon sequestration and solar absorption are unclear and need investigated. Older leaves accumulate damage and dirt and thus eventually have lower reflectance (Toomey *et al.* 2009), however reduced leaf turnover also serves to maintain canopy structure, potentially contributing to the increases in leaf area index witnessed over western equatorial Africa (Zhu *et al.* 2016).

Lopé, and the evergreen-forested region of WEA, is anomalous within the climatic context of tropical forests. According to Neotropical estimates the habitat with ~1500mm rainfall per year should be a "dry" forest and be expected to exhibit deciduous phenology (Reich 1995). A recent analysis of irradiance across central Africa emphasised the unique case of the SW Gabon region (concurrent with the *Aucoumea* range) with its light deficient climate (Philippon *et al.* 2019). The cloudiness and cool temperatures of the long dry season compensate for the drought and reduce evapotranspiration. How the plant community experiences reduced rainfall over time may also be intercepted by the cloudiness of the site. Further information is needed on future projections for cloud cover and aerosol optical depth during the dry seasons to understand the ecological implications of the drying trend and the potential ecological risks associated with changes to dry season cloud cover (Philippon *et al.* 2019).

The global environment is changing and phenology is likely to be an important aspect of the ecological response. How tropical forest phenology is responding to global change was considered sufficiently important for me to be invited to present an early version of this analysis at a side event at the United Nations Framework Convention on Climate Change (UNFCCC) Conference of Parties (COP) 21 in December 2015. The described changes in tropical forest leaf turnover are likely to have implications for human and animal users of the forest, forest productivity and forest-climate feedbacks. As such this research will be shared with both the academic community and relevant parties within Gabon (ANPN and the Ministry of Water and Forests; Figure 1.5) in order to facilitate its inclusion within national and global

research initiatives that influence decision-making in governmental policy and multilateral conventions (such as the UNFCCC).

7.4 THE SOCIAL IMPACTS OF TROPICAL PHENOLOGY

7.4.1 SUMMARY OF RESULTS

Finally, in Chapter 6 we assess the influence of raw resource availability on successful NTFP commercialisation for integrated conservation and development. We combine over 15 years' scientific monitoring of *Baillonella toxisperma* (known as Moabi) at Lopé National Park with indigenous knowledge of Moabi oil producers in rural Gabon, to describe the factors that influence Moabi harvest success and explore subsequent impacts on the rest of the Moabi oil value chain. We show that Moabi fruit production is highly variable between years and regions although the climatic or biotic factors that influence this variability are currently unknown. We consider that at the present time, Moabi harvest is limited more by the effort involved in harvest and oil production than by raw resource availability, but that this may change. Movement towards centralised, mechanised oil production is likely to result in direct purchase of raw nuts from rural producers (as has happened in commercialisation of Argan and Shea oil; Lybbert *et al.* 2002; Elias & Carney 2007) and release some of the current limitations on fruit harvest.

7.4.2 SYNTHESIS AND APPLICATIONS

ANPN has engaged with NTFP commercialisation as an integrated conservation and development outreach tool in accordance with the government-wide commitment to poverty reduction. However, without careful consideration, NTFP commercialisation can fail both its objectives of poverty reduction and biodiversity protection (Arnold & Pérez 2001). The contribution that NTFP commercialization can make to poverty alleviation is strongly influenced by market forces while the benefits are often distributed unequally within rural communities (Heubach *et al.* 2011). For the biodiversity protection aspect of NTFP commercialisation to be successful,

the NTFP value of the resource needs to be higher than its timber value. Extraction of Moabi trees for timber is currently temporarily banned in Gabon (Iponga *et al.* 2018). Successful commercialisation of Moabi oil has the potential to lend greater weight to this legislation and encourage popular support for this policy.

In order to aid successful commercialisation of this NTFP, both for poverty reduction and biodiversity protection objectives, the variability in Moabi fruit availability needs to be addressed within the business model of market developers. We recommend that current Moabi commercialisation partnerships incorporate either an insurance-type scheme to compensate participants or develop other NTFPs alongside Moabi to form a diverse "safety-net" and reduce economic shocks to Moabi oil producers when Moabi fruits are scarce. We shared an initial version of this report with the Directorate for NTFPs (Ministry of Water and Forests; Figure 1.5) in Gabon in February 2016 and will be delivering our final recommendations to both ANPN and Gabon Boutique. The final version of this Chapter will be made available in the academic literature to contribute to new efforts to assess the effectiveness of integrated conservation and development projects (ICDPs) in west and central Africa (e.g. a recent assessment of ICDP effectiveness related to wild meat; Wicander & Coad 2018).

7.5 PATHWAYS TO IMPACT FROM THIS THESIS

In Figure 7.2 we summarise the potential and realised pathways for impact from the results presented in this thesis as discussed in the previous sections. There are four main areas to which this research can contribute: ANPN Research (1) and Integrated Conservation and Development (2), global research initiatives and networks (3) and government policy and multilateral conventions (4). ANPN has made significant investments in research including their long-term commitment to the SEGC research program at Lopé NP. They have also invested in integrated conservation and development initiatives such as their partnership with Gabon Boutique to develop NTFP commercialisation in NP buffer zones. In Chapters 2, 3 and 6 we have made direct recommendations for ways in which these prior investments can be

made most effective for their stated aims. The remaining two areas that this research contributes to are interlinked (Figure 1.7); Global research initiatives and research networks make available the evidence upon which government policy and multilateral conventions can be formed. Of particular relevance to the work presented in this thesis is the development of Gabonese government policy and legislation on NTFP use and protection of tree species of high NTFP value (Iponga *et al.* 2018) as well as multilateral agreements on climate change adaptation (i.e. UNFCCC), fair and equitable sharing of the benefits of genetic resources (i.e. the Nagoya protocol of the Convention on Biological Diversity, CDB) and the protection of threatened biodiversity (i.e. the Global Strategy for Plant Conservation and the Aichi Biodiversity Targets of the CBD).

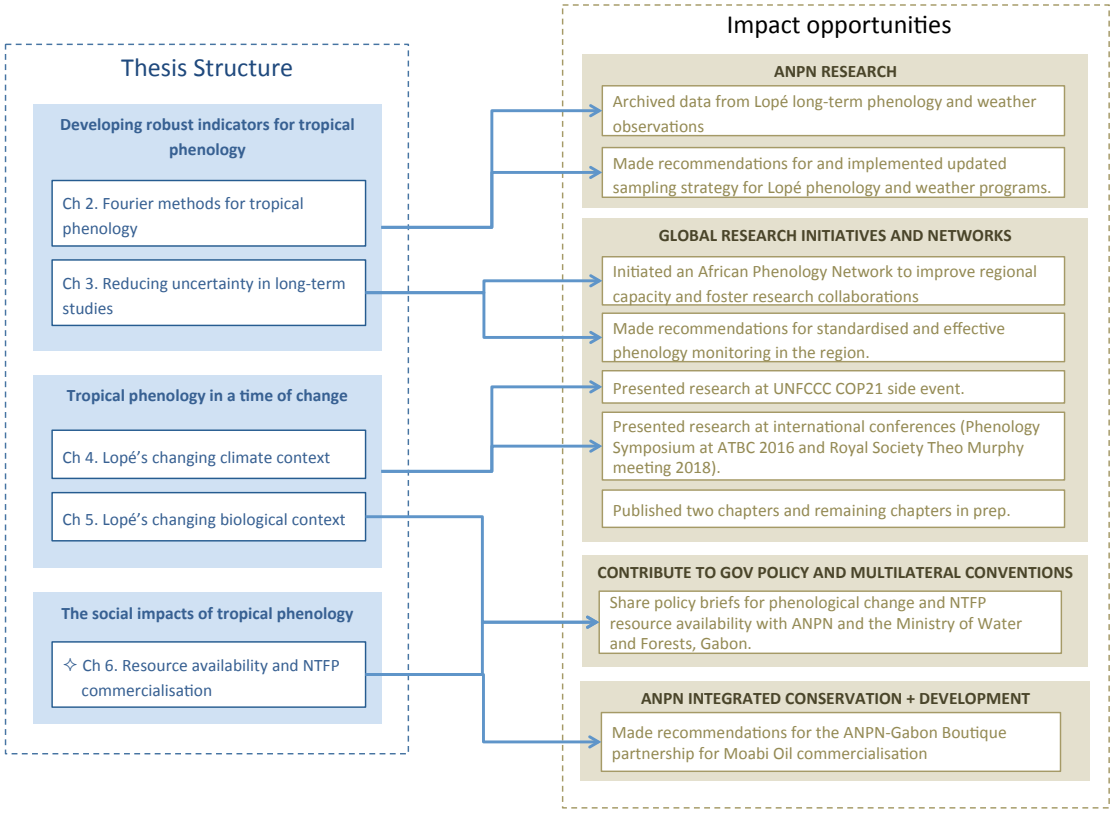

Figure 7.2. Potential and realised pathways for impact from the work presented in this thesis.

7.6. GENERAL CONCLUSIONS

In this thesis we have shown that regularly cycling and synchronised phenology is common in tropical tree communities despite the superficially

"aseasonal" tropical environment where plant growth is possible throughout the year. However the presence of regular, semi-annual and annual cycles in some species should not detract from the diversity in reproductive and leafing strategies found among the tropical tree community, with irregular cycles, cycles other than 12 months and unsynchronised populations all evident. We have shown that this biological diversity and the complexity of the ecosystem require long-term (6+ years) field observations to overcome the problems of poor visibility, rapidly occurring biological events and irregular or inconsistent cycles.

Our evidence supports the idea that western equatorial Africa experiences a strongly seasonal environment with predictable changes in rainfall, temperature, relative humidity, solar radiation and wind speed. The long dry season in this region is unique both within central Africa and the global tropics for its light deficiency. The relative importance of water and light availability for tropical tree phenology has been a question of debate for some time, although the focus thus far has been on tropical forest regions where water and light availability are asynchronous (Pau *et al.* 2010; Wu *et al.* 2017b; Detto *et al.* 2018; Wright & Calderón 2018). The co-occurrence of moisture and light at Lopé leads to an interesting scenario where the plant community "has it all" in the bright, rainy seasons, and responds by maximising leaf emergence and development at those times and suppressing leaf turnover during the cloudy long dry season. While we can see that moist and light conditions are important for the timing of leaf phenology we are limited in how far we can contribute to the debate on their relative importance at Lopé as the factors cannot be considered independently on seasonal scales.

Besides seasonality, the climatic regime in western equatorial Africa is markedly dry and light deficient throughout the year compared to other evergreen tropical forests and thus makes an important case study to understand the survival strategies of tropical trees. There is a growing awareness that reduced evapotranspiration during the cloudy, long dry season facilitates the very presence of evergreen forest communities in this

region despite relatively low annual rainfall (Philippon *et al.* 2019). If trees are able to access enough soil moisture for their photosynthetic needs, then the long dry season may not be a biological drought even if there is a climatological water deficit.

Using the evidence available from Lopé we have also shown that predictions of increased deciduousness associated with long-term warming and drying in western equatorial Africa are not yet evident. In fact we show that dominant canopy trees at Lopé are becoming more evergreen with fewer deciduous events since 1986. Once again it appears that the long dry season cloud may be playing an important role in intercepting the effects of long-term climate change on the ecological community. Seasonally reduced evapotranspiration and long-term increases in CO_2 availability are likely to be reducing water stress by improving water use efficiency.

7.7 FUTURE WORK AND FINAL REMARKS

Priorities for tropical phenology research identified at a recent Royal Society Theo Murphy meeting on tropical phenology (January 2018; https://royalsociety.org/science-events-and-lectures/2018/01/tropical-phenology/) were to: (1) harmonise data collection and analytical methods between research sites to facilitate cross-site comparisons, (2) develop the interface between ground-observed phenology and remote sensing, (3) invest in long-term "super-sites" (such as Lopé NP) in order to maintain valuable continuous data records and (4) expand data observations throughout the tropics using new research approaches such as citizen science phenology observations and phenocam networks.

We have already made progress on the first two priorities identified above by the methodological advances presented in Chapters 2 and 3 and the canopy-wide analysis of leaf turnover in Chapter 5, which is compatible with remote sensing observations of the upper canopy. The proposal to spatially expand phenological observations outside of the long-term super-sites lends itself most easily to our NTFP study in Chapter 6. NTFPs are easily recognized and

of great cultural importance to rural and urban dwellers in the region making them ideal for citizen science phenology ("sticking power" described in Chapter 3).

An obvious avenue for future work resulting from this thesis is to design a research program to elucidate the mechanisms for the CO_2 effect on leaf turnover demonstrated in Chapter 6. We have proposed a traits analysis of historical leaf collections in the region (sourced from herbaria) to test the effects of elevated CO_2 on stomatal density (Beerling & Kelly 1997), leaf thickness and number of chloroplasts (Pritchard *et al.* 1999; Tricker *et al.* 2004). Another aspect to pursue would be to test for the influence of climatological extremes on phenological activity. The close synchrony between minimum daily temperature and solar radiation at Lopé prevented them both from being included in the same explanatory model for leaf turnover at seasonal scales in Chapter 6 and we chose to include solar radiation as there is greater evidence in the literature for light limitation of new leaf production. However previous analyses at Lopé have shown that extreme low temperatures (below 19°c) are a trigger for flowering for some species following the long dry season (Tutin & Fernandez 1993). A predictive modeling approach, similar to Wright and Caldéron's recent analysis of phenological cues for flowering in Panama (2018), could be used to test for the impacts of minimum temperature at seasonal and interannual scales. Finally, it will be of great value to test the influence of reduced leaf turnover and the warming and drying trends at Lopé on the reproductive phenology of tree species as changes to flower and fruit production will have many cascading impacts for forest regeneration and also the animal and human users of the forest.

Phenology has the potential to be an important indicator of environmental change (Rosenzweig *et al.* 2007; Pereira *et al.* 2013) and an early warning of cascading effects for species' interactions within ecosystems (Butt *et al.* 2015; Morellato *et al.* 2016). There have been a number of calls for more quantitative assessment of the impacts of climate on tropical phenology (Butt *et al.* 2015; Mendoza *et al.* 2017) and to correct the temperate (Northern

hemisphere) bias of current climate change studies (Feeley *et al.* 2017). This thesis answers these calls by making available, for the first time in over two decades, a rare long-term tropical phenology record. The work presented here also provides novel analytical methods and insights into tropical forest function that have regional and global importance for forest regeneration and productivity, resource availability for human and animal users of the forest and climate-vegetation feedbacks.

LITERATURE CITED

Abernethy, K., Bush, E.R., Forget, P.M., Mendoza, I. & Morellato, L.P.C. (2018). Current issues in tropical phenology: a synthesis. *Biotropica*, **50**, 477–482.

Abernethy, K., Maisels, F. & White, L.J.T. (2016). Environmental Issues in Central Africa. *Annual Review of Environment and Resources*, **41**, 1–33.

Adamescu, G.S., Plumptre, A.J., Abernethy, K.A., Polansky, L., Bush, E.R., Chapman, C.A., Shoo, L.P., Fayolle, A., Janmaat, K.R.L., Robbins, M.M., Ndangalasi, H.J., Cordeiro, N.J., Gilby, I.C., Wittig, R.M., Breuer, T., Hockemba, M.B., Sanz, C.M., Morgan, D.B., Pusey, A.E., Mugerwa, B., Gilagiza, B., Tutin, C., Ewango, C.E.N., Sheil, D., Dimoto, E., Baya, F., Bujo, F., Ssali, F., Dikangadissi, J., Jeffery, K., Valenta, K., White, L., Masozera, M., Wilson, M.L., Bitariho, R., Ebika, S.T.N., Gourlet-Fleury, S., Mulindahabi, F. & Beale, C.M. (2018). Annual cycles are the most common reproductive strategy in African tropical tree communities. *Biotropica*, **50**, 418–430.

Adamowski, K., Prokoph, A. & Adamowski, J. (2009). Development of a new method of wavelet aided trend detection and estimation. *Hydrological Processes*, **23**, 2686–2696.

Adams, W.M., Aveling, R., Brockington, D., Dickson, B., Elliott, J., Hutton, J., Roe, D., Vira, B. & Wolmer, W. (2004). Biodiversity conservation and the eradication of poverty. *Science (New York, N.Y.)*, **306**, 1146–9.

Adole, T., Dash, J. & Atkinson, P.M. (2016). A systematic review of vegetation phenology in Africa. *Ecological Informatics*, **34**, 117–128.

Agostinelli, C. & Lund, U. (2013). R package 'circular': Circular Statistics.

Alberton, B., Torres, S., Cancian, L.F., Borges, B.D., Almeida, J., Mariano, G.C.,

Patricia, L. & Morellato, C. (2017). Introducing digital cameras to monitor plant phenology in the tropics : applications for conservation. *Perspectives in Ecology and Conservation*, **15**, 82–90.

Alexander Shenkin, Bentley, L.P., Oliveras, I., Salinas, N., Adu-Bredu, S., Marimon, B.H., Marimon, B., Peprah, T., Lopez Choque, E., Rodriguez, L.T., Arenas, E.R.C., Adonteng, C., Seidu, J., Passos, F.B., Reis, S.M., Blonder, B., Silman, M., Enquist, B.J., Asner, G.P. & Yadvinder Malhi. Evaluating General And Ecological Drivers Of Tropical Tree Crown Size And Shape. *American Naturalist, In Review.*

Alfaro-Sánchez, R., Muller-Landau, H.C., Wright, S.J. & Camarero, J.J. (2017). Growth and reproduction respond differently to climate in three Neotropical tree species. *Oecologia*, **184**, 531–541.

Anderson, D.P., Nordhelm, E. V, Moermond, T., Bi, Z.B.G., Boesch, C., Nordheim, E. V, Moermond, T.C. & Cocody, D. (2005). Factors Influencing Tree Phenology in Taï National Park , Côte d'Ivoire. *Biotropica*, **37**, 631–640.

Aono, Y. & Kazui, K. (2008). Phenological data series of cherry tree flowering in Kyoto, Japan, and its application to reconstruction of springtime temperatures since the 9th century. *International Journal of Climatology*, **28**, 905–914.

Archibald, S., Staver, A.C. & Levin, S.A. (2011). Evolution of human-driven fire regimes in Africa. *PNAS*, **109**, 847–852.

Del Arco, J.M., Escudero, A. & Garrido, M. V. (1991). Effects of site characteristics on nitrogen retraslocation from senescing leaves. *Ecology*, **72**, 701–709.

Arnold, J. & Pérez, M. (2001). Can non-timber forest products match tropical forest conservation and development objectives? *Ecological economics*, **39**, 437–447.

Asefi-najafabady, S. & Saatchi, S. (2013). Response of African humid tropical forests to recent rainfall anomalies. *Philosophical transactions of the Royal Society of London. Series B, Biological sciences*, **368**, 20120306,.

Asshoff, R., Zotz, G. & Körner, C. (2006). Growth and phenology of mature temperate forest trees in elevated CO2. *Global Change Biology*, **12**, 848–861.

Awono, A. & Levang, P. (2018). Contribution of environmental products to the household economy in Cameroon: essential, complementary or trivial? *Forestry Research and Engineering: International Journal*, **2**, 1–14.

Babweteera, F., Plumptre, A.J., Adamescu, G.S., Shoo, L.P., Beale, C.M., Reynolds, V., Nyeko, P. & Muhanguzi, G. (2018). The ecology of tree reproduction in an African medium altitude rain forest. *Biotropica*, **50**, 405–417.

Balas, N., Nicholson, S.E. & Klotter, D. (2007). The relationship of rainfall variability in West Central Africa to sea-surface temperature fluctuations. *International Journal of Climatology*, **27**, 1335–1349.

Barlow, J., França, F., Gardner, T.A., Hicks, C.C., Lennox, G.D., Berenguer, E., Castello, L., Economo, E.P., Ferreira, J., Guénard, B., Gontijo Leal, C., Isaac, V., Lees, A.C., Parr, C.L., Wilson, S.K., Young, P.J. & Graham, N.A.J. (2018). The future of hyperdiverse tropical ecosystems. *Nature*, **559**, 517–526.

Battipaglia, G., Zalloni, E., Castaldi, S., Marzaioli, F., Cazzolla-Gatti, R., Lasserre, B., Tognetti, R., Marchetti, M. & Valentini, R. (2015). Long tree-ring chronologies provide evidence of recent tree growth decrease in a central african tropical forest. *PLoS ONE*, **12**, e0180932.

Bauters, M., Drake, T.W., Verbeeck, H., Bodé, S., Hervé-Fernández, P., Zito, P., Podgorski, D.C., Boyemba, F., Makelele, I., Cizungu Ntaboba, L., Spencer, R.G.M. & Boeckx, P. (2018). High fire-derived nitrogen deposition on central African forests. *Proceedings of the National Academy of Sciences*, **115**, 549–554.

Beerling, D.J. & Kelly, C.K. (1997). Stomatal density responses of temperate woodland plants over the past seven decades of CO2 increase: A comparison of salisbury (1927) with contemporary data. *American Journal of Botany*, **84**, 1572–1583.

Behera, S., Brandt, P. & Reverdin, G. (2013). The tropical ocean circulation

and dynamics. *International Geophysics vol. 103*, pp. 385–412. Academic Press.

Belcher, B. & Schreckenberg, K. (2007). Commercialisation of non-timber forest products: a reality check. *Development Policy Review*, **25**, 355–377.

Bell, S., Cornford, D. & Bastin, L. (2015). How good are citizen weather stations? Addressing a biased opinion. *Weather*, **70**, 75–84.

Blaser, J., Sarre, A., Poore, D. & Johnson, S. (2011). *Status of Tropical Forest Management 2011. International Tropical Timber Organisation Technical Series No 38.*

Bloomfield, P. (2000). *Fourier analysis of time series: an introduction*. John Wiley & Sons.

Bonan, G.B. (2008). Forests and climate change: forcings, feedbacks, and the climate benefits of forests. *Science (New York, N.Y.)*, **320**, 1444–1449.

Borchert, R., Renner, S.S., Calle, Z., Havarrete, D., Tye, A., Gautier, L., Spichiger, R. & Von Hildebrand, P. (2005). Photoperiodic induction of synchronous flowering near the Equator. *Nature*, **433**, 627–629.

Bristow, K. & Campbell, G. (1984). On the relationship between incoming solar radiation and daily maximum and minimum temperature. *Agricultural and Forest Meteorology*, **31**, 159–166.

Bush, E.R., Abernethy, K.A., Jeffery, K., Tutin, C., White, L., Dimoto, E., Dikangadissi, J.T., Jump, A.S. & Bunnefeld, N. (2017). Fourier analysis to detect phenological cycles using tropical field data and simulations. *Methods in Ecology and Evolution*, **8**, 530–540.

Bush, E.R., Bunnefeld, N., Dimoto, N., Dikangadissi, J.T., Jeffery, K., Tutin, C., White, L. & Abernethy, K.A. (2018). Towards effective monitoring of tropical phenology: Maximising returns and reducing uncertainty in long-term studies. *Biotropica*, **50**, 455–464.

Butt, N., Seabrook, L., Maron, M., Law, B.S., Dawson, T., Syktus, J. & Mcalpine, C. (2015). Cascading effects of climate extremes on vertebrate fauna through changes to low-latitude tree flowering and fruiting phenology.

Global Change Biology, **21**, 3267–3277.

Camberlin, P., Janicot, S. & Poccard, I. (2001). Seasonality and atmospheric dynamics of the teleconnection between African rainfall and tropical sea-surface temperature: Atlantic vs. ENSO. *International Journal of Climatology*, **21**, 973–1005.

Campos, L.Z., Nascimento, A.L.B., Albuquerque, U.P. & Araújo, E.L. (2018). Use of local ecological knowledge as phenology indicator in native food species in the semiarid region of Northeast Brazil. *Ecological Indicators*, **95**, 75–84.

Cannon, C.H., Curran, L.M., Marshall, A.J. & Leighton, M. (2007). Long-term reproductive behaviour of woody plants across seven Bornean forest types in the Gunung Palung National Park (Indonesia): Suprannual synchrony, temporal productivity and fruiting diversity. *Ecology Letters*, **10**, 956–969.

Cazelles, B., Chavez, M., Berteaux, D., Ménard, F., Vik, J.O., Jenouvrier, S. & Stenseth, N.C. (2008). Wavelet analysis of ecological time series. *Oecologia*, **156**, 287–304.

Central Intelligence Agency. (2018). Gabon country profile. *The World Factbook 2013-14. Washington DC.* URL https://www.cia.gov/library/publications/the-world-factbook/geos/gb.html [accessed 26 November 2018]

Chalfin, B. (2000). Risky Business : Economic Uncertainty , Market Reforms and Female Livelihoods in Northeast Ghana. *Development and Change*, **31**, 987–1008.

Chambers, L.E., Altwegg, R., Barbraud, C., Barnard, P., Beaumont, L.J., Crawford, R.J.M., Durant, J.M., Hughes, L., Keatley, M.R., Low, M., Morellato, P.C., Poloczanska, E.S., Ruoppolo, V., Vanstreels, R.E.T., Woehler, E.J. & Wolfaardt, A.C. (2013). Phenological Changes in the Southern Hemisphere. *PLoS ONE*, **8**, e75514.

Chapman, C.A., Bonnell, T.R., Sengupta, R., Goldberg, T.L. & Rothman, J.M. (2013). Is Markhamia lutea's abundance determined by animal foraging?

Forest Ecology and Management, **308**, 62–66.

Chapman, C. a., Chapman, L.J., Struhsaker, T.T., Zanne, A.E., Clark, C.J. & Poulsen, J.R. (2005). A long-term evaluation of fruiting phenology: importance of climate change. *Journal of Tropical Ecology*, **21**, 31–45.

Chapman, C.A., Valenta, K., Bonnel, T.R., Brown, K.A. & Chapman, L.J. (2018). Solar radiation and ENSO predict fruiting phenology patterns in a 15-year record from Kibale National Park, Uganda. *Biotropica*, **50**, 384–395.

Chapman, C.A., Wrangham, R.W., Chapman, L.J., Kennard, D.K. & Zanne, a. E. (1999). Fruit and flower phenology at two sites in Kibale National Park, Uganda. *Journal of Tropical Ecology*, **15**, 189–211.

Chen, Y.-Y., Satake, A., Sun, I.-F., Kosugi, Y., Tani, M., Numata, S., Hubbell, S.P., Fletcher, C., Nur Supardi, M.N. & Wright, S.J. (2017). Species-specific flowering cues among general flowering Shorea species at the Pasoh Research Forest, Malaysia. *Journal of Ecology*, **106**, 586–598.

Chuine, I. (2010). Why does phenology drive species distribution? *Philosophical Transactions of the Royal Society B: Biological Sciences*, **365**, 3149–3160.

Clark, D.A. (2007). Detecting Tropical Forests ' Responses to Global Climatic and Atmospheric Change : Current Challenges and a Way Forward. **39**, 4–19.

Cleland, E.E., Chuine, I., Menzel, A., Mooney, H. a. & Schwartz, M.D. (2007). Shifting plant phenology in response to global change. *Trends in Ecology and Evolution*, **22**, 357–365.

Collins, J.M. (2011). Temperature variability over Africa. *Journal of Climate*, **24**, 3649–3666.

Cook, B.I., Wolkovich, E.M., Davies, T.J., Ault, T.R., Betancourt, J.L., Allen, J.M., Bolmgren, K., Cleland, E.E., Crimmins, T.M., Kraft, N.J.B., Lancaster, L.T., Mazer, S.J., McCabe, G.J., McGill, B.J., Parmesan, C., Pau, S., Regetz, J., Salamin, N., Schwartz, M.D. & Travers, S.E. (2012). Sensitivity of Spring Phenology to Warming Across Temporal and Spatial Climate Gradients

in Two Independent Databases. *Ecosystems*, **15**, 1283–1294.

Couralet, C., Van Den Bulcke, J., Ngoma, L.M., Van Acker, J. & Beeckman, H. (2013). Phenology in functional groups of central african rainforest trees. *Journal of Tropical Forest Science*, **25**, 361–374.

da Cunha, A.R. (2015). Evaluation of measurement errors of temperature and relative humidity from HOBO data logger under different conditions of exposure to solar radiation. *Environmental Monitoring and Assessment*, **187**.

Cusack, D., Karpman, J., Ashdown, D., Cao, Q., Ciochina, M., Halternman, S., Lydon, S. & Neupane, A. (2013). Global change effects on humid tropical forests: Evidence for biogeochemical and biodiversity shifts at an ecosystem scale. *Review of Geophysics*, **54**, 523–610.

Dai, A., Trenberth, K.E. & Karl, T.R. (1999). Effects of clouds, soil moisture, precipitation, and water vapor on diurnal temperature range. *Journal of Climate*, **12**, 2451–2473.

Davis, C.C., Willis, C.G., Connolly, B., Kelly, C. & Ellison, A.M. (2015). Herbarium records are reliable sources of phenological change driven by climate and provide novel insights into species??? phenological cueing mechanisms. *American Journal of Botany*, **102**, 1599–1609.

Detto, M., Wright, S.J., Calderón, O. & Muller-landau, H.C. (2018). Resource acquisition and reproductive strategies of tropical forest in response to the El Niño–Southern Oscillation. *Nature Communications*, **9**, 913.

Dezfuli, A.K., Zaitchik, B.F. & Gnanadesikan, A. (2015). Regional atmospheric circulation and rainfall variability in south equatorial Africa. *Journal of Climate*, **28**, 809–818.

Dlugokencky, E.J., Thoning, K.W., Lang, P.M. & Tans, P.P. (2017). NOAA Greenhouse Gas Reference from Atmospheric Carbon Dioxide. *Dry Air Mole Fractions from the NOAA ESRL Carbon Cycle Cooperative. Global Air Sampling Network.*

Doucet, J.L., Kouadio, Y.L., Monticelli, D. & Lejeune, P. (2009). Enrichment of

logging gaps with moabi (Baillonella toxisperma Pierre) in a Central African rain forest. *Forest Ecology and Management*, **258**, 2407–2415.

Elias, M. & Carney, J. (2007). African shea butter: a feminized subsidy from nature. *Nature as local heritage in Africa*, **77**, 37–62.

Endamana, D., Angu, K.A., Akwah, G.., Shepherd, G. & Ntumwel, B.C. (2016). Contribution of non-timber forest products to cash and non-cash income of remote forest communities in Central Africa. *International Forestry Review*, **18**, 280–295.

FAO. (2016). FAOSTAT - Karite nuts (sheanuts) Value of Agricultural Production. URL http://www.fao.org/faostat/en/#search/shea

Farnsworth, A., White, E., Williams, C.J.R., Black, E. & Kniveton, R. (2011). Understanding the Large Scale Driving Mechanisms of Rainfall Variability over Central Africa. *African Climate and Climate Change*, pp. 101–122. Springer, Dordecht.

Fauset, S., Baker, T.R., Lewis, S.L., Feldpausch, T.R., Affum-Baffoe, K., Foli, E.G., Hamer, K.C. & Swaine, M.D. (2012). Drought-induced shifts in the floristic and functional composition of tropical forests in Ghana. *Ecology Letters*, **15**, 1120–1129.

Feeley, K.J., Stroud, J.T. & Perez, T.M. (2017). Most 'global' reviews of species' responses to climate change are not truly global. *Diversity and Distributions*, **23.3**, 231–234.

Fu, C., Ji, Z. & Wei, Z. (2017). Spatial patterns of ENSO's interannual influences on lilacs vary with time and periodicity. *Atmospheric Research*, **186**, 95–106.

Gond, V., Fayolle, A., Pennec, A., Cornu, G., Mayaux, P., Doumenge, C., Fauvet, N., Gourlet-fleury, S., B, P.T.R.S. & Camberlin, P. (2013). Vegetation structure and greenness in Central Africa from Modis multi-temporal data. *Philosophical transactions of the Royal Society of London. Series B, Biological sciences*, **368**, 20120309.

Gouhier, T.C., Grinsted, A. & Simko, V. (2018). R package biwavelet: Conduct

Univariate and Bivariate Wavelet Analyses.

Guan, K., Wolf, A., Medvigy, D., Caylor, K., Pan, M. & Wood, E.F. (2013). Seasonal coupling of canopy structure and function in African tropical forests and its environmental controls. *Ecosphere*, **4**, 1–21.

Habib, E., Krajewski, W.F. & Ciach, G.J. (2001). Estimation of Rainfall Interstation Correlation. *Journal of Hydrometeorology*, **2**, 621–629.

Hall, P. & Bawa, K. (1993). Methods to assess the impact of extraction of non-timber tropical forest products on plant populations. *Economic Botany*, **47**, 234–247.

Hanes, J.M., Richardson, A.D. & Klosterman, S. (2013). Mesic temperate deciduous forest phenology. *Phenology: An Integrative Environmental Science* (ed M.D. Schwartz), pp. 211–224. Springer.

Hansen, M.C., Potapov, P. V, Moore, R., Hancher, M., Turubanova, S.A., Tyukavina, A., Thau, D., Stehman, S. V, Goetz, S.J., Loveland, T.R., Kommareddy, A., Egorov, A., Chini, L., Justice, C.O. & Townshend, J.R.G. (2013). High-Resolution Global Maps of 21st-Century Forest Cover Change. *Science*, **342**, 850–853.

Hansen, M.C., Roy, D.P., Lindquist, E., Adusei, B., Justice, C.O. & Altstatt, A. (2008). A method for integrating MODIS and Landsat data for systematic monitoring of forest cover and change in the Congo Basin. *Remote Sensing of Environment*, **112**, 2495–2513.

Harris, I., Jones, P.D., Osborn, T.J. & Lister, D.H. (2014). Updated high-resolution grids of monthly climatic observations - the CRU TS3.10 Dataset. *International Journal of Climatology*, **34**, 623–642.

Hartmann, D.L., Klein Tank, A.M.G., Rusticucci, M., Alexander, L. V., Brönnimann, S., Charabi, Y.A.R., Dentener, F.J., Dlugokencky, E.J., Easterling, D.R., Kaplan, A., Soden, B.J., Thorne, P.W., Wild, M. & Zhai, P. (2013). Observations: Atmosphere and surface. *Climate Change 2013 the Physical Science Basis: Working Group I Contribution to the Fifth Assessment Report of the Intergovernmental Panel on Climate Change* (eds T.F. Stocker, D. Qin, G.-K. Plattner, M. Tignor, S.K. Allen, J. Boschung,

A. Nauels, Y. Xia, V. Bex & P.M. Midgley), pp. 159–254. Cambridge University Press, Cambridge, United Kingdom and New York, NY, USA.

Heubach, K., Wittig, R., Nuppenau, E.A. & Hahn, K. (2011). The economic importance of non-timber forest products (NTFPs) for livelihood maintenance of rural west African communities: A case study from northern Benin. *Ecological Economics*, **70**, 1991–2001.

Holben, B.N., Eck, T.F., Slutsker, I., Tanré, D., Buis, J.P., Setzer, A., Vermote, E., Reagan, J.A., Kaufman, Y.J., Nakajima, T., Lavenu, F., Jankowiak, I. & Smirnov, A. (1998). AERONET—A Federated Instrument Network and Data Archive for Aerosol Characterization. *Remote Sensing of Environment*, **66**, 1–16.

Hudson, I.L., Kang, I. & Keatley, M.R. (2010). Wavelet analysis of flowering and climatic niche identification. *Phenological Research: Methods for Environmental and Climate Change Analysis* (eds I.L. Hudson & M.R. Keatley), pp. 361–391. Springer.

Hudson, I.L. & Keatley, M. (2010). *Phenological Research.* (I.L. Hudson & M.R. Keatley, Eds.). Springer.

Huete, A.R. & Saleska, S.R. (2010). Remote sensing of tropical forest phenology : Issues and controversies. *International Archives of the Photogrammetry, Remote Sensing and Spatial Information Science*, **38**, 539–541.

Hughes, L. (2000). Biological consequences of global warming: is the signal already aparrent? *Trends in Ecology & Evolution*, **15**, 56–61.

Humboldt-University of Berlin. (2012). International Phenological Gardens. URL https://www.agrar.hu-berlin.de/en/institut-en/departments/dntw-en/agrarmet-en/phaenologie/ipg/ipg_allg-e [accessed 5 January 2017]

Ingram, V. & Schure, J. (2010). *Review of Non Timber Forest Products (NTFPs) in Central Africa, Cameroon. Yaounde: CIFOR/FORENET Project.* Yaounde, Cameroon.

Iponga, D.M., Mikolo-Yobo, C., Lescuyer, G., Assoumou, F.M., Levang, P., Tieguhong, J.C. & Ngoye, A. (2018). The contribution of NTFP-gathering to rural people's livelihoods around two timber concessions in Gabon. *Agroforestry Systems*, **92**, 157–168.

James, R. & Washington, R. (2013). Changes in African temperature and precipitation associated with degrees of global warming. *Climatic Change*, **117**, 859–872.

James, R., Washington, R. & Rowell, D.P. (2013). Implications of global warming for the climate of African rainforests. *Philosophical Transactions of the Royal Society B: Biological Sciences*, **368**, 20120298,.

Jenkins, G. (2014). A comparison between two types of widely used weather stations. *Weather*, **69**, 105–110.

Ju, J. & Roy, D.P. (2008). The availability of cloud-free Landsat ETM+ data over the conterminous United States and globally. *Remote Sensing of Environment*, **112**, 1196–1211.

Kidd, C., Becker, A., Huffman, G.J., Muller, C.L., Joe, P., Skofronick-Jackson, G. & Kirschbaum, D.B. (2017). So, how much of the Earth's surface is covered by rain gauges? *Bulletin of the American Meteorological Society*, **98**, 69–78.

Kikuzawa, K. (1995). The Basis for Variation in Leaf Longevity of Plants. *Vegetatio*, **121**, 89–100.

Kikuzawa, K. & Ackerly, D. (1999). Significance of leaf longevity in plants. *Plant Species Biology*, **14**, 39–45.

Kinnaird, M.F. (1992). Competition for a Forest Palm: Use of Phoenix reclinata by Human and Nonhuman Primates. *Conservation Biology*, **6**, 101–107.

Kitajima, K., Mulkey, S.S., Samaniego, M. & Wright, S.J. (2002). Decline of photosynthetic capacity with leaf age and position in two tropical pioneer tree species. *American Journal of Botany*, **89**, 1925–1932.

Kitayama, K., Ushio, M. & Aiba, S.I. Celestially determined annual seasonality

of equatorial tropical rain forests. *bioRxiv PREPRINT*, 454058.

Koch, G.W., Amthor, J.S. & Goulden, M.L. (1994). Diurnal patterns of leaf photosynthesis, conductance and water potential at the top of a lowland rain forest canopy in Cameroon: Measurements from the Radeau des Cimes. *Tree Physiology*, **14**, 347–360.

Kothe, S., Pfeifroth, U., Cremer, R., Trentmann, J. & Hollmann, R. (2017). A Satellite-Based Sunshine Duration Climate Data Record for Europe and Africa. *Remote Sensing*, **9**, 429.

Kuhnert, P.M., Martin, T.G. & Griffiths, S.P. (2010). A guide to eliciting and using expert knowledge in Bayesian ecological models. *Ecology Letters*, **13**, 900–914.

Laraque, A., Mahé, G., Orange, D. & Marieu, B. (2001). Spatiotemporal variations in hydrological regimes within Central Africa during the twentieth century. *Journal of Hydrology,* **245**, **1–4,** 104–117.

Lasky, J.R., Uriarte, M. & Muscarella, R. (2016). Synchrony, compensatory dynamics, and the functional trait basis of phenological diversity in a tropical dry forest tree community: effects of rainfall seasonality. *Environmental Research Letters*, **11**, 115003.

Lewis, S.L., Lloyd, J., Sitch, S., Mitchard, E.T. a. & Laurance, W.F. (2009). Changing Ecology of Tropical Forests: Evidence and Drivers. *Annual Review of Ecology, Evolution, and Systematics*, **40**, 529–549.

Lewis, S.L., Sonké, B., Sunderland, T., Begne, S.K., Lopez-gonzalez, G., Heijden, G.M.F. Van Der, Phillips, O.L., Affum-baffoe, K., Baker, T.R., Banin, L., Bastin, J., Beeckman, H., Boeckx, P., Bogaert, J., Cannière, C. De, Clark, C.J., Collins, M., Djagbletey, G., Djuikouo, M.N.K., Doucet, J., Ewango, C.E.N., Fauset, S., Feldpausch, T.R., Ernest, G., Gillet, J., Hamilton, A.C., Harris, D.J., Hart, T.B., Haulleville, T. De, Hladik, A., Hufkens, K., Huygens, D., Jeanmart, P., Jeffery, K.J., Leal, M.E., Lloyd, J., Lovett, J.C., Makana, J., Malhi, Y., Andrew, R., Ojo, L., Peh, K.S., Pickavance, G., Poulsen, J.R., Reitsma, J.M., Sheil, D., Simo, M., Steppe, K., Taedoumg, H.E., Talbot, J., James, R.D., Taylor, D., Thomas, S.C., Toirambe, B., Verbeeck, H., Vleminckx, J., Lee, J.,

White, T., Willcock, S., Woell, H., Zemagho, L., B, P.T.R.S., Sonke, B., Poulsen, R. & Thomas, C. (2013). Above-ground biomass and structure of 260 African tropical forests. *Philosophical transactions of the Royal Society of London. Series B, Biological sciences*, **368**, 20120295.

Lindenmayer, D.B. & Laurance, W.F. (2017). The ecology, distribution, conservation and management of large old trees. *Biological Reviews*, **92**, 1434–1458.

Lopes, A.P. (2016). Leaf flush drives dry season green-up of the Central Amazon. *Remote Sensing of Environment*, **182**, 90–98.

Louppe, D. (2005). Baillonella toxisperma Pierre. [Internet] Record from PROTA4U. *PROTA (Plant Resources of Tropical Africa / Ressources végétales de l'Afrique tropicale)* (eds D. Louppe, A.A. Oteng-Amoako & M. Brink). Wageningen, Netherlands.

Lybbert, T.J., Aboudrare, A., Chaloud, D., Magnan, N. & Nash, M. (2011). Booming markets for Moroccan argan oil appear to benefit some rural households while threatening the endemic argan forest. *PNAS*, **108**, 13963–13968.

Lybbert, T.J., Barrett, C.B. & Narjisse, H. (2002). Market-based conservation and local benefits: the case of argan oil in Morocco. *Ecological Economics*, **41**, 125–144.

Mahe, G., Lienou, G., Descroix, L., Bamba, F., Paturel, J.E., Laraque, A., Meddi, M., Habaieb, H., Adeaga, O., Dieulin, C., Chahnez Kotti, F. & Khomsi, K. (2013). The rivers of Africa: Witness of climate change and human impact on the environment. *Hydrological Processes*, **27**, 2105–2114.

Maidment, R.I., Allan, R.P. & Black, E. (2015). Recent observed and simulated changes in precipitation over Africa. *Geophysical Research Letters*, **42**, 8155–8164.

Maidment, R.I., Grimes, D., Allan, R.P., Tarnavsky, E., Stringer, M., Hewison, T., Roebeling, R. & Black, E. (2014). The 30-year TAMSAT African Rainfall Climatology And Time-series (TARCAT) Dataset. *Journal of Geophysical Research: Atmospheres*, **119.18**, 10–619.

Maidment, R.I., Grimes, D., Black, E., Tarnavsky, E., Young, M., Greatrex, H., Allan, R.P., Stein, T., Nkonde, E., Senkunda, S. & Alcántara, E.M.U. (2017). A new, long-term daily satellite-based rainfall dataset for operational monitoring in Africa. *Scientific Data*, **4**, 1–19.

Malhi, Y., Adu-bredu, S., Asare, R.A., Lewis, S.L., Mayaux, P. & B, P.T.R.S. (2013). The past, present and future of Africa's rainforests. *Philosophical transactions of the Royal Society of London. Series B, Biological sciences*, **368**, 20120293.

Malhi, Y. & Wright, J. (2004). Spatial patterns and recent trends in the climate of tropical rainforest regions. *Philosophical Transactions of the Royal Society B: Biological Sciences*, **359**, 311–329.

Man&Nature. (2017). Moani, Bush Mango and Cocoa Vegetable Butter serving conservation of Dja Reserve. URL http://www.manandnature.org/images/soutenus/MaN_Cameroun_MoabiEN_2018.pdf

Martin, T.G., Burgman, M.A., Fidler, F., Kuhnert, P.M., Low-Choy, S., Mcbride, M. & Mengersen, K. (2012). Eliciting Expert Knowledge in Conservation Science. *Conservation Biology*, **26**, 29–38.

Mayaux, P., Pekel, J.-F., Desclée, B., Donnay, F., Lupi, A., Achard, F., Clerici, M., Bodart, C., Brink, A., Nasi, R. & Belward, A. (2013). State and evolution of the African rainforests between 1990 and 2010. *Philosophical transactions of the Royal Society of London. Series B, Biological sciences*, **368**, 20120300.

Meko, D.. (2015). *Applied Time Series Analysis, Online notes for course (Geosciences 585A) offered at the University of Arizona*.

Mendoza, I., Condit, R.S., Wright, S.J., Caubère, A., Châtelet, P., Hardy, I. & Forget, P.M. (2018). Inter-annual variability of fruit timing and quantity at Nouragues (French Guiana): insights from hierarchical Bayesian analyses. *Biotropica*, **50**, 431–441.

Mendoza, I., Peres, C.A. & Morellato, L.P.C. (2017). Continental-scale patterns and climatic drivers of fruiting phenology: A quantitative Neotropical

review. *Global and Planetary Change*, **148**, 227–241.

Menne, M.J., Durre, I., Vose, R.S., Gleason, B.E. & Houston, T.G. (2012). An Overview of the Global Historical Climatology Network-Daily Database. *Journal of Atmospheric and Oceanic Technology*, **29**, 897–910.

Menzel, A. (2002). Phenology: It's importance to the global change community. *Climatic Change*, **54**, 379–385.

Menzel, A., Sparks, T.H., Estrella, N., Koch, E., Aaasa, A., Ahas, R., Alm-Kübler, K., Bissolli, P., Braslavská, O., Briede, A., Chmielewski, F.M., Crepinsek, Z., Curnel, Y., Dahl, Å., Defila, C., Donnelly, A., Filella, Y., Jatczak, K., Måge, F., Mestre, A., Nordli, Ø., Peñuelas, J., Pirinen, P., Remišová, V., Scheifinger, H., Striz, M., Susnik, A., Van Vliet, A.J.H., Wielgolaski, F.E., Zach, S. & Zust, A. (2006). European phenological response to climate change matches the warming pattern. *Global Change Biology*, **12**, 1969–1976.

Mitchard, E.T.A. (2018). The tropical forest carbon cycle and climate change. *Nature*, **559**, 527–534.

Momont, L. (2007). *Sélection de l'habitat et organisation sociale de l'éléphant de forêt, Loxodonta africana cyclotis (Matschie 1900), au Gabon*. Muséum National d'histoire Naturelle, Paris.

Morellato, L.P.C., Alberton, B., Alvarado, S.T., Borges, B., Buisson, E., Camargo, M.G.G., Cancian, L.F., Carstensen, D.W., Escobar, D.F.E., Leite, P.T.P., Mendoza, I., Rocha, N.M.W.B., Soares, N.C., Silva, T.S.F., Staggemeier, V.G., Streher, A.S., Vargas, B.C. & Peres, C.A. (2016). Linking plant phenology to conservation biology. *Biological Conservation*, **195**, 60–72.

Morton, D.C., Nagol, J., Carabajal, C.C., Rosette, J., Palace, M., Cook, B.D., Vermote, E.F., Harding, D.J. & North, P.R.J. (2014). Amazon forests maintain consistent canopy structure and greenness during the dry season. *Nature*, **506**, 221.

Morton, J.F.. & Voss, G.L.. (1987). The Argan Tree (Argania sideroxylon , Sapotaceae), a Desert Source of Edible Oil. *Economic Botany*, **41**, 221–233.

Munzimi, Y., Hansen, M., Adusei, B. & Senay, G. (2015). Characterizing Congo Basin Rainfall and Climate Using Tropical Rainfall Measuring Mission (TRMM) Satellite Data and Limited Rain Gauge Ground Observations. *Journal of Applied Metereology and Climatology*, **54**, 541–555.

Nagai, S., Ichie, T., Yoneyama, A., Kobayashi, H., Inoue, T., Ishii, R., Suzuki, R. & Itioka, T. (2016). Usability of time-lapse digital camera images to detect characteristics of tree phenology in a tropical rainforest. *Ecological Informatics*, **32**, 91–106.

National Climate Data Centre. (2014). El Nino/Southern Oscillation (ENSO) Technical Discussion | Teleconnections | National Climatic Data Center (NCDC). *Climate Monitoring*. URL http://www.ncdc.noaa.gov/teleconnections/enso/enso-tech.php [accessed 16 July 2014]

National Weather Service. (2018). Inter-Tropical Convergence Zone. *Jet Stream - An Online School for Weather*. URL https://www.weather.gov/jetstream/itcz [accessed 3 December 2018]

Naughton-Treves, L., BuckHolland, M. & Brandon, K. (2005). The role of protected areas in conserving biodiversity and sustaining local livelihoods. *Annual Review of Environment and Resources*, **30**, 219–52.

Ndiade-Bourobou, D., Hardy, O.J., Favreau, B., Moussavou, H., Nzengue, E., Mignot, A. & Bouvet, J.M. (2010). Long-distance seed and pollen dispersal inferred from spatial genetic structure in the very low-density rainforest tree, Baillonella toxisperma Pierre, in Central Africa. *Molecular Ecology*, **19**, 4949–4962.

Neto, E.M.F.L., Almeida, A.L.S., Peroni, N., Castro, C.C. & Albuquerque, U.P. (2013). Phenology of Spondias tuberosa Arruda (Anacardiaceae) under different landscape management regimes and a proposal for a rapid phenological diagnosis using local knowledge. *Journal of Ethnobiology and Ethnomedicine*, **9**, 1–13.

Newbery, D.M., Chuyong, G.B. & Zimmermann, L. (2006). Mast fruiting of large ectomycorrhizal African rain forest trees: importance of dry season

intensity and resource-limitation hypothesis. **170**, 561–579.

Newstrom, L., Frankie, G. & Baker, H. (1994). A new classification for plant phenology based on flowering patterns in lowland tropical rain forest trees at La Selva, Costa Rica. *Biotropica*, **26**, 141–159.

Newton, A.C., Marshall, E., Schreckenberg, K., Golicher, D., Velde, D.W., Edouard, F. & Arancibia, E. (2006). Use of a Bayesian Belief Network to Predict the Impacts of Commercializing Non-timber Forest Products on Livelihoods. **11**, 24.

Niang, I., Ruppel, O.C., Abdrabo, M.A., Essel, A., Lennard, C., Padgham, J. & Urquhart, P. (2014). Africa. *Climate Change 2014: Impacts, Adaptation and Vulnerability - Contributions of the Working Group II to the Fifth Assessment Report of the Intergovernmental Panel on Climate Change.* (eds V.R. Barros, C.B. Field, D.J. Dokken, M.D. Mastrandrea, K.J. Mach, T.E. Bilir, M. Chatterjee, K.L. Ebi, Y.O. Estrada, R.C. Genova, B. Girma, E.S. Kissel, A.N. Levy, S. MacCracken, P.R. Mastrandrea & L.L. White), pp. 1199–1265. Cambirgde University Press, Cambirgde, UK and New York, NY, USA.

Nicholson, S.E. & Grist, J.P. (2003). The seasonal evolution of the atmospheric circulation over West Africa and equatorial Africa. *Journal of Climate*, **16**, 1013–1030.

Nikiema, A. & Umali, B.. (2007). Vitellaria paradoxa C.F.Gaertn. [Internet] Record from PROTA4U. *PROTA (Plant Resources of Tropical Africa / Ressources végétales de l'Afrique tropicale)* (eds H.A.M. van der Vossen & G.S. Mkamilo). Wageningen, Netherlands.

NOAA. (2018). U.S. Daily Climate Normals (1981-2010). *National Centers for Environmental Information*. URL https://data.nodc.noaa.gov/cgi-bin/iso?id=gov.noaa.ncdc:C00823 [accessed 26 November 2018]

Norden, N., Chave, J., Belbenoit, P., Caubère, A., Châtelet, P., Forget, P.M. & Thébaud, C. (2007). Mast fruiting is a frequent strategy in woody species of eastern South America. *PLoS ONE*, **2.10**, e1079.

Obeso, J.R. (2002). The costs of reproduction in plants. *New phytologist*, **155**,

321–348.

Osnas, J.L.D., Lichstein, J.W., Reich, P.B. & Pacala, S.W. (2013). Global Leaf Trait Relationships: Mass, Are, and the Leaf Economics Spectrum. *Science*, **340**, 741–745.

Otto, F.E.L., Jones, R.G., Halladay, K. & Allen, M.R. (2013). Attribution of changes in precipitation patterns in African rainforests. *Philosophical transactions of the Royal Society of London. Series B, Biological sciences*, **368**, 20120299.

Ouédraogo, D.-Y., Fayolle, A., Gourlet-Fleury, S., Mortier, F., Freycon, V., Fauvet, N., Rabaud, S., Cornu, G., Benedet, F., Gillet, J.-F., Oslisly, R., Doucet, J.-L., Lejeune, P. & Favier, C. (2016). The determinants of tropical forest deciduousness: disentangling the effects of rainfall and geology in central Africa. *Journal of Ecology*, **104**, 924–935.

Pachauri, R.K., Allen, M.R., Barros, V.R., Broome, J., Cramer, W., Christ, R., Church, J.A., Clarke, L., Dahe, Q., Dasgupta, P. & Dubash, N.K. (2014). *2014: Climate Change 2014: Synthesis Report. Contribution of Working Groups I, II and III to the Fifth Assessment Report of the Intergovernmental Panel on Climate Change. IPCC.*

Parcs Gabon. (2018). L'Agence Nationale des Parcs Nationaux. URL https://web.archive.org/web/20131027114012/http://www.parcsgabon.org/l-anpn/l-agence [accessed 24 November 2018]

Parmesan, C. (2006). Ecological and Evolutionary Responses to Recent Climate Change. *Annual Review of Ecology Evolution and Systematics*, **37**, 637–669.

Parmesan, C. & Yohe, G. (2003). A globally coherent fingerprint of climate change impacts across natural systems. *Nature*, **421**, 37.

Pau, S., Okamoto, D.K., Calderón, O. & Wright, S.J. (2017). Long-term increases in tropical flowering activity across growth forms in response to rising CO2 and climate change. *Global Change Biology*, **24**, 2105–2116.

Pau, S., Okin, G.S. & Gillespie, T.W. (2010). Asynchronous response of tropical

forest leaf phenology to seasonal and el Niño-driven drought. *PloS one*, **5**, e11325.

Pau, S., Wolkovich, E.M., Cook, B.I., Nytch, C.J., Regetz, J., Zimmerman, J.K. & Joseph Wright, S. (2013). Clouds and temperature drive dynamic changes in tropical flower production. *Nature Climate Change*, **3**, 838–842.

Pereira, H.M., et al., Ferrier, S., Walters, M., Geller, G.N., Jongman, R.H.G., Scholes, R.J., Bruford, M.W., Brummitt, N., Butchart, S.H.M., Cardoso, A.C., Coops, N.C., Dulloo, E., Faith, D.P., Freyhof, J., Gregory, R.D., Heip, C., Höft, R., Hurtt, G., Jetz, W., Karp, D.S., M. A. McGeoch, D.O., Onoda, Y., Pettorelli, N., Reyers, B., Sayre, R., Scharlemann, J.P.W., Stuart, S.N., Turak, E., Walpole, M. & Wegmann, M. (2013). Essential Biodiversity Variables. *Science*, **339**, 277–278.

Pfeifroth, U., Kothe, S., Müller, R., Trentmann, J., Hollmann, R., Fuchs, P. & Werscheck, M. (2017). *Surface Radiation Data Set - Heliosat (SARAH) - Edition 2*.

Philippon, N., Cornu, G., Monteil, L., Gond, V., Moron, V., Pergaud, J., Sèze, G., Bigot, S., Camberlin, P., Doumenge, C., Fayolle, A. & Ngomanda, A. (2019). The light-deficient climates of western Central African evergreen forests The light-de fi cient climates of western Central African evergreen forests. *Environmental Research Letters*, **14**, 34007.

Philippon, N., Martiny, N., Camberlin, P., Hoffman, M.T. & Gond, V. (2014). Timing and patterns of the ENSO signal in Africa over the last 30 years: Insights from Normalized Difference Vegetation Index Data. *Journal of Climate*, **27**, 2509–2532.

PlantUse English Contributors. (2015). Aucoumea klaineana (PROTA). URL https://uses.plantnet-project.org/e/index.php?title=Aucoumea_klaineana_(PROTA)&oldid=199003

Plenderleith, K. & Brown, N. (2004). Moabi (Baillonella toxisperma). *The key non-timber forest products of central africa: state of the knowledge* (eds

L.E. Clark & T.C.H. Sunderland), pp. p141-162. USAID, Bureau for Africa, Office of Sustainable Development.

Plumptre, A.J. (2011). *The Ecological Impact of Long-term Changes in Africa's Rift Valley*. Nova Science.

Polansky, L. & Boesch, C. (2013). Long-term Changes in Fruit Phenology in a West African Lowland Tropical Rain Forest are Not Explained by Rainfall. *Biotropica*, **45**, 434–440.

Polansky, L., Douglas-Hamilton, I. & Wittemyer, G. (2013). Using diel movement behavior to infer foraging strategies related to ecological and social factors in elephants. *Movement Ecology*, **1**, 13.

Polansky, L. & Robbins, M.M. (2013). Generalized additive mixed models for disentangling long-term trends, local anomalies, and seasonality in fruit tree phenology. *Ecology and Evolution*, **3**, 3141–3151.

Polansky, L., Wittemyer, G., Cross, P.C., Tambling, C.J. & Wayne, M. (2010). Fourier and wavelet analyses of animal location time series data. **91**, 1506–1518.

Pouliot, M. (2012). Contribution of 'women's gold' to West African livelihoods: the case of shea (Vitellaria paradoxa) in Burkina Faso. *Economic Botany*, **66**, 237–248.

Preethi, B., Sabin, T.P., Adedoyin, J.A. & Ashok, K. (2015). Impacts of the ENSO Modoki and other tropical indo-pacific climate-drivers on African rainfall. *Scientific Reports*, **5**, 1–15.

Press, W.H., Teukolsky, S.A., Vetterling, W.T. & Flannery, B.P. (1992). *Numerical Recipes in C: The Art of Scientific Computing*, Secondn. Cambridge University Press, Cambridge.

Primack, R.B., Higuchi, H. & Miller-Rushing, A.J. (2009). The impact of climate change on cherry trees and other species in Japan. *Biological Conservation*, **142**, 1943–1949.

Pritchard, S., Rogers, H., Prior, S. & Peterson, C. (1999). Elevated CO2 and plant sturcture: a review. *Global Change Biology*, **5**, 807–837.

Rasolofoson, R.A., Hanauer, M.M., Pappinen, A., Fisher, B. & Ricketts, T.H. (2018). Impacts of forests on children's diet in rural areas across 27 developing countries. *Science Advances*, **4**, eaat2853.

Regan, H.M., Colyvan, M., Burgman, M. a, Applications, E. & Apr, N. (2008). A Taxonomy and Treatment of Uncertainty for Ecology and Conservation Biology. *Ecological Applications*, **12**, 618–628.

Reich, P.B. (1995). Phenology of tropical forests: patterns, causes, and consequences. *Canadian Journal of Botany*, **73**, 164–174.

Reich, P.B., Uhl, C., Walters, M.B., Prugh, L. & David, S. (2004). Leaf Demography and Phenology in Amazonian Rain Forest : A Census of 40 000 Leaves of 23 Tree Species. *Ecological Monographs*, **74**, 3–23.

Richardson, A.D., Keenan, T.F., Migliavacca, M., Ryu, Y., Sonnentag, O. & Toomey, M. (2013). Climate change, phenology, and phenological control of vegetation feedbacks to the climate system. *Agricultural and Forest Meteorology*, **169**, 156–173.

van Rij, J., Wieling, M., Baayen, R. & van Rijn, H. (2017). itsadug: Interpreting Time Series and Autocorrelated Data Using GAMMs. R package version 2.3.

Rohde, R., Muller, R.A., Jacobsen, R., Muller, E., Perlmutter, S., Rosenfeld, A., Wurtele, J., Groom, D. & Wickham, C. (2013). A new estimate of the average Earth surface land temperature spanning 1753 to 2011. *Geoinfor Geostat Overview 1*, **7**, 2.

Rosenzweig, C., Casassa, G., Karoly, D.J., Imeson, A., Liu, C., Menzel, A., Rawlins, S., Root, T.L., Seguin, B. & Tryjanowski, P. (2007). Assessment of observed changes and responses in natural and managed systems. *Climate Change 2007: Impacts, Adaptation and Vulnerability. Contribution of Working Group II to the Fourth Assessment Report of the Intergovernmental Panel on Climate Change* (eds M.L. Parry, O.F. Canziani, J.P. Palutikof, P.J. van der Linden & C.E. Hanson), pp. 79–131. Cambirgde University Press, Cambirgde, UK.

Saji, N.H. & Yamagata, T. (2003). Possible impacts of Indian Ocean dipole

mode events on global climate. *Climate Research*, **25**, 151–169.

Sakai, S. (2001). Phenological diversity in tropical forests. *Population Ecology*, **43**, 77–86.

Sakai, S., Harrison, R.D., Momose, K., Kuraji, K., Nagamasu, H., Yasunari, T., Chong, L. & Nakashizuka, T. (2006). Irregular droughts trigger mass flowering in aseasonal tropical forests in Asia. *American Journal of Botany*, **93**, 1134–1139.

van Schaik, C.P., Terborgh, J.W. & Wright, J.S. (1993). The phenology of tropical forests: Adaptive significance and consequences for primary consumers. *Annual Review of Ecology and Systematics*, **24**, 353–377.

Schefuss, E., Schouten, S. & Schneider, R.R. (2005). Climatic controls on central African hydrology during the past 20 , 000 years. *Nature*, **437**, 1003–1006.

Schielzeth, H. (2010). Simple means to improve the interpretability ofregression coefficients. *Methods in Ecology and Evolution*, **1**, 103–113.

Schwartz, M.D., Ahas, R. & Aasa, A. (2006). Onset of spring starting earlier across the Northern Hemisphere. *Global Change Biology*, **12**, 343–351.

Seiwa, K. (1999). Changes in leaf phenology are dependent on tree height in Acer mono, a deciduous broad-leaved tree. *Annals of Botany*, **83**, 355–361.

Shackleton, C. & Sheona, S. (2004). The importance of non-timber forest products in rural livelihood security and as safety nets: a review of evidence from South Africa. *South African Journal of Science*, **100**, 658–664.

Singh, K.P. & Kushwaha, C.P. (2016). Deciduousness in tropical trees and its potential as indicator of climate change: A review. *Ecological Indicators*, **69**, 699–706.

Singh, K.P. & Kushwaha, C.P. (2005). Emerging paradigms of tree phenology in dry tropics. *Current Science*, **89**, 964–975.

Struhsaker, T.T., Struhsaker, P.J. & Siex, K.S. (2005). Conserving Africa's rain

forests: Problems in protected areas and possible solutions. *Biological Conservation*, **123**, 45–54.

Suggitt, A.J., Platts, P.J., Barata, I.M., Bennie, J.J., Burgess, M.D., Bystriakova, N., Duffield, S., Ewing, S.R., Gillingham, P.K., Harper, A.B., Hartley, A.J., Hemming, D.L., Maclean, I.M.D., Maltby, K., Marshall, H.H., Morecroft, M.D., Pearce-Higgins, J.W., Pearce-Kelly, P., Phillimore, A.B., Price, J.T., Pyke, A., Stewart, J.E., Warren, R. & Hill, J.K. (2017). Conducting robust ecological analyses with climate data. *Oikos*, **126**, 1533–1541.

Suzuki, T. (2011). Seasonal variation of the ITCZ and its characteristics over central Africa. *Theoretical and Applied Climatology*, **103**, 39–60.

Taylor, G., Tallis, M.J., Giardina, C.P., Percy, K.E., Miglietta, F., Gupta, P.S., Gioli, B., Calfapietra, C., Gielen, B., Kubiske, M.E., Scarascia-Mugnozza, G.E., Ket, K., Long, S.P. & Karnosky, D.F. (2008). Future atmospheric CO2 leads to delayed autumnal senescence. *Global Change Biology*, **14**, 264–275.

Team, R.C. (2015). R: A language and environment for statistical computing.

Team, R.C., Wuertz, D., Setz, T. & Chalabi, Y. (2015). timeSeries: Rmetrics - Financial Time Series Objects.

Texier, N., Deblauwe, V., Stévart, T., Sonké, B., Simo-Droissart, M., Azandi, L., Bose, R., Djuikouo, M.N., Kamdem, G., Kamdem, N., Mayogo, S., Zemagho, L. & Droissart, V. (2018). Spatio-temporal patterns of orchids flowering in Cameroonian rainforests. *International Journal of Biometeorology*, **62**, 1931–1944.

Ticktin, T. (2004). The ecological implications of harvesting non-timber forest products. *Journal of Ecology*, **41**, 11–21.

Ting, S., Hartley, S. & Burns, K.C. (2008). Global patterns in fruiting seasons. *Global Ecology and Biogeography*, **17**, 648–657.

Todd, M.C. & Washington, R. (2004). Climate variability in central equatorial Africa: Influence from the Atlantic sector. *Geophysical Research Letters*, **31**, 1–4.

Tokinaga, H. & Xie, S.P. (2011). Weakening of the equatorial Atlantic cold

tongue over the past six decades. *Nature Geoscience*, **4**, 222–226.

Toomey, M., Roberts, D. & Nelson, B. (2009). The influence of epiphylls on remote sensing of humid forests. *Remote Sensing of Environment*, **113**, 1787–1798.

Trabucco, A. & Zomer, R.J. (2009). *Global Potential Evapo-Transpiration (Global-PET) and Global Aridity Index (Global-Aridity) Geo-Database*.

Tricker, P.J., Calfapietra, C., Kuzminsky, E., Puleggi, R., Ferris, R., Nathoo, M., Pleasants, L.J., Alston, V., De Angelis, P. & Taylor, G. (2004). Long-term acclimation of leaf production, development, longevity and quality following 3 yr exposure to free-air CO2 enrichment during canopy closure in Populus. *New Phytologist*, **162**, 413–426.

Tutin, C.E.G. (1998). Gorillas and their food plants in the Lopé Reserve, Gabon. *Chorology, Taxonomy and Ecology of the Floras of Africa and Madagascar* (eds C.R. Huxley, J.M. Lock & D.F. Cutler), pp. 227–243.

Tutin, C.E.G. & Fernandez, M. (1993). Relationships between minimum temperature and fruit production in some tropical forest trees in Gabon. *Journal of Tropical Ecology*, **9**, 241–248.

Tutin, C.E.G. & Fernandez, M. (1987). Sympatric gorilla and chimpanzees in Gabon. *AnthroQuest*, **37**, 3–6.

Tutin, C.E.G., Fernandez, M., Rogers, M.E., Willimson, E.A. & McGrew, W.C. (1991a). Foraging profiles of sympatric lowland gorillas and chimpanzees in the Lope Reserve Gabon. *Philosophical Transactions of the Royal Society of London B*, **334**, 179–186.

Tutin, C.E., Ham, R.M., White, L.J. & Harrison, M.J. (1997). The primate community of the Lopé Reserve, Gabon: diets, responses to fruit scarcity, and effects on biomass. *American journal of primatology*, **42**, 1–24.

Tutin, C.E.G. & White, L.J.T. (1998). Primates, phenology and frugivory: Present, past and future patterns in the Lope Reserve, Gabon. *Dynamics of Tropical Communities: 37th Symposium of the British Ecological Society* (eds D.M. Newbery, H.H.T. Prins & N. Brown), pp. 309–338. Blackwell

Science, Oxford.

Tutin, C.E.G., Williamson, E.A., Rogers, M.E. & Fernandez, M. (1991b). A case study of a plant-animal interaction: Cola lizae and lowland gorillas in the Lope Reserve, Gabon. *Journal of Tropical Ecology*, **7**, 181–199.

UNdata. (2018). Gabon Country Profile. URL http://data.un.org/en/iso/ga.html

University of East Anglia Climatic Research Unit, Harris, I.C.. & Jones, P.D. (2017). *CRU TS4.01: Climatic Research Unit (CRU) Time-Series (TS) version 4.01 of high-resolution gridded data of month-by-month variation in climate (Jan. 1901- Dec. 2016).*

USA National Phenology Network (USA-NPN). (2017). Nature's Notebook. Connecting people with nature to benefit our changing planet. URL https://www.usanpn.org/natures_notebook# [accessed 5 January 2017]

Veuthey, S. & Gerber, J.F. (2010). Logging conflicts in Southern Cameroon: A feminist ecological economics perspective. *Ecological Economics*, **70**, 170–177.

van Vliet, A.J.H. (2010). Societal Adaptation Options to Changes in Phenology. *Phenological Research* (eds I.L. Hudson & M.R. Keatley), pp. 75–98. Springer Netherlands, Dordrecht.

Voysey, B. (1995). *Seed dispersal by gorillas in the Lope Reserve, Gabon*. The University of Edinburgh, Edinburgh.

Voysey, B.C., McDonald, K.E., Rogers, M.E., Tutin, C.E.G. & Parnell, R.J. (1999). Gorillas and seed dispersal in the Lope Reserve, Gabon. I: Gorilla acquisition by trees. *Journal of Tropical Ecology*, **15**, 23–38.

Walther, G., Post, E., Convey, P., Menzel, A., Parmesan, C., Beebee, T.J.C., Fromentin, J., HoeghGuldberg, O. & Bairlein, F. (2002). Ecological responses to recent climate change. *Nature*, **416**, 389–395.

Washington, R., James, R., Pearce, H., Pokam, W.M. & Moufouma-Okia, W. (2013). Congo Basin rainfall climatology: can we believe the climate models? *Philosophical transactions of the Royal Society of London. Series*

B, Biological sciences, **368**, 20120296.

Wezel, A. & Lykke, A.M. (2006). Woody vegetation change in Sahelian West Africa: Evidence from local knowledge. *Environment, Development and Sustainability*, **8**, 553–567.

White, L. (1998). Baillonella toxisperma. *The IUCN Red List of Threatened Species*, **e.T33039A9**. URL http://dx.doi.org/10.2305/IUCN.UK.1998.RLTS.T33039A9752397.en [accessed 7 March 2017]

White, E.C. (2007). *Ecology of Mandrillus sphinx: Ranging, diet and social structure of a mandrill horde in Lopé national park, Gabon*.

White, L.J.T. (1992). *Vegetation history and logging damage: effects on rainforest mammals in the Lope' Reserve, Gabon*. University of Edinburgh.

White, L.J.T. (1995). *Vegetation Study- Final Report. Projet ECOFAC - Composante Gabon in collaboration with the Wildlife Conservation Society*.

White, L. & Abernethy, K. (1997). *A guide to the vegetation of the Lopé Reserve. Wildlife Cons. Society, ECOFAC Gabon*. Libreville.

White, L. & Edwards, A. (2000). *Conservation research in the African rain forests: a technical handbook. Wildlife Conservation Society*. New York.

Wicander, S. & Coad, L. (2018). Can the Provision of Alternative Livelihoods Reduce the Impact of Wild Meat Hunting in West and Central Africa? *Conservation and Society*, **16**, 441–458.

Wich, S.A. & Schaik, C.P. Van. (2000). The impact of El Niño on mast fruiting in Sumatra and elsewhere in Malesia. *Journal of Tropical Ecology*, **16**, 563–577.

Willis, K.J., Bennett, K.D., Burrough, S.L., Macias-Fauria, M. & Tovar, C. (2013). Determining the response of African biota to climate change : using the past to model the future. *Philosophical transactions of the royal society*, **368**, 20120491.

Wittemyer, G., Polansky, L., Douglas-Hamilton, I. & Getz, W.M. (2008).

Disentangling the effects of forage, social rank, and risk on movement autocorrelation of elephants using Fourier and wavelet analyses. *Proceedings of the National Academy of Sciences of the United States of America*, **105**, 19108–13.

Wolter, K. (2018). Multivariate ENSO Index (MEI). URL https://www.esrl.noaa.gov/psd/enso/mei/ [accessed 24 July 2018]

Wolter, K. & Timlin, M.S. (1998). Measuring the strength of ENSO events: How does 1997/98 rank? *Weather*, **53**, 315–324.

Wolter, K. & Timlin, M.S. (1993). Monitoring ENSO in COADS with a seasonally adjusted principal component index. *Proc. of the 17th Climate Diagnostics Workshop*, pp. 52–57. Norman, OK, NOAA/NMC/CAC, NSSL, Oklahoma Clim. Survey, CIMMS and the School of Meteor., Univ. of Oklahoma.

World Bank. (2018). Gabon Country Profile. *DataBank - World Development Indicators*. URL http://databank.worldbank.org/data/views/reports/reportwidget.aspx?Report_Name=CountryProfile&Id=b450fd57&tbar=y&dd=y&inf=n&zm=n&country=GAB

Wright, S. (1996). Phenological responses to seasonality in tropical forest plants. *Tropical forest plant ecophysiology*, pp. 440–460. Springer, Boston, MA.

Wright, S.. J. & Calderon, O. (1995). Phylogenetic Patterns among Tropical Flowering Phenologies. *Journal of Ecology*, **83**, 937–948.

Wright, J.S. & Calderon, 0. (2006). Seasonal, El Nino and longer term changes in flower and seed production in a moist tropical forest. *Ecology letters*, **9**, 35–44.

Wright, S.J. & Calderón, O. (2018). Solar irradiance as the proximate cue for flowering in a tropical moist forest. *Biotropica*, **50**, 374–383.

Wright, S.J., Carrasco, C., Calderon, O. & Paton, S. (1999). The El Nino Southern Oscillation, variable fruit production, and famine in a tropical

forest. *Ecology*, **80**, 1632–1647.

Wright, S. & Cornejo, F. (1990). Seasonal drought and leaf fall in a tropical forest. *Ecology*, **71**, 1165–1175.

Wright, I.J., Reich, P.B., Westoby, M., Ackerly, D.D., Baruch, Z., Bongers, F., Cavender-Bares, J., Chapin, T., Cornellssen, J.H.C., Diemer, M., Flexas, J., Garnier, E., Groom, P.K., Gulias, J., Hikosaka, K., Lamont, B.B., Lee, T., Lee, W., Lusk, C., Midgley, J.J., Navas, M.L., Niinemets, Ü., Oleksyn, J., Osada, H., Poorter, H., Pool, P., Prior, L., Pyankov, V.I., Roumet, C., Thomas, S.C., Tjoelker, M.G., Veneklaas, E.J. & Villar, R. (2004). The worldwide leaf economics spectrum. *Nature*, **428**, 821–827.

Wright, J.S. & van Schaik, C.P. (1994). Light and the phenology of tropical trees. *The American Naturalist*, **143**, 192–199.

Wu, J., Chavana-Bryant, C., Prohaska, N., Serbin, S.P., Guan, K., Albert, L.P., Yang, X., van Leeuwen, W.J.D., Garnello, A.J., Martins, G., Malhi, Y., Gerard, F., Oliviera, R.C. & Saleska, S.R. (2017a). Convergence in relationships between leaf traits, spectra and age across diverse canopy environments and two contrasting tropical forests. *New Phytologist*, **214**, 1033–1048.

Wu, J., Guan, K., Hayek, M., Restrepo-Coupe, N., Wiedemann, K.T., Xu, X., Wehr, R., Christoffersen, B.O., Miao, G., da Silva, R., de Araujo, A.C., Oliviera, R.C., Camargo, P.B., Monson, R.K., Huete, A.R. & Saleska, S.R. (2017b). Partitioning controls on Amazon forest photosynthesis between environmental and biotic factors at hourly to inter-annual time scales. *Global Change Biology*, **23**, 1240–1257.

Wu, J., Kobayashi, H., Stark, S.C., Meng, R., Guan, K., Tran, N.N., Gao, S., Yang, W., Restrepo-Coupe, N., Miura, T., Oliviera, R.C., Rogers, A., Dye, D.G., Nelson, B.W., Serbin, S.P., Huete, A.R. & Saleska, S.R. (2018). Biological processes dominate seasonality of remotely sensed canopy greenness in an Amazon evergreen forest. *New Phytologist*, **217**, 1507–1520.

Wunder, S. (2001). Poverty alleviation and tropical forests-what scope for synergies? *World Development*, **29**, 1817–1833.

Yang, Z., Wang, J., Ichoku, C., Hyer, E. & Zeng, J. (2013). Mesoscale modeling

and satellite observation of transport and mixing of smoke and dust particles over northern sub-Saharan African region. *Journal of Geophysical Research Atmospheres*, **118**, 12139–12157.

Zalamea, P.-C., Munoz, F., Stevenson, P.R., Paine, C.E.T., Sarmiento, C., Sabatier, D. & Heuret, P. (2011). Continental-scale patterns of Cecropia reproductive phenology: evidence from herbarium specimens. *Proceedings of the Royal Society B: Biological Sciences*, **278**, 2437–45.

Zhang, Y.-J., Sack, L., Cao, K.-F., Wei, X.-M. & Li, N. (2017). Speed versus endurance tradeoff in plants: Leaves with higher photosynthetic rates show stronger seasonal declines. *Scientific Reports*, **7**, 42085.

Zhang, Y., Tan, Z., Song, Q., Yu, G. & Sun, X. (2010). Respiration controls the unexpected seasonal pattern of carbon flux in an Asian tropical rain forest. *Atmospheric Environment*, **44**, 3886–3893.

Zhou, L., Tian, Y., Myneni, R.B., Ciais, P., Saatchi, S., Liu, Y.Y., Piao, S., Chen, H., Vermote, E.F., Song, C. & Hwang, T. (2014). Widespread decline of Congo rainforest greenness in the past decade. *Nature*, **508**, 86–90.

Zhu, Z., Piao, S., Myneni, R.B., Huang, M., Zeng, Z., Canadell, J.G., Ciais, P., Sitch, S., Friedlingstein, P., Arneth, A., Cao, C., Cheng, L., Kato, E., Koven, C., Li, Y., Lian, X., Liu, Y., Liu, R., Mao, J., Pan, Y., Peng, S., Peuelas, J., Poulter, B., Pugh, T.A.M., Stocker, B.D., Viovy, N., Wang, X., Wang, Y., Xiao, Z., Yang, H., Zaehle, S. & Zeng, N. (2016). Greening of the Earth and its drivers. *Nature Climate Change*, **6**, 791–795.

Zimmerman, J.K., Wright, S.J., Calderón, O., Pagan, M.A., Paton, S., Zimmerman, Jess, K., Wright, Joseph, S., Calderon, O, Aponte, P., M, Paton & S. (2007). Flowering and fruiting phenologies of seasonal and aseasonal neotropical forests: the role of annual changes in irradiance. *Journal of Tropical Ecology*, **23**, 231.

Zunzunegui, M., Ain-lhout, F., Jáuregui, J., Barradas, M.C.D., Boutaleb, S., Álvarez-cansino, L. & Esquivias, M.P. (2010). Fruit production under different environmental and management conditions of argan , Argania spinosa (L .). *Journal of Arid Environments*, **74**, 1138–1145.

APPENDICES

APPENDIX A: POWER ANALYSIS OF SIMULATED DATA TO SHOW THE IMPACT OF NULL HYPOTHESIS CHOICE FOR DETECTING PERIODICITY.

Two credible null hypotheses with which to compare a Fourier spectral estimate are; (1) the null continuum of the spectrum – an extreme smooth of the periodogram such that only the underlying shape remains - and (2) the white noise spectrum – the mean spectral value (Meko 2015) (Figure A1).

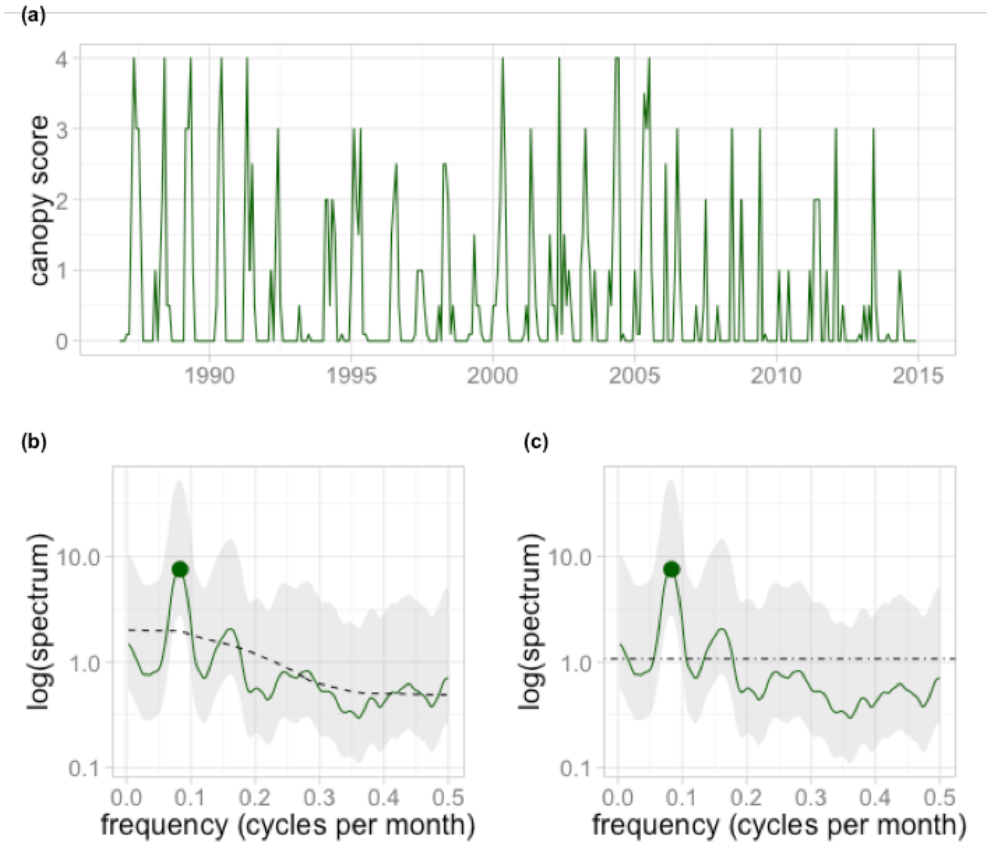

Figure A1. Null hypothesis choice. a) Time series plot shows flowering canopy scores each month from 1987 to 2015 for an individual tree. b) and c) show smoothed periodograms (Daniell filter spans [7 9]) for these flowering scores (green line) for which a dominant peak is obvious at 0.083 cycles per month (wavelength=12 months). 95% confidence intervals (grey shades) for the smoothed spectrum are used to test the null hypotheses that the dominant peak (the frequency with the highest spectral estimate, represented by green dots) of the periodogram is not different from b) a "null continuum" where the periodogram is smoothed using extreme spans (Daniell filter spans [75 79]) such that only the underlying shape of the spectrum remains (black dashed line) or c) "white noise", where all variation in the spectrum is apportioned equally to each frequency (black dashed line).

We did a power analysis to show the impact of null hypothesis choice for detecting periodicity using time series data simulated to represent a repeating 12-month flowering cycle with varying levels of noise (regularity of the cycle and observation uncertainty). We simulated 10,000 individual time series representing a 10-year long, annually repeating, flowering cycle with a peak month of June with two key variables allowed to vary between simulated "individuals"; the regularity of the peak month (to represent process uncertainty) and the detectability of flowering events (to represent observation uncertainty). For each year of data, we generated monthly scores of zero (no-flowering) and a flowering peak of three-months duration with scores randomly chosen from a distribution of canopy scores similar to that found in our long-term field fata from Lopé (see code in supporting information for more details). Regularity was determined by choosing the location of the flowering peak each year from a truncated normal distribution (2:11) with mean 6 and standard deviation randomly selected from 0.1 to 8 (standard deviation was consistent for each "individual" but allowed to vary between individuals). Once the time series was constructed, detectability was determined by replacing a certain percentage of randomly chosen positive flowering scores with zeros (from 0 – 80%). Examples of these simulated data are shown in Figure A2.

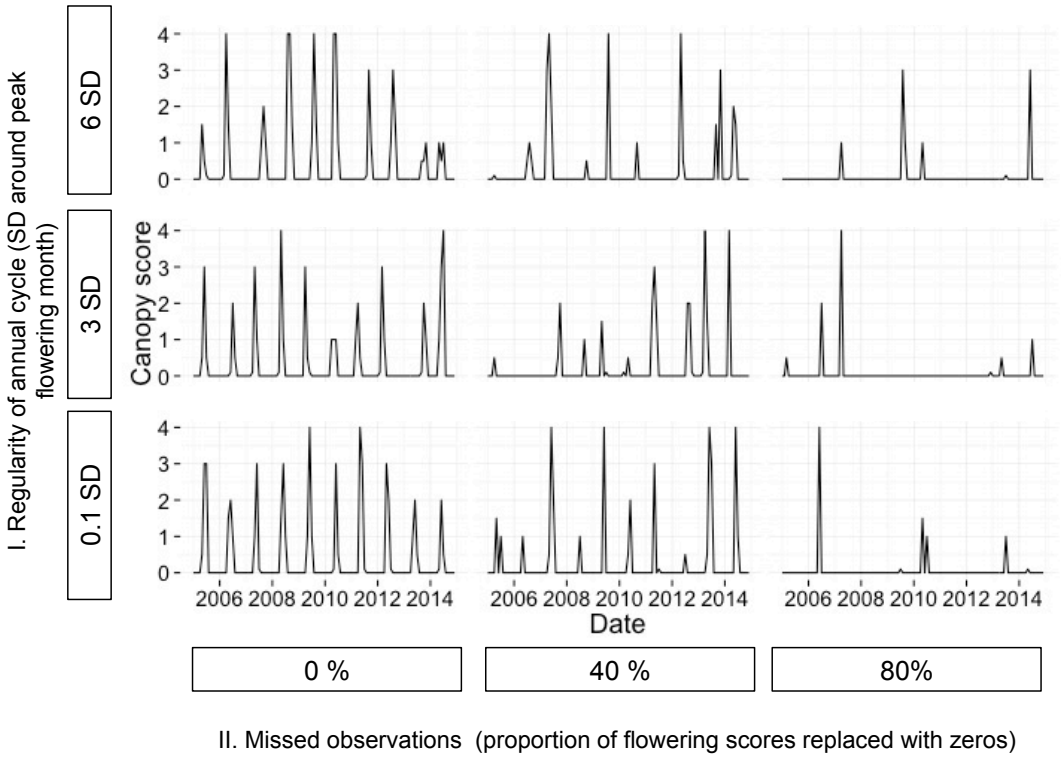

Figure A2. Example simulated data in six different noise scenarios. In each scenario, peak month each year was chosen from a truncated normal distributions with mean six and standard deviation 0.1, three or six, and positive flowering scores randomly replaced with zeros at a rate of 0, 40 or 80%.

We prefer null hypothesis testing using a null continuum spectrum rather than a white noise spectrum as it results in fewer false positive results (detection of significant cycles outside of expected frequency range) at medium to high noise scenarios (e.g. greater than 2SD around peak flowering month), which are more likely to be representative of empirical data than the highly regular simulated data, however this also results in a loss of sensitivity to some cycles (Figure A3).

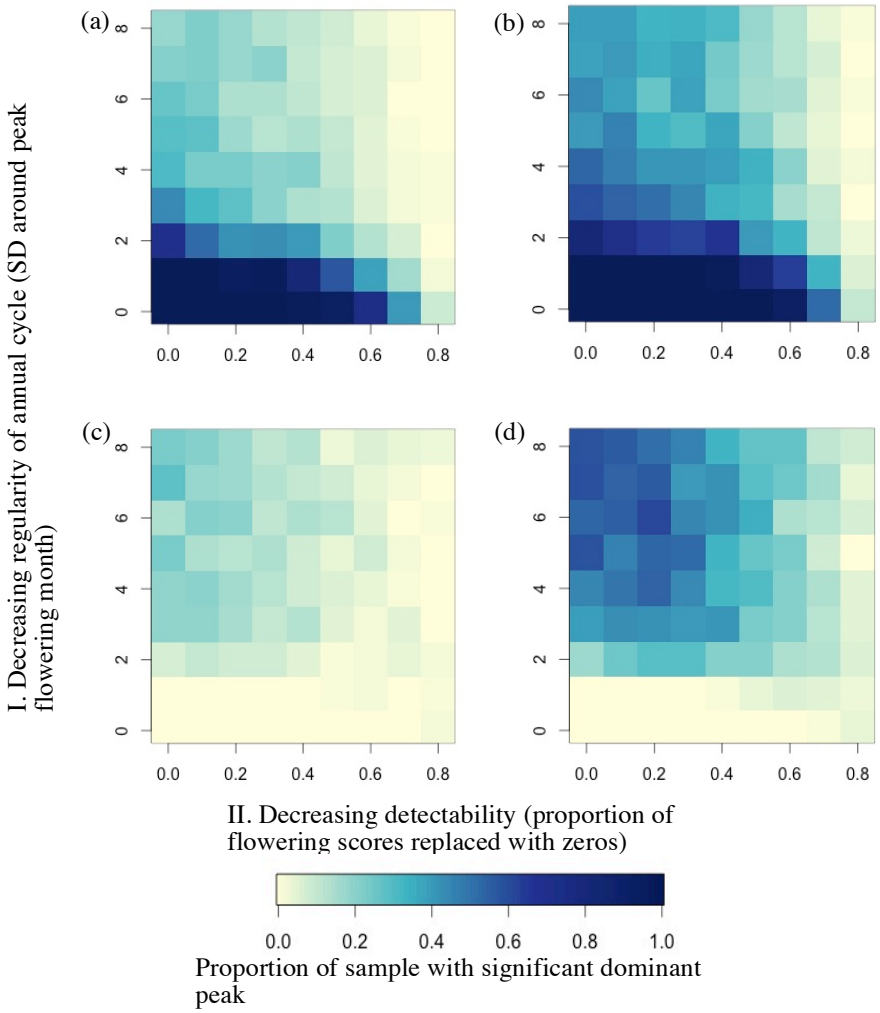

Figure A6. Power analysis of simulated data to show the impact of null hypothesis choice and length and noise of time series for detecting periodicity. Data simulated to represent a 10-year time series of a repeating 12-month flowering cycle with varying levels of noise. The shading of each matrix plot shows the likelihood of detecting a dominant peak using Fourier analysis within the expected wavelength interval and significant when compared to (a) "null continuum" and (b) "white noise" null hypotheses and the likelihood of detecting a dominant peak falling outside of the expected wavelength band and significant when compared to (c) "null continuum" and (d) "white noise" null hypotheses.

APPENDIX B: DEMONSTRATION OF FOURIER ANALYSIS FOR THREE CASE STUDY SPECIES AND COMPARISON WITH OTHER COMMON METHODS FOR QUANTIFYING FLOWERING PHENOLOGY.

Demonstration of Fourier analysis for three case study species

Here we show Fourier outputs in detail for three different species; *Antidesma vogelianum* (n=21), *Pentadesma butyracea* (n=14) and *Duboscia. macrocarpa* (n=11). Researchers from Lopé National Park, have observed individual tree canopies, using binoculars from the ground, at the beginning of each month since 1986 and noted the proportion of the canopy covered by flowers, recorded as scores from 0 to 4 (Tutin & Fernandez 1993; Tutin & White 1998). Initial observation of the mean proportions of individuals in flower each month over the years shows that flowers appear on a six-monthly cycle for *A. vogelianum*, peaking in June and December each year, on an annual (or multiple of annual) cycle for *P. butyracea* peaking between May - June each year and can occur in any month in a non-synchronised manner for *D. macrocarpa* (Figure B1 A, D and G). To further describe these cycles and extract quantitative indicators we ran Fourier analysis and a confidence test of the dominant spectral estimate for each individual. To estimate the relative phase of the dominant cycle for each individual we ran co-Fourier analysis of the data against a simulated time series of the same frequency, with phase 0, by convention for our data peaking on Jan 1st 1986.

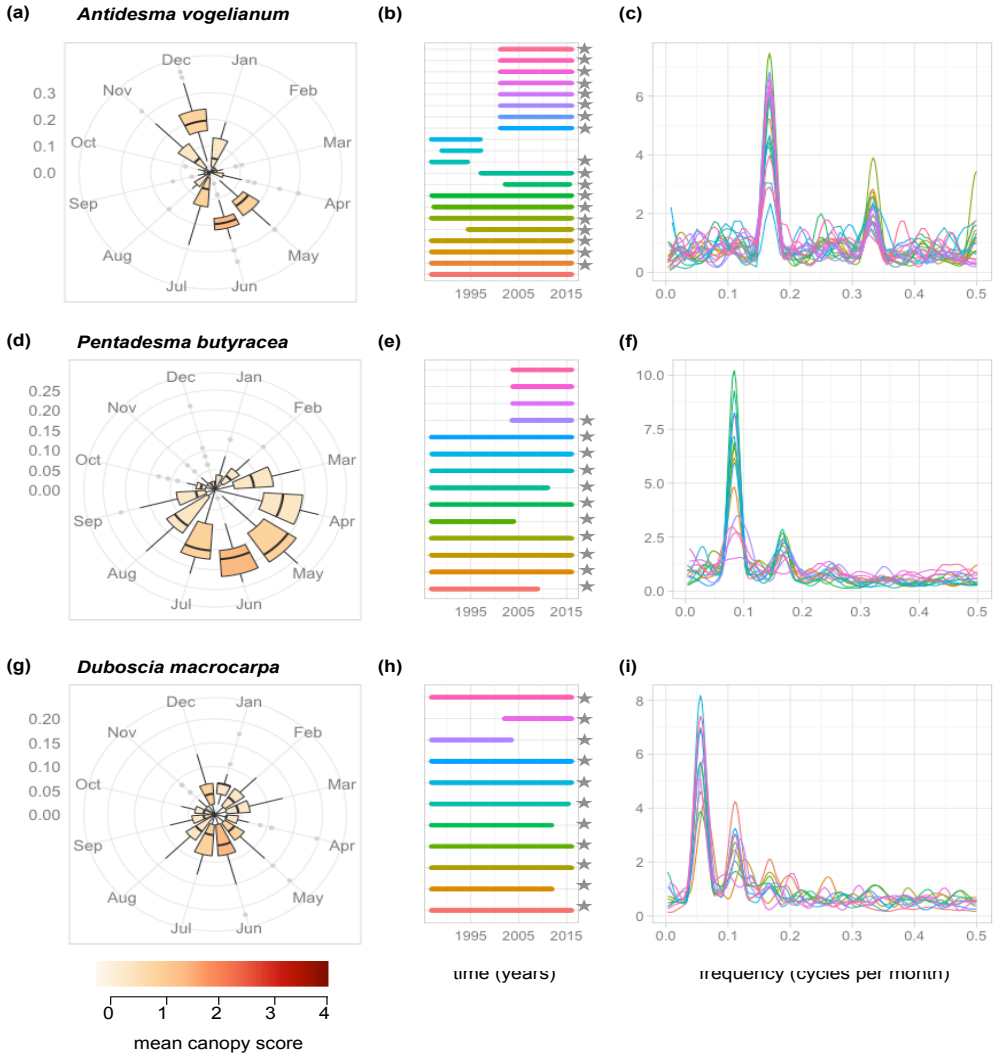

Figure B1. Fourier analysis of three tropical trees species. A. vogelianum (n=21), P. butyracea (n=14) and D. macrocarpa (n=11). Plots (a), (d) and (g) show circular boxplots of the proportion of individuals in flower each month between years. Coloured fill represents mean canopy score for flowering between individuals and years. Plots (b), (e) and (h) show the length of each individual time series, between 1986 and 2016. Plots (c), (e) and (i) show smoothed standardised periodograms for each individual (coloured according to duration plot). Dominant peaks in the spectral estimates (s(f)) indicate cycles in the data. Stars next to the duration plots indicate a significant dominant peak for that individual when compared to a null hypothesis of no periodicity.

Table B1. Quantitative descriptors of flowering cycles derived from Fourier analysis for three species.

Quantitative description of flowering cycles	***A. vogelianum***	***P. butyracea***	***D. macrocarpa***
Number of individuals in sample	21	14	11
Number of individuals with significant dominant cycles	19	12	11
Mean cycle length + SD (months)	6 + 0	12 + 0.25	17.9 + 0.99
Modal cycle length (months)	6	12	18
Cycle length of simulated cosine curve for co-Fourier analysis (months)	6	12	18
Mean phase difference to simulated cosine curve (radians)	-1.26	2.27	0.94
Timing of peak events (months since Jan 1st)	4.8 10.8	4.34	2.69 8.69
Timing of peak events (calendar month)	late May late November	mid-May	mid-March mid-September
Synchronicity: SD of mean phase difference (radians)	0.21	0.24	1.68
Synchronicity: SD of mean phase difference (months)	0.20	0.46	4.8

The common dominant flowering cycle for *A. vogelianum* individuals was 6 months long, synchronised between individuals (SD peak month = 0.2 months) peaking twice each calendar year in late May- early June and late November – early December (Table B1).

The common dominant flowering cycle for *P. butyracea* individuals was 12 months long, synchronised between individuals (SD peak month = 0.46 months) peaking once each calendar year in mid-May (Table B1).

The common dominant flowering cycle for *D. macrocarpa* individuals was 18 months long and not well synchronised between individuals (SD peak month = 4.8 months). In this context, although mean peak months for flowering are possible to calculate for the population (mid March and mid September in alternating calendar years), they have little biological meaning (Table B1).

Comparison of Fourier with other common methods for quantifying flowering phenology

We identified four key questions commonly asked when quantifying seasonal phenology activity; 1) Is there a regular cycle? 2) How long is the cycle? 3) What is the peak timing of the phenology event? 4) How synchronised are the phenology events? We asked these questions using four different methods (graphical representation of time series data, circular statistics on both species summaries and individual data records, autocorrelation analyses and GAMs; Tables B2-4 and Figures B2-4) commonly used in the literature to quantify seasonal characteristics of phenology data. We contrasted the outputs of these methods alongside those derived from Fourier analyses for phenology as we present it in this paper. This allows comparison of the different methods' abilities to provide information and the nature of that information – for example, is it quantitative and inclusive of uncertainty or variance?

We find that Fourier analysis overcomes the difficulties associated with circular statistics regarding non-annual cycles. In the literature, the solution given for the handling of non-annual species within circular statistics is to use autocorrelation analyses to fist identify non-annual cycles and then to exclude those species form further analysis (Zimmerman *et al.* 2007) or to analyse reproductive events separately (Wright *et al.* 1999). In comparison, Fourier analysis is flexible to non-annual species, as demonstrated in the where the cycle strength, wavelength, phase and synchronicity is calculated for species *A. voglieanum* and *D. macrocarpa*, which have a 6-month and an 18-month cycles respectively. Fourier analysis, as we present it, also provides a more comprehensive suite of information about the seasonal cycle, including both measures of variance and confidence. The sinusoidal basis of Fourier assumes regular phenological activity, and as such the method compares negatively to some other methods when information on the variation in phenophase intensity between months or years is required. It is also worth noting the power of such analysis at the level of the individual.

It is only with Fourier analysis at the level of the individual that the 18-month unsynchronized cycle of *D. macrocarpa* trees can be identified.

Table B2. Methods comparison for quantifying flowering phenology of Antidesma vogelianum. N = 21 individuals, mean time series length = 232 ± 94 months - see Figure B2 for illustrations.

	Graphical representation (individual)	Circular statistics (species)	Circular statistics (individuals)	Autocorrelation analysis (species)	GAM annual smooth (species)	Fourier (species)	Fourier (individuals)
Figure 2	**A**	**B**		**C**	**D**	**E**	**F**
Cycle regularity	**Regular.** Visual inspection of each time series, cycles appear regular.	**Regular cycle.** Visual inspection of circular raw data graph, cycle appears to be regular	**Regular cycle.** Visual inspection of circular raw data graphs, cycles appear to be regular	**Regular cycle.** There are significant lags.	**Regular.** Visual inspection of annual smooth, peaks appear to be regularly spaced.	**Significant regular cycle.** Spectral estimate for dominant cycle= 0.03.	**Significant regular cycle for 19 /21 individuals.** Mean normalised s(f) for dominant cycle = 5.6 ± 1.1 SD.
Cycle length	**Sub-annual cycle of 6 months long**. Visual inspection of each time series, cycles appear to be around 6 months long	**Cycle neither unimodal nor continuous.** Length of mean vector=0.14; Raleigh test of uniformity p=0.96; Rao's spacing test of uniformity p<0.001	**Unclear.** High dispersion of values for all individuals, mean length of mean vector = 0.14 ± 0.07.	**Subannual cycle in flower production as a species.** Significant lag at 6 months.	**Sub-annual cycle**. Visual inspection of annual smooth, appear to be two significant peaks a year, 6 months apart.	**Sub-annual cycle of 6 months long**. Dominant frequency = 0.167 cycles per month (Dominant wavelength = 6 months)	**Sub-annual cycle of 6 months long.** Mean of all significant dominant cycles = 0.167 ± 0 SD cycles per month (Dominant wavelength = 6 months).
Peak timing	**May-June and December**	**Unclear**. Angle of mean vector = 1.99 radians (3.8 months since Jan 1st), but high dispersion of values, see cycle length.	**Unclear.** Mean angle of mean vector = 2.2 radians (4.2 months since Jan 1st) , but high dispersion of values, see cycle length.	NA	**Jun and Dec.** Highest values for annual smooth found in June and December.	**Repeating cycle peaking every 6 months in late Jun and late Dec .** Phase = -0.14 radians (months c(5.9, 11.9))	**Repeating cycle every 6 months in late May and late Nov.** Mean phase = -1.26 radians (months c(4.8, 10.8))
Synchrony	**Synchronised.** Visual inspection of all time series show cycle to be synchronised	NA	**Not well synchronised.** SD of mean angle of mean vector = 1.02 radians (1.95 months)	NA	NA	NA	**Well synchronised.** SD of mean phase = 0.21 radians (0.20 months)

Figure B2. Methods comparison for quantifying flowering phenology of Antidesma vogelianum, N = 21 individuals, mean time series length = 232 ± 94 months - see Table B2.

A. Time series graphs (individuals)

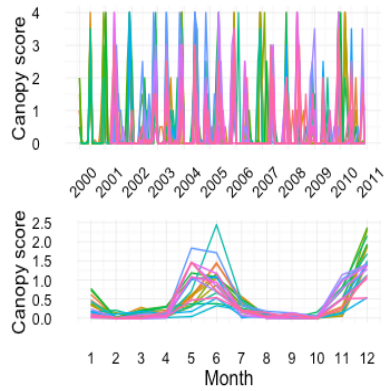

B. Raw circular data graph

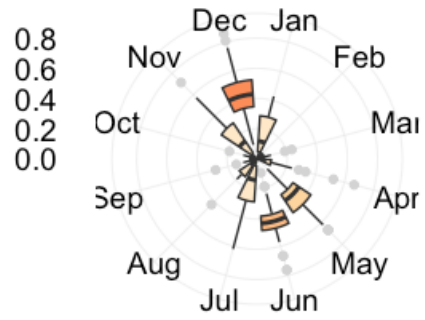

C. Autocorrelation analysis (species)

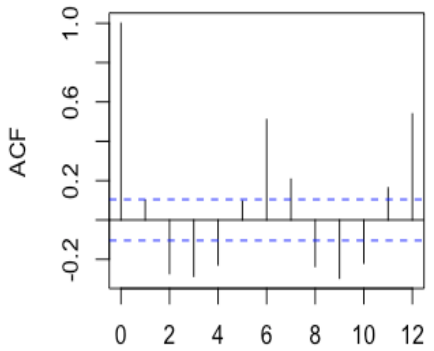

D. GAM annual smooth (species)

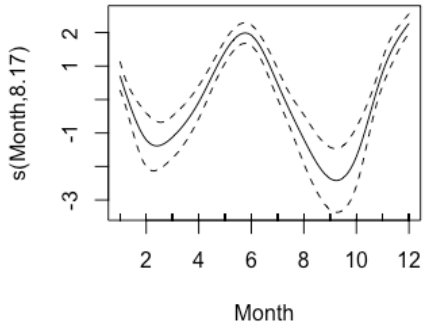

E. Fourier for species (individuals combined)

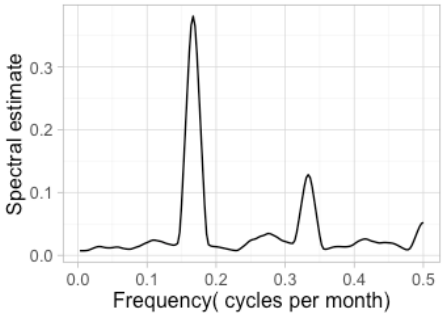

F. Fourier for individuals

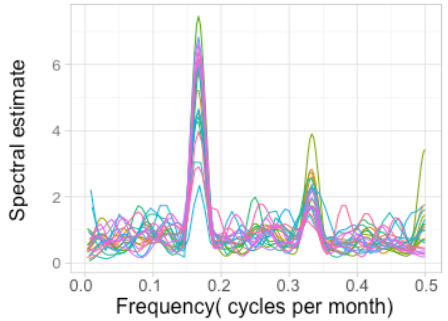

Table B3. Methods comparison for quantifying flowering phenology of Pentadesma butyracea. N=14 individuals, mean time series length = 274 ± 92 months - see Figure B3 for illustrations.

	Time series (individual)	Circular statistics (species)	Circular statistics (individuals)	Autocorrelation analysis (species)	GAM annual smooth (species)	Fourier (species)	Fourier (individuals)
Figure 3	**A**	**B**		**C**	**D**	**E**	**F**
Cycle regularity	**Regular.** Visual inspection of each time series, cycles appear regular.	**Unclear.** Visual inspection of raw circular data graph, unclear how regular cycle is.	**Regular cycle.** Visual inspection of circular raw data graphs, cycles appear to be regular	**Regular cycle.** There are significant lags.	**Unclear.** Visual inspection of annual smooth, one broad peak per pear.	**Significant regular cycle.** Spectral estimate for dominant cycle= 0.07.	**Significant regular cycle for 12/14 individuals.** Mean normalised s(f) for dominant cycle = 6.7 ± 2.2 SD.
Cycle length	**Annual cycle**. Visual inspection of each time series, cycles appear to be around 12 months long, one peak per year.	**Cycle is unimodal and not continuous.** Length of mean vector=0.59; Raleigh test of uniformity p<0.001; Rao's spacing test of uniformity p<0.05	**Cycle is unimodal.** Low dispersion of values for all individuals, mean length of mean vector = 0.46 ± 0.09.	**Annual cycle in flower production as a species.** Strongest significant lag at 12 months.	**Annual cycle**. Visual inspection of annual smooth, appears to be one significant peak a year.	**Annual cycle**. Dominant frequency = 0.083 cycles per month (1 cycle per year). Dominant wavelength= 12 months.	**Annual cycle.** Mean of all significant dominant cycles = 0.083 ± 0.0 SD cycles per month (1 cycle per year). Dominant wavelength = 12 ± 0.25 SD months.
Peak timing	**May-June**	**Mid-May.** Angle of mean vector = 2.41 radians (month 5.6).	**Mid-May.** Mean angle of mean vector = 2.88 radians (5.5 months).	NA	**Mid-May.** Highest values for annual smooth found in May.	**Repeating cycle peaking every 12 months in Mid-June.** Phase = 2.82 radians (month 5.4 months)	**Repeating cycle peaking every 12 months in mid-May.** Mean phase = 2.27 radians (month 4.3)
Synchrony	**Synchronised.** Visual inspection of all time series, cycles appear to be synchronised	NA	**Well synchronised.** SD of mean angle of mean vector = 0.27 radians (0.52 months)	NA	NA	NA	**Well synchronised.** SD of mean phase = 0.24 radians (0.46 months)

Figure B3. Methods comparison for quantifying flowering phenology of Pentadesma butyracea.N=14 individuals, mean time series length = 274 ± 92 months - see Table SB3.

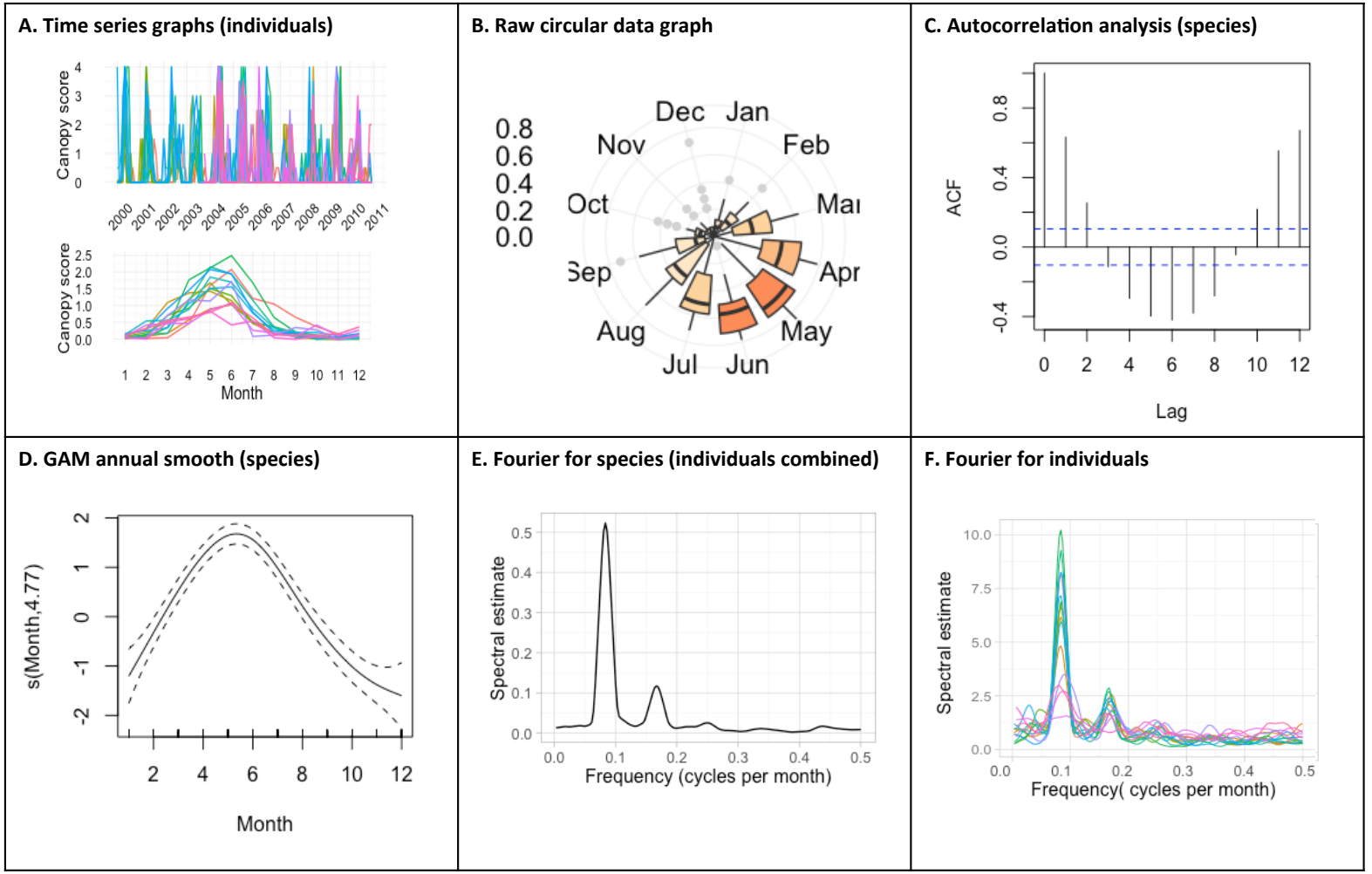

Table B4. Methods comparison for quantifying flowering phenology of Duboscia macrocarpa. N=11 individuals, mean time series length = 313 ± 66 months - see Figure B4 for illustrations.

	Time series (individual)	Circular statistics (species)	Circular statistics (individuals)	Autocorrelation analysis (species)	GAM annual smooth (species)	Fourier (species)	Fourier (individuals)
Figure 4	**A**	**B**		**C**	**D**	**E**	**F**
Cycle regularity	**Unclear.** Visual inspection of each time series, cycles difficult to differentiate.	**Unclear.** Visual inspection of raw circular data graph, unclear how regular cycle is.	**Unclear.**	**Regular cycle.** There are significant lags.	**Irregular.** Visual inspection of annual smooth, two broad peaks per pear of different intensity.	**Significant regular cycle.** Spectral estimate for dominant cycle= 0.05.	**Significant regular cycle for 11/11 individuals.** Mean normalised s(f) for dominant cycle = 5.9 ± 1.4 SD.
Cycle length	**Unclear**. Visual inspection of each time series, cycles unclear but appear to be supra-annual.	**Cycle is neither uniform nor unimodal.** Length of mean vector=0.26; Raleigh test of uniformity p=0.01; Rao's spacing test of uniformity p<0.05	**Cycle is neither uniform nor unimodal.** High dispersion of values for all individuals, mean length of mean vector = 0.16 ± 0.07.	**18-month cycle as a species.** Strongest significant lag at 18 months, also significant lag at 6 months.	**6-month cycle as a species**. Visual inspection of annual smooth, appears to be two significant peaks a year.	**6-month cycle as a species**. Dominant frequency = 0.167 cycles per month (2 cycles per year). Dominant wavelength= 6 months. Another strong peak observed at 18 months.	**18-month cycle.** Mean of all significant dominant cycles = 0.056 ± 0.0 SD cycles per month (1 cycle per year). Dominant wavelength = 17.9 ± 1.0 SD months.
Peak timing	**May-June and Dec-Jan.** Pattern apparent but much variation.	**No peak timing.** Angle of mean vector = 2.53 radians (month 4.8), but length of mean vector is very low.	**No peak timing.** Mean angle of mean vector = 2.28 radians (month 4.35), but see length of mean vector is very low.	NA	**May.-Jun and Dec-Jan.** Highest values for annual smooth found in May-Jun and Dec-Jan.	**Repeating cycle peaking every 6 months in mid-March and mid-Sep .** Phase = 0.85 radians (months c(2.5, 8.5))	**Repeating cycle peaking every 18 months on average in mid-March and mid-Sep .** Mean phase = 0.9 radians (months c(2.7, 8.7))
Synchrony	**Unclear.** Cycles difficult to differentiate but perhaps some loose synchronisation.	NA	**Not well synchronised.** SD of mean angle of mean vector = 0.72 radians (1.37 months)	NA	NA	NA	**Not synchronised.** SD of mean phase = 1.68 radians (4.8 months)

Figure B4. Methods comparison for quantifying flowering phenology of Duboscia macrocarpa. N=11 individuals, mean time series length = 313 + 66 months - see Figure B4 for illustrations.

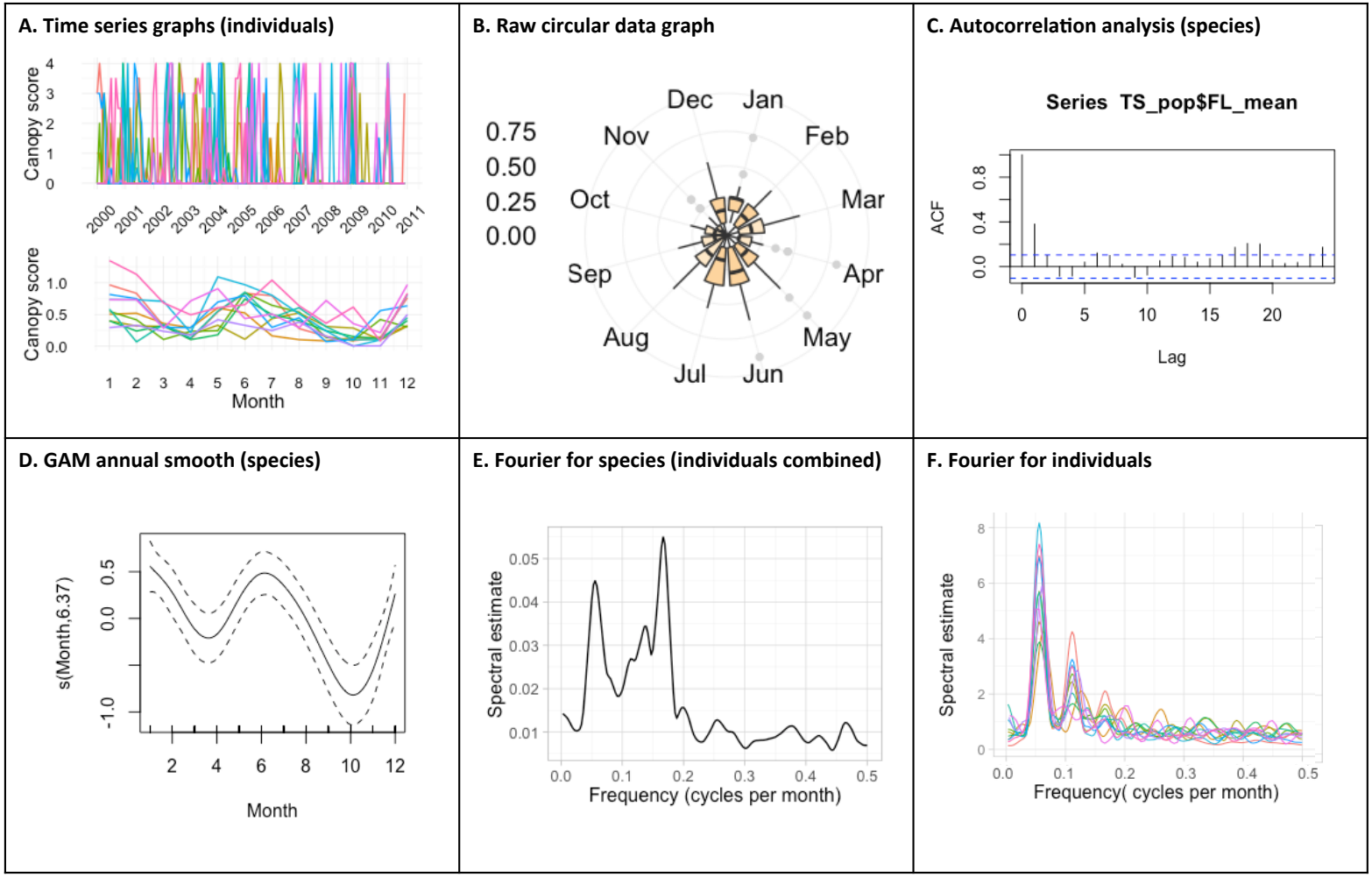

APPENDIX C: PREPARING LOPÉ WEATHER DATA

Rainfall

Rainfall has been recorded using two pieces of equipment at Lopé NP: a manual rain gauge (total precipitation for the preceding 24 hour period recorded at 8am each day) and a VantagePro weather station (precipitation recorded every 30 mins) (Figure C1).

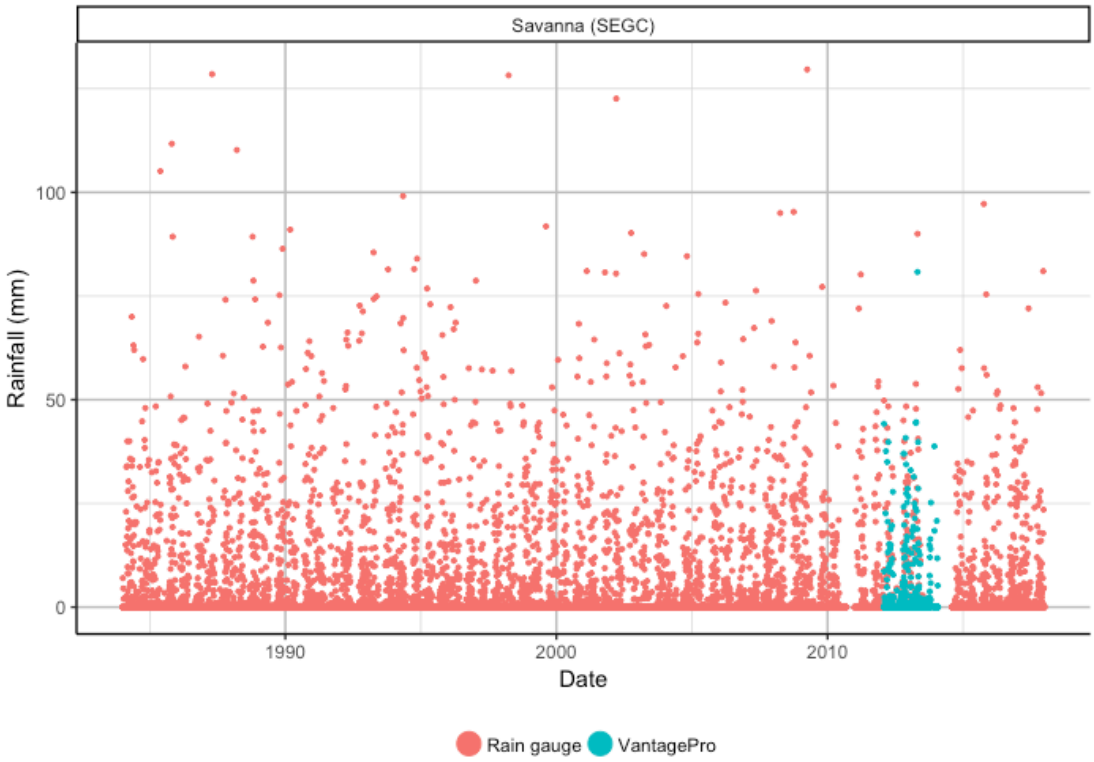

Figure C1. Time series plot of rainfall observations at Lopé NP, 1984-2018. Coloured dots show unprojected daily observations from both the rain gauge and the VantagePro weather station.

First, we adjusted the 24-hr period for the VantagePro data to begin and end at 8am to match the rain gauge. When we compared simultaneous measurements (2012-2014) we found that the weather station consistently underestimated rainfall compared to the rain gauge (Figure C2).

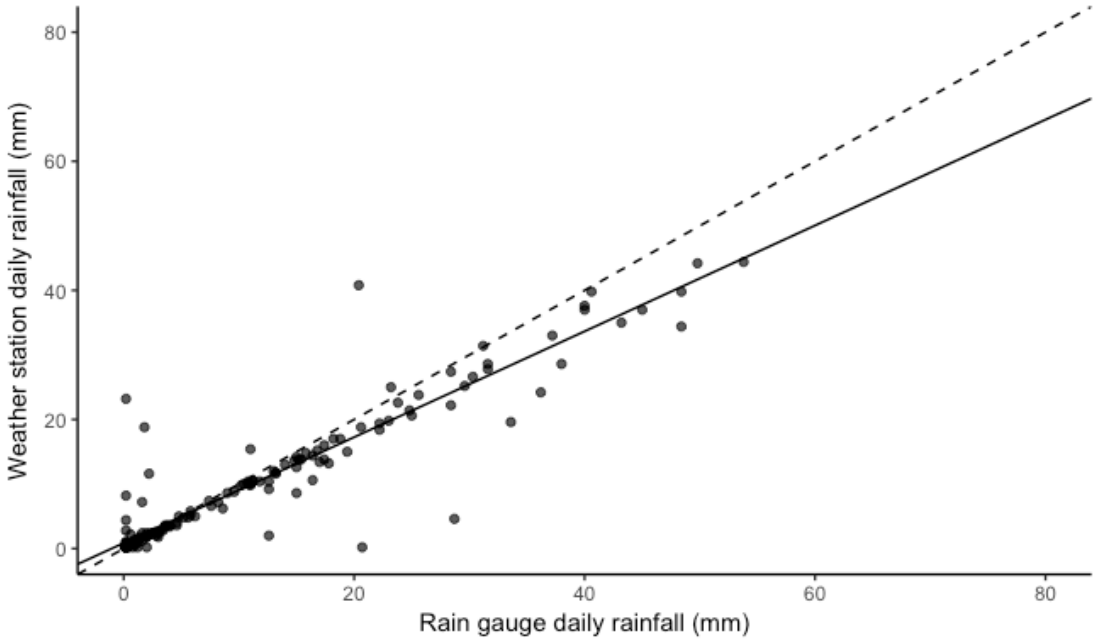

Figure C2. Comparison of simultaneous non-zero rainfall observations from the weather station and the rain gauge at Lopé NP, 2012-2014. The dotted line indicates the expected 1:1 relationship. The solid line indicates the model prediction.

To standardise the data record we used rain gauge-rainfall to predict weather station-rainfall for all simultaneous non-zero daily records within a general linear model (GLM, family=Poisson; Table C1).

Table C1 Estimates from a general linear model (family=Poisson) to standardise Lopé rainfall observations. Rainfall observations from the weather station (VantagePro) were used to predict rain-gauge rainfall for all simultaneous non-zero observations.

Predictor	**Estimate**	**SE**	**T value**	**P value**
Intercept	0.86	0.42	2.05	<0.05
Rainfall (rain gauge)	0.82	0.02	35.67	<0.0001

We extracted the intercept and slope from the GLM to reproject the weather station data and calculated mean daily rainfall for each day with more than one record. Between 1st January 1984 and 31st December 2017 there were 369 days with no rainfall observations (3% total number of days). Where

possible we filled these gaps using the 10-day running mean for the time-series, but 308 missing daily observations remained in three blocks: 2010-09-16 - 2010-12-26 (lost rain gauge data), 2013-10-31 - 2013-11-30 and 2014-02-02 - 2014-07-26 (lost VantagePro data due to lightning strike on equipment). For further analyses requiring complete monthly timeseries (Fourier and Wavelet methods) we filled missing months using the mean value for corresponding calendar month (Figure C3). All data selection procedures described above are shown as a flow chart in Figure C4.

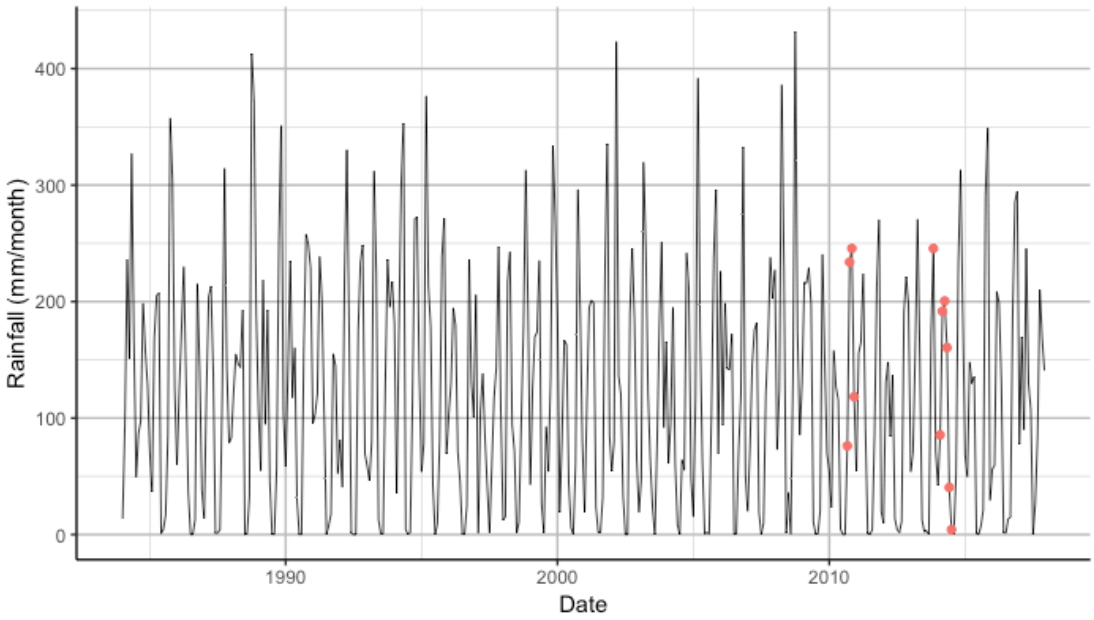

Figure C3. Time series plot of monthly rainfall at Lopé NP, 1984-2018. The line shows the calibrated data filled with the 10-day running mean to give total monthly rainfall. Red dots indicate missing months, which were filled using the mean value for the corresponding calendar month.

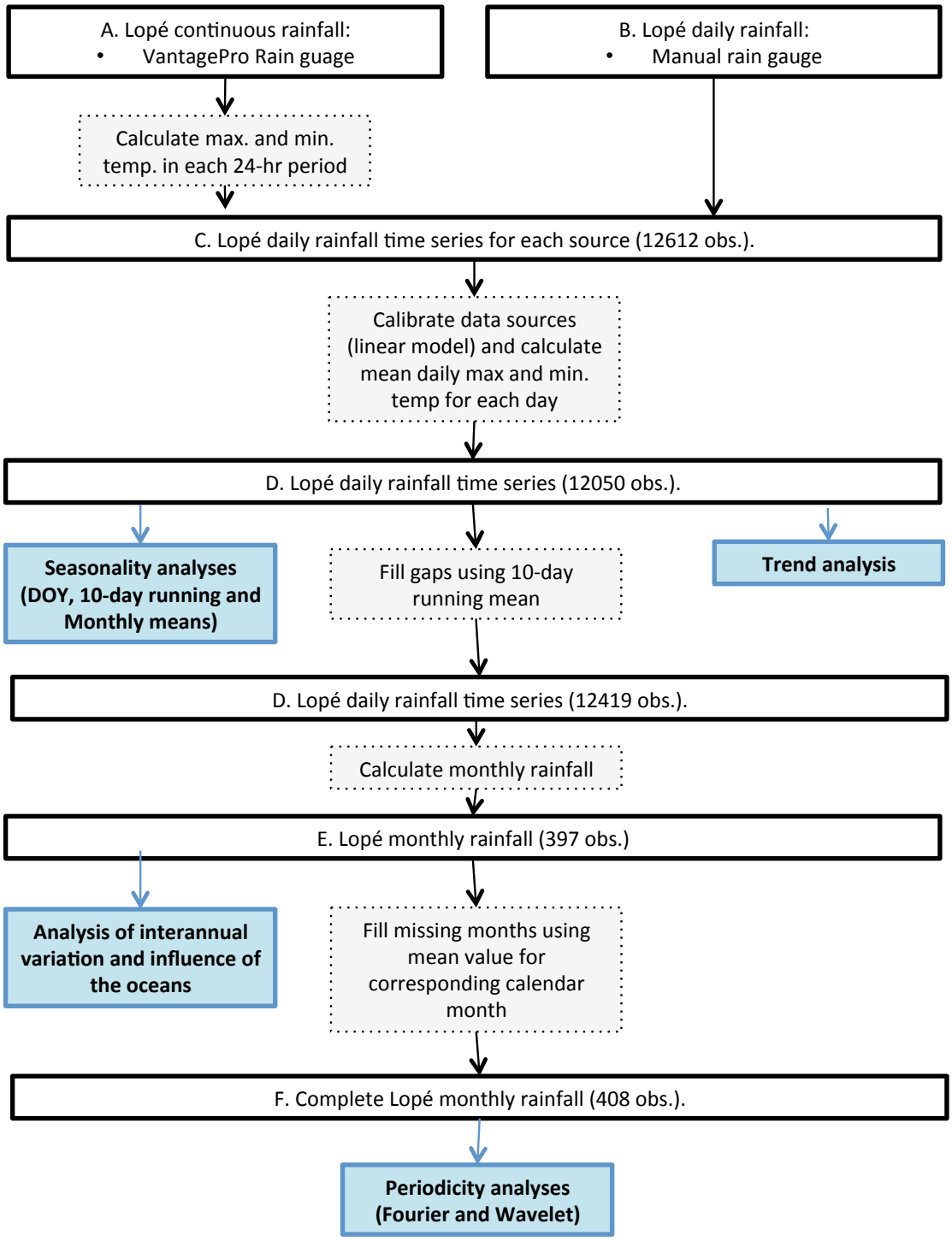

Figure C4 Diagram to show data selection for rainfall analyses. Bold boxes indicate data packages. Grey dashed boxes indicate processes. Blue boxes indicate analyses.

Temperature

Maximum and minimum daily temperatures have been recorded at Lopé using six different pieces of equipment at the two sites from 1984 to the present (Figure C5).

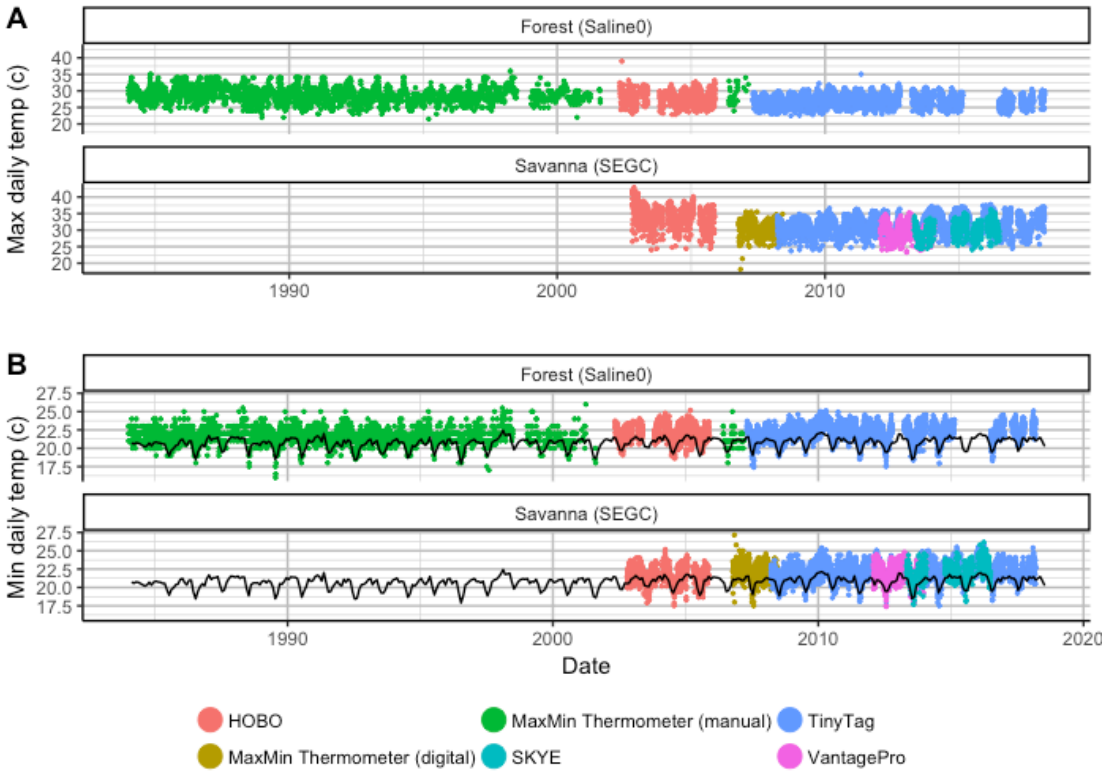

Figure C5 Time series plots of maximum (A) and minimum (B) daily temperature observations at Lopé NP, 1984-2018. Coloured dots show the unprojected daily observations from both sites (forest and savanna) using different equipment. The black line shows monthly mean minimum daily temperature from the Berkeley dataset.

The manual max/min thermometer showed the highest and lowest temperature since last reset and was recorded at irregular intervals. In the case of multi-day intervals between data observations it is impossible to know which day temperature extremes occurred on. We therefore assigned the recorded observations to the mid-date between the current and previous observations for all multiday intervals outside of three major breaks where the equipment was out of use: 1998/07 - 1999/01, 2001/03 - 2001/08 and 2001/08 - 2006/06. The digital max/min thermometer showed the highest

and lowest temperatures of the previous 24hrs (usually recorded between 8 and 9am). The automatic units collected data in intervals up to 30 minutes long. We calculated minimum and maximum daily temperature for the continuous data records using a 24hr period from 8am-8am to match the thermometer data.

The three major challenges for using this Lopé temperature record for long-term analyses are 1) the impacts of solar radiation during the day on maximum daily air temperature measurements, 2) lack of simultaneous recording pre-2007 to quantify the differing sensitivities of recording equipment (e.g. to sunlight) and 3) missing data. We describe here (and in diagram form in Figure C8) how we addressed these challenges.

Maximum daily temperature is usually the highest temperature recorded during daylight hours and is strongly influenced by surface solar radiation, while minimum daily temperature usually occurs at night and is thus less impacted by irradiance effects (Bristow & Campbell 1984; Dai *et al.* 1999). While various attempts were made to shade the recording equipment at Lopé, it has since been shown that specialised solar radiation shields are necessary for accurate recording of maximum daily air temperature (Jenkins 2014; Bell *et al.* 2015; da Cunha 2015). However recent experience at Lopé using specialist TinyTag solar shields has shown that they increase the likelihood of termite invasion, which has resulted in equipment failure in some cases. The relative exposure of the savanna site (away from the forest canopy) and the dynamic nature of the "shaded" forest site (increasing and decreasing irradiance in response to canopy changes) has interacted with the differing sensitivities of each recording unit and led to variability in the means and ranges of maximum temperature data derived from different equipment (Figure C6).

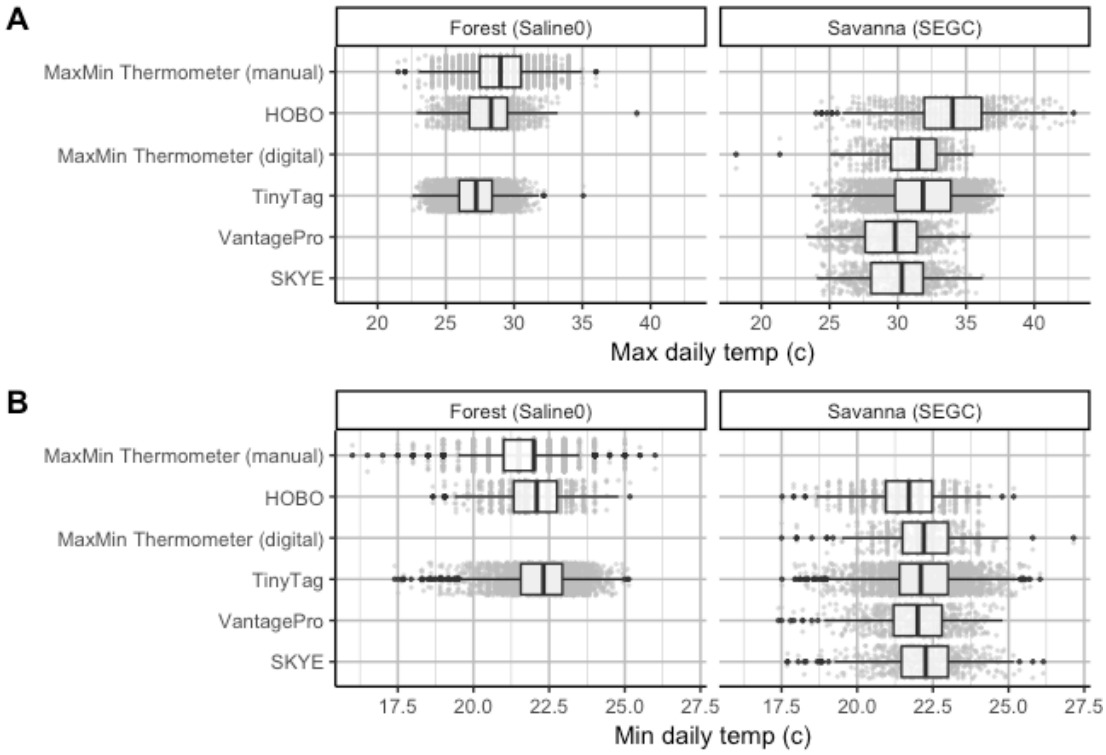

Figure C6 Boxplots of maximum (A) and minimum (B) daily temperature at Lopé NP, 1984-2018. Lopé forest observations cover the period 1984 - 2018 and Lopé savanna observations cover the period 2002 – 2018. Grey dots show the daily data collected at both sites (forest and savanna) using different equipment. Boxplots show the median (vertical bar), interquartile range (25th and 75th centiles; filled box), the normal range (no more than 1.5 times the interquartile range from the 25th and 75th centiles, horizontal black lines) and the outliers (outside of the normal range, black dots).

Because of the lack of simultaneous recording (pre-2007) to evaluate these differences and the dynamic nature of sunlight effects over time even for observations deriving from the same equipment (e.g. canopy changing) we chose to use maximum and minimum daily temperature observations from all equipment to assess mean seasonality (Day of Year and Monthly means) and periodicity (Fourier and Wavelet analyses) for each site, but only minimum daily temperature for long-term assessments of change and inter-annual variability. As Fourier and Wavelet analyses require continuous timeseries, we summarised all max and min data (25538 daily max and min observations) to monthly mean timeseries for each site, excluding months with fewer than five observations. We filled missing months using the mean

value for the corresponding calendar month from the entire time series (Figure C7).

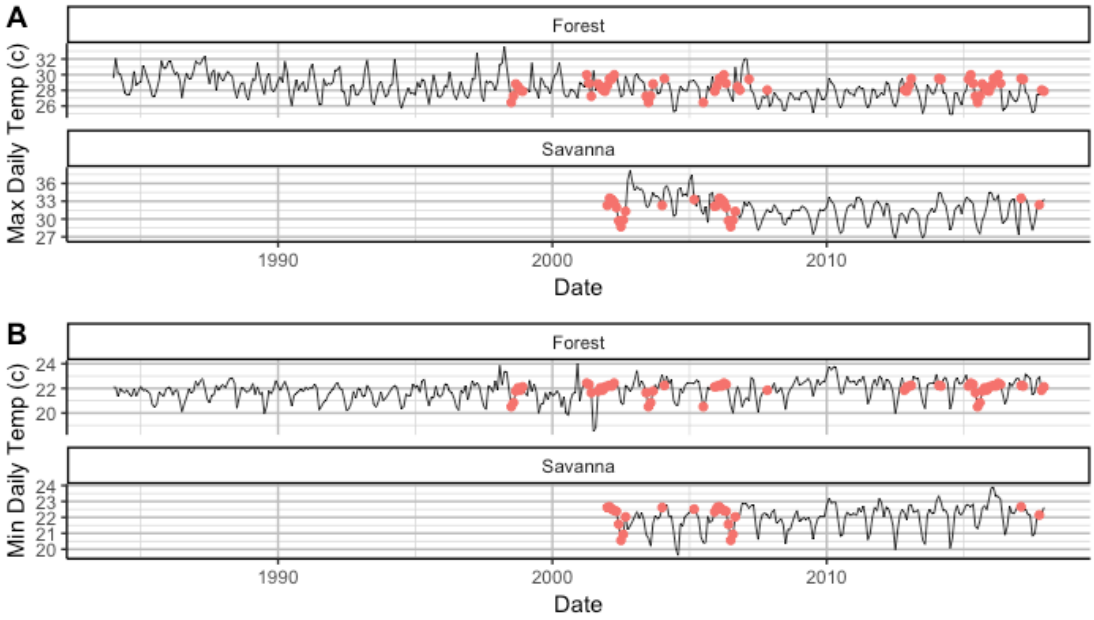

Figure C7 Time series plot of monthly mean maximum (A) and minimum (B) daily temperature observations at Lopé NP, 1984-2018. The line shows the monthly means for each site. Red dots indicate missing months, which were filled using the mean value for the corresponding calendar month.

For long-term analyses we combined minimum temperature data from both sites (mean minimum temperature from simultaneous TinyTag recordings are 22.3°c ±1.1 sd in the forest and 22.0°c ± 1.2 sd in the savanna) and calculated the mean daily minimum temperature from all sites and equipment for each day in the time series (8217 observations from 3/1/1984 to 31/12/2017, 34% days missing). We used this daily time series for trend analysis and to calculate monthly timeseries. First we calculated the average daily low temperature for each month (monthly mean of minimum daily temperature) excluding months with fewer than five observations (overall mean number of observations per month for all equipment = 22.3). The manual max/min thermometer used from 1984 to 2002 does however accurately record the extreme lows in daily minimum temperature for the entire interval between observations. In order to make best use of this information we also calculated extreme daily low temperature for each

month (monthly minimum of minimum daily temperature) for the Lopé time-series. We included all months, no matter the number of observations, from the manual thermometer record but only months with more than five observations for all other data collection methods.

In the final Lopé minimum temperature record there are 36 monthly observations missing (9% total number of months) for the average low temperature timeseries and 24 monthly observations missing (6% total number of months) for the extreme low temperature timeseries between Janvuary 1984 and December 2017. All data selection procedures described above are shown as a flow chart in Figure C8.

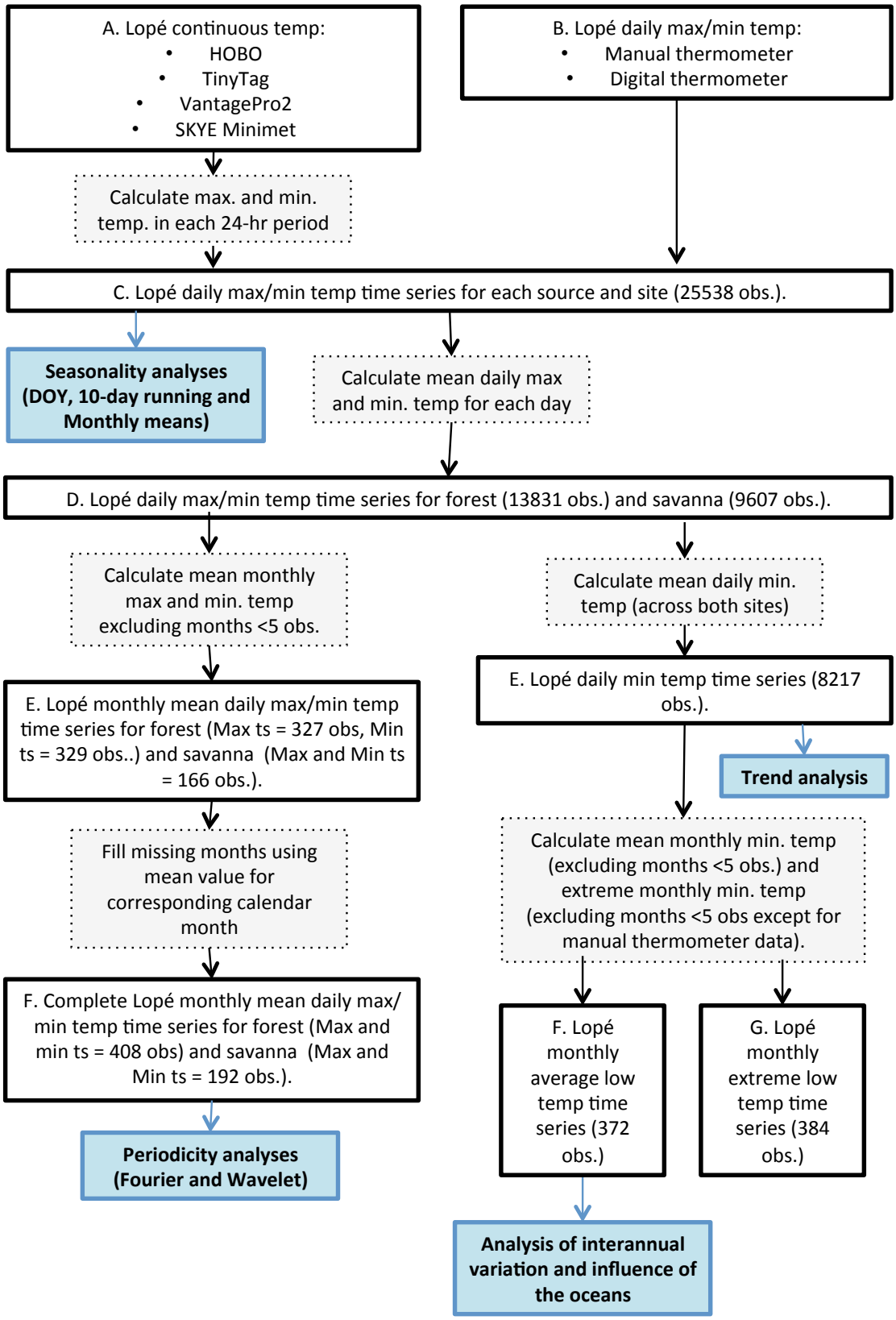

Figure C8 Diagram to show data selection for temperature analyses. Bold boxes indicate data packages. Grey dashed boxes indicate processes. Blue boxes indicate analyses.

Relative Humidity

Relative humidity (RH) has been recorded at Lopé using five different types of equipment (wet/dry bulb, HOBO units, TinyTags, and both weather stations) at the two sites (savanna and forest) from 1985 to the present (Figure C9).

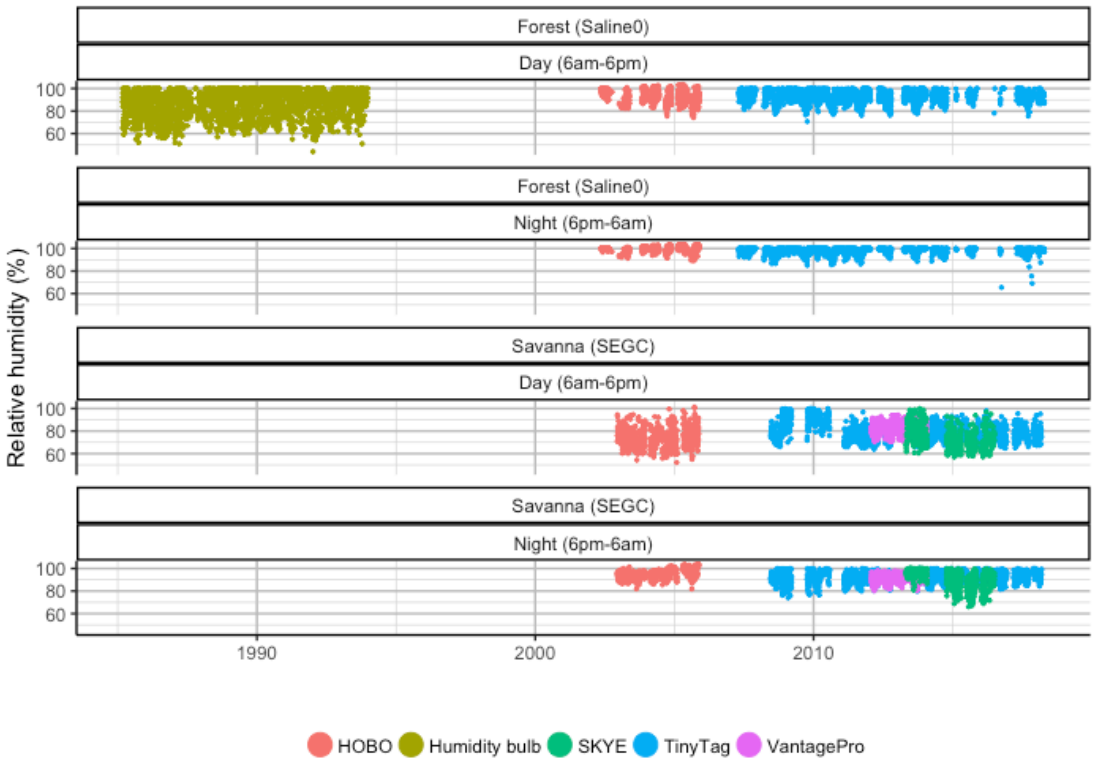

Figure C9 Time series plots of day and night relative humidity at Lopé NP 1983-2018. Coloured dots show daily observations from both sites (forest and savanna) and different equipment. Humidity bulb observations were recorded once per day at different times. The remaining observations are mean values for the day or night from automated data collection with intervals up to 30 minutes long.

The four major challenges in creating a Lopé humidity record for long-term analyses are 1) the impacts of solar radiation and water saturation on humidity measurements and the differing sensitivities of recording equipment to these, 2) the variable observation times pre-2002 using the wet-dry bulb, 3) drift in measurement errors over time and low frequency of equipment calibration and 4) missing data.

We know that direct solar radiation leads to underestimation of RH (da Cunha 2015) and that accurate data requires specialised solar screens, which were not used at Lopé before 2017. To avoid errors in our dataset associated with solar radiation we separated day (6am-6pm) and night (6pm-6am) observations for the data derived from the automatic units and calculated the mean humidity for each session per 24-hour period (6am-6am; Figure C9). Restricting further analyses to night time data also precluded the humidity bulb data as it was only collected during the daytime. In any case, it proved difficult to use this data for seasonal or inter-annual analyses as it was recorded at different times each day depending on the research station schedule (usually between 7am and 6pm). The TinyTag manufacturers (GEMINI) advised us that erroneous 0% RH observations represented a shorting of the internal circuit under conditions of water saturation and so we removed all zeroes before calculating daily means.

In 2016/17 all TinyTag humidity units were calibrated in the UK and were found to be over measuring relative humidity by 3.9 - 13.4% (at an applied humidity of 77-78%). Following these checks, two units were replaced and the humidity channels on the remainder were adjusted. However is very difficult to know when the measurement drift occurred between 2010 and 2016 and how to remove this error. None of the units were calibrated regularly and as a result were often used outside of expiry periods meaning that this measurement drift may be an issue for the other data too. For example, HOBO units often measured RH >100% (Figure C10) and the SKYE data shows downward drift over time in 2015/2016 (Figure C9).

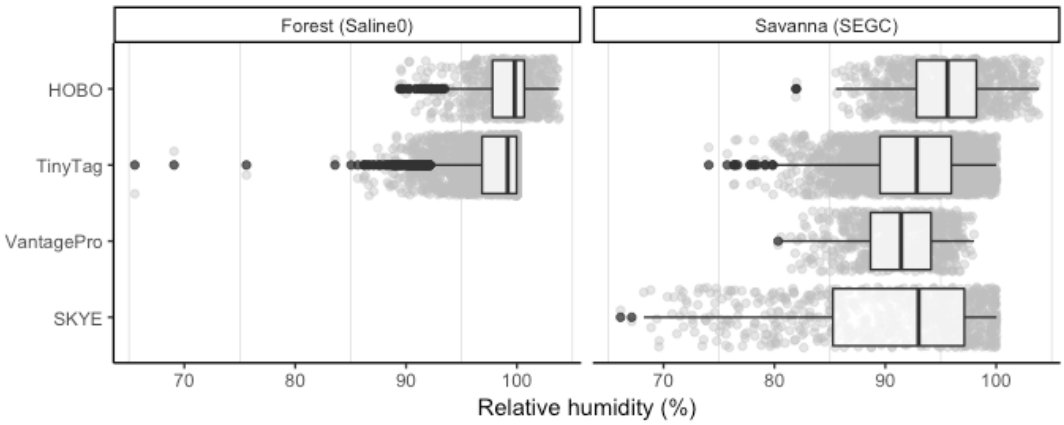

Figure C10 Boxplots of night-time relative humidity at Lopé NP, 2002-2018. Grey dots show the daily (night-time) data observations from both sites (forest and savanna) using different equipment. Boxplots show the median (vertical bar), interquartile range (25th and 75th centiles; filled box), the normal range (no more than 1.5 times the interquartile range from the 25th and 75th centiles, horizontal black lines) and the outliers (outside of the normal range, black dots).

Because of the data problems described above, we chose to use the full night time RH automated data record to assess mean seasonality (Day of Year and Monthly means) and periodicity (Fourier and Wavelet analyses; complete monthly mean time series shown in Figure C11) for each site, but not for long-term assessments of change and inter-annual variability.

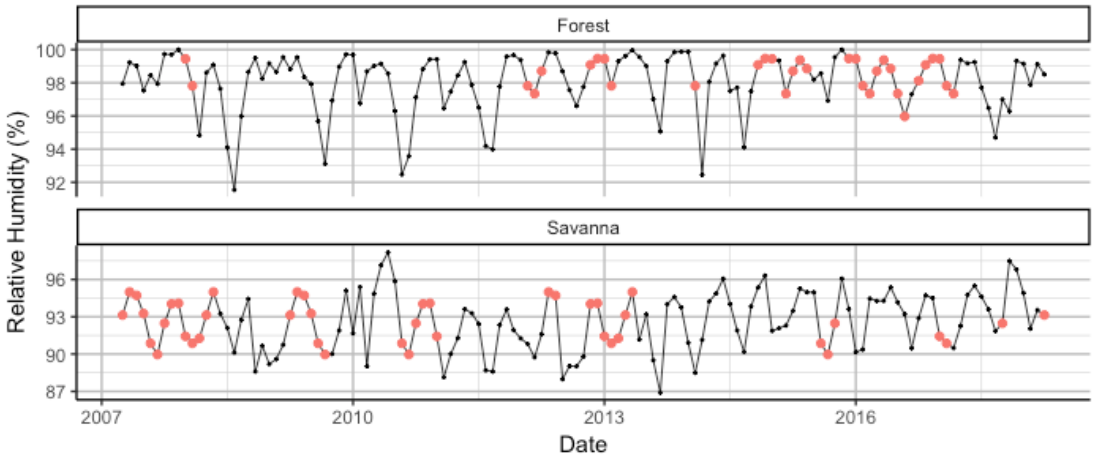

Figure C11 Time series plot of monthly mean relative humidity observations at Lopé NP, 2007-2018. The line shows the monthly means for each site. Red dots indicate missing months, which were filled using the mean value for the corresponding calendar month.

Solar Radiation

Solar radiation has been recorded at Lopé using two weather stations in the savanna from 2012 to 2016 (Figure C12). Because the data is short and patchy we can only use it to demonstrate seasonality and periodicity (Fourier analysis using the continuous time series showin in Figure C13) not long-term trends or interannual variation.

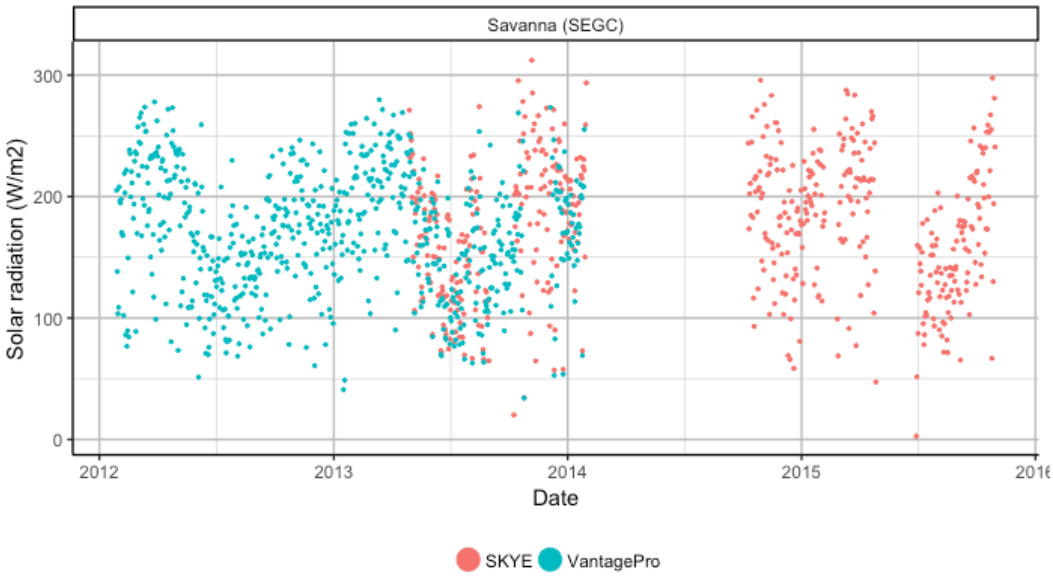

Figure S4.1.12 Time series plots of surface solar radiation at Lopé NP, 2012-2016. Coloured dots show daily mean observations from different equipment.

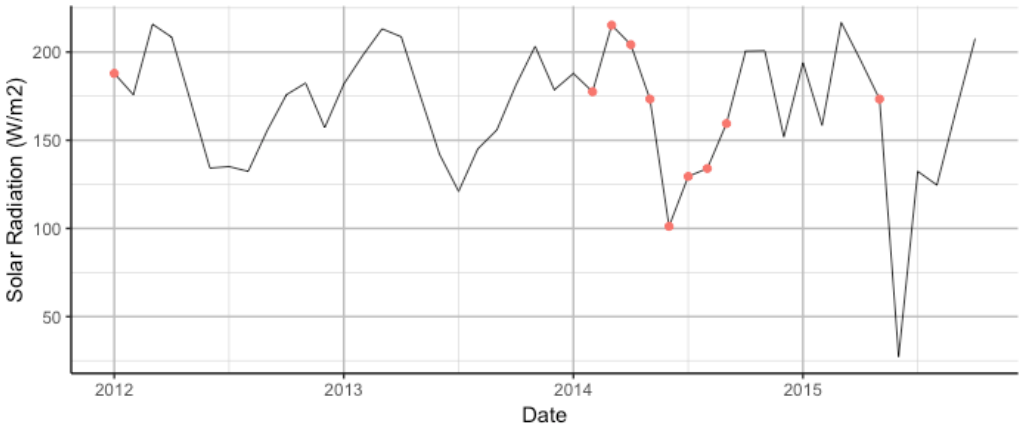

Figure C13 Time series plot of monthly mean solar radiation observations at Lopé NP, 2012-2016. The line shows the monthly means for each site. Red dots indicate missing months, which were filled using the mean value for the corresponding calendar month.

Wind Speed and Direction

Wind speed and direction have been recorded at Lopé using two weather stations in the savanna from 2012 to 2016 (Figure C14).

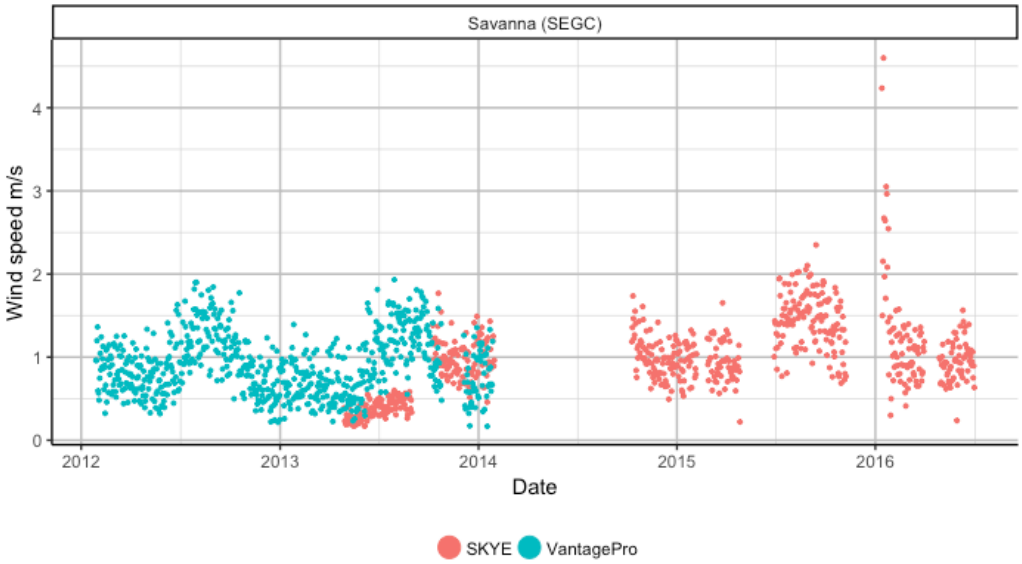

Figure C14 *Time series plot of wind speed at Lopé NP, 2012-2017. Coloured dots show daily mean observations from different equipment.*

Because the windspeed data is short and patchy we can only use it to demonstrate seasonality and periodicity (Fourier analysis using the continuous time series shown in Figure C15) not long-term trends or interannual variation.

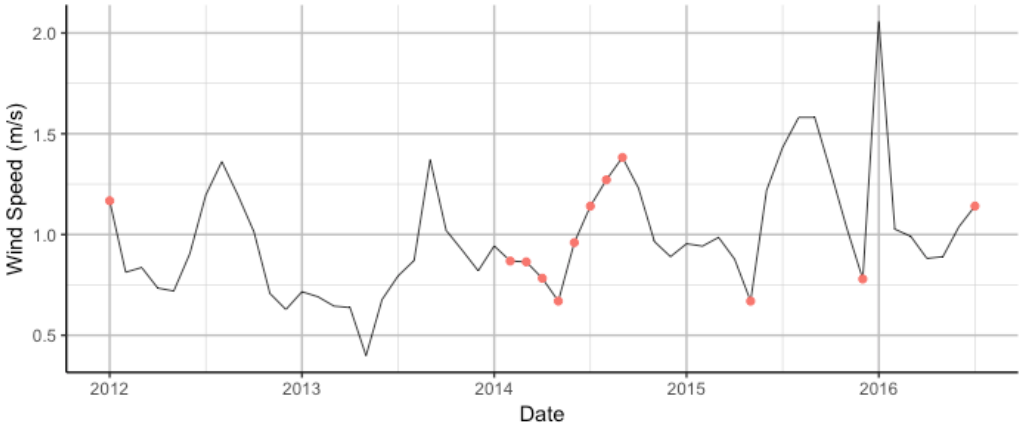

Figure C15 Time series plot of monthly mean wind speed observations at Lopé NP, 2012-2016. The line shows the monthly means for each site. Red dots indicate missing months, which were filled using the mean value for the corresponding calendar month.

The two different weather stations also recorded wind direction data but the seasonal summaries of wind direction are very different from each station (Figure C16). Wind measurements are highly influenced by local turbulence for these types of weather stations (Bell *et al.* 2015). Because of the localised nature of the measurements, the disagreements between the weather stations and the short and patchy nature of the record we exclude wind direction from current analyses until there is a more extensive data record at Lopé.

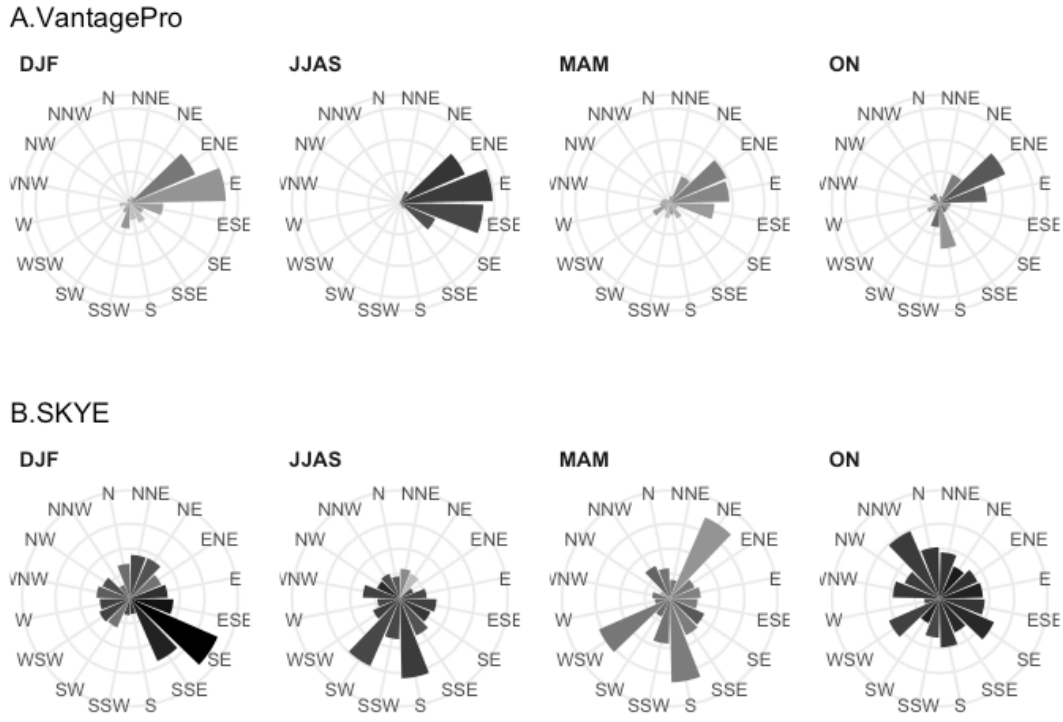

Figure C16 Rose diagrams to show wind direction at Lopé NP, 2012-2016. Circular bar plots show the mean proportion of time spent in each wind direction in each season (DJF: Dec-Feb, JJAS: Jun-Sep, MAM: Mar-May, ON: Oct-Nov) for each piece of equipment. The shade of the bar indicates mean wind speed (Dark fill: high speeds, Light fill: low speeds).

Aerosol Optical Thickness

We downloaded the AERONET level 2.0 data product (automatically cloud-cleared and manually quality assured) from the NASA website and extracted data for the wavelengths 440, 550 and 675nm as relevant for photosynthetically active radiation (PAR: 400-700nm; Figure C17).).

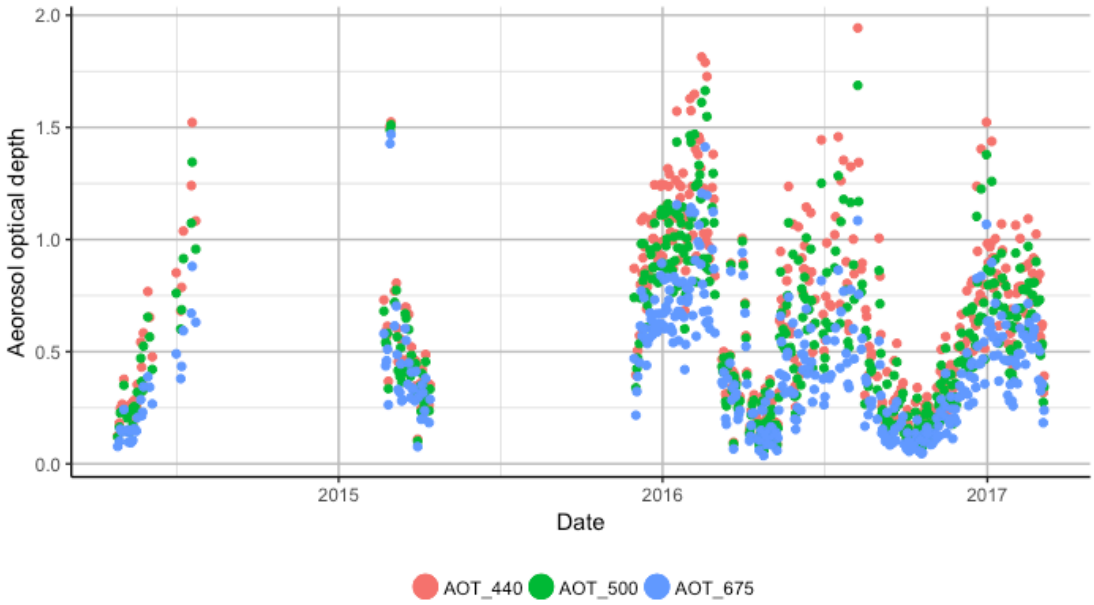

Figure C17 Time series plot of Aerosol Optical Depth at Lopé NP, 2014-2017. Coloured dots show daily mean observations at different aerosol optical depths relevant for photosynthetically active radiation (440, 500 and 675nm).

Due to equipment error and data removal due to cloudiness, 61% of data between 24-04-2014 and 06-03-2017 is missing. Data availability is strongly seasonal and is most sparse in the months June-November (85% data points are missing in August) and most dense in March (only 35% data points missing). Because the data is short and patchy we can only use it to demonstrate seasonality and periodicity (Fourier analysis using the continuous time series shown in Figure C18) not long-term trends or interannual variation.

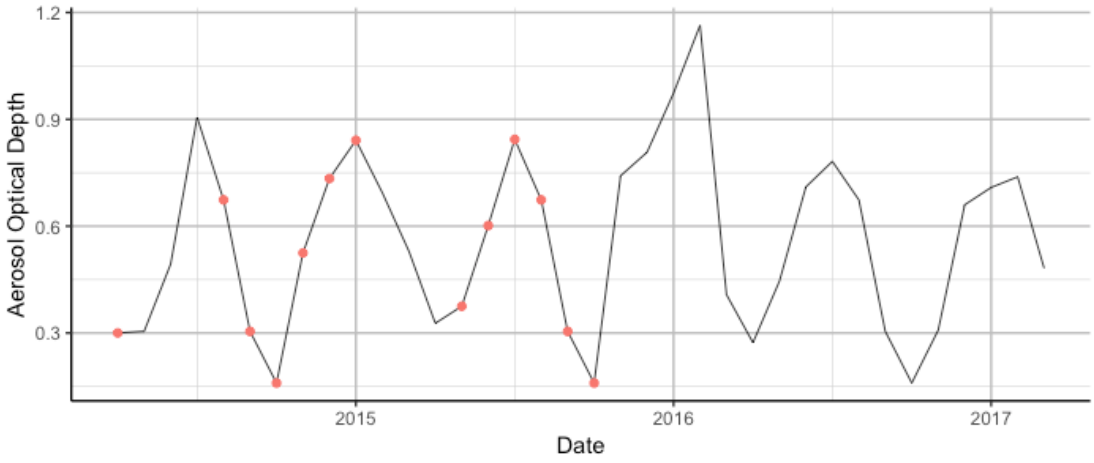

Figure C18 Time series plot of monthly mean Aerosol Optical Depth observations at Lopé NP, 2012-2017. The line shows the monthly means for each site. Red dots indicate missing months, which were filled using the mean value for the corresponding calendar month.